Universitetet
i Stavanger

FACULTY OF SCIENCE AND TECHNOLOGY

MASTER'S THESIS

Study programme/specialisation: Offhore Technology - Marine- and Subsea Technology	Spring / ~~Autumn~~ semester, 2018.. Open/~~Confidential~~
Author: Marie Engedal Andreassen	…………………………………… (signature of author)

Programme coordinator: Professor Muk Chen Ong

Supervisor(s):   Professor II Jan Inge Dalane

Title of master's thesis:

Installation of subsea equipment in utra-deep water using Fibre rope deployment system

Credits: 30

| Keywords:

- Fibre rope deployment method
- Marine Operations
- SIMO
- Subsea Installation
- 4000m water depth | Number of pages: …..198………….

+ supplemental material/other: ..20………

Stavanger,…..15.06.2018………..
date/year |

Abstract

As the demands for installation at deeper waters is increased, technology for such installations must be adapted to the conditions of the deep and ultra-deep water depths. This thesis provides information of such installations methods, including non-conventional installations methods.

The main focus of the thesis is using fibre rope deployment system to deploy equipment at water depths up to 4000 m. The use of fibre rope instead of the traditional steel wire is popular due to the similar specific gravity to water, which makes the fibre rope naturally buoyant in water. This cancels the self-weight problem of the steel wire as hoist line. Due to the different properties of the fibre rope, a new and cutting-edge technology was developed by the industry for deployment using fibre rope.

To investigate the possibilities of deploying equipment to water depths of 4000m, numerous simulations were conducted using the simulation program the SIMO. The results of the simulations show no significant problems using fibre rope to deploy various common subsea equipment. However, the positioning of the equipment is demonstrated to be a major challenge at these

Acknowledgements

I would like to thank my supervisor, Prof II. Jan Inge Dalane, for providing this interesting topic, as well as providing important information and feedback throughout the writing process.

Thank you to Postdoctoral Lin Li for providing necessary help with the simulation.

I would also like to thank Even Sandøy Nærum in Subsea 7 for providing help with the SIMO simulation program.

Thank you to my family and friends for supporting me and giving me useful advice throughout the thesis.

Table of Contents

List of figures

List of tables

List of Abbreviations

AHC	Active heave compensation
A&R	Abandonment and retrieval
AHTS	Anchor handling tug supply
ART	Active rope tension
BOB	Braid optimized for bending
CoB	Centre of buoyancy
CoF	Centre of force
CoG	Centre of gravity
CT	Constant tension
CTCU	Cable traction control unit
FRDS	Fibre rope deployment system
HMPE	High modulus polyethylene
HPU	Hydraulic power unit
Hs	Wave height
IDD	Inboard damping device
JIP	joint industry project
LCP	Liquid crystal polymer
MBL	Minimum breaking load
MODU	Mobile offshore drilling units
OBD	Over boarding device
ODD	Outboard damping device
PIM	Pendulous installation method
RMS	Rope management system
SIM	Sheave installation method
StW	Storage winch
SWL	Safe working load
Te	Tonnes
TLP	Tension leg platform
Tp	wave period/peak period

1. Introduction

As the unexplored reservoirs in the shallow water areas are reducing, the Oil and Gas industry sees the need to explore in deeper waters. Installations in deeper waters mean large technical challenges and the need for new and improved technology. Today the record for the deepest drilling and completion of a subsea well is in the Tobago field in the Gulf of Mexico, at 2934m water depth (Offshore Energy Today staff, 2011). As well as the challenges of the depth, the industry experiences challenges with metocean conditions, weight and size of the subsea equipment, and seabed layout.

This thesis investigates the installations at water depth down to 4000 m. The main gaps in technology from 3000m to 4000m is related to equipment and installation process. The majority of deepwater or ultra-deepwater production today occurs in four countries: Brazil, United States, Angola and Norway. The United States and Brazil together accounted for more than 90% of the global ultra-deepwater production in 2015 (Manning, 2016).

When operating in ultra-deepwater there are several uncertainties that must be considered. Vessel and equipment availability, new installation methods considering time, cost and robust operational limits, capacity of fibre rope, design tools and analysis methodology, wave motions, currents in different layers, reduce risk, and position and accuracy.

1.1. Introduction to Fibre Rope Deployment Method

The fibre Rope Deployment system (FRDS) is investigated as the used method for the installation process. The use of traditional steel wire rope is getting less attractive as the water depth increases. At depths of 3000m, the wire accounts for about half the load on the winch. This leaves a limited useful payload compared with the rope diameter. Synthetic fibre robes avoid this limitation. The specific gravity of the synthetic material is about the same as for water, so the ropes weight in water is negligible (Gjerde, 2015).

The major difference in properties between the steel wire and fibre rope has to be considereded when developing a fibre handling system. Fibre rope have lower axial stifffness, thus increased rope elongation. They are more exposed to abrasive wear and tear, subjected to contant cyclic bending causing internal heat buildup, and lowvariable and variable fricton coefficients. The fibre roope handling system requires active heave compensation.

Figure 1.1: CTCU Fibre rope deployment system from Rolls-Royce Maritime (ODIM). (Rolls-Royse Marine AS, 2010)

Compared with steel wire systems, the fibre rope deployment system sees a significant decrease in needed work load for the winch. The work load will stay approximately the same throughout the deployment process. The decrease in load also decreases the power output of the crane, reducing the cost of the operation. A smaller vessel is needed for the FRDS system and the deployment time is significantly reduced.

1.2. Objective and scope

The goal for the thesis is to acquire knowledge of subsea installation, and carry out simulations using the Fibre Rope Deployment system in ultra-deepwater up to 4000m.

This thesis includes a brief introduction of deepwater installation, including the installation methods currently used. The fibre rope deployment method is explained with great detail, including handling system, field experience and potential fibre rope cranes. Theory for vessel motions and lifting operations are provided. The main objective of the thesis using the simulation program SIMO to simulate deployment of various subsea equipment at the water depth of 4000 m, and briefly discuss the results. The method for the simulation including data input, environment and sling position is briefly explained and discussed. is the method and results of deepwater installation simulations using SIMA. The main issued related to deployment to 4000 m, in relatable current and wave conditions, are discussed in this thesis.

2. Deepwater installation

2.1. Offshore lifting operations
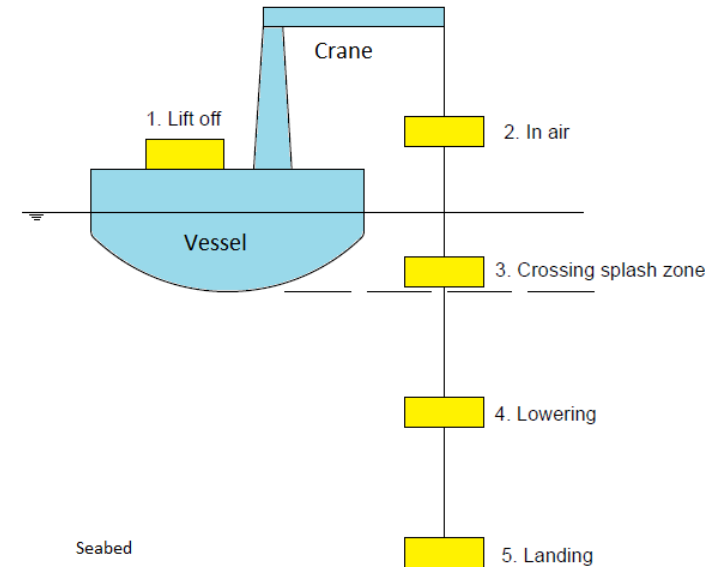
Figure 2.1: Illustration of steps for offshore lifting operations

During the installation of a subsea structure, the lifted structure is exposed to dynamic loading due to the motions of the installation vessel, as well as the direct action of the waves. Following are the main steps of a subsea lifting operation with accordance to Bai and Bai (2010) and Mouhandiz and Troost (2013).

1. Lift off
2. In air
3. Splash zone
4. Lowering
5. Landing

2.1.1. Lift off

During lift off there are three steps; slack wire, load transfer and hanging off the hook. During lift off the subsea structure is lifted from either the deck of the lifting vessel or a separate barge using a lifting crane, shown in the Figure 2.2 and Figure 2.3. When lifting from a barge it is critical to avoid recontact with the barge. This can be avoided by determining the minimum crane lifting speed. This is determined by using the criteria that the crane lifting velocity should be greater than the relative vertical velocity between the manifold base and the barge. Another important aspect is to avoid unacceptable tension in the lifting wire, such as snap loads due to slack in the sling. (Bai & Bai, 2010)
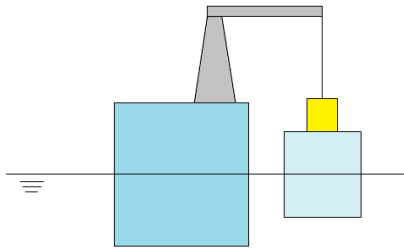
Figure 2.2: Lift off from barge
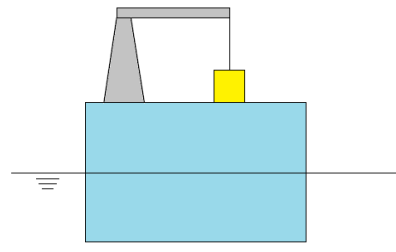
Figure 2.3: Lift off from deck

2.1.2. In air

After lift off the structure is hanging freely in air from the crane. When starting to deploy the structure over the side of the vessel, it is important to have enough clearance between the structure and the vessel. Any transverse motion can cause minimal clearance. During over boarding, the vessel loading condition and orientation can be optimized with respect to the incoming waves. Resulting in less structure motions and thus higher workability. (Mouhandiz & Troost, 2013)

One of the limiting criteria is the pendulum motion of a structure due to crane tip movement. In order to control the movement of the structure bumper frames and tugger lines can be use. It is also important to take account of the weather conditions, and avoid weather where the structure pendulum movements are too big.

2.1.3. Splash zone

This is the phase where the structure is submerged though the water surface and into the water. Here it is important that the maximum loads on the structure is defined. In the splash zone phase, the loads on the structure can be very high due to a combination of the motions of the installation vessel and the motion of the surface waves.

During the passage through the splash zone it is important to determine the wave load. When the structure is submerged to the seabed it is important to determine the added mass and damping. The added mass and drag coefficients are immersion dependent. When analyzing, it is important that the installed structure is exposed to extreme, direct wave loading. A way to improve the workability and safety of the phase, shielding by the vessel can be taken into account. The shielding effect causes a reduction of wave height at the lee side of the vessel. (Bai & Bai, 2010)

Alternative step: Transferring to A&R Wire

In some cases, where the crane wire is not long enough for the water depth, the structure is lowered to about 100m water depth to transfer the load from the crane to an Abandonment and Retrieval (A&R) Wire. When the structure reaches the transfer depth, the payout on the crane wire is stopped, the A&R winch is deployed and connected to the lowering yoke with the help of an ROV. The load is then transferred from the crane main hook to the A&R winch. (Bai & Bai, 2010)

2.1.4. Lowering

After passing the splash zone, or after transferring the structure load to the A&R winch, the structure is lowered further to the seabed. To determine the peak vertical motions of the structure during the lowering procedure, the resonance depth has to be calculated. Resonance occurs where the wave period corresponding to the max heave motion of the vessel, in a particular wave period range, matches the natural period of the lowering system. The natural period of the lowering system depends on the length of the lowering wire/rope. At a certain length of the wire, resonance may occur. The corresponding water depth is defined as the resonance depth. (Bai & Bai, 2010)

As well as resonance, the maximum hoist wire dynamics and the hydrostatic forces should be investigated. In some cases, to avoid hydrostatic pressure differences in the structure, the lowering is stopped. During the stop the components reestablishes equal hydrostatic pressure with respect to the ambient condition. After this process is completed, the lowering speed is increased. (Mouhandiz & Troost, 2013)

The weight of the submerged structure and the self-weight of the wire will cause static elongation of the hoist line. As the length of the wire increases, the stiffness of the wire will change. The mass of the system will increase during the deployment phase, if the wire has a self-weight or the structure is filled with water.

2.1.5. Landing

During landing and positioning of the structure on the seabed, it is important to consider the vertical offset and motions due to the static stretch in the wire. In addition, the horizontal offset is important for landing of the structure onto the seabed at the correct position and orientation. To reach the right position of the subsea structure, the structure can be positions by moving the installation vessel, or by the use of a ROV (Remotely operated vehicle). Another solution is to use an arrangement with clump weigh.

The maximum allowable touchdown velocity should be specified in the installation criteria. To satisfy the criteria, the installation may be performed in heave compensation mode. The seabed might consist of

mud, clay or sand. The touchdown velocity is therefore limited to the value for which the installed subsea structure structural integrity is not affected. (Mouhandiz & Troost, 2013) (Bai & Bai, 2010)

2.2. Deepwater deployment technology

The best available deepwater deployment systems today still face the challenge of meeting the requirement for deploying subsea structures that are more than 300 tonnes to water depths beyond 3000m. One of the main problems is the self-weight of the steel systems which makes the wire rope systems inefficient and impractical on most of the deepwater installation vessels. Use of synthetic fibre ropes that are essentially neutral buoyant in sea water, could be used to overcome this problem. This eliminates the self-weight of the deployment system ropes on the lifting and lowering capacity of the ultra-deep water deployment system. The most appropriate candidate of the fibre ropes is the High modulus polyethylene (HMPE). This is because the HMPE material has a very high strength-to-weight ratio, good elongation properties and dynamic toughness. Below is an overview of the most common deepwater deployment technologies and their challenges. This section is written with accordance to He, et al. (2012) (He, et al., 2012)

2.2.1. Single wire deployment system:

The single wire deployment system uses a simple wire drum to install small and medium size subsea equipment. The installed equipment is lifted from the deck of the installation vessel and is lowered through the splash zone, and is deployed to a water depth between 50 and 100m. At this water depth, the load is transferred to a winch wire, before further lowering though the water columns until it lands on the seabed at the installation position.

At large water depths, the deployment system requires an anti-rotation system. There are three types of wire used for this system including ordinary wire, rotation resistance wire and low rotation wire. The ordinary wire is not torque balanced and could rotate up to 360° per meter under a tension load of 20% minimum breaking load (MBL). The rotation resistant wire consists of two layers of strains in opposite direction. The low rotation wire is made to counter balance the torque by the layers of strands. Unlike the ordinary wire the low rotation wire rotates approximately 2° per meter of wire under a tension load of 20% MBL. Due to the free rotation of the wire under tension, wire damage or loss of end termination could occur. When the tension is removed, the rotation tries to unwind. Of the wire types mentioned above, only the low rotation wire is suitable for deepwater installations. During deepwater installations the loads

on the drum flanges is increased, this accumulates significantly at the flanges when the load is large, resulting in damage to the drum flanges.

Figure 2.4 is a 400Te deployment system equipped with a traction winch, an active heave compensation system (AHC) and a storage winch with a steel wire of Ø109mm. This system can be operated at a lowering speed of 500 m/hour (0.14 m/s) and work at a maximum water depth of 2000 m. (He, et al., 2012)
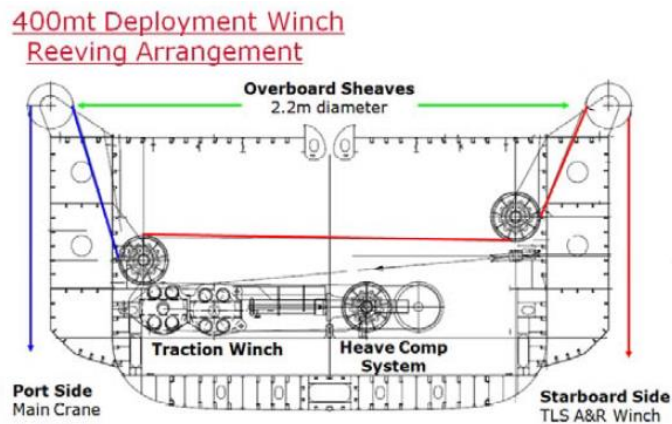
Figure 2.4: 400Te deployment winch reeving arrangement. (He, et al., 2012)

2.2.2. Modular winch system

The self-weight of the steel wire causes a single wire system to loose its lift capacity, this problem becomes progressively worse in deep water. Steel wire rope technology with a multi-fall lowering system is mature and durable. However, it is difficult to manufacture sufficient long lengths of steel wire. The manufacture capability is usually of 200Te steel wire at 2900 m lengths and 5 inches in diameter. The safety working load (SWL) of such wires are at 350 tonnes. The long wires needed for deep water depths will even cause significant problems for the low rotation wires, and will further complicate the entangle problems with multi-fall systems. (He, et al., 2012)

A solution to these problems is using a modular winch system, often called a module handling system. This system is used for lifting/lowering of special subsea modules. It consists of up to 6 winch units ranging from 5Te to 70Te lifting capacity, with an operating capacity down to 2000m water depth. Each winch uses an electrical drive with built in AHC system and active rope tension (ART) controls. This system helps compensate for the vessel movements with the sea bottom. One disadvantage is that the system has a peak power consumption at 300kW. The system also needs a special control and operation system.

Figure 2.5 is a dual winch tandem deployment system with a 250Te lowering capacity at water depths up to 3000m.
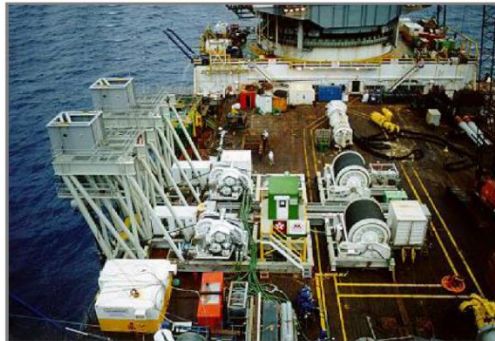
Figure 2.5: Dual Winch Tandem Deployment System. (He, et al., 2012)

To compensate for the self-weight problem of the steel wire deployments systems a new and approved system using fibre rope has been developed. The system is used in a single-fall or a two-fall deployment system. Below is some basic information about the fibre rope deployment systems (FRDS). A more in depth technical description is found in chapter 3.

2.2.3. Single-fall FRDS system:

Using the FRDS together with a conventional steel wire crane can be used for ultra-deep water deployment. The crane is used for lift-off and over boarding the vessel and deploying the installed object to a specific water depth, for example 50 m. At this water depth, the load is transferred from the winch to the FRDS before the installed object is deployed to the seabed. (He, et al., 2012)

One example of a FRDS is the 46Te Cable Traction Control Unit (CTCU) developed by ODIM Alitec AS. The CTCU unit consists of a series of sheaves with individual drives used to de-tension the rope, as well as controlling the speed and the torque on each individual sheave. The purpose is to avoid accumulated slip due to rope elongation and variations of diameter due to splices. In addition to the CTCU, a storage winch is used to store the ropes at low tension while maintaining a constant back tension for the CTCU. The ODIM CTCU with the highest capacity has been designed with a 125Te SWL.

2.2.4. Two-fall FRDS system:

The 125Te FRDS described above can be used in a two-fall configuration. The two-fall FRDS has a total capacity of 250Te SWL at water depths deeper than 3000m.

2.3. Installation methods

Deepwater installation methods are classified as either conventional or non-conventional methods. The methods are listed in Table 2.1 below.

Table 2.1: Conventional and non-conventional installation methods. (He, et al., 2012)

Conventional	Non-conventional
- Cranes of heavy lift vessels - A-frames of offshore support vessels - Drilling riser of drill vessel - Deepwater construction vessels	- Special construction vessels - Sheave installation method - Pendulous installation method - Pencil buoy method - Modular winch system

All of the installation systems and methods have been developed and successfully used in deepwater applications.

2.3.1. Deepwater construction vessel (DCV)

The subsea hardware and suction anchors are transported to the installation site via a barge. The subsea hardware and suction anchor is pre-fitted with two high-performance synthetic slings, for each installation object. Technip's Deep Blue vessel is equipped with a 400Te outboard crane. One of the slings is connected to the crane and the hardware is lifted off the barge and lifted though the splash zone and deployed to a water depth of approximately 100m. A remotely operated vehicle (ROV) is then used to capture a special grommet attached to the second sling, and transports the grommet to the hoop of Deep Blue's A&R winch. When the load is completely transferred to the A&R winch, the other sling will be freed from the outboard crane. The hardware is then lowered onto the seafloor for installation (He, et al., 2012). The DCV is often used for installing larger equipment such as foundations, moorings, SPARs, TLPs, and integrated topsides. (Offshore Fleet Journal, u.d.)

2.3.2. MODU drilling riser

the MODU drilling riser system is an expensive day rate vessel. It is often used to install wellheads, Christmas trees and BOP's. But it is rarely used to install manifolds. This is due to the low availability and

the extremely expensive day rates. In addition, most of the drilling semisubmersibles have lifting capacities when installing 300Te subsea hardware at up to 1000m water depth. (He, et al., 2012)

Figure 2.6 and Figure 2.7 show the installation of a 240Te manifold in 940m water depth in December 1997 by Petrobras.

Figure 2.6:SEMI Drilling riser for installing 240Te Manifold. Courtesy of Petrobras. (He, et al., 2012)
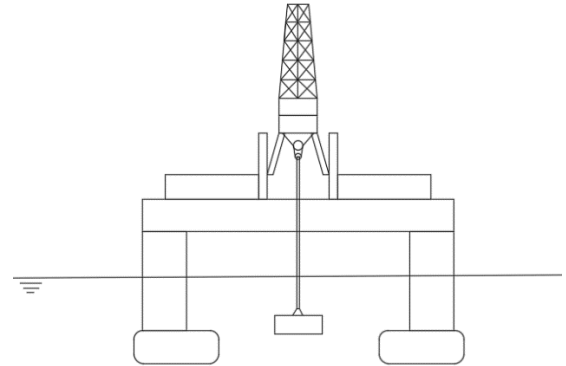
Figure 2.7: Schematic Illustration of Manifold Installation.

2.3.3. Heavy lift vessel

There is a limited of heavy lift vessels that are suitable for lifting 300 tonnes subsea hardware ate water depths beyond 3000m. Some of the available vessels include Heerema's Balder, Saipem 7000, Jumbo Offshore's Javelin and Fairplayer. The heavy lift vessels are specialized in deepwater installation and are very capable and efficient. The main problem is the low availability of the vessels and the high cost. (He, et al., 2012)

Figure 2.8: installation of the Åsgard subsea compressor manifold station in summer of 203 from the Saipem 7000. Courtesy of Statoil. (Davies & Ramberg, 2016)

2.3.4. Offshore support vessels and A-frame

Small offshore support vessels include ROV support vessels, diving support vessels, field support vessels, Anchor Handling Tug Supply (AHTS) vessels. They have A-frames and conventional rope deployment systems. They have a limited capacity of installing 200Te subsea structure in water depths up to 1000m. Most are used to only install compact subsea hardware in shallow water. However, if a heavy duty FRDS system is used onboard instead of the conventional rope deployment system, a small support vessel with a capable A-Frame can be used to install 300Te subsea hardware at water depths beyond 3000m. (He, et al., 2012)

Figure 2.9: AHTS with A-Frame for Manifold Installation. Courtesy of TTS Group ASA. (TTS Group ASA, 2017)

2.3.5. Sheave installation method (SIM)

The sheave installation method was developed to install the 175Te *Roncador Manifold I* to a water depth of 1885m in 2002. It is based on a two-fall configuration of a conventional deployment system. The major difference of the conventional deployment system is that the fixed end from the dead point is relocated from the installation vessel to another vessel. There is a total of 3 vessels. The first is a semisubmersible rig that is used for lift-off and deployment of the manifold though the splash zone. The semisubmersible provides heave motion compensation during lowering though the splash zone and during landing at the sea bottom. The semisubmersible used in this case the Pride South America, which is a DP-3 drilling vessel with a crane with the capacity of lifting 300Te at a maximum water depth of 1000m. The second vessel is an Anchor handling tug supply (AHTS) 1 vessel that is used to provide the fixed point for the dead end of the wire when lowering the manifold through the water column. The third vessel is a AHTS 2 that is located

at an adequate distance from AHTS 1. AHTS 2 provides assistance to orient the manifold as well as avoiding potential twist induced by the two-fall configuration system. A schematic illustrate of the vessels are shown in Figure 2.12. (He, et al., 2012)

Figure 2.10: Lif-off and overboard the Manifold. (He, et al., 2012)

Figure 2.11: Lowering of Manifold though splash zone. (He, et al., 2012)
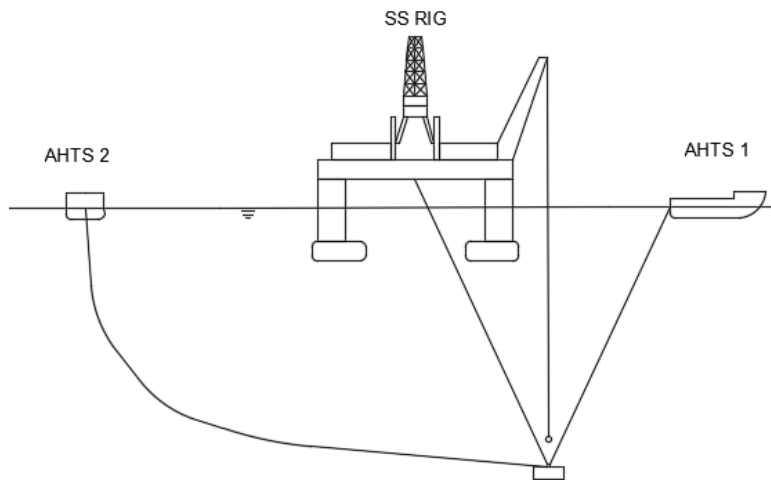
Figure 2.12: Schematic Illustration of Sheave Installation Method

2.3.6. Pendulous installation method

The pendulous installation method (PIM) is a non-conventional method installed by Petrobras due to the low availability and high cost of the conventional installation methods, such as construction vessels and heavy lift vessels. PIM uses two conventional small vessels with a FRDS and without any special rigging onboard. The fibre rope deployment system has a capacity of 300Te in water depths up to 3000m. The method uses a steel wire winch system to launch the manifold in a pendulum motion. The deployment line is made up of polyester ropes to deploy the manifold to the seabed. (He, et al., 2012)

Figure 2.13: Dummy manifold for full-scale test (16.6m*8.5m*5.2m). Courtesy of Petrobras. (He, et al., 2012)

The first vessel is equipped with a crane for lift-off and overboarding of the manifold into the seawater through the slash zone. When the manifold is lowered to a specific water depth, say 50m in this case, the load is transferred from the crane to a launch winch wire. The deployment line is pre-rigged with lifting slings for lifting of the manifold and buoyancy elements that helps reduce the winch capacity required for both the launch winch and the deployment winch. The deployment line is pre-deployed at a certain length to ensure that the manifold is maintained in a vertical position approximately 50m above the seabed. It is important to take account the elongation of the polyester rope, to avoid premature touchdown of the manifold. Once the load is transferred from the crane to the launch winch wire, lunching can start by paying out the launch line, while the deployment winch is at breaking mode. During the pendulous movement, the load is gradually transferred form the launch line to the deployment line. The pendulous motion is complete once the manifold has swung from the bottom of the first vessel, 50m below sea surface, to the bottom of the second vessel, 50m above sea bottom.

This method prevents axial resonance as the ropes are much longer than the lengths that would fall into the resonance region when deployed though the water column. The method allows the lift lines to undergo gradual tension after pre-paid. After the pendulous launch, an ROV is used to disconnect the launch line by pulling the trigger sling. Once the launch line is disconnected the deployment winch can deploy the manifold vertically the last meters until the manifold reaches its position and lands on the seabed.

The pendulous installation method is cost effective, however deploying manifolds with complex geometries may cause hydrodynamic instability. Figure 2.14 and Figure 2.15 show the PIM for a 280Te Manifold at 1900m water depth.
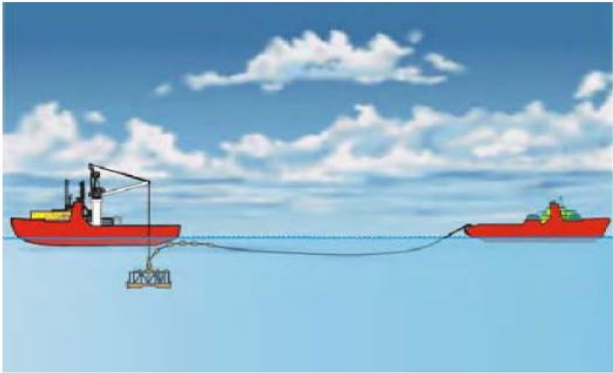
Figure 2.14: Illustration of manifold overboarding. Courtesy of Petrobras. (He, et al., 2012)
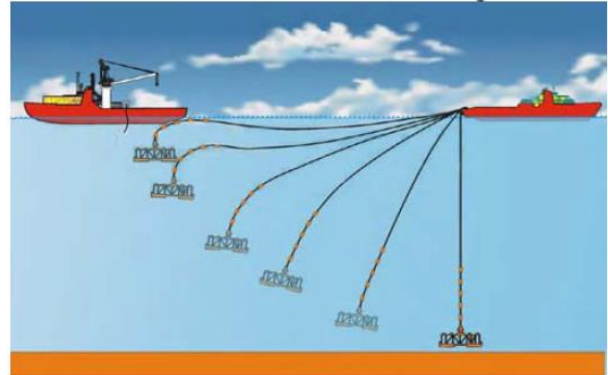
Figure 2.15: Illustration of pendulous Motion to Lower Manifold. Courtesy of Petrobras. (He, et al., 2012)

2.3.7. Pencil buoy method

The Pencil Buoy Method (PBM) is a subsurface transportation and installation method developed by Aker Solutions. The system required a crane barge used for lift-off from barge at an inshore transfer location with sufficient water depth. The load is then transferred from the barge crane to a top-class AHTS vessel. The AHTS vessel includes a tug winch wire and a tubular buoyancy tank shaped as a pencil. The pencil tank is launched from the stern deck by paying out the towing winch line, while the tug vessel is slowly moving forward. The weight of the installed structure and rigging are suspended from the Pencil Buoy during wet tow. The pencil buoy is a steel structure with internal ring stiffeners. In consists of many watertight compartments. The compartments are made to satisfy the requirement due to one compartment damage. During towing to the installation location, the vessel maintains a speed 3.0 to 3,5 knots. Once the AHTS vessel arrives at the installation location, the towing wire is winched in and the weight of the installation structure is transferred from the Pencil Buoy to the towing winch wire. The buoy is then disconnected. During the load transfer the AHTS vessel moves slowly forward to avoid contact between the tug vessel stern and the pencil buoy. The system requires a passive heave compensator during deployment to the sea bed. The deployment of the structure to the sea bed is similar to other deepwater installations. (He, et al., 2012)

The lift-off and lowering through the splash zone is done at a sheltered location rather than in offshore operation. The subsurface wet tow was designed for installation during unrestricted summer storms. The subsurface wet tow causes complex hydrodynamic problems on the cargo structure and the pencil buoy due to wave and current action. There are three generations of PBM. The first generation has a cargo capacity of 150Te, the second has a cargo capacity of 250Te and the third generation has a cargo capacity of 350Te.

The figure bellow shows the setup and the pre-launch position of the Pencil Buoy Method.
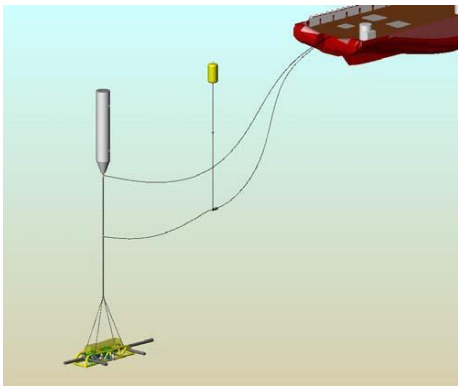
Figure 2.16: Setup for Pencil Buoy Method. Courtesy of Aker Solutions. (He, et al., 2012)

Figure 2.17: Photo of slender Pencil shaped buoy at pre-launch. Courtesy of Aker Solutions.

2.3.8. Free-fall installation – torpedo anchor piles

The free-fall installation used to install torpedo anchors. The torpedo anchors are used for mooring of deep-water offshore facilities, including risers and floating structures. The anchors are installed by dynamically penetrating the soil by kinetic energy. This is achieved by free fall of the anchor through the water column. The anchor is a cone-tipped cylindrical steel pipe, filled with concrete and scrap metal as ballast. The special feature of the torpedo anchor are conical tip, stabilizing fins, ballast and omni-direction chain attachment on the top of the pile. These features are used to penetrate the seabed within the target tolerance, and prevent fluttering and unacceptable resultant vertical tilt angles. Due to the ballast location at the bottom of the anchor torpedo, the anchor will have a low centre of gravity which helps with stability during free fall.

A mooring anchor is attached to the top of the torpedo anchor. A ROV is used to monitor the mooring component being laid out toward the anchor drop location. This allows pre-alignment of the mooring arm. The anchor is then deployed to the proposed drop location, usually 30m above the seabed. The ROV

controls that the anchor is in the right position and height. Then an acoustic release-hook is triggered and the anchor is dropped into the soil. The mooring chain forms an inverse catenary shape, shown in step 6 in Figure 2.19, once the mooring line is loaded to cut in the embedded anchor chain. This shape helps reduce the horizontal load on top of the anchor, and increase the lateral capacity. When designing such anchors, one must take account the estimation of the embedded depth, as well as the short-term and long-term pull-out capacities. Torpedo anchors were first made as an inexpensive and an easily installed anchor for riser flowline restraint. There are three different types of torpedo anchors made; T-24 for flowline restraint, T-43 for MODUs, and T-98 for permanent FPSO anchors. The soil needed for installation of torpedo anchors are usually soft to medium clay soil, this soil is the same soil that works well for suction piles and plate anchors. (He, et al., 2012)

Figure 2.18: Torpedo anchor piles in combination with polyester rope. (He, et al., 2012)
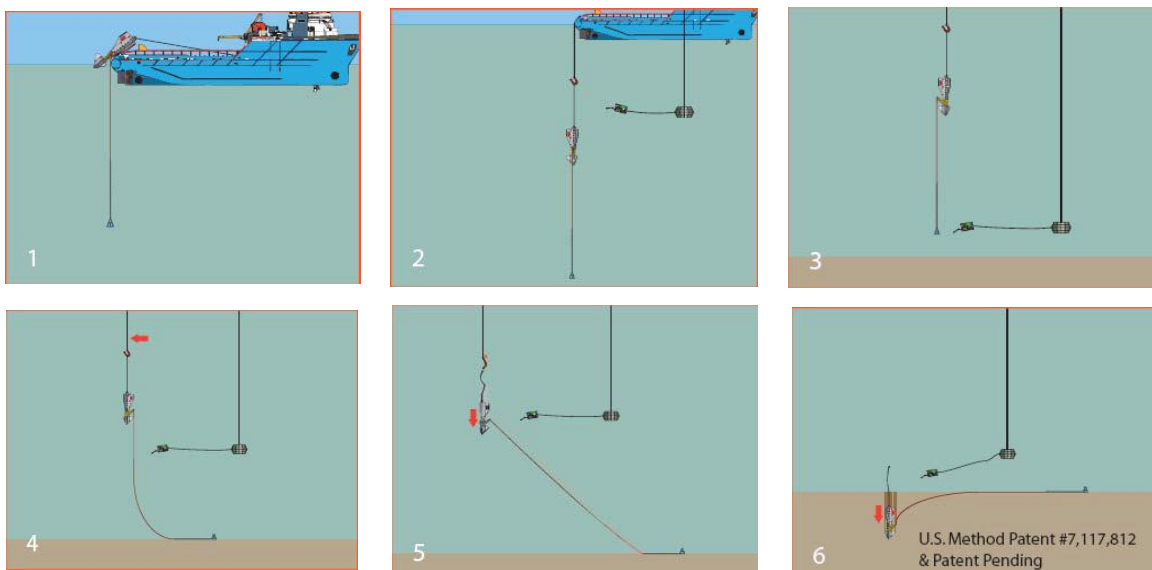
Figure 2.19: Typical Free-fall steps for anchors. (He, et al., 2012)

3. Fibre rope deployment system

In the following chapter, the fibre rope deployment system is described with great detail. The chapter includes information about fibre rope, fibre rope handling systems, rope management system, field experience and fibre rope cranes.

3.1. Fibre rope

The traditional hoisting lines used for lifting and mooring in deepwater exploration and production are steel and chain wire. Steel and chain wires have limitations in deepwater, primarily due to their self-weight. Also, the size of the handling systems tends to be very large, not only in size and weight, but also in terms of investment and operation. (Bull, et al., 2007)

Use of synthetic fibre rope provide a potential solution to the self-weight problems. The three main fibre rope material options for deepwater applications are aramid, polyester and High modulus polyethylene (HMPE), see Table 3.1. Other alternatives are high-strength zylon, vectran and nylon. (He, et al., 2012)

Table 3.1: Weights and Sizes of Deployment Ropes Based on 1000Te MBL. (He, et al., 2012)

Parameter	HMPE	Aramid	Polyester	Nylon	Steel
Weight in air [kg/m]	8.4	12.0	23	25	58
Weight in Water [kg/m]	Neutral	3.3	5.9	2.5	49
Overall Diameter [mm]	125	120	175	200	110

The HMPE rope is the best candidate for ultra-deep water development systems. The HMPE fibre has a high-modulus and high-strength, is essentially neutrally buoyant in water and excellent mechanical properties with low density. This results in a high performance-on-weight basis and makes it one of the strongest manmade fibres. The high strength and high modulus in the fibre direction yields for resistance against deformation. The main characteristics of the HMPE rope includes high strength, low density, low elongation at break, long fatigue life, and resistance to most chemicals and sea water. The mechanical properties of the HMPE is influenced by temperature change. The strength and modulus increases in sub-ambient temperatures, usually ranging from 10-45°C, but decrease at higher temperatures. (He, et al., 2012)

Important features for fibre rope used as lifting line in heave compensation systems are (Bunes, Ingeberg, Torben, & Teigen, 2008):

- High cyclic bend over sheave performance

- Torque free construction

- Field inspectable and reparable

- High strength to weight ratio

The fibre rope from Puget Sound Rope is used in the many if the current developments. It is commonly referred to as Braid Optimized for Bending (BOB) and is a 12x12 braided construction. This assures a torque free rope, as well as a rope that can easily be inspected internally and repaired offshore by trained personnel. Repair of the rope will typically give an incline splice with a diameter 50% above the nominal rope size.

A blend of HMPE and liquid crystal polymer (LCP) fibres have been used to provide good temperature resistance and good creep properties. A lubricant coating is used to reduce the friction between the fibres. This reduced the internal wear and heat built up in cyclic bend over sheave operation. A typical minimum D:d ratio requirement for heave compensating sheaves is 30:1 for this rope. D is the pitch diameter, rotation diameter, of the rope and d is the rope diameter.

3.1.1. Comparison between steel wire and fibre rope

Figure 3.1 and Figure 3.2 shows a comparison between steel wire and fibre rope with regard to the required working load for a winch system and with respect to the weight of the lifting line in air. A safety factor of 4 has been used on the calculations for both the fibre rope and steel wire.
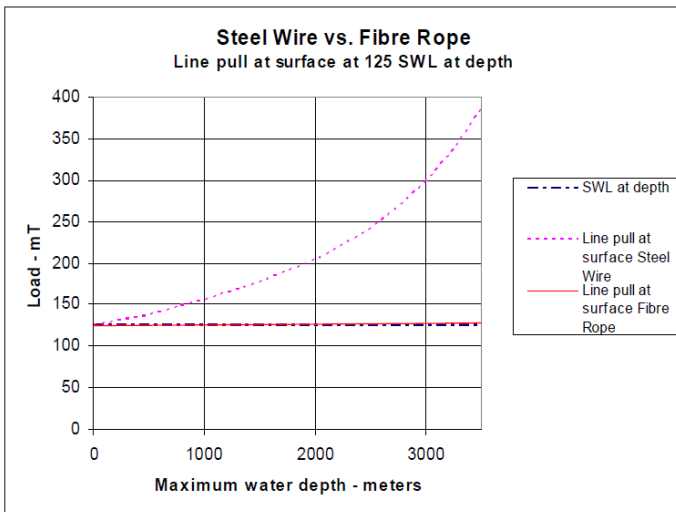
Figure 3.1: Line-pull at surface. (Ingeberg & Torben, 2011)
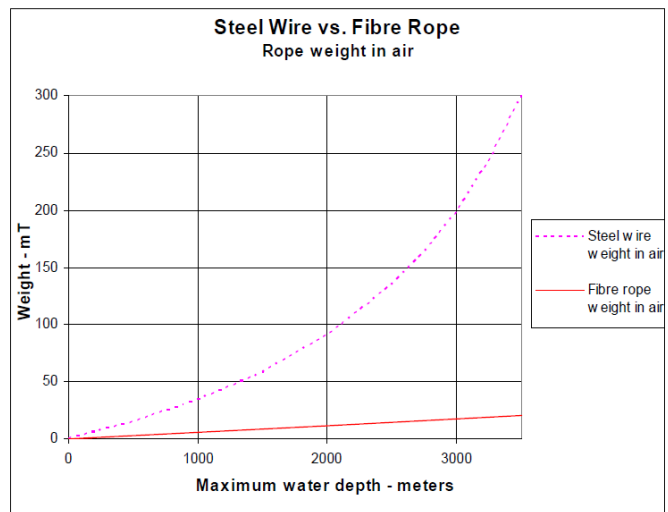
Figure 3.2: Rope Weight in air. (Ingeberg & Torben, 2011)

At 3000m water depth, the required working load for the steel wire winch will be around 300Te, while only 127Te working load is required for the fibre rope winch.

Another interesting aspect is the weight of the lifting line with regard to the fabrication, handling and transportation. The weight in air of the steel wire for this case will be approximately 200Te, while the corresponding fibre rope weight will only be 20Te, which is 10% of the steel weight. The high weight of the steel wire represents a challenge with regard to logistics and handling. As well as getting close to the practical limits and capabilities of today's industry.

In addition, the power supply needed for the active heave compensation (AHC) system is influenced by the hoist line material, due to the different weight capacity. Using the same values as the example above, for system rated at 3000m water depth, the steel wire system required a peak power at 4.4MW and the fibre rope systems requires a peak power at 1.9MW. These values represent the minimum installed power needed for the motors in the handling system.

Hoist line properties

Below is a comparison between a hoist line made of steel wire, and one maid of HMPE fibre rope. These values are taken from the Launch and Hoist line used for the pendulous installation method for installation of a manifold in the South China Sea. (He, Wang, Xu, Zhang, & Zhu, 2013)

Table 3.2: Properties for steel wire and HMPE rope. (He, Wang, Xu, Zhang, & Zhu, 2013)

	Steel wire	HMPE rope
Diameter [mm]	127	155
Length [m]	2000	1400
Mass in Air [kg/m]	57.8	15.0
Weight in Sea Water [kgf/m]	44.7	~0
Minimum Break Load [Te]	1000	1200
Axial stiffness, EA [MN]	965	250

3.1.2. Challenges

Although the motivation and potential saving using fibre rope is quite obvious, the utilization of fibre ropes for lifting lines is not completely straight forward. The major differences in properties of fibre rope

compared to steel ropes need to be taken into account when designing a fibre rope handling system. The main challenges are listed below and briefly described. (Bunes, Ingeberg, Torben, & Teigen, 2008)

Traction unit

- During subsea installation, the handling system deploys a heavy object, but recovers an empty hook. During recovery of the empty hook it is necessary to avoid spooling of the rope onto the drum at very low tension. A traction unit is required for handling systems using fibre ropes. This is also important when later deploying a heavy object to avoid the high-tension rope to be squeezed into softly spooled layers.

- The rope is recommended to be stored at a tension below 10% of the Minimum Breaking Load (MBL) to avoid excessive creep of the rope in the storage winch. Using a typical safety factor of 4-5, the working load will represent 20-25% of the MBL. This is above the recommended storage tension. Therefore, a traction unit is also needed during the recovery of operations with heavy payload.

Elongation

- Due to the low axial stiffness of the fibre rope, significant elongation of the rope as tension is increased though the traction winch. The elongation causes damaging slippage between the fibre rope and the traction winch drums when using a traditional traction winch.

Fatigue life

- Fibre ropes are more exposed to adhesive wear and tear compared to steel wire.

- Fatigue life of the fibre rope when subjected to constant cyclic bending e.g. during heave compensation modes, must be managed. This is also the case for steel wire. An additional challenge with fibre rope is related to the internal heat build-up and the sensibility to heat of the fibres.

Splices

- A fibre rope with a braided construction and without a jacket can easily be spliced if necessary. This opens up the possibility to handle the fatigue life of the whole rope by cutting out and replacing the worn sections. Therefore, the fibre rope requires a traction winch system that can handle splices.

Friction

- Due to rope coating, contaminations and temperature, fibre ropes have a very low and variable coefficient of friction. This is challenging when designing a traction winch unit that is dependent on friction.

Resonance

- Since the fibre rope has a low axial stiffness, resonant conditions can be seen at more shallow water depths compared to steel wire systems.

3.2. Handling systems

ODIM, a Norway based company, have developed a Cable Traction Control Unit (CTCU) system for handling of sensitive cables like Seismic cables, fibre optic cables and from 2002 also fibre ropes. Described below is a dedicated CTCU system for deep water installation using a fibre rope as hoist line. This system has a SWL of 46Te with a dynamic factor of 1.3. (Bunes, Ingeberg, Torben, & Teigen, 2008)
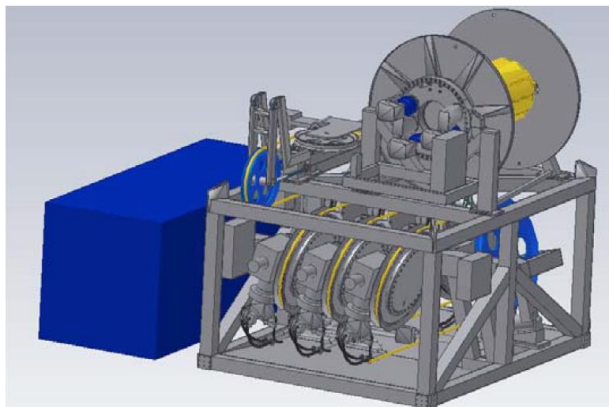
Figure 3.3: 46Te CTCU system. (Bunes, Ingeberg, Torben, & Teigen, 2008)

Main parts of the CTCU system:

- CTCU: a series of sheaves with individual drive used to de-tension the rope
- StW: Storage Winch to store the rope at low tension. Also assuring a constant back tension for the CTCU to assure frictional capacity.
- IDD: Inboard Damping Device that smoothens the tension between the CTCU and the StW
- ODD: Outboard Damping Device used for constant tension and pull limit control (optional)
- OBD: Over Boarding Device

- HPU: Hydraulic Power Unit with accumulators that supplies the system with high and low-pressure oil
- Control system: Computer system used for dynamic control of individual machines and interactions between the machines. The control system also includes

The fibre rope is stores at constant tension in the storage winch on top of the structure. For the 46Te unit the storage winch was designed for 4500m of 56mm rope. From the storage winch, the rope is fed through the spooling device and inboard damping device, before entering the individual sheaves of the CTCU. From the CTCU the rope is guided over the ODD device before entering the overboarding device. (Bunes, Ingeberg, Torben, & Teigen, 2008)

Important features of the CTCU traction unit:

- Active load distribution: the load is shared between the sheaves within the physical limitations of each sheave.
- Slip control: controls the speed of the sheaves. It compensates for the rope load elongation and the differences in diameter due to splices.
- Anti spin control: Detects and reacts on emerging spinning of the rope by comparing the sheave speed with the measured rope speed.
- D:d ratio in accordance with the requirement for cyclic bend of the fibre rope over the sheave. The general minimum D:d ratio from manufactures today is 30:1. The 46Te system was designed with a D:d ratio of 33:1. This gives the opportunity of using larger size ropes.
- Differentiated sheave protective coatings designed with regard to the load and friction capacity of each sheave
- Sheave groove profile allowing for splice handling
- Rope pre-conditioning: used to bring the rope size down to a nominal size, when spoiling of a new rope for the first time.

The needed features for functioning during deep water installation and construction operations are present in the handling system. Following are the present measures of the CTCU system (Bunes, Ingeberg, Torben, & Teigen, 2008):

- High speed deployment of heavy loads
- High speed deployment and recovery of empty hook

- Powerful and accurate active heave compensation: gives speed capacity of 2% and 95% accuracy according to signal representing vessel motions

- Accurate constant tension function (CT)

- Pull limit: Active limitation of allowed pulling force. Can be combined with the AHC. This can also be extended to a splash zone transition function.

- Automatic landing function: automatic transition from the AHC system to the CT system upon landing. This can be combined with the Pull limit.

- Automatic lift-off function: automatic transition from the AHC system to the CT system during lift-off. Can be combined with the Pull limit.

- Crane mode: Brake handling according to requirements for offshore cranes. The FRDS can be integrated with a crane, A-frame or other overboarding devices as well as handle the payload in air or and on deck.

3.3. Rope management system

For the CTCU based FRDS, a rope management system (RMS) has been developed as a built-in part of the winch control system. Real time signals on position and applied tension at any part of the rope is available in the system. The information is compared with geometrical data of the FRDS, for example sheave diameter and distance between the sheaves. With the technology mentioned above, the RMS is able to count the number of bends at every position of the rope. Then each bend is weighted according to a factor given by e.g. the bend radius and the rope tension at each point. (Bunes, Ingeberg, Torben, & Teigen, 2008)

The rope is split into rope segments with a configurable length. The rope data is recorded for each rope segment. The data is processed and displayed in real time on the winch operator computer. The main screen for the RMS is shown in the figure below. Alarms that give warnings of inspection and replacement of a rope segment that have reached a certain configured alarm limed is implemented as a part of the alarm system for the FRDS. All the data is stored so that the data can be post processed. The post processed data can for instance be used to find a new factor for bend weighing. (Bunes, Ingeberg, Torben, & Teigen, 2008)
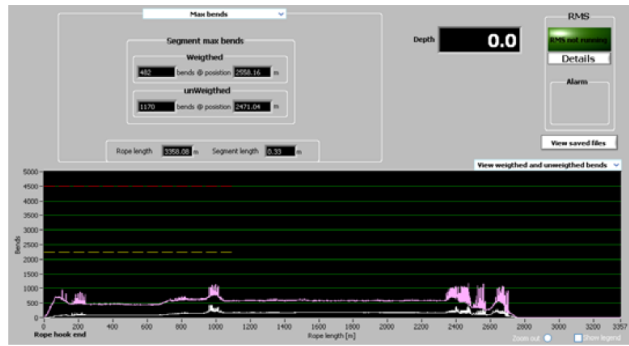
Figure 3.4: main screen of the RMS. (Bunes, Ingeberg, Torben, & Teigen, 2008)

The RMS can also manage data for rope configuration. Such as when a section of the rope is cut out or a new section of rope is spliced in. When a section of the rope has reached its retirement criteria or the operator would like to check the condition of the rope, the section can be sent to a laboratory for testing of residual strength. The RMS is a powerful tool to speed up and assure quality in rope wear and retirement calculations.

3.4. Field experience

In this section pilot tests and field experience of the CTCU fibre rope deployment method is described. The tests described are the 46Te SWL pilot tests and field pilot test, installation in gulf of Mexico sing the 46Te CTCU, and The 250Te CTCU in two-fall configuration field test.

3.4.1. Pilot tests 46 Te

The 46Te SWL Fibre rope deployment system was built and tested in 2003-2004 by a joint industry project (JIP). It was conducted by the Norwegian company ODIM. The system was tested offshore and inshore on a barge. Table 3.3 shows the technical specification of the 46Te FRDS. (Bull, et al., 2007)

Table 3.3: Technical specifications of the 46Te SWL FRDS by ODIM. (Rolls-Royse Marine AS, 2010)

Safe working load (SWL)	46Te
Maximum dynamic load	73.6Te (Dynamic amplification Factor of 1.6)
Launch/Recovery speed at SWL	1.0/0.5 m/s
Launch/Recovery speed at 50% SWL	2.0/1.0 m/s
AHC speed	2.0 m/s
Constant tension range	5-45Te
Fibre rope diameter	56mm
Storage winch capacity	4500m +
Peak power consumption	850 kW

The first test conducted was a factory acceptance test, where the basic features of the rope handling was tested. Later the system was tested in an 8-week period inshore on a barge. The installed object used was a clump weight of 35mT in water. Information about the winch and rope performance was found by conducting extensive testing of the AHC system. The rope used for this test was 225m of 56mm BOB rope described in section 3.1. The test was conducted at a water depth of 100m. Test was conducted inshore in shallow water and with limited vessel motions.

The rope performance was tested by running in active heave compensation with temperature sensors on the inside of the rope. These sensors were used to monitor the temperature build-up in the rope caused by cyclic bending over the sheaves. Tests of the rope cooling was also conducted. The results from the teste were used to establish the rope retirement criteria.

A 4-fall configuration test with 18mm rope was also conducted to demonstrate that the rope would not induce torque on the lifted object.
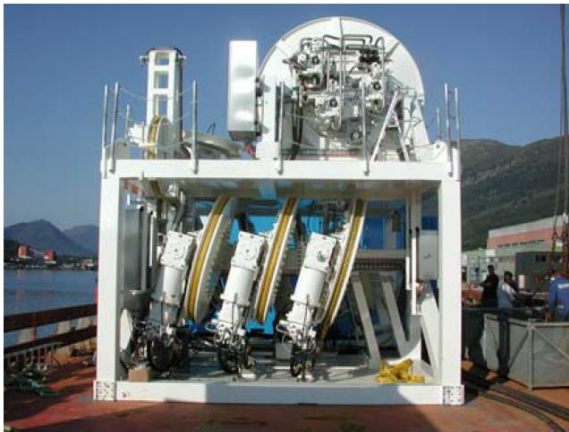
Figure 3.5: CTCU system on barge. (Ingberg & Torben, 2006)

Figure 3.6:Inshore testing from barge. (Ingberg & Torben, 2006)

3.4.2. Field pilot 46Te

To prove that the systems works in deep water and in an offshore environment a field pilot was conducted. Hydro and the Ormen Lange project provided the JIP with the opportunity of installing three gravity anchors at 855m water depth at the Ormen Lange field off the west coast of Norway. The pilot was conducted in April 2005. (Bull, et al., 2007)

Table 3.4 show the data of the anchors:

Table 3.4: Data of gravity anchors. (Bull, et al., 2007)

Weight in air [Te]	**35.4**
Weight in water [Te]	30.8
Footprint [m]	7 x 7
Skirt length [m]	3
Trapped water [m³]	150

Due to the large amount of trapped water, there will be a significant added mass. This will cause resonant conditions during the deployment of landing of the anchors. This provides the opportunity to test the active heave compensated fibre rope handling system in resonant conditions.

The installation was performed by Geoconsult and the vessel used was the Geofjord. Geofjord I a high utility ROV/construction support vessel. The vessel has a flush deck and a 6 x 6 moonpool. The CTCU was installed though the moonpool. The anchors were launched over the side using a vessel crane and the load was then transferred to the CTCU at 100-200m water depth.

Figure 3.7: Gravity anchors. (Bull, et al., 2007)

Figure 3.8: Geofjord at ODIM site during mobilization. (Bull, et al., 2007)

A test was conducted during the installation of the anchors. Two of the anchors were instrumented with a Motion Reference Unit (MRU) and data logger. The purpose of the test was to compare the measure

motion of the anchor with the measure vessel motions at the boarding point for the rope. The data was used for analysis of the AHC and the amplification of the vessel motions to the anchors motion.

The main steps for the installation of the anchors

- Launching of anchors from deck to 100-200 meters using a vessel crane
- Load transfer from vessel crane to CTCU
- Lowering to 5 meters above seabed
- Positioning, landing and penetration of the anchors
- Recovery of equipment

Anchor 1 and 2 was lowered in steps, stopping at approximately every 100m for conduction of test. The tests were conducted with and without Active Heave Compensation. The landing and penetration of the anchors were done with AHC. The AHC proved to be more than sufficiently accurate for anchor installation, and effectively reduced oscillations in outboard tension that would normally have been caused by vessel motions. The landing and penetration was performed with great ease and high precision, without any form of disturbances due to residual motion on the anchors. Careful monitoring of the rope was done as the load was gradually reduced during penetration. The rope showed no sign of rotation at all.

The results of field test showed the effect of the AHC on rope tension. Without AHC, the tension varied from 24 to 40mT, and when the AHC was engaged the variations reduced to ± 1mT. The results clearly showed the importance of the AHC during deployment and installation of modules with potentially high hydrodynamic loads.

3.4.3. Installation in Gulf of Mexico

In 2006 the 46Te system was hired by Subsea 7 for doing installation work in the Gulf of Mexico at water depths down to 2750m.

A rope management procedure was developed before the installation work was launched. The management procedure involved three principle sub-tasks:

- Development of a conservative rope life retirement criterion.
- Development of winch software which would track the progress of the rope towards repair or retirement
- Development of operating procedures for rope inspection and repair.

Mobilization

The FRDS was mobilized on Toisa Perseus in September 2006. The system is installed to work over the side of the vessel. (Bunes, Ingeberg, Torben, & Teigen, 2008)

Figure 3.9: FRDS installed on Toisa Perseus. (Bunes, Ingeberg, Torben, & Teigen, 2008)

A clump weigh of 0.8Te was used to assure tension on the FRDS during recovery of the empty hook. To avoid damage on the rope during ROV handling of the hook, a 25 meters pennant with protective jacket on sub-ropes is used between the clump weight and the ROV hook.

Installation tasks

The installation in Gulf of Mexico started in September 2006 and lasted for 9 months. 190 deployments and recoveries were performed in water depths from 2000 to 2750m. The operations included in the project was installation of mudmats, manifolds, spool pieces, jumpers and X-mas tree, and lowering and stabbing of second end of umbilicals. (Bunes, Ingeberg, Torben, & Teigen, 2008)

Main steps for the installations tasks:

- Deploying units using a vessel crane to 1000m water depth
- Transfer the load to the CTCU
- Deployment of payload to a few meters above seabed
- Positioning and landing with active heave compensation

While deploying the payloads to the seabed, the vessel crane recovered to deck and deployed the next unit to 1000m. With this procedure, the ROV used for load transfer from the crane to the CTCU did not have to go all the way back to the surface.

In January 2008, 320 lifts had been completed with the fibre rope deployment system in the Gulf of Mexico. The general feedback from the operator received by ODIM was very positive. The high-speed capability of the system had provided considerable time saving for the ultra-deep water installations.

The rope had also performed well without any major issues. The first inspection of the fibre rope was carried out after 6 months and 140 installations. During a full internal and external inspection of the part of the rope that had experienced the highest amount of bend cycles, no broken or damaged fibres were detected, and the outer layer was also found to be in good condition.

After approximately 300 lifts by the end of 2007, the limit for taking out a sample was met. A segment of the rope was cut out and sent to a laboratory for a residual strength test. The data from this test was combined with the recorded bend history of the section from the RMS to adjust the retirement criteria and improve the wear calculations for the rope.

3.4.4. Field Pilot 250Te in two-fall configuration

 A new DEMO 2000 funded project with the main objective of scaling up the 46Te SWL unit to a 125Te SWL unit was launched in September 2006. The project included a field pilot at the end that demonstrated a two-fall operation in deep water using fibre rope. The system was designed with a capacity of 250Te in a water depth of 3000m in two-fall operation. (Bunes, Ingeberg, Torben, & Teigen, 2008)

The following table shows the technical specifications for the 125Te and 250Te CTCU fibre rope deployment systems.

Table 3.5: Technical specifications of the 125Teand 250Te SWL FRDS by ODIM. (Rolls-Royse Marine AS, 2010)

Safe working load (SWL)	125 Te	250 Te
Maximum dynamic load	162.5 Te (Dynamic amplification Factor of 1.3)	325 Te (Dynamic amplification Factor of 1.3)
Launch/Recovery speed at SWL	0.5/0.3 m/s	0.5/0.3 m/s
Launch/Recovery speed at 50% SWL	1.0/0.6 m/s	1.0/0.6 m/s
AHC speed	1.5 m/s	1.5 m/s
Constant tension range	15-110 Te	30-200 Te
Fibre rope diameter	88 mm	136mm
Storage winch capacity	7000 m +	4000 m +
Peak power consumption	1000 kW	2000 kW

According to Torben and Ingberg (2011) the 250Te FRDs JIP aimed to demonstrate that deepwater lifting operations can be performed safely and successfully by using fibre rope deployment system in two-fall configuration based on the CTCU technology in combination with a torque free fibre rope instead of steel wire as the lifting line. (Ingeberg & Torben, 2011)

The key product for this field test was the 125Te CTCU designed for two-fall operation with lifting capacity of 250Te. For the field pilot to be possible, the system had to be mobilized on a vessel with additional equipment for handling the test weight and the two-fall arrangement.

The 125Te CTCU system and a module handling system from ODIM-Rolls-Royce was purchased by Aker Oilfield Services. The system was to be played on the Skandi Santos newbuilding for operation I Brazil, on a five-year contact with Petrobras for installing X-mas trees. The vessel had to be provided with some additional equipment to be completely adequate platform for conducting the field pilot.

System description

The equipment needed for performing the two-fall lift was a torque free rope combined with a handling system to minimize the introduction to twist in the rope during operation. The system also needed a two-fall block suitable for deepwater operations and a hang-off point for the dead end of the rope.

The rope used was an 88mm braid optimized for bending (BOB) rope with the same properties as explained in section 3.1. The rope has a maximum bending load of 567Te, which represents a 4.5 safety factor compared with the working load of the 125Te FRDS in single fall configuration.

The fibre rope deployment system is shown in Figure 3.10.
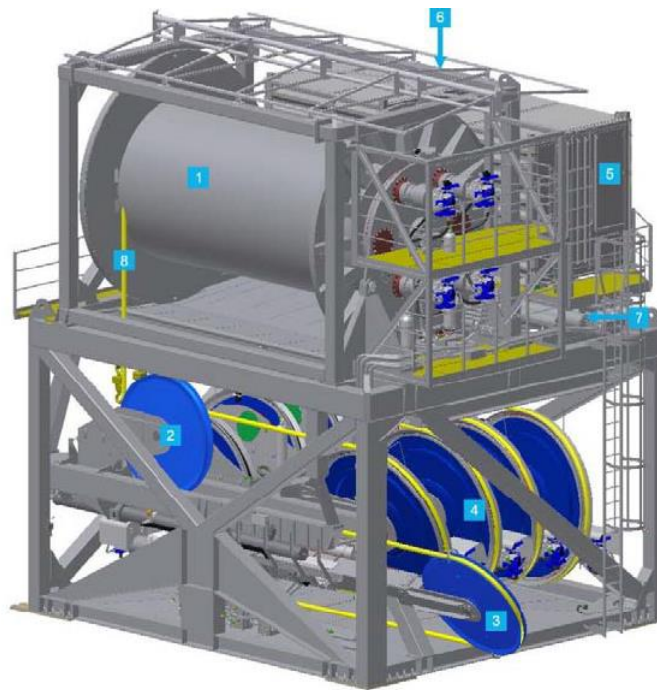
Figure 3.10: 125/250Te fibre rope deployment system. (Ingeberg & Torben, 2011)

The main components of the system are numbered in Figure 3.10 and are listed below:

1. Storage winch
2. Spooling winch
3. Inboard damping device
4. Cable traction control unit, CTCU
5. StW electrical container
6. CTCU electrical container
7. Accumulator units
8. Fibre rope
9. Cable counter (not visible in figure 3.10)

The two-fall system

According to Torben and Ingberg (2011) the two-fall block was designed and sized for the scope of the test and not for the full capacity of the system the working load was 110Te, and consisted of the following elements:

- Sheave with grooves suitable for 88mm fibre rope
- Frame with rope guides to prevent derailing
- Weight at bottom to secure stability/low centre of gravity
- Frame with bumper bars for instrument package
- Hinged arm to counteract twist with remotely operated vehicle (ROV) (contingency measure)
- Pad eye for 120Te shackle
- 300-bar pressure rating

The dead end of the rope was fixed in the two-fall configuration by using a hang-off beam installed on the top of the skidding rails on the main moonpool hatch of the vessel. The beam was secured using hatch clamps and turn buckles. Figure 3.11 and Figure 3.12 shows the two-fall block and the beam installed on the moonpool.
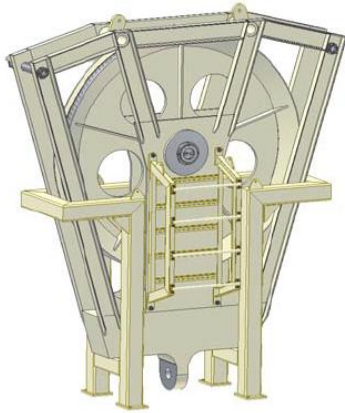
Figure 3.11: Two-fall block. (Ingeberg & Torben, 2011)
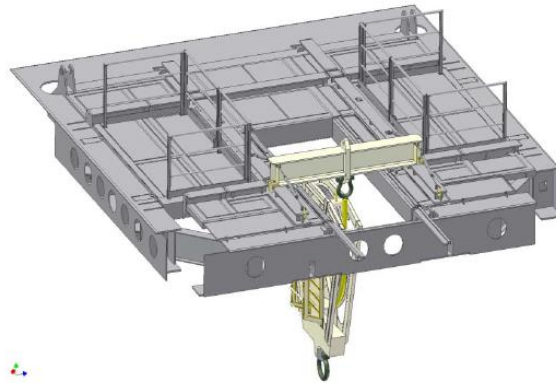
Figure 3.12: Beam installed on the moonpool. (Ingeberg & Torben, 2011)

Test instrumentation

There were two different methods used for monitoring twist during the two-fall test. The first test was real-time monitoring by comparing vessel and ROV headings. Every 100m the ROV was aligned with the two-fall block for performing readings, while the vessel handling remained fixed. The other method was twist logging based upon an instrumentation package installed on the two-fall block. (Ingeberg & Torben, 2011)

Vessel

Skandi Santos was outfitted with a complete module handling system from ODIM-Rolls-Royce, with the following subsystems according to Torben and Ingberg (2011):

- Main lift system: used for handling modules between the moonpool hatch and the seabed
- Test cursor systems: handle and stack modules brought by a skidding system on deck
- Skid system: securing and transporting modules on aft deck and in tower area
- Moonpool tower system: base for main and test cursor system
- Hydraulic system: provide and distributes hydraulic energy for all consumers
- Control system: implements system functionality and user interface

Figure 3.13: Skandi Santos with complete module handling system. (Ingeberg & Torben, 2011)

Field pilot execution

The scope of the two-fall field pilot test was 100Te to 1000m water depth. The test was scheduled for December 2009 when weather in Norway was generally harsh. The final test site location was chosen to be at the test site used by the Ormen Lange project for deepwater testing of pipeline repair system. At the location, the water depth was 940m. the area had been rock dumped and sea conditions were predictable. (Ingeberg & Torben, 2011)

Three test procedures for the sea trials were used. The first was an offshore tuning procedure used for tuning and verification of the active heave compensation system. The second was a sea acceptance test (SAT) used for functional verification of the complete module handling system. The last test was two-fall test procedure with installation and recovery operations with a 100Te payload.

The SAT test was performed to establish the system's ability to perform deepwater installation and recovery operations using fibre rope. The conclusion from the tests was that the system had the specified functionality, performance and accuracy, and that deepwater installation and recovery could be performed safely using the CTCU-based 125Te FRDS.

The two-fall test was done on December 14th in 2009. The test included the installation of an instrumentation package with local logging of heading and depth data.

Main steps of the two-fall test (Ingeberg & Torben, 2011):

- The two-fall block is launched though the moonpool with the 100Te clump weight overboarded using a vessel crane.
- At 150m depth the load is transferred from the vessel crane to the two-fall block

- Test 1:
  - deploy the 100Te clump weight in steps of 100m and verifying twist in real time using vessel and ROV heading information
  - At 900m water depth, the AHC mode was entered and auto landing function initiated.
  - Tension in the at the bottom of the two-fall block was reduced from 90Te to 64Te during landing operations
  - After landing: constant tension setpoint gradually reduced so the tension at the bottom of the two-fall block was reduced from 64Te to 11Te, and back to 64Te before initiation of auto lift-off.
  - Recovery from 900m to 200m done in steps of 100m for real-time twist monitoring
  - At 200m load of clump weight transferred to vessel crane

- Test 2:
  - deploy empty hook to 900m
  - Recovery of empty hook to 100m in 100m steps
- Two-fall block recovered to deck
- Data secured

The following conclusions were made after the field test according to Torben and Ingberg (2011)

- Load transfer from the crane can introduce an intermittent twist owing to the direction of pull. This should be handled by careful planning of the load transfer operation
- Deployment and recovery of a heavy load was demonstrated with a very low level of twist, showing that the restoring toque from the geometry of the two-fall system was dominant in relation to disturbances during the test
- Unloading landing and tension reduction from 90Te to 11Te gave only a small change in twist. As expected, twist was greater during this test than with the high-load test owing to a reduced restoring torque from the geometry of the two-fall arrangement at low loads
- It was observed that some twist had been introduced to the rope before the two-fall test. This is considered to be one of the torque-creating factors which must be counterbalanced by the restoring torque. But the fact that the test was successful even with this disturbance indicates that the system is quite robust with regard to such issues

- The current profile logged prior to the test indicated that the current was very small and probably not a significant source of disturbance. In real operations, this could be a significant factor which must be controlled.

3.5. Cranes

Several cranes have been developed for fibre rope deployment. A fibre rope crane is combined with proven fibre rope handling technology. This eliminates the need for a vessel crane and the transferring of load step during the deployment. Following is the description of three such cranes, two by Rolls-Royce and one by NOV.

3.5.1. NOV Trident crane

According to NOV, the crane has a sleek outward design that provides a glimpse into what lies beneath the surface. The lifting system is innovative and allows the unit to maintain its full lifting capacity at any operational depth. (National Oilwell Varco, Rig systems, 2017)

Figure 3.14: NOV Trident crane. (National Oilwell Varco, Rig systems, 2017)

The hoisting system includes a patent pending "Winch on king" concept and a spooling system designed specifically for the use of fibre rope. The system utilized a unique rope protection system that ensures that the rope temperature is conditioned, and protects the rope from environmental exposure. The design allows for the use of fibre rope, hybrid rope or steel wire.

Crane features:

- Lower weight
- Reduced installation and commissioning – compared to below deck winch systems
- Lower centre of gravity of crane system – compared with winch above deck

- Electrically and/or hydraulically operated

3.5.2. Rolls-Royce Fibre rope crane

Rolls-Royce have developed three different fibre rope cranes. The first two are FRC 150t and FRC 250t

The crane structure has an integrated operator cabin and the fibre rope runs over large diameter sheaves. Below the deck is a compact CTCU which forms the crane winch, provides active heave compensation and stores the rope on a reel. The system has a track record of over 10 years. Due to the naturally buoyant fibre rope, the crane can handle loads at its full capacity down to 4500mwater depth. (Rolls-Royce Marine AS, 2017)

General design features:

- Filed proven CTCU technology for fibre rope handling
- Smart integration in vessel – below deck
- Innovative crane structure – reduced weight
- High-end control system
- Active heave compensation
- Constant tension, with auto landing and auto lift-off mode
- Pull limit and controlled emergency pay-out function
- State-of-art operator cabin
- High quality – low maintenance, robust and field proven technology
- Cost efficient logistics for rope replacement
- In-field splicing of rope
- Easy inspection of rope
- Rope management system – full wear traceability
- DNV GL certification

Table 3.6: Technical data of fibre rope cranes. (Rolls-Royce Marine AS, 2017)

SWL	150t	250t
Operation depth	4500 m	4500m
Min outreach	7m	11m
Max outreach	31m	40m
Winch speed	0-1.5 m/s (all layers)	0-1.5 m/s (all layers)
AHC capacity (Peak to peak)	4.8m at 10s period (150t, all layers)	3.2m at 10s period (250t, all layers)
Heavy lift capacity (double fall)	300Te at 2250m	500Te at 2250m
Aux winch capacity	10/20Te	10/20Te
Tugger winch capacity	5Te	5Te
Slewing	+/- 200 degrees rotation	+/- 200 degrees rotation
Peak power consumption	1300kW	2300kW

Figure 3.15: Rolls-Royce Fibre rope crane. (Rolls-Royce Marine AS, 2017)

3.5.3. Rolls-Royce dual draglink crane

The last fibre rope crane from Rolls-Royce is the dual draglink crane, DDC50FR. The crane has the same design features as the two other cranes, but has a smaller specific weight limit. (Rolls-Royce Marine AS, 2017)

Table 3.7: Technical data of fibre rope cranes (Rolls-Royce Marine AS, 2017)

SWL	50t
Operation depth	3000 m
Min outreach	3m
Max outreach	20m
AHC capacity (Peak to peak)	6m at 8s period (50t, all layers)
Heavy lift capacity (double fall)	100Te at 1500m
Tugger winch capacity	3Te
Slewing	+/- 360 degrees rotation
Peak power consumption	850kW

4. Equipment

To cover the effectiveness of the fibre rope deployment method, I will look at the installation of several types of subsea equipment. This is to establish the effect of the size and geometry of the equipment when it comes to installing at ultra-deep water. Due to the light weight of the fibre rope, it is important to look at the effect of the displacement of the installed object. Therefore, it is of interest to investigate the effect of the weight of the installed objects. The weights of the installed objects range from 5 tonnes to 190 tonnes.

The dimensions and weight of the following equipment is given by Øystein Aa Myklebust.

4.1. Tubing head spool

A tubing head spool is a wellhead component that supports the tubing hanger and provides a means of attaching the Christmas tree to the wellhead. The tubing head is attached to the casing spool used to hang the tubing and is used to seal the annulus between the tubing and the casing. (Schlumberger, 2018)

The top spool on a wellhead assembly contains the highest pressure in the wellhead, and contains a load shoulder to hang the tubing hanger and tubing string. The tubing head is a necessary component when drilling and completing a well as is provides a mean to support and test the BOP while completing a well. When the well is completed, the tree is installed on top of the head with a tubing head adapter. (FMC Technologies, 2018)

Figure 4.1: tubing head spool

Figure 4.2: Tubing Head spool

Table 4.1: Dimensions of Tubing head spool

	Typical Dimensions
Length [m]	4
Width [m]	5
Height [m]	3
Weight [tonnes]	25

4.2. Suction anchor

A suction anchor (also called suction caissons or suction piles) is a long steel cylinder topped with a pile top or cap. The cap comprises valves to assist with embedment as well as connections that differ depending on the use of the anchor. Suction anchors have been used effectively as mooring anchors since the 1990s. (InterMoor, 2018)

When installing the suction pile, it is lowered to the seabed. Loads are resisted though the structure with mooring padeyes or pile top footings to the soil via direct bearing and skin friction. The suction anchor is then self-penetrating the soil, usually up to 60% of its own length under its own weight. How much it self penetrates depends on the soil conditions and the pile properties. The remainder of the embedment is achieved through suction: a remote-operated vehicle (ROV) pumps water out of the top suction port after sealing pile top valves. Pile top and ROV instrumentation contribute to precise installation. (InterMoor, 2018)

Figure 4.3: Suction anchors. (EPG, 2018)

Figure 4.4: Suction anchor. (EPG, 2018)

Table 4.2: Dimensions of Suction Anchor

	Typical Dimensions
Height [m]	10
Diameter [m]	5
Weight [tonnes]	70

4.3. Valve tree

Subsea trees are complex configurations of valves and other component. They are installed at the wellhead to monitor and control production flow, and manage gas or fluid injection. Valve orientation can either be vertical with production tubing suspended in the wellhead, or horizontal with production tubing suspended in the tree. When it comes to design and materials, water depth has the most significant design implications because it determines operating pressure, structural integrity requirements and type of topside vessel involved. Today, the capabilities are at water depths from 0-3000m. (Company, 2011)

Figure 4.5: DHXT^{TM} horizontal tree. (GE Oil&Gas, 2018)

Table 4.3: Dimensions of Valve tree

	Typical Dimensions
Length [m]	4
Width [m]	5
Height [m]	3
Weight [tonnes]	50

4.4. Well jumper

A subsea jumper is a short pipe connector that is used to transport production fluid between two subsea components, for example, a tree and manifold, a manifold and another manifold, or a manifold and an export sled. It may also connect other subsea structures such as PLEM/PLETs and riser bases. In addition to being used to transport production fluid, it can also be used to inject water into a well. A well jumper is a jumper connected between a well add a manifold. (Cheveron, Statoil, 2018)

Figure 4.6: Well jumper with spreader beam. Picture provided by Equinor.
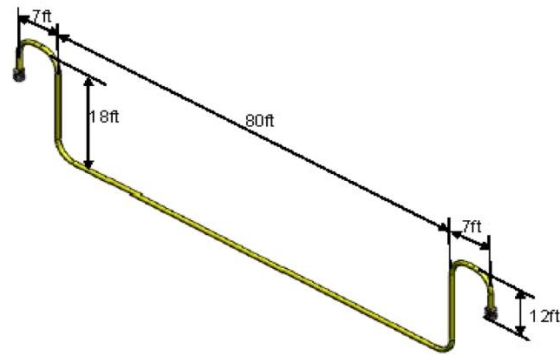
Figure 4.7: Well jumper with dimension. (Lu, Chun, Manzano-Ruiz, Janardhanan, & Perng)

Table 4.4: Dimensions of well jumper

	Typical Dimensions
Diameter [m]	6-7"
Length [m]	30
Weight [tonnes]	5*

*calculated by using slender elements

The weight when installing the well jumper will be slightly higher due to the extra weight of the spreader beam used during installation.

4.5. Drill Centre Template

A subsea template is a large steel structure which is used as a base for various subsea structures such as wells, subsea trees and manifold. The size of the template is dependent on the number of structures

attached to it. (FishSAFE, u.d.) A drill centre template (DCT) is a subsea template with well slots, complete with a protective structure. Typically the DCT would have 4well slots with 30" casing, but many variations can be designed. (Aquaterra Energy)

Figure 4.8: Drill Centre Template. (Aquaterra Energy, u.d.)
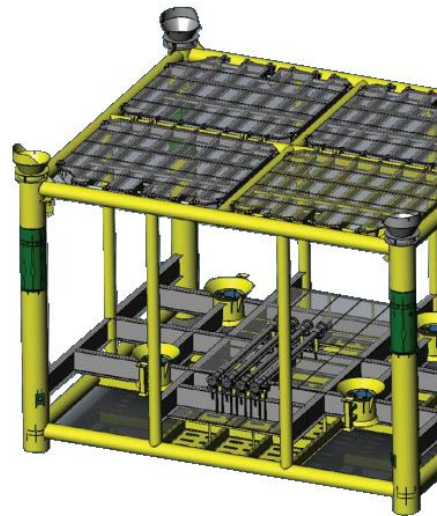
Figure 4.9: Drill Centre template.

Table 4.5: Dimensions of Drill Centre Template

	Dimensions
Length [m]	11.4
Width [m]	13m
Height [m]	9.6m
Weight [tonnes]	190*

*calculated by using slender elements

5. Theory

This chapter look into the theory for vessel motions, linear waves and subsea lifting.

5.1. Vessel motions
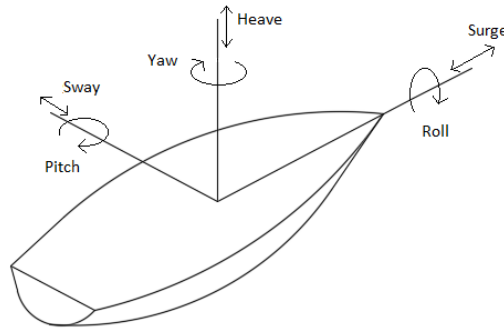
Figure 5.1: The six DOF of vessel

The vessels motions experienced by the vessel can be described by six degrees of freedom (DOF). The six DOF consist of three translational motions and three rotational motions. The translational motions are Heave, Surge and Sway, and the rotational motions are Roll, Pitch and Yaw. The rotational motions are the same for all points of the vessel, while the translational motions are coupled and depends on the motion of the other DOF. (Gudmestad, 2015)

The importance of the six DOF varies depending on the operation. For example, heave motion is the most important for vertical operations (deployment) and roll is most important for crane operations over the side (Lift-off and overboarding). Heave and roll will be the main focus for this chapter, as they are the most important vessel motions during ultradeep sea offshore lifting and installation. This section is written with accordance to Gudmestad (2015).

5.1.1. Heave motion

Heave motion is the vertical up and down motion of the vessel along the vertical axis.

Table 5.1: symbol and unit for heave and roll motions

	Position	Velocity	Acceleration
Translational motion (heave)	$z(t)$	$\dot{z}(t)$	$\ddot{z}(t)$
Rotational motion (roll)	Angle $\theta(t)$	Angular velocity $\dot{\theta}(t)$	Angular acceleration $\ddot{\theta}(t)$

Equation of motion:

$$m\ddot{z}(t) + c\dot{z}(t) + kz(t) = F(t)$$

$m = mass$

$c = damping$

$k = stiffness$

The solution to the equation of motion is: $z(t) = z_h(t) + z_p(t)$

$z_h(t) = $ the solution of the homogenous equation, $m\ddot{z}(t) + c\dot{z}(t) + kz(t) = 0$

$z_p(t) = $ a particular solution of the full equation.

The homogenous solution $z_h(t)$

For a case with no damping *(z=0)* and with initial conditions *z(t=0)* and $\dot{z}(t=0) = (H/2)(1/\omega)$ the solution is:

$$z_h(t) = \frac{H}{2}sin\omega_0 t$$

Where

$$\omega_0 = \sqrt{\frac{k}{m}}, \quad T_0 = \frac{2\pi}{\omega_0} = 2\pi\sqrt{\frac{m}{k}}$$

$\omega_0 = eigen\ frequency$

$T_0 = eigen\ period$

It is always important to avoid resonances. We therefore need to find ω_{heave} to determine when there is resonance between the heave motion and the waves, and ω_{roll} to determine when there is resonance between the roll motion and the waves.

Table 5.2: homogenous solution and amplitude

	Homogenous solution	Amplitude
A. Displacement	$z_h(t) = \frac{H}{2}sin\omega_0 t$	$z_{h\ maz}(t) = \frac{H}{2}$
B. Velocity	$\dot{z}_h(t) = \frac{H}{2}\omega_0 cos\omega_0 t$	$\dot{z}_{h\ max}(t) = \frac{H}{2}\omega_0$
C. Acceleration	$\ddot{z}_h(t) = -\frac{H}{2}\omega_0^2 sin\omega_0 t$	$\ddot{z}_h(t) = \frac{H}{2}\omega_0^2$

46

D. Mass, m

The mass includes the mass of the vessel m_v and the added mass m_a. The added mass is the water particles that is moved due to the movement of the vessel with amplitudes that decline away from the vessel.

E. Stiffness, k

The stiffness is the resistance against the vertical motion. For heave motion, the stiffness is the resistance against the vertical motion.

$$k = A_w \rho g \quad [N/m]$$

A_w = area in waterline [m²]
$m = m_a + \rho \nabla$ [kg]
$\nabla = A_w d$ = volume displacement of the vessel
d = vessel draft [m]

The eigen frequency and the eigen period then becomes:

$$\omega_0 = \sqrt{\frac{k}{m}} = \sqrt{\frac{A_w \rho g}{m_a + \rho \nabla}}, \quad T_0 = 2\pi \sqrt{\frac{m_a + \rho \nabla}{A_w \rho g}}$$

If we have a case where $m_a \ll \rho \nabla$ and a barge where $\nabla = A_w \cdot d$, we get the following heave period of the barge:

$$T_{heave\ barge} = 2\pi \sqrt{\frac{m_a + \rho \cdot A_w \cdot d}{A_w \cdot \rho \cdot g}}$$

If the added mass is small:

$$T_{heave\ barge} = 2\pi \sqrt{\frac{d}{g}}$$

T_h becomes large if there is a large added mass. The added mass can be increased by mounting spoiler on the barge, called bilge keels.

When determining the particular solution, a case of regular sinusoidal forcing is considered, such that:

$$F(t) = F_0 sin\omega t$$

The particular solution is given by:

$$z_p(t) = \frac{F_0}{k} \cdot DAF \cdot \sin(\omega t - \theta)$$

For a case with no damping, d = 0

$$z_p = \frac{F_0}{k}\left(\frac{1}{1 - \beta^2}\right)\sin(\omega t)$$

> $DAF =$ dynamic amplification factor

$$\beta = \frac{\omega}{\omega_0} = \frac{excitation\ frequency}{eigen\ frequency}$$

The system will behave qusistatically with $\beta \approx 0$ and $DAF \approx 1$, for a system where $\omega \ll \omega_0$ or $T \gg T_0$

$$z(t) = \frac{F_0}{k} sin\omega t$$

When $\omega \sim \omega_0$, the resonance in the system will be limited by the damping, c.

Table 5.3: the particular solution of heave

	Particular solution, $z_p(t)$
Vertical velocity	$\dot{z}_p(t) = \frac{F_0}{k} DAF\omega\cos(\omega t - \theta)$
Vertical acceleration	$\ddot{z}_p(t) = -\frac{F_0}{k} DAF\omega^2\sin(\omega t - \theta)$

5.1.2. Roll motion
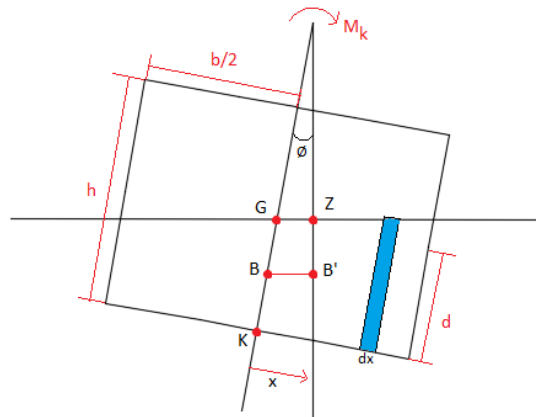
Figure 5.2: Roll motion of barge

Roll motion is the side-to-side rotational motions of the vessel.

Equation of motion for roll motion:

$$I_T\ddot{\theta}(t) + c_r\dot{\theta}(t) + k_r\theta(t) = M(t)$$

I_T = transverse mass moment of inertia [kgm²]

$k_r\theta(t)$ = uprighting moment = uprighting arm x buoyancy force

$$k_r\theta(t) = GZ \cdot \rho g \nabla = GZ \cdot \Delta = \text{GMsin}\theta \cdot \Delta$$

∇ = submerged volume

Δ = mass of displaced water = $\rho g \nabla$

For small angles, θ, $sin\theta \sim \theta$ and

$$k_r\theta(t) = GM \cdot \theta(t) \cdot \Delta$$

$$k_r = GM \cdot \Delta$$

The homogeneous solution, $\theta(t)$

For a case with no damping, $c_r = 0$ and with initial conditions $\theta(t = 0) = 0$ and $\dot{\theta}(t) = \theta_0\omega_r$, the homogenous solution is given by:

$$\theta_h(t) = \theta_0 sin\omega_r t$$

The eigen frequency of the roll is given by

$$\omega_r = \sqrt{\frac{\Delta \cdot GM}{I_T}} \quad \rightarrow \quad T_{roll} = 2\pi \sqrt{\frac{I_T}{\Delta \cdot GM}}$$

The transverse mass moment of inertia for a volume with respect to an axis through the centre of gravity is:

$$I_T = \int_v x^2 dm = \int_v x^2 \cdot \rho \cdot dV$$

$dV = submerged\ volume = (d + x\theta) \cdot l$

The mass moment of inertia is:

$$I_T = pd \frac{b^3}{12} l$$

$$\omega_{roll} = \sqrt{12} \sqrt{\frac{g \cdot GM}{b}}$$

Roll period for a ship:

$$T_{roll} = c_r \frac{b}{\sqrt{GM}}$$

Where

$$c_r = \frac{2\pi}{\sqrt{12g}}$$

- For a typical bare: $c_r = 0.6$
- For a ship gemometry: $c_r = 0.8$
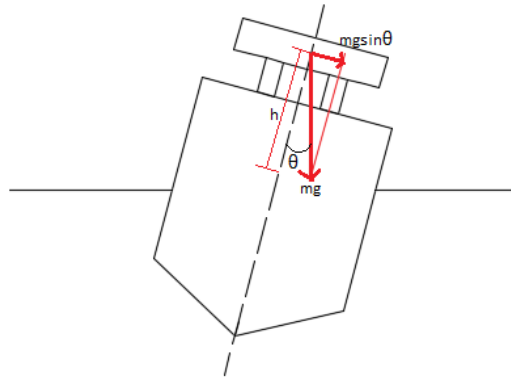
Figure 5.3: Roll motion of vessel

Angular roll:

$$\theta_h(t) = \theta_0 sin\theta\omega t$$

Maximum angular roll

$$\theta_{h\ max} = \theta_0$$

The angular roll is significant for the forces on cargo and for comfort.

Table 5.4: The homogenous solution and amplitude for roll

	Homogenous solution	Max
Angular roll	$\theta_h(t) = \theta_0 sin\theta\omega t$	$\theta_{h\ max} = \theta_0$
Angular velocity	$\dot{\theta}_h(t) = \theta_0\omega cos\theta\omega t$	$\dot{\theta}_{h\ max} = \theta_0\omega$
Angular acceleration	$\ddot{\theta}_h(t) = -\theta_0\omega^2 sin\theta\omega t$	$\ddot{\theta}_{h\ max} = \theta_0\omega^2$

The transverse velocity at distance r from the centre of the roll is given by:

$$V_\theta = \dot{\theta}_{h\ max} \cdot r = \theta_0\omega r$$

The transverse velocity is significant for handling of cargo, comfort and landing of helicopter.

The transverse force is given by:

$$K = m\ddot{\theta}r$$

$$K_{max} = m\theta_0\omega^2 r$$

The transverse force is significant for handling of cargo, sea fastening and comfort.

5.2. Linear wave theory

Due to the extreme water depth, the installation process is most affected by the waves during lift-off and though the splash zone. The linear wave theory puts the use to linearized boundary conditions, whereas higher-order wave theories do not. The linearity results in regular waves with sinusoidal shape, while higher-order waves will have higher crests than troughs. (Gudmestad, 2015)

5.2.1. Surface profile

A sinusoidal wave has the following surface profile:

$$\xi = \xi(x,t) = \xi_0 sin(\omega t - kx)$$

ξ_0: amplitude

ω: wave (angular) frequency

t: time

k: constant, often called the wave number

x: position

The surface profile equation is derived from the potential function by using the dynamic boundary conditions:

$$\varphi(x,z,t) = \frac{\xi_0 g}{\omega} \underbrace{\frac{coshk(z+d)}{\cosh(kd)}}_{depth\ dependent} \underbrace{\cos(\omega t - kx)}_{regular\ linear\ wave}$$

Where $\frac{coshk(z+d)}{\cosh(kd)}$ is the depth dependent part, and $\cos(\omega t - kx)$ is a regular linear wave.

The dynamic linear boundary condition:

$$\xi = -\frac{1}{g}\frac{\partial \varphi}{\partial t}_{|z=0}$$

The amplitude of a higher-order wave is approximately 10% higher than the amplitude of a linear wave. This is something that must be taken account for when simulating using linear waves.

The surface profile of a typical sinusoidal wave in two dimensional (2D) is shown in figure XX

52
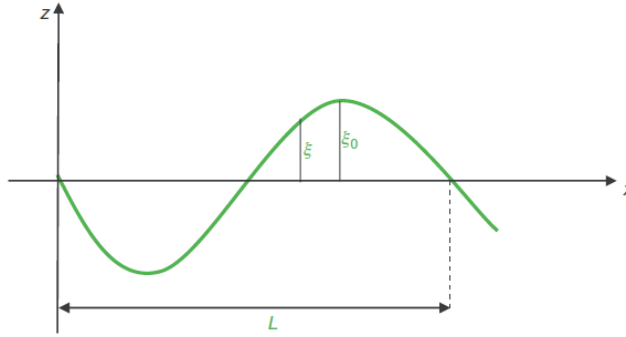
Figure 5.4: sinusoidal wave profile

The surface profile is independent on x and can be evaluated when t=0. In the figure L is the wavelength and is the distance between the two neighbouring wave crests, or the two wave troughs.

From the wave profile we have the following properties:

$$\xi\left(\frac{L}{2},0\right) = 0 \Rightarrow \xi_0 \sin\left(-k\frac{L}{2}\right) = 0$$

$$\xi(L,0) = 0 \Rightarrow \xi_0 \sin(-kL) = 0$$

From these properties, it follows that

$$k\frac{L}{2} = \pi \Rightarrow k = \frac{2\pi}{L}$$

From the previous equations we see that if we have a way to find k, we can calculate the wave length, L, and vice versa.

The surface profile is also dependent on time, t, and is found by evaluating the profile for x=0. The wave period, T, is the time between two neighbouring wave crests or wave troughs.

From the wave profile we have the following properties:

$$\xi\left(0,\frac{T}{2}\right) = 0 \Rightarrow \xi_0 \sin\left(\omega\frac{T}{2}\right) = 0$$

$$\xi(0,T) = 0 \Rightarrow \xi_0 \sin(\omega T) = 0$$

From these properties, it follows that:

$$\omega\frac{T}{2} = \pi \Rightarrow \omega = \frac{2\pi}{T}$$

53

The argument of the sine in the surface profile, $\omega t - kx$, is in general called the phase. We consider two points at different positions on the surface profile as shown in the figure below.

The two positions are:

- $t = t_0, x = x_0$
- $t = t_1 = t_0 + \Delta t, x = x_1 = x_0 + \Delta x$
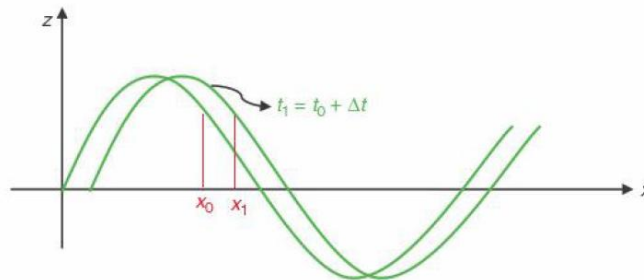
Figure 5.5:movement of a point

The wave profile at the two points will be equal if

$$\xi_0 \sin(\omega_0 - kx_0) = \xi_1 \sin(\omega_1 - kx_1)$$

$$\Rightarrow \omega t_0 - kx_0 = \omega t_1 - kx_1$$

$$\Rightarrow k(x_1 - x_0) = \omega(t_1 - t_0)$$

$$\Rightarrow \frac{\Delta x}{\Delta t} = \frac{x_1 - x_0}{t_1 - t_0} = \frac{\omega}{k}$$

Or

$$x_1 = x_0 + \frac{\omega}{k}(t_1 - t_0)$$

Further, we have

$$c = \lim_{\Delta t \to 0} \frac{\Delta x}{\Delta t} = \lim_{\Delta t \to 0} \frac{\omega}{k} = \frac{\omega}{k}$$

$$c = \frac{2\pi/T}{2\pi/L} = \frac{L}{T}$$

c: phase velocity associated with the wave

In the case of deep water, the following relation hold between k and ω.

$$\omega^2 = gk \tanh kd$$

In deep water $\tanh kd \approx 1$

$$\rightarrow k = \frac{\omega^2}{g}$$

For deep water waves, the phase velocity is given as:

$$c = \frac{\omega}{k} = \frac{\omega}{\omega^2/g} = \frac{g}{\omega} = \frac{g}{2\pi/T} = \frac{gT}{2\pi}$$

The phase velocity in deep water is proportional to the wave period, T. This means that long periodic waves have a wave form that moves faster than the short periodic waves. Swells may thus indicate that there is low pressure (a storm) approaching.

5.2.2. Deep water adjustments

In deep water, that is $d \gg 1$, we ca make some simplifications. In general, we can write:

$$\cosh d = \frac{e^d + e^{-d}}{2} \approx \frac{e^d}{2}$$

$$\sinh d = \frac{e^d - e^{-d}}{2} \approx \frac{e^d}{2}$$

$$\tanh d = \frac{\sinh d}{\cosh d} \approx \frac{e^d/2}{e^d/2} = 1$$

5.2.3. The JONSWAP spectrum

The JONSWAP spectrum was established during a joint research project, the "JOint North Se WAve Project", and was developed from wave measurements in the Southern North Sea. The JONSWAP spectrum is to be used in this thesis for the wave data. The spectrum is defined as:

$$S(\omega) = \frac{\alpha g^2}{\omega^5} \exp(-\beta \left(\frac{\omega}{\omega_p}\right)^{-4} \gamma \exp\left(-\frac{(\omega - \omega_p)^2}{2\sigma^2 \omega_p^2}\right)$$

α: spectral parameter

ω_p : peak frequency, $\omega_p = \frac{2\pi}{T_p}$

γ : peakedness parameter

β : form parameter, default value $\beta = 1.25$

σ : spectral parameter with default values

$$\sigma_a = 0.07 \quad for \quad \omega < \omega_p$$

$$\sigma_b = 0.09 \quad for \quad \omega > \omega_p$$

The spectrum describes the sea conditions under developing wave conditions as well as fully developed sea conditions. The parameters of the spectrum are normally determined by the parameters Hs and tp. The spectrum assumes the same direction of the swell and wind generated wave components.

Significant wave height, Hs, is often used instead of α to parametrize he spectrum. The program uses the following equations to specify α.

$$\alpha = \left(\frac{H_s \omega_p^2}{4g}\right)^2 \frac{1}{0.065\gamma^{0.803} + 0.135}$$

Or

$$\alpha = 5.061 \frac{H_s^2}{T_p^4} (1 - 0.287 \ln(\gamma))$$

In the program, γ may normally be taken as

$$\gamma = \exp\left[3.484\left(1 - 0.1975\delta \frac{T_p^4}{H_s^2}\right)\right]$$

$$\delta = 0.036 - 0.0056 \frac{T_p}{\sqrt{H_s}}$$

The alternative used for specifying the spectrum in this thesis is:

- H_s, T_p, assuming $\beta = 1.25$, $\sigma_a = 0.07$ and $\sigma_b = 0.09$, γ is calculated from the equation above, and α is calculated from either of the two equations mentioned above.
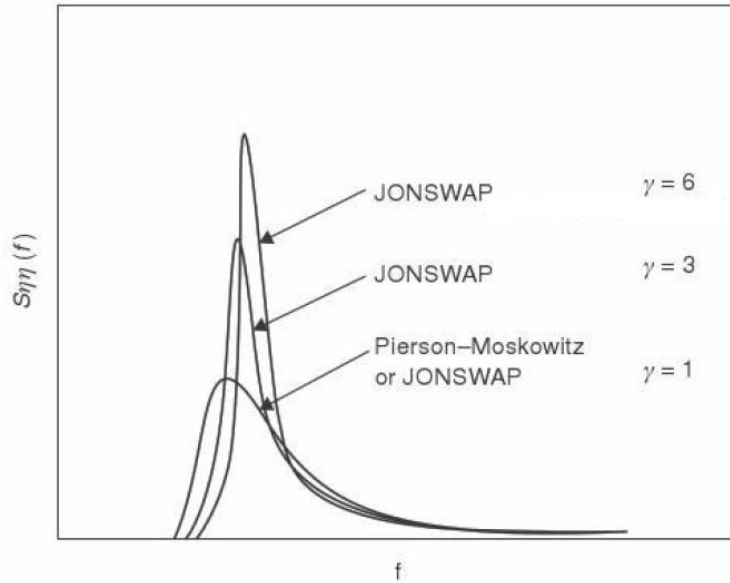
Figure 5.6: comparison of JONSWAP and Pierson-Moskowitz spectra having same Hs and same zero crossing period, Tz

5.3. Lifting through wave zone

The following forces should be considered when assessing the response of the object, when lifted though the splash zone according to DVN (2009):

- Force in hoisting line/cable
- Weight of object (in air)
- Buoyancy force
- Steady force due to current
- Inertia force
- Wave damping force
- Drag force
- Wave excitation force
- Slamming force

The force $F_{line}(t)$ in the hoisting line is the sum of a mean force F_0 and a dynamic force $F_{dyn}(t)$ due to motion of crane tip and wave excitation on object. The mean force is a slowly varying force, partly due to the lowering velocity and partly due to water ingress into the object after submergence. The following chapters are written with accordance to DNV-RP-H103 (2013). (DNV, 2009)

5.3.1. Weight on object

The Weight of the object is taken as;

$$W_0 = Mg \quad [N]$$

M = mass of object including pre-filled water within object [kg]

g = acceleration of gravity [m/s²]

5.3.2. Buoyancy force

The buoyancy force for a submerged object is equal to the weight of the displaced water

$$F_B(t) = \rho g V(t) \quad [N]$$

ρ = mass density of water [kg/m³]

$V(t)$ = displaced volume of water [m³]

During the water entry of an object lowered though the free surface, the buoyancy force is given by the weight of the instantaneous displaced water. For a totally submerged object the buoyancy force may vary with time in a case of continued water ingress into the object. The direction of the buoyancy force is opposite to gravity. If the centre of buoyancy is not vertically above the centre of gravity, the buoyancy force will exert a rotational moment on the lifted object.

Gor a submerged object, the submerged weight W of the object is defined as

$$W(t) = W_0 - F_B(t) = [M - \rho V(t)] \cdot g \quad [N]$$

Static weight of a submerged object:

$$F_{static} = Mg - \rho V g \quad [N]$$

5.3.3. Steady force due to current

The steady force due to ocean current can be taken as a quadratic drag force (DNV, 2009)

$$F_c = \frac{1}{2} \rho C_{DSi} A_{pi} U_c(z_0)^2 \quad [N]$$

C_{DSi} = the steady state drag coefficient in the current direction i

A_{pi} = projected area in direction i [m²]

$U_c(z_0)$ = current velocity at depth z_0 of object [m/s]

The steady current force is opposed by the horizontal component of the hoisting line force.

5.3.4. Inertia force due to moving object

The inertia force in direction $i (i = 1,2,3)$ on an object moving in pure translation can be calculated from (DNV, 2009)

$$F_{I,i} = -(M\delta_{ij} + A_{ij})\ddot{x}_j \quad [N]$$

Where summation over j is assumed.

M = structural mass [kg]

δ_{ij} = 1 if $i = j$ or 0 if $i \neq j$

A_{ij} = added mass in direction t due to acceleration j [kg]

$\ddot{x}_j$ = acceleration of object in direction j ($x_1 = x, x_2 = y$ and $x_3 = z$) [m/s²]

The added mass is usually expressed in terms of an added mass coefficient C_A^{ij} defined by:

$$A_{ij} = \rho C_A^{ij} V_R$$

V_R = reference volume of the object [m³]

C_A^{ij} = added mass coefficient

For rotational motion (typically yaw motion) of lifted object the inertia effects are given by the mass moments of inertia M_{ij} and the added moments of inertia A_{ij} where $ij = 4,5,6$ as well as coupling coefficients with dimension mass multiplied by length.

A general object in pure translational motion may be destabilized due to the Munk moment which can e expressed in terms of the translational added mass coefficients.

5.3.5. Wave damping force

In general, when an object moves in vicinity of a free surface, outgoing surface waves will be created. The energy of these waves comes from the work done to dampen the motion of the object. The resulting force on the object is the wave damping force. (DNV, 2009)

The wave damping force F_{wd} is proportional to the velocity of the object

$$F_{wd} = B_{ij}\dot{x}_j \quad [N]$$

B_{ij} = wave generation damping coefficient [kg/s]

$\dot{x}_j$ = velocity of lifted object [m/s]

For oscillatory motion of the object, the wave damping force vanishes for high frequencies and for low frequencies. Wave damping can be neglected if;

$$T \gg \sqrt{\frac{2\pi D}{g}} \quad [s]$$

Where T is the period of the oscillatory motion, D is a characteristic dimension of the object normal to the direction of motion and g is the acceleration of gravity. For transparent structures composed of several slender elements, the characteristic dimension is the cross-sectional dimension of the slender elements.

5.3.6. Wave excitation force

The wave excitation forces and moments are the loads on the structure when it is restrained from any motion response and here are incident waves. (DNV, 2009)

When the characteristic dimensions of the object is considerably smaller than the wave length, the wave excitation force in direction i of a fully submerged object is found from:

$$F_{Wi} = \rho V \left(\delta_{ij} + C_A^{ij} \right) \dot{v}_j + F_{Di} \quad [N]$$

V = submerged volume of object (taken to still water level z=0) [m³]

F_{Di} = viscous drag excitation force [N]

For a partly submerged object the excitation force un direction i is found from

$$F_{Wi} = \rho g A_w \varsigma(t) \delta_{i3} + \rho V \left(\delta_{ij} + C_A^{ij} \right) \dot{v}_j \quad [N]$$

Where the first terms is the hydrostatic force associated with the elevation of the incident wave at the location of the object.

A_w = water plane area [m²]

$\varsigma(t)$ = wave surface elevation [m]

δ_{i3} = 1 if i=3 (vertically), and 0 if i = 1 or i =2 (horizontally)

5.3.7. Viscous drag force

The viscous drag force in direction i can be expressed by the equation (DNV, 2009)

$$F_{di} = \frac{1}{2}\rho C_D A_p |v_r| v_{ri} \quad [N]$$

C_D = drag coefficient in oscillatory fluid

A_p = projected area normal to motion/flow direction [m²]

v_r = total relative velocity [m/s]

$v_{ri} = v_i - \dot{x}_i$ = relative velocity component in dir. i [m/s]

If the damping of an oscillating object is calculated by a quadratic drag formulation, the drag coefficient C_D depends on the oscillation amplitude. The oscillation amplitude is usually expressed in terms of the non-dimensional Keulegan-Carpenter (KC) number as defined as

$$KC = 2\pi \frac{z_m}{D} \quad [-]$$

z_m = oscillation amplitude [m]

D = characteristic length of object, normally the smallest dimension transverse to the direction of oscillation [m]

The dependence of KC-number for force coefficients (inertia and damping) also applies to objects exposed to oscillatory water particle motion in the wave zone. For regular waves, the KC-number can be taken as

$$KC = \frac{\pi H}{D} \quad [-]$$

Where H is the regular wave height. For irregular wave conditions, the KC-number can be taken as

$$KC = \frac{(\sqrt{2}\sigma_v)T_z}{D} \quad [-]$$

σ_v = standard deviation of water particle velocity [m/s]

T_z = zero up-crossing periods [s]

5.3.8. Slamming force

The slamming force on an object lowered though the free surface with constant slamming velocity, v_s (assumed positive) in still water can be written in terms of a slamming coefficient C_s as (DNV, 2009)

$$F_s(t) = \frac{1}{2}\rho C_s A_p v_s^2 \quad [N]$$

Where C_s is defined by

$$C_s = \frac{2}{\rho A_p V_s} \frac{dA_{33}^\infty}{dt} = \frac{2}{\rho A_p} \frac{dA_{33}^\infty}{dh} \quad [-]$$

Where A_{33}^∞ is the instantaneous high-frequency limit heave added mass and dA_{33}^∞/dh is the rate of change of added mass with submergence.

$h = submergence\ relative\ to\ surface\ elevation\ [m]$

The slamming impact velocity may be calculated by:

$$v_s = v_c + \sqrt{c_{ct}^2 + v_w^2} \quad [m/s]$$

$v_c = hook\ lowering\ velocity,\ typically\ 0.5\ [m/s]$
$v_{ct} = characteristic\ single\ amplitude\ vertical\ velocity\ of\ the\ crane\ tip\ [m/s]$
$v_w = characteristic\ vertical\ water\ particle\ velocity$

For water entry in waves the relative velocity between lowered object and sea surface must be applied, so that the slamming force can be taken as

$$F_s(t) = \frac{1}{2}\rho C_s A_p (\dot{\varsigma} - \dot{\eta})^2 \quad [N]$$

$\dot{\varsigma} = vertical\ velocity\ of\ sea\ surface\ [m/s]$
$\dot{\eta} = the\ vertical\ motion\ of\ the\ object\ [m/s]$

The sectional slamming force on a horizontal cylinder can be written in terms of a slamming coefficient, C_s;

$$F_s(t) = \frac{1}{2}\rho C_s D v_s^2 \quad [N/m]$$

$$C_s = \frac{2}{\rho D} \frac{dA_{33}^\infty}{dh} \quad [-]$$

Where D is the diameter of the cylinder [m].

5.3.9. Equation of vertical motion of lifted object when lowered into wave zone

Combining the expression for buoyancy, inertia, wave excitation, slamming and drag damping forces valid for wave lengths much longer than the dimensions of the object, the equation of vertical motion $\eta(t)$ for the lowered object can be taken as (DNV, 2009)

$$(M + A_{33})\ddot{\eta} = B_{33}^{(1)}(v_3 - \dot{\eta}) + B_{33}^{(2)}(v_3 - \dot{\eta})|(v_3 - \dot{\eta})| + (\rho V + A_{33})\dot{v}_3 + \frac{dA_{33}^\infty}{dh}(\dot{\varsigma} - \dot{\eta})^2 + \rho g V(t)$$
$$- Mg + F_{line}(t)$$

$B_{33}^{(1)}$ = the linear damping coefficient [kg/s]

$B_{33}^{(2)}$ = the quadratic damping coefficient [kg/m]

v_3 = water particle velocity [m/s]

$\dot{v}_3$ = water particle acceleration [m/s2]

$F_{line}(t)$ = force in hoisting line [N]

The force in the hoisting line is given by

$$F_{line}(t) = Mg - \rho g V(t) + K(z_{ct} - \eta) \quad [N]$$

K = hoisting line stiffness [N/m]

z_{ct} = motion of crane tip [m]

η = motion of object [m]

The velocity and acceleration of the lowered object are

$$\dot{\eta} = \dot{\tilde{\eta}} + v_c \quad [m/s]$$

$$\ddot{\eta} = \ddot{\tilde{\eta}} \quad [m/s^2]$$

$\tilde{\eta}$ = the wave induced motion of the object [m/s]

v_c = a constant lowering velocity (negative during lowering and vice versa) [m/s]

5.3.10. Hydrodynamic loads on slender elements

The hydrodynamic force exerted on a slender object can be estimated by summing up sectional forces acting on each strip of the structure. For slender structural members having cross-sectional dimensions considerably smaller than the wave length, wave loads may be calculated using Morisons's load formula being a sum of an inertia force proportional to acceleration and drag force proportional to the square of

the velocity. Morison's load formula is normally applicable when the wave length is more than 5 times the characteristic cross-sectional dimension. (DNV, 2009)
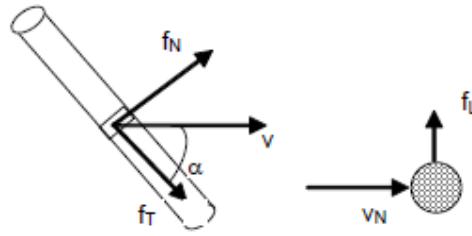
Figure 5.7: Normal force f_N, tangential force f_T and lift force f_L on a slender structure

The sectional normal force on a slender structure is given by

$$f_N = -\rho C_A A \ddot{x}_N + \rho(1 + C_A)A\dot{v}_N + \frac{1}{2}\rho C_D D v_{rN}|v_{rN}| \quad [N/m]$$

A = cross-sectional area [m²]
D = diameter or characteristic cross-sectional dimensions [m]
$\ddot{x}_N$ = acceleration of element normal to element [m/s²]
v_{rN} = relative velocity normal to element [m/s]
$\dot{v}_N$ = water particle acceleration in normal dir. [m/s²]

5.3.11. Hydrodynamic coefficients

In general, the hydrodynamic force coefficients depend on the following (DNV, 2009)

- Geometry

- Reynolds number: $Re = \frac{v_m D}{v}$ based on the maximum velocity v_m

- Keulegan-Carpenter number: $KC = \frac{v_m T}{D}$

    v = fluid kinematic viscosity [m/s²]
    Y = wave period of period of oscillation
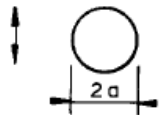
In addition, the following may have influence on the force coefficients; aspect ratio, angle of inclination to the flow, surface roughness, perforation ratio, frequency of oscillation, proximity to free surface and proximity to solid boundary.

5.3.12. Added mass coefficients for simple bodies

The sectional (2D) added mass of for a slender element is $a_{ij} = \rho C_A A_R, i,j = 1,2 \, [kg/m]$ where A_R is the reference area, usually taken as the cross-sectional area.

Added mass for a simple circular structure is given by Appendix A in DNV-RP-H103 as

Table 5.5: Added mass coefficient

Section through body	C_A	$A_R \, [m^2]$
	1.0	πa^2

5.3.13. Drag coefficients for simple bodies
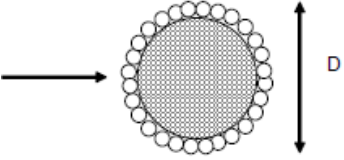
The drag coefficient for circular cylinders depends strongly on the roughness k of the cylinder. For high Reynolds numbers ($Re > 10^6$) and large KC number, the steady drag-coefficient C_{DS} may be taken as

$$C_{DS}(\Delta) = \begin{cases} 0.65 & ; \Delta < 10^{-4} \\ (29 + 4 \cdot log_{10}(\Delta))/20 & ; 10^{-4} < \Delta < 10^{-2} \\ 1.05 & ; \Delta > 10^{-2} \end{cases}$$

where $\Delta = k/D$ is the non-dimensional roughness.

For non-circular cross-sectional steady flow C_{DS} is given in Appendix B in DNC-RP-H103;

Table 5.6: Drag coefficient

Geometry	Drag coefficient, C_{DS}	
Wire and chains	Type ($Re = 10^4 - 10^7$)	C_{DS}
	Wire, six strands	1.5-1.8
	Wire, spiral no sheathing	1.4-1.6
	Wire, spiral with sheathing	1.0-1.2
	Chain, stud (relative chain diameter	2.2-2.6
	Chain, stud less (relative chain diameter)	2.0-2.4

5.4. Lifting though wave zone – simplified method

5.4.1. Hydrodynamic forces

The following chapter is written with accordance to DNV-RP-H103 (2009).

Crane tip motions

Using the simplified motion, it is assumed that the vertical motion of the structure is equal to the vertical motion of the crane tip. More accurate calculations should be made if amplification due to vertical resonance is present. Resonance amplification may be present if the crane tip oscillation period or the wave period is close to the resonance period, T_0. Of the hoisting system (DNV, 2009):

$$T_0 = 2\pi \sqrt{\frac{M + A_{33} + \theta \cdot mL}{K}} \quad [s]$$

m = mass of hoisting line per unit length [kg/m]

L = length of hoisting line [m]

M = mass of object in air [kg]

A_{33} = heave mass off object [kg]

θ = adjustment factor taking into account the effect of mass of hoisting line and possible soft springs

Mass force

The characteristic mass force on an object item due to combined acceleration of object and water particles may be taken as (DNV, 2009):

$$F_{Mi} = \sqrt{[(M_i + A_{33i}) \cdot a_{ct}]^2 + [(\rho V_i + A_{33i}) \cdot a_w]^2} \quad [N]$$

a_{ct} = characteristic simple amplitude vertical acceleration of crane tip [m/s²]

V_i = volume of displaced water of object item relative to the still water level [m³]

a_w = characteristic vertical water particle acceleration [m/s²]

Hydrodynamic force

The characteristic hydrodynamic force on an object when lowered though water surface is a time dependent function of slamming impact force, varying buoyancy, hydrodynamic mass forces and drag forces. (DNV, 2009)

The following combination of the various load components is acceptable in the simplified method:

$$F_{hyd} = \sqrt{(F_D + F_{slam})^2 + (F_M + F_\rho)^2} \quad [N]$$

F_D = characteristic hydrodynamic drag force [N]

F_{slam} = characteristic slamming impact force [N]

F_M = characteristic hydrodynamic mass force [N]

F_ρ = characteristic varying buoyancy force [N]

The structure may be divided into main items and surfaces contributing to the hydrodynamic force. The water particle velocity and acceleration should be related to the vertical centre of gravity for each main item when calculating mass and drag forces. These force contributions should then be found by:

$$F_M = \sum_i F_{Mi} \quad and \quad F_D = \sum_i F_{Di} \quad [N]$$

Where F_{Mi} and F_{Di} are the individual force contributions from each main item.

5.4.2. Accept criteria

Accept criteria for the calculated hydrodynamic forces. (DNV, 2009)

Characteristic total force

The characteristic total force on an object lowered though water surface should be taken as:

$$F_{total} = F_{static} + F_{hyd} \quad [N]$$

In cases where snap loads occur the characteristic total force on the object should be taken as:

$$F_{total} = F_{static} + F_{snap} \quad [N]$$

F_{static} = static weight of object [N]

F_{hyd} = characteristic hydrodynamic force [N]

F_{snap} = characteristic snap force [N]

The slack sling criterion

Snap forces shall as far as possible be avoided. Weather criteria should be adjusted to ensure this. Snap forces in the slings or hoist line may occur if the hydrodynamic force exceeds the static weight of the object.

The following criterion should be fulfilled in order to ensure that snap loads are avoided in the slings or hoist line:

$$F_{hyd} \leq 0.9 \cdot F_{static-min} \quad [N]$$

Where

$$F_{static-min} = M_{min}g - \rho V g \quad [N]$$

Capacity checks

In addition to the slack sling criterion, the capacity of lifted structure and lifting equipment should be checked. The characteristic total force on the object should be calculated applying the maximum static weight.

$$F_{static-max} = M_{max}g - \rho V g \quad [N]$$

The capacity checks related to the weight of the object in air. Hence, converted dynamic amplification factor (DAF) should be equivalent to a factor valid in air. The dollowing relation should be applied in he equations given in DNV-OS-H205:

$$DAF_{conv} = \frac{F_{total}}{Mg} \quad [-]$$

$DAF_{conv} = $ *is the converted dynamic simplification facor*
$F_{total} = $ *the largest of* $F_{total} = F_{static} + F_{hyd}$ *and* $F_{total} = F_{static} + F_{snap}$

5.4.3. Snap forces in slings or hoisting lines

Snap forces may occur of the slack sling criterion is not fulfilled. (DNV, 2009)

Snap force

Characteristic snap load may be taken as:

$$F_{snap} = v_{snap}\sqrt{K \cdot (M + A_{33})} \quad [N]$$

$v_{snap} = $ *characteristic snap velocity [m/s]*

Snap velocity

The snap velocity may be taken as:

$$v_{snap} = v_{ff} + C \cdot v_r \quad [m/s]$$

v_{ff} = free fall velocity [m/s]

v_r = characteristic vertical relative velocity between object and water particle [m/s]

C = correction factor

The vertical relative velocity between the object and water particles may be taken as:

$$v_r = v_c + \sqrt{c_{ct}^2 + v_w^2} \quad [m/s]$$

Two values for hook lowering velocity should be applied; $v_c = 0$ and v_c = typical lowering velocity. In addition, a retrieval case should be covered applying a v_c equal to a typical hoisting velocity. The highest snap velocity for the three options should be applied in the snap force calculation.

The correction factor should be taken as:

$$
\begin{array}{lll}
C = 1 & for & v_{ff} < 0.2v_r \\
C = \cos\left[\pi\left(\frac{v_{ff}}{v_r} - 0.2\right)\right] & for & 0.2v_r < v_{ff} < 0.7v_r \\
C = 0 & for & v_{ff} > 0.7v_r
\end{array}
$$

The free fall velocity of the object may be taken as:

$$v_{eff} = \sqrt{\frac{2F_{static}}{\rho A_p C_D}} \quad [m/s]$$

Snap force due to lift-off

Snap forced due to lift off from e.g. a barge should be taken into considerations.

Snap loads during lift off may be calculated according applying a characteristic snap velocity equal to:

$$v_{snap} = v_c + v_{rct} \quad [m/s]$$

v_{rct} = characteristic vertical relative velocity between object and crane tip [m/s]

Stiffness of hoisting system

The stiffness of the hoisting system may be calculated by:

$$\frac{1}{K} = \frac{1}{k_{rigging}} + \frac{1}{k_{line}} + \frac{1}{k_{soft}} + \frac{1}{k_{block}} + \frac{1}{k_{boom}} + \frac{1}{k_{other}}$$

K = total stiffness of hoisting system [N/m]

$k_{rigging}$ = stiffness of rigging, spreader bar, etc

k_{line} = stiffness of hoist line(s)

k_{soft} = stiffness of soft strop or passive heave compensation system if used.

k_{block} = stiffness of multiple lines in a block if used

k_{boom} = stiffness of crane boom

k_{other} = other stiffness contributions, if any

The line stiffness may be calculated by:

$$k_{line} = \frac{EA}{L} \quad [N/m]$$

E = modulus of rope elasticity [N/m²]

A = effective cross section areas of line(s). The areas are summarized if there are multiple parallel lines [m²]

L = length of line(s). If multiple lines the distance from block to crane tip is normally applied [m]

The effective cross section area of one wire line is found by:

$$A_{wire} = \frac{\pi \cdot D^2}{4} \cdot c_F \quad [m^2]$$

c_F = fill-factor of wire rope

D = the rope diameter [m]

5.5. Deepwater lowering operations

This chapter is written with accordance to DNV-RP-H103 (2009). (DNV, 2009)

- Stretched length of cable due to cable own weight and weight of lifted object
- Horizontal offset due to current where he current velocity may be time-dependent and its magnitude and direction may vary with water depth
- Dynamics of lifted object due to wave induced motion of crane tip on vessel
- Methods for controlling vertical motion of lifted object

In this part, we will describe the forces action on the vertical lift wire and the lowered object beneath the wave zone and down to the seabed.

5.5.1. Static forces on cable length of a cable.

Stretched length of the cable, Ls

A vertical cable will stretch due to its own weight and the weight of the lifted object at the end of the cable (DNV, 2009)

$$L_s = L \left[1 + \frac{W + \frac{1}{2}wL}{EA} \right] \ [m]$$

$L_s = stretched\ length\ of\ cable\ [m]$
$W = Mg\text{-}\rho g V = fully\ submerged\ weight\ of\ lifted\ object\ [N]$
$w = mg\text{-}\rho g A = fully\ submerged\ weight\ per\ unit\ length\ of\ cable\ [M/m]$
$E = modulus\ of\ elasticity\ of\ cable\ [N/m2]$
$A = nominal\ cross\ sectional\ area\ of\ cable\ [m2]$

5.5.2. Horizontal offset due to current

For an axially stiff cable with negligible bending stiffness the offset of a vertical cable with a heavy weight W_0 at the end of the cable in an arbitrary current with unidirectional (in x-direction) velocity profile $U_c(z)$ is given by (DNV, 2009);

$$\xi(z) = \int_z^0 \left[\frac{F_{d0} + \left(\frac{1}{2}\right) \rho \int_{-L}^{z_1} C_{Dn}[U_c(z_2)]^2 dz_2}{W + w(z_1 + L)} \right] dz_1 \ \ [m]$$

Where

$$F_{D0} = \frac{1}{2} \rho C_{Dx} A_x [U_z(-L)]^2 \ \ [N]$$

is the hydrodynamic drag force on the lifted object.

$\xi(z) = horizontal\ offset\ at\ vertical\ position\ z\ [m]$
$\xi_L = horizontal\ offset\ at\ end\ of\ cable\ z = -L\ [m]$
$L = un\text{-}stretched\ length\ of\ cable\ [m]$
$C_{Dn} = drag\ coefficient\ for\ normal\ flow\ past\ cable$
$C_{Dx} = drag\ coefficient\ for\ horizontal\ flow\ past\ lifted\ object$

D_c = cable diameter [m]

A_x = x-projected area of lifted object [m²]

$U_c(z)$ = current velocity at depth z [m/s]

z_1, z_2 = integration variables [m]
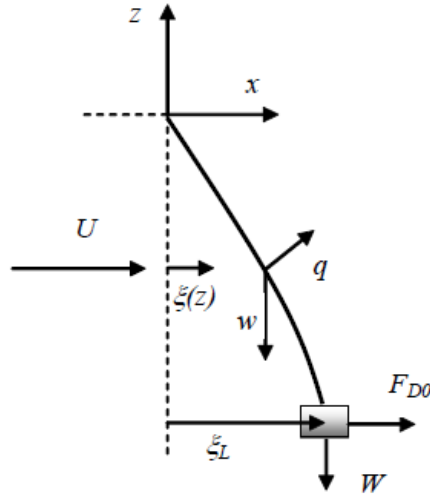
Figure 5.8: Horizontal offset due to uniform current. Curvature of cable determined by $F_{D0}/W < q/w$.

For a uniform current U_c and cable properties D_c, C_{Dn} the horizontal offset can be derived by;

$$\xi(z) = L\left(\frac{q}{w}\kappa - \lambda\right)\ln\left[\frac{\kappa + \frac{z}{L} + 1}{\kappa + 1}\right] - \frac{q}{w}z \quad [m]$$

Where the top of the cable is at z =0 and the lifted object is at the end of the cable at z = -L

Horizontal offset of the lifted object:

$$\xi(z) = L\left(\frac{q}{w}\kappa - \lambda\right)\ln\left[\frac{\kappa +}{\kappa + 1}\right] - \frac{qL}{w} \quad [m]$$

Where;

$$\kappa = \frac{W}{wL}$$

And

$$\lambda = \frac{F_{D0}}{wL}$$

The hydrodynamic drag force per unit length of cable, q, is given by;

$$q = \frac{1}{2}\rho C_{Dn} D_c U_c^2 \quad [N/m]$$

Vatical displacement

For installation of modules on seabed it is important to control the distance from the seabed to the lower part of the lifted object at the end of the cable. The difference Δz of vertical position of the lower end of the cable between the real vertical position of the lower end of the cable between the real condition and a vertical un-stretched condition has two contributions

$$\Delta z = \Delta z_G + \Delta z_E$$

Δz_G = vertical geometric displacement due to curvature of the cable
Δz_E = vertical elastic displacement due to stretching of cable

The vertical displacement due to curvature of the cable:

$$\frac{\Delta z_G}{L} \approx \frac{q}{w}\left(\frac{q}{w}\kappa - \lambda\right)\left\{\ln\left[\frac{\kappa + }{\kappa + 1}\right] + \frac{1}{2}\left[\frac{1 - \frac{\lambda w}{\kappa q}}{1 + \kappa}\right]\right\} + \frac{1}{2}\left(\frac{q}{w}\right)^2 \quad [-]$$

The vertical displacement due to stretching of the cable:

$$\frac{\Delta z_E}{L} \approx -\frac{1}{EA}\left[W + \frac{1}{2}(wL - q\xi_L)\right] \quad [-]$$

Vertical cable stiffness

The vertical cable stiffness is the force that has to be applied to the lifted object at the lower end of the cable per unit vertical displacement;

$$k_V = \frac{dF_V}{dz} \quad [m/N]$$

The vertical stiffness is the sum of the elastic stiffness k_E and the geometric stiffness k_g.

$$\frac{1}{k_V} = \frac{1}{k_E} + \frac{1}{k_G} \quad [N/m$$

The elastic stiffness is given by:

$$k_E = \frac{EA}{L} \quad [m]$$

The non-linear geometric stiffness k_G is given by:

$$\frac{1}{k_G} = -\frac{\partial (\Delta z_G)}{\partial W} = -\frac{q^2}{w^3}\left[\ln\left(\frac{\kappa}{\kappa+1}\right) + \frac{1}{2}\frac{\kappa+3}{(\kappa+1)^2}\right] + \frac{q}{w^2}\frac{\lambda}{\kappa}\frac{1}{(\kappa+1)^2} + \frac{1}{w}\left(\frac{\lambda}{\kappa}\right)^2\frac{2\kappa+1}{2(\kappa+1)^2} \quad [m/N]$$

Horizontal stiffness

The horizontal stiffness k_H of lifted object is the horizontal force that ha been applied to the lower end of the cable per unit horizontal displacement.

$$k_H = \frac{dF_H}{dx} \quad [N/m]$$

The horizontal stiffness is given by:

$$\frac{1}{k_H} = \frac{\partial \xi_L}{\partial F_{DO}} = \frac{1}{w}\ln\left[\frac{\kappa+1}{\kappa}\right] \quad [m/N]$$

The horizontal stiffness is not influenced by the current drag on the cable and the lifted object. This expression for horizontal stiffness is valid for static loads only.

When the lifted object is much heavier than the weight of the cable the horizontal cable stiffness reduces to the stiffness of the mathematical pendulum:

$$\kappa = \frac{W}{wL} \gg 1 \quad \rightarrow \quad k_H = w\kappa = \frac{W}{L} \quad [N/m]$$

Cable payout – quasi-static loads

The quasi-static tension T(s) at the top of the cable during payout for deep-water lowering operations is given by

$$T(s) = W + ws + \frac{1}{2}\rho C_{Df}\pi D_c s v_c |v_c| + \frac{1}{2}\rho C_{Dz}A_p v_c |v_c| \quad [N]$$

$s = length\ of\ cable\ payout\ [m]$

$C_{Df} = cable\ longitudinal\ friction\ coefficient$

$C_{Dz} = drag\ coefficient\ for\ vertical\ flow\ past\ lifted\ object$

For cable payout length s, the necessary payout velocity to produce a slack condition is found by setting T = 0 in the equation above. The formula above neglects the effect of current and water particle velocity due to waves and is therefore only valid for still water.

5.5.3. Dynamic forces on cable and lifted objects

for typical lifting operations from a floating vessel it is normally acceptable to assume the motions of the vessel is not affected by the motions of the lifted object. The following method is based on the following assumptions (DNV, 2009):

- Mass and assed mass of lifted object is much smaller than the displacement of the vessel
- The objects contribution to moment of inertia around CoG/ centre plane of vessel is much smaller than the vessel moment of inertia.
- The motion of the cranetip is vertical
- The effect of current can be neglected

Dynamic drag forces

Due to motion of the crane tip and lifted object, dynamic drag forces will act on the cable. The drag forces restrict the change of shape of the cable. As the velocity/accelerations of the crane tip increases, the elastic stiffness becomes increasingly important. (DNV, 2009)

Natural frequencies of a straight vertical cable

The natural frequency of a straight vertical cable is given by

$$= \omega_j v_j \sqrt{\frac{EA}{m}} \quad [rad/s] \ ; \ j = 0,1,2,..$$

The exact solution for the wave numbers v_j are given by the equation (assuming un-damped oscillations);

$$v_j L tan(v_j L) = \varepsilon = \frac{mL}{M + A_{33}} \quad [-]$$

$\omega_j = 2\pi/T_j = angular\ natural\ frequencies$

$T_j = eigen\ periods\ [s]$

$v_j = corresponding\ wave\ numbers\ [1/m]$

$\varepsilon = mass\ ratio$

The first eigen period for un-damped oscillations of the lifted object in the presence of crane master and/or soft slings may be taken as (DNV, 2009):

$$T_0 = \frac{2\pi}{\omega_0} = 2\pi\sqrt{\frac{M + A_{33} + \theta * mL}{K}}$$

Where

$$K = \left(\frac{1}{k_c} + \frac{1}{k_s} + \frac{L}{EA}\right)$$

k_c = stiffness of crane master at top of cable [kg/s²]

k_s = stiffness of soft sling or crane master at lifted object [kg/s²]

θ = adjustment factor to account for the cable mass

The adjustment factor to account for the cable mass is given by the general formula

$$\theta = \frac{1 + c + \frac{c^2}{3}}{(1 + c + \frac{c}{s})^2}$$

Where

$$c = \frac{k_c L}{EA} \ and \ s = \frac{k_s L}{EA}$$

The following limiting values for the adjustment factor may be applied:

- $\theta \sim 1/3$ if the stiffness EA/L is the dominant soft stiffness (c and s are both large numbers)
- $\theta \sim 0$ if the dominant soft spring is located just above the lifted object ($s \ll 1$ and $c > 1$)
- $\theta \sim 1$ if the dominant soft spring is located at the crane tip (($c \ll 1$ and $s > 1$)

In case of soft springs at both ends of the cable ($s \ll 1$ and $c \ll 1$), the adjustment factor can be approximated by

$$\theta = \left(\frac{s}{s + c}\right)^2$$

For straight vertical cables, the higher Eigenperiods are given by

$$T_j = \frac{2\pi}{\omega_j} \quad [s]; \quad j = 1,2,..$$
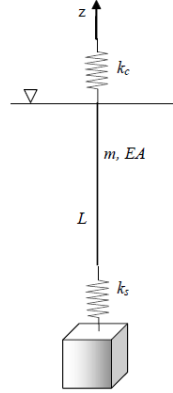
Figure 5.9: Forces oscillation of lifted object in cable with crane master at top of cable and soft sling at top of lifted object

Response of lifted object in a straight vertical cable exposed to forced vertical oscillation

When a deeply submerged object is lifted from a vessel in waves, the vertical motion of the object is governed by the motion of the top of the cable, fixed to the oscillating vessel. (DNV, 2009)

The vertical motion of a straight vertical cable with the lifted object at vertical position z = -L caused by forced oscillation of the top of the cable with frequency ω and amplitude η_a is given by;

$$\left|\frac{\eta(z)}{\eta_a}\right| = \left|\frac{kEA\cos[k(z+L)] + (-\omega^2 M' + i\omega\Sigma)\sin[k(z+L)]}{kEA\cos(kL) + (-\omega^2 M' + i\omega\Sigma)\sin(kL)}\right| \quad [m/m]$$

Where || means the absolute value of a complex number and mass M' = M+A_{33}

The complex wave number k is given by

$$k = k_r + ik_i = \sqrt{\frac{m}{EA}}\sqrt{\omega^2 - i\omega\left(\frac{\sigma}{m}\right)} \quad [m^{-1}]$$

Where the positive square root is understood. $i = \sqrt{-1}$ is the imaginary unit and m is the mass per unit length of cable. The functions cos(u) and sin(u) are the complex cosine and sine functions of complex numbers $u = u_r + iu_i$ as defined in Abramowitz and Stegun (1965).

σ and Σ are linear damping coefficients for cable motion and motion of lifted object respectively defined by equivalent linearization.

77
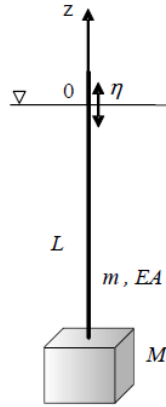
Figure 5.10: Forced oscillation of lifted in cable

The linear damping coefficient for cable for cable motion is defined by;

$$\sigma = \sqrt{2\pi}\rho C_{df} D_c \omega \eta_a \quad [kg/ms]$$

And the longitudinal cable friction force per unit length is given by

$$f_v = \frac{1}{2}\rho C_{df}\pi D |\dot{\eta}|\dot{\eta} \quad [N/m]$$

Where the vertical motion along the cable is given by:

$$\dot{\eta} = \frac{\partial n}{\partial t} \quad [m/s]$$

The linear damping coefficient for motion of lifted object is defined by;

$$\Sigma = \sqrt{\frac{2}{\pi}}\rho C_{Dz} A_p \omega \eta_a \quad [kg/s]$$

And the vertical drag force for lifted object is given by

$$F_v = \frac{1}{2}\rho C_{dz} A_p |\dot{\eta}_L|\dot{\eta}_L \quad [N]$$

And where

$$\eta_L = \eta(-L) = motion\ of\ lifted\ object\ [m]$$

The amplitude of the vertical motion of the lifted object caused by a forced oscillation of top of the cable with frequency ω and amplitude η_a is given by η_L ;

$$\frac{|\eta_L|}{\eta_a} = \left|\frac{kEA}{kEAcos(kL) + (-\omega^2 M' + i\omega\Sigma)\sin(kL)}\right| \quad [m/m]$$

The ratio between the motion of the lifted object and the motion at the top of the cable, is the motion transfer function

$$H_L(\omega) = \frac{\eta_L}{\eta_a} \quad [m/m]$$

The amplitude of the dynamic force $F_d(z)$ in the cable at position z is given by;

$$\frac{F_d(z)}{\eta_a k_E} = \left|\frac{-(kL)^2 k_E \sin[k(z+L)] + (kL)h(\omega)\cos[k(z+L)]}{(kL)k_E \cos(kL) + h(\omega)\sin(kL)}\right|$$

Where

$$h(\omega) = -\omega^2 M' + i\omega\Sigma$$

$$k_E = \frac{EA}{L}$$

The dynamic force varies along the length of the cable. If the amplitude of the dynamic force exceeds the static tension in the cable, a slack wire condition occurs.

The amplitude of the dynamic force F_{d0} at the top of the cable is obtained by setting z = 0 in the expression above. Similar, the dynamic force at the lifted object is obtained by setting z=L.

The motion of the lifted object due to a general irregular wave induced motion at top of the cable is obtained by combining transfer functions for motion of lifted object and motion of the top of cable at crane tip position. The response spectrum of the lifted object is given by;

$$S_L(\omega) = [H_L(\omega)H_a(\omega)]^2 S(\omega) \quad [m^2 s]$$

Where $H_a(\omega)$ is the transfer function for crane tip motion, $S(\omega)$ is the wave spectrum and $H_L(\omega)$ is the motion transfer function defined above.

Horizontal motion response of lifted object in a straight vertical cable

The first eigen period for un-damped oscillations of the lifted object may be taken as

79

$$T_{0h} \approx 2\pi \sqrt{\frac{\left(M + A_{11} + \frac{mL}{3}\right) * L}{W + 0.45wL}}$$

A_{11} = surge added mass of lifted object [kg]

Applying added mass in sway, A_{22}, in the equation above will give the eigenperiod for sway motion of the lifted object.

If the ocean current energy spectrum is non-zero in a range of frequencies close to $f_0 = 1/T_{0h}$ horizontal oscillations of the lifted object can be excited. Likewise, the oscillations may be excited by horizontal motion of the crane tip. Such oscillations may be highly damped due to viscous drag on cable and lifted object.

5.5.4. Heave compensation (move to end of vessel motions)

Various motion control devices may be used to compensate for the vertical motion of the vessel. The most commonly used device is a heave compensator. (DNV, 2009)

Heave compensator

A heave compensator may be used to control the motion of the lifted object and tension in cable during lifting operation. They may be divided into three main groups:

- Passive heave compensator
- Active heave compensator
- Combined passive/active systems

A passive heave compensator is in principle a pure spring damper system which does not require input of energy during operation. An active heave compensator may use actively controlled winches and hydraulic pistons. The active system is controlled by reference signal. In a combination system the active system is working in parallel with the passive.

Examples of input reference signals to an active heave compensator are:

- Wire tension
- Crane top motion
- Winch or hydraulic piston motion

- Position of lifted object

- Vessel motion

- Wave height/current velocity

6. SIMO modelling

6.1. SIMO

The program used for the simulations is SIMO, Simulation of Marine Operations. According to SINTEF (2003) SIMO is a computer program for simulation of complex, genera, multi-body marine operations. The program has a complete environment model (wind, waves and stationary current), which is required for position-keeping (mooring and/or DP) analysis. It also includes models for mooring systems and DP with trustees. (Marintek, 2003)

6.2. Inputs

6.2.1. Vessel

The vessel used was given by the supervisor. The geometry file used was taken from the SIMA homework provided in OFF600. The geometry file was only used for visual purposes and scaled to fit the given vessel data.

Table 6.1: Data input for vessel

	Values
LPP	137.7 m
Width	27m
Draught	6.438m
TA (Draught at the aft of the boat)	6.407m
TF (Draught at the front of the boat)	6.469m
Accumulated mass	1.69e+07

The vessel data input was provided with fixed force elongation as shown in Figure 6.1. The fixed force elongation makes the vessel stay positioned.
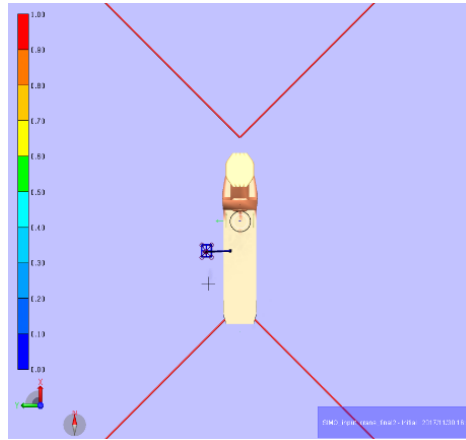
Figure 6.1: Vessel with fixed force elongation

6.2.2. Crane

The crane is made up of 3 slender elements. The design of the crane is design with correlation to the Rolls Royce subsea crane provided in section 3.5.2 and given cranetip point. There are two different coordinates of the slender elements used due to the differences in equipment size. See section 7.6 for more information.

Figure 6.2: Crane 1

Figure 6.3: Crane 2

Table 6.2: Coordinates and data for crane 1

	X (End 1)	Y (End 1)	Z (End 1)	X (End 2)	Y (End 2)	Z (End 2)	Specific volume	Distributed mass
Crane 1	-24.5	8	2	-24.5	8	18	4.9	1
Crane 2	-24.5	8	18	-24.5	27.5	46	0.8	1
Crane 3	-24.5	27.5	46	-24.5	27.5	30	0.5	1

Table 6.3: Coordinates and data for crane 2

	X (End 1)	Y (End 1)	Z (End 1)	X (End 2)	Y (End 2)	Z (End 2)	Specific volume	Distributed mass
Crane 1	-24.5	8	2	-24.5	8	18	4.9	1
Crane 2	-24.5	8	18	-24.5	24.25	48	0.8	1
Crane 3	-24.5	24.25	48	-24.5	24.25	32	0.5	1

6.2.3. Winch

The winch is located at the body point at the cranetip. The data input for the winch is provided in Table 6.4.

Table 6.4: winch data iinput.

Acceleration [m/s²]	1
Maximum speed [m/s]	1.5
Maximum length [m]	4500
Drum length [m]	4500

The maximum length is the maximum wire length that can be added to the drum, and the drum length is the initial wire length at the drum.

The speed of the deployment of the equipment is set to be different for deploying through the splash zone, and deploying though the water column. The following intervals are used:

Table 6.5: Winch speed

Start time [s]	Stop time [s]	Speed [m/s]
4	175	0.2
175	5500*	0.75

The second interval stop time, marked with *, varies for the different equipment. The following stop times are used for the different equipment.

Table 6.6: Stop times for installed equipment

	Stop time [s]
Suction Anchor	5067
Valve tree	5200
Spreader beam	5300
Template	5300
Tubing head spool	5500

6.2.4. Hook body

The hook has a distributed mass of 4000kg and have the same properties of the hook provided in the *SIMA modelling from scratch I SIMO* example, provided in in OFF600. The same geometry file was used for visual purposes.

Figure 6.4: Hook geometry

Due to the geometry of the different equipment, the hook has two different sets of body points.

Table 6.7: Hook body point set 1				Table 6.8: Hook body point set 2			
Name	**x**	**y**	**Z**	**Name**	**x**	**y**	**Z**
Hook point	0	0	0	**Hook point**	0	0	0
Hook point 1	0	-0.2	-1.8	**Hook point 1**	-0.14	-0.14	-1.8
Hook point 2	-0.2	0	-1.8	**Hook point 2**	-0.14	0.014	-1.8
Hook point 3	0	0.2	-1.8	**Hook point 3**	0.14	0.14	-1.8
Hook point 4	0.2	0	-1.8	**Hook point 4**	0.14	-0.14	-1.8

Body point set 1 is used for the suction anchor and the tubing head spool. For the well jumper body point 2 and 4 are used from body pint set 1. Body point set 2 is used for the valve tree and the drill centre template.

6.2.5. Installed body

All the installed bodies are made up of slender elements. The inputs needed for the slender elements are specific volume, distributed mass, number of strips, coordinate end point 1, end point 2, quadratic drag and added mass.

The distributed mass is calculated from the inner and outer diameter of each slender element. The formula is given below:

$$w_p = \frac{\pi}{4} * \rho_m \left(d_0^2 - d_i^2 \right) \ [kg/m]$$

w_p = weight of empty pipe per unit length (kg/m)

ρ_m = density of pipe material (kg/m3)

d_0 = outside diameter (m)

$d_i = d_0 - 2t$: inside diameter (m)

t = wall thickness

The material used is steel with a density of 7850 kg/m^3.

The formula used for added mass:

$$m_a = \rho * C_A * A_R \ [kg/m]$$

The formula used for quadratic drag:

Table 6.9: Calculation of Drag Force

	Formula	Units
Drag force	$F_D = \dfrac{1}{2} * \rho * v^2 * C_d * A$ $F_D = \dfrac{1}{2} * \rho * v^2 * C_d * L * D$	N
Move Length and square velocity to the left side*	$\dfrac{F_D}{v^2 * L} = \dfrac{1}{2} * \rho * C_d * D$	$\dfrac{N * s^2}{m^3}$

*The simulation calculates the drag force according to the length and the change of velocity as the manifold gets lowered into the water.

C_A and C_d is assumed to be 1 for all the slender elements.

6.2.5.1.   Tubing head spool
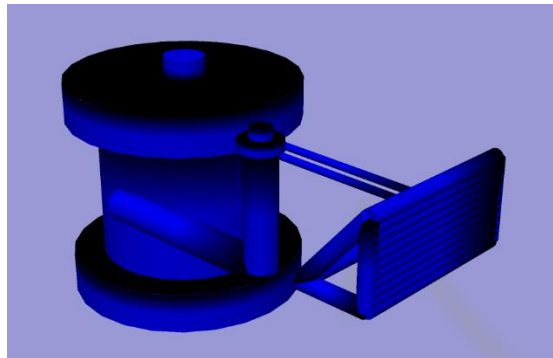
Figure 6.5: Tubing head spool

Table 6.10 show the data input for each slender element in the tubing head spool. The Tubing head spool consist of a total of 29 slender elements.

Table 6.10: Data input for slender elements in SIMO, tubing head spool

Outer diameter [m]	Wall thickness [mm]	Distributed mass [kg/m]	Specific volume [m²/m]	Added mass [kg/m]	Quadratic drag [Ns²/m³]
0.100m	6	14.3	0.00785398	8.050	51.250
0.250m	solid	29	0.04908739	50.315	128.125
0.250m	12.5 (5%)	75.1	0.04908739	50.315	128.125
0.250m	15 mm	89.7	0.04908739	50.315	128.125
0.375m	22.5 mm	202	0.04908739	113.208	192.188
0.500m	30 mm	359	0.11044662	201.258	256.250
2.150m	129 mm	6631	3.63050301	372.266	1101.875
2.900m	174 mm	12065	6.60519855	6770.329	1486.250

The wall thickness is calculated as 6% of the outer diameter of each slender elements. One of the slender elements are calculated as solid, while one with the wall thickness of 5% of the outer diameter.

6.2.5.2. Suction anchor
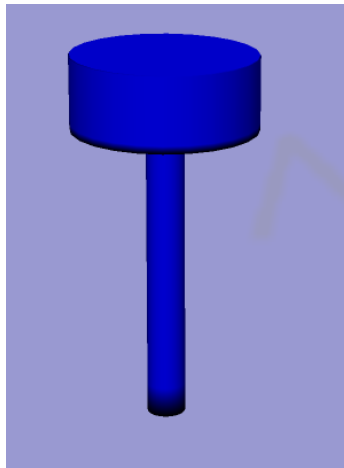
Figure 6.6: Suction anchor in slender elements

The suction anchor consists of two slender elements. The data input for each slender element is shown in Table 6.11.

Table 6.11: Data input for slender elements in SIMO, suction anchor

Outer diameter [m]	Wall thickness [mm]	Distributed mass [kg/m]	Specific volume [m²/m]	Added mass [kg/m]	Quadratic drag [Ns²/m³]
5 m	0.1	160280	19.6349541	20125.8279	2562.5
5 m (0.5m)	0.05	48000	0.78539816	20125.8279	2562.5

In SIMO, the slender elements are created as solid cylinders and designed with the specific volume of each slender element. As the suction anchor is a hollow cylinder with a thin wall thickness, the bottom part of the suction anchor is designed as a thin cylinder in SIMO. The reason for this is to gain the effect of water coming into the suction anchor as it is deployed in water. The distributed mass is calculated with a wall thickness of 0.1m for the upper cylinder and 0.05m for the bottom cylinder to reach the appropriate weight of the suction anchor.

6.2.5.3. Well jumper
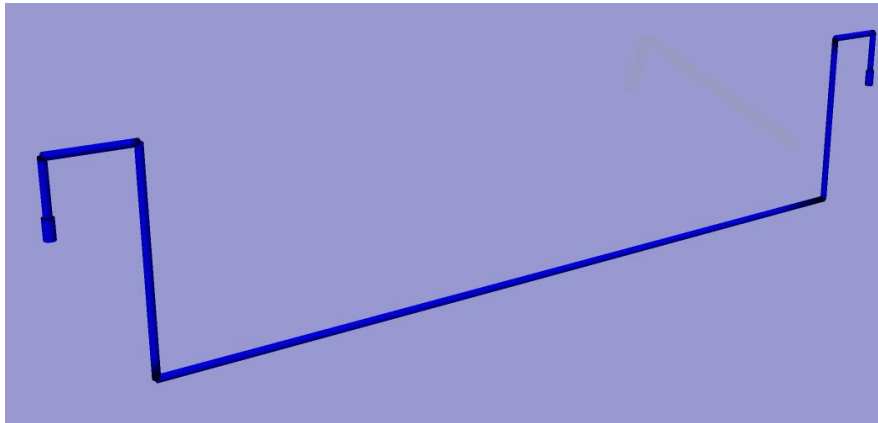
Figure 6.7: Well jumper

The well jumper consists of 9 slender elements. The data input for the slender elements are provided in Table 6.12.

Table 6.12: Data input for slender elements in SIMO, well jumper

Outer diameter [m]	Wall thickness [mm]	Distributed mass [kg/m]	Specific volume [m²/m]	Added mass [kg/m]	Quadratic drag [Ns²/m³]
0.254 (10")	25.4 mm (1")	151	0.05067075	51.938	130.175
0.1778 (7")	25.4 mm (1")	103	0.02482867	25.449	91.123
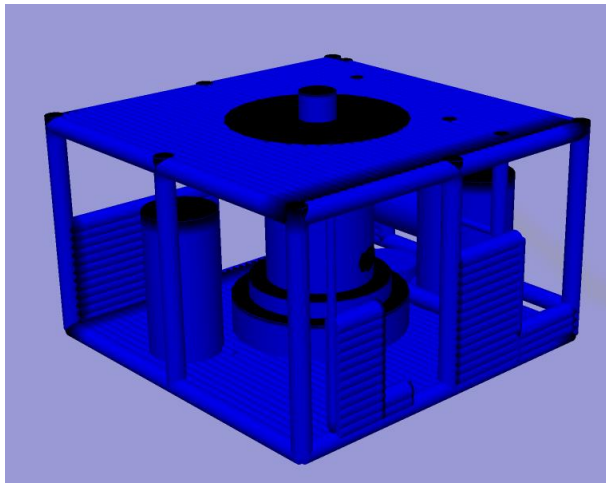
Figure 6.8: valve tree
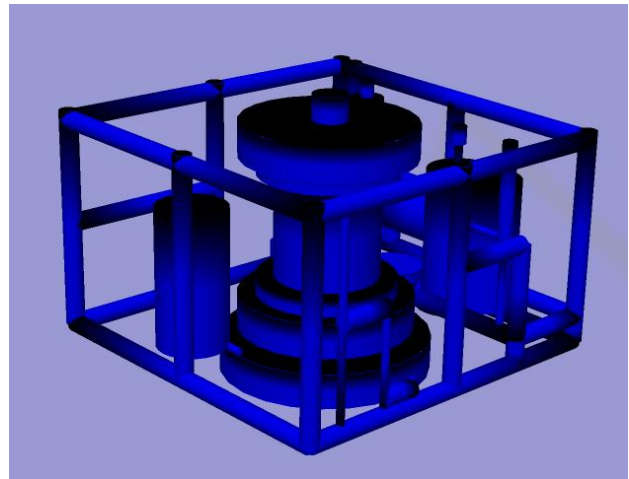
Figure 6.9: valve tree, simplified

Figure 6.8 show the model of the valve tree consisting of 193 slender elements. The number of slender elements was too much for the program to calculate to a water depth of 4000m. Therefore, the valve tree was modified to a simplified model consisting of 60 slender elements, shown in Figure 6.9. The data input for the slender elements are provided in Table 6.13.

Table 6.13: Data input for slender elements in SIMO, valve tree

Outer diameter [m]	Wall thickness [mm]	Distributed mass [kg/m]	Specific volume [m²/m]	Added mass [kg/m]	Quadratic drag [Ns²/m³]
0.001	0.00003	0.00071765	7.85398E-07	0.001	0.513
0.1	0.003	7.17649718	0.007853982	8.050	51.250
0.2	0.006	28.7059887	0.031415927	32.201	102.500
0.25	0.0075	44.8531074	0.049087385	50.315	128.125
0.5	0.015	179.412429	0.196349541	201.258	256.250
0.75	0.0225	403.677966	0.441786467	452.831	384.375
1	0.03	717.649718	0.785398163	805.033	512.500
1.5	0.045	1614.71187	1.767145868	1811.325	768.750
2	0.06	2870.59887	3.141592654	3220.132	1025.000
2.5	0.075	4485.31074	4.908738521	5031.457	1281.250
3	0.09	6458.84746	7.068583471	7245.298	1537.500

The wall thickness for each slender element is calculated as 3% of the outer diameter.

6.2.5.5.   *Drill centre template*
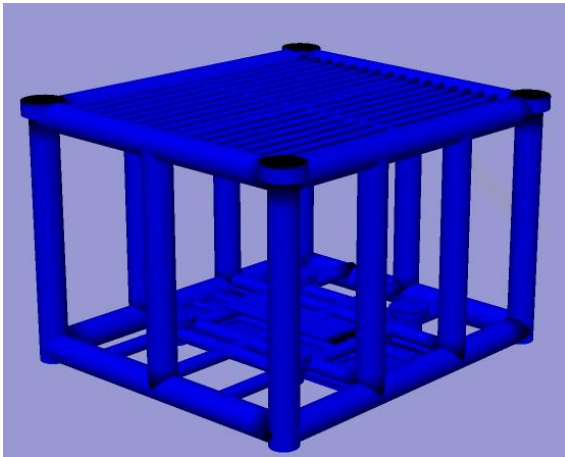
| *Figure 6.10: Drill centre template* | *Figure 6.11: Drill centre template, simplified* |
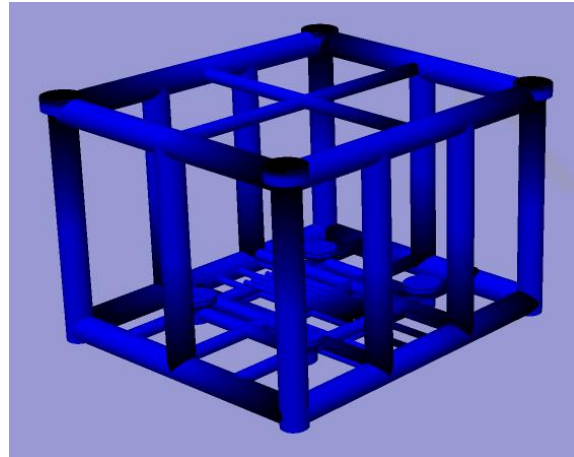
The same issue as for the valve tree occurred for the modelled drill centre consisting og 202 slender elements, shown in Figure 6.10. The model was modified to a simplified model consisting of 52 slender elements, shown in Figure 6.11. The data input for the slender elements are provided in Table 6.14.

Table 6.14: Data input for slender elements in SIMO, drill centre template

Outer diameter [m]	Wall thickness [mm]	Distributed mass [kg/m]	Specific volume [m²/m]	Added mass [kg/m]	Quadratic drag [Ns²/m³]
0.2	0.012	55.6363493	0.03141593	32.2013247	102.5
0.25	0.015	86.9317957	0.04908739	50.3145698	128.125
0.5	0.03	347.727183	0.19634954	201.258279	256.25
1	0.06	1390.90873	0.78539816	805.033117	512.5
1.5	0.09	3129.54465	1.76714587	1811.32451	768.75

Here, the wall thickness is calculated as 6% of the outer diameter.

6.3. Simple wire coupling

Simple wire coupling provides inputs for length, flexibility, damping, axial stiffness (EA) and breaking strength. Simple wire coupling does not take account for the weight of the rope in air and in water. For the slings, simple wire coupling is used. Each sling is a wire rope with fibre core, with a diameter of 0.03m. the SIMO software experiences trouble if the axial stiffness is too high for short slings, therefore the axial stiffness of the ropes is calculated using the following equations (OrcaFlex):

$$E = 1.03 \times 10^8 \frac{kN}{m^2}$$

$$A = 0.455 \frac{\pi d^2}{4}$$

$$Axial\ stiffness = E \times A = 3.67 \times 10^7 d^2\ kN$$

E = Young's Modulus for a 6x19 strand group with fibre core

A = assumed metallic area

6.4. Lift line coupling

In addition to the data inputs provided in the simple wire coupling, the lift line coupling provides inputs such as quadratic drag, weight in air and weight in water to weight in air ratio.

6.4.1. Winch using lift line coupling

The rope data was retrieved from *Lankorst Ropes' LankoDeep® AHC* rope and *Samson Quantum-12 rope, and* Table 3.2 *in section 3.1.1.*

Table 6.15: Rope properties. (Samson Rope Tenchnologies, inc, 2014) (Lankhorst Ropes)

	Values
Diameter	0.134 m
Weight in air	119.9 N/m
Weight in water	-3.1 N/m
Ratio	-0.026
Transverse drag coefficient	2 Ns^2/kg
Minimum breaking load	10300500 N (1050Te)
Axial Strength (EA)	250 MN

The transverse drag coefficient is interpolated from DNV-RP-H103, Appendix B. In the source, the drag coefficient is given for a wire with 6 strands, where the drag coefficient is given as 1.5-1.8. As the fibre rope used in the SIMO model is a fibre rope with 12 strands, a slightly higher drag coefficient of 2 is used.

The steel rope and fibre rope compared has similar minimum breaking loads of around 1000Te. The comparison was made to look at the effect of the self-weigh of the two materials in water. The steel rope values are retrieved from table 3.2 in chapter 3.1.1, while the Fibre rope properties are the same as in Table 6.15 above.

Table 6.16: Steel wire and fibre rope properties. (Lankhorst Ropes)

	Fibre rope (HMPE)	Steel
Diameter	0.134 m	0.127 m
Weight in air	119.9 N/m	567 N/m
Weight in water	-3.1 N/m	438.5 N/m
Ratio	-0.026	0.77
Transverse drag coefficient	2 Ns^2/kg	2 Ns^2/kg
Minimum breaking load	10300500 N (1050Te)	9810000 N (1000Te)
Axial Strength (EA)	250MN	965MN

Figure 6.12 shows a comparison between the submerged weight of the steel and the fibre ropes, including an equipment with a mass of 103 tonnes.
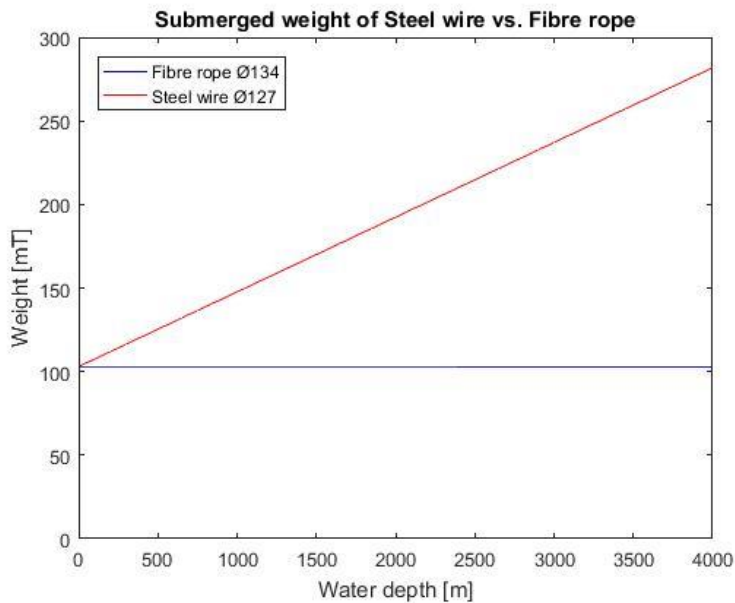
Figure 6.12: Submerged weight in water including installed object

7. Sling position

When installing equipment, it is important to look at the sling positions of the slings. This following chapter goes in depth on the importance of the sling positions.

7.1. Lifting in air

7.1.1. Centre of Gravity (CoG)

When preparing a lift and attaching the rigging it is important to follow a Rigging Study made for the lift, and to ensure that the centre of gravity is directly under the hook block of the lifting crane. When a load is lifted by a crane, the CoG is always hanging vertically beneath the hook. If the CoG is not directly beneath the hook once the load is lifted, then the load will tilt until it is. To make sure that the load stays horizontal when lifted, we either change the lift point position of one of the slings, or lengthen or shorten one of the slings to ensure the CoG is exactly under the hook when the load is lifted. (WSH Council, 2014)
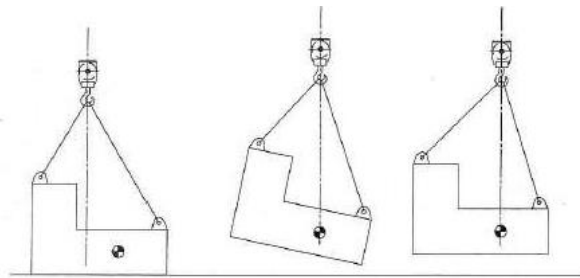
Figure 7.1: CoG beneath the hook. (WSH Council, 2014)

When the CoG is not equally spaced between the rigging points, the slings and fitting will not carry an equal share of the load. The slings connected closest to the CoG will carry the greatest share of the load.

LOAD ON SLING CALCULATED
TENSION 1 = LOAD X D2 X S1/(H(D1+D2))
TENSION 2 = LOAD X D1 X S2/(H(D1+D2))
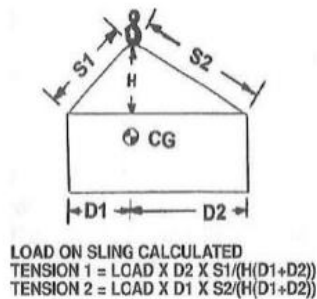
Figure 7.2: Tension in slings. (WSH Council, 2014)

7.2. Lifting in water

When lifting an object though the water column, it is important to take account the centre of buoyancy (CoB) as well as the centre of gravity. The hook should now be vertically above the centre of force, and not the centre of gravity.

The centre of force (CoF) is calculated using the following formula.

$$CoF = \frac{(B * CoB) - (mg * CoG)}{mg - B}$$

$$F = mg - B$$

$CoF = Centre\ of\ Force$

$CoB = Centre\ of\ Buoyancy$

$CoG = Centre\ of\ Gravity$

$B = buoyancy$

$m = mass\ of\ lifted\ object$

$g = gravity$
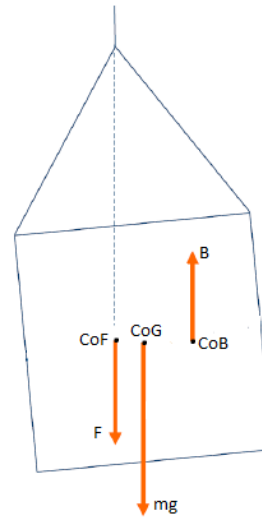
Figure 7.3: Centre of force

The force centre, CoF, will be vertically below the hook. This leads to a heel angle of the load. If the centre of the vertical added mass is not in line with F, we will have vertical excitation and therefore tilting oscillations. Lifting at points below CoG should be analysed with care.

One important question to ask when arranging the slings is "is the structure designed for the loads occurring during lifting and deployment?". We must take account the hydrodynamic forces. Limited lifting height may give large compressive forces from the slings.

7.3. Sling angles/lengths

In any lifting operation the rigging equipment will be selected based in the weight of the load to be lifted. However, there are times when the angle of the slings gets overlooked and what appears as the SWL on the tag or certificate is not sufficient to do the job.
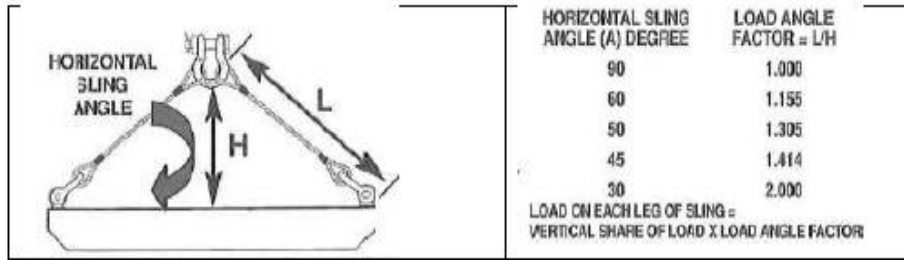
Figure 7.4: Load angle factor. (WSH Council, 2014)

Tension in each sling:

$$T = \frac{L}{H} * \frac{W}{n}$$

T = Tension in each sling

L = Length of sling

H = height between hook and load

n = number of slings
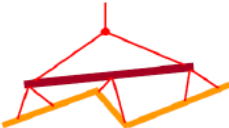
Rigging is advised to proceed at 60 degrees as far as possible. Slings should also be selected with at least a 20% extra SWL as lifting is typically carried out at 60 degrees sling angles. When the rigging exceeds this sling angle, detailed calculations should be done to determine the actual load on each leg of sling.

According to GL Noble Denton "The sling angle should not normally be less than 45º to the horizontal although for lifts that are installed at an angle this may not be the case, e.g. flare booms installed by a single crane, the upper rigging may be less than 45º". (Replaced by DNVGL-ST-N001) (Technical standards committe, 2015)

7.4. Lifting measures

Sometimes lifting measures are needed when lifting certain objects. This is most common for un-symmetric structures and long structures. There are three different types of measure shown the table below:

Table 7.1: Lifting measures

Lifting frames	Spreader beam	Reinforcement (compression bar)

7.5. Calculating optimal sling angle and length

To calculate the optimal sling angle and length we start by looking at the position of the slings when installing the tubing head spool. The hook is located above the centre of gravity of the wellhead, and the hook points on the wellhead are located one meter from the centre of gravity in each direction. Figure 7.5 and Figure 7.6 show two different locations of the wellhead compared to the hook location.
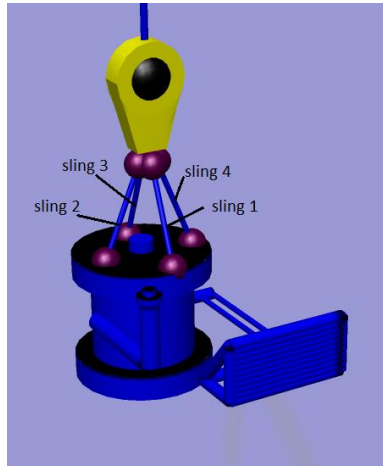
Figure 7.5: Tubing head spool z position, 20m
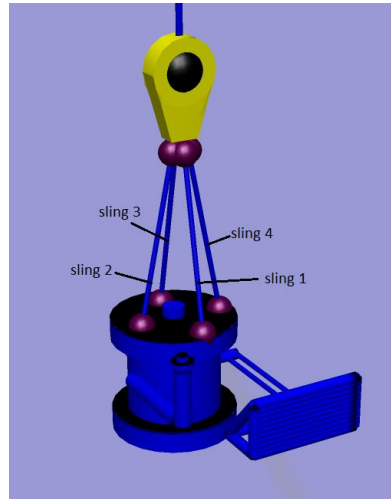
Figure 7.6: Tubing head spool z position, 18m

Since all four slings are symtric, we will look at sling 1 for further reasearch. The figure below shows the location of the connetion points.
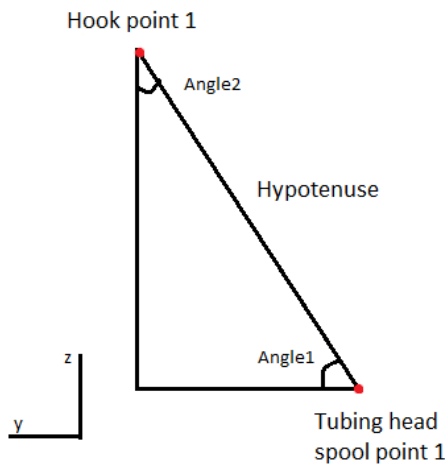
Figure 7.7: position of body points

7.5.1. Alternative 1: Tubing head spool z position at 20m

The first alternative is to position the tubing head spool at 20m above the mean sea level. The coordinates of the body point are given in Table 7.2. The coordinates of the hook point 1 and tubing head spool point 1 are relative to the coordinates to the hook body and the tubing head spool body, respectively. The coordinates are then modified according to the body centre coordinate, located on the vessel, of the whole model (x0, y0, z0).

Table 7.2: Coordinates for data input, 20m

Sling 1	Body point coordinates relative to body coordinates			Body coordinates relative to centre coordinates			Body point coordinates relative to centre coordinates		
	x	y	z	x1	y1	z1	x0	y0	z0
Hook point 1	0.00	-0.20	-1.80	-24.50	27.50	25.00	-24.50	27.30	23.20
Tubing head spool point 1	-0.95	-0.64	1.25	-23.46	27.14	20.00	-24.41	26.50	21.25

Using Pythagoras theorem, the length of the sling is calculated, shown in Table 7.3.

Table 7.3: Data results for 20m

length in y-direction	0.80
length in x-direction	-0.09
hypotenuse1	0.81
length in z-direction, H	1.95
hypotenuse2, L	2.11
L/H (Load angle factor)	1.08
angle1	67.56
angle2	22.44

When placing the wellhead at 20m above the mean water level, we get a load angle factor of 1.08. this means that each of the four slings is added an extra load of 0.08 of the actual load on the sling. A simulation deploying the tubing head spool, for a simulation time of 200m, providing data for the tension in the slings. The results from SIMO are shown in Figure 7.8 and Table 7.4.
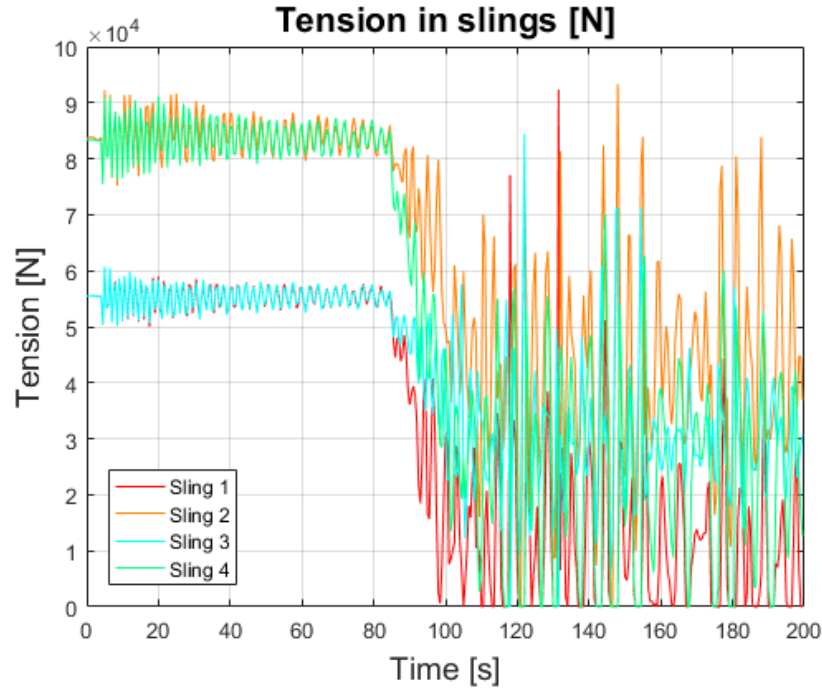
Figure 7.8: Tension in the slings, 20m

The tension in slings 2 and 4 are higher when the tubing head spool is lifted above water, than in slings 1 and 4, shown in Figure 7.8. This might be due to a slight unbalance of the tubing head spool. The statistics for the tension in the slings are provided in Table 7.4. As the tubing head is lifted though the splash zone and deployed through the water column, the mean tension decreases in all slings. However, the standard deviation indicates large variations in tension. The large variations might indicate snap forces in the slings.

Table 7.4: Statistics for tension in slings, 20m

	Max [N]	Min [N]	Mean [N] (total)	Standard deviation [N]	Mean [N] (water)
sling 1	92315	0	31705	23536	12955
sling 2	93356	0	62189	23867	44713
sling 3	84378	0	42110	14672	31677
sling 4	91207	0	51765	31490	26435

7.5.2. Alternative 2: tubing head spool z position at 18m

The second alternative is to position the tubing head spool 18m above the mean sea level. The new coordinates are given in

Table 7.5.

Table 7.5: Coordinates for data input, 18m

sling 1	Body point coordinates relative to body coordinates			Body coordinates relative to centre coordinates			Body point coordinates relative to centre coordinates		
	x	y	z	x1	y1	z1	x0	y0	z0
hook point 1	0.00	-0.20	-1.80	-24.50	27.50	25.00	-24.50	27.30	23.20
Tubing head spool point 1	-0.95	-0.64	1.25	-23.46	27.14	18.00	-24.41	26.50	19.25

The additional length in z direction, increases the length of the sling, and thus decreases the load angle factor. The calculated results for the tubing head spool positioned at 18m above water is given in Table 7.6.

Table 7.6: Data results for 18m

length in y-direction	0.80
length in x-direction	-0.09
hypotenuse1	0.81
length in z-direction, L	3.95
hypotenuse2, H	4.03
L/H (Load angle factor)	1.02
angle1	78.48
angle2	11.52

Due to the increased z value, and thus increased length of the sling, the load angle factor is reduced to 1.02. This results in an added with a factor of 0.02 per sling.
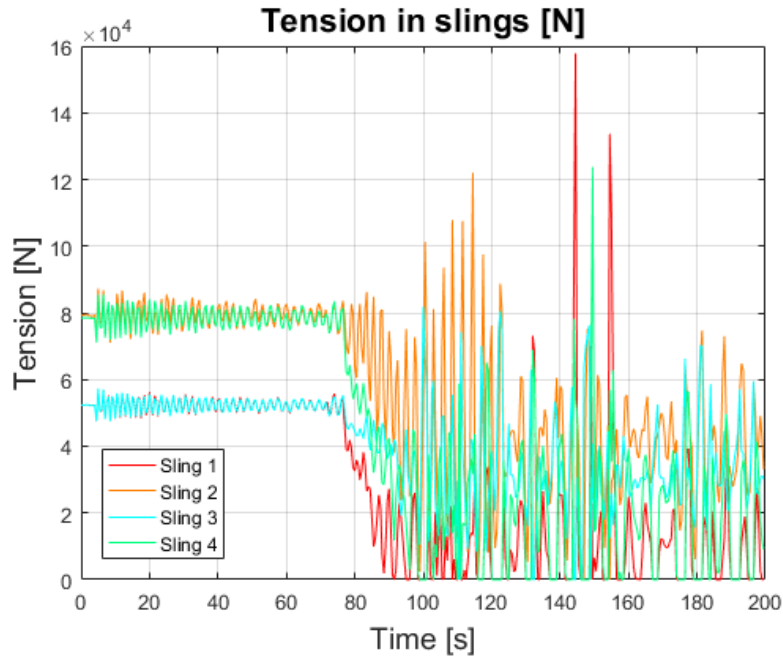
Figure 7.9: Tension in the slings, 18m

As with alternative 1, the tension in slings 2 and 4 are higher when lifted above water level, than for the tension in sling 1 and 3. However, there is a slight decrease in the tension for all slings. The mean value of the tension in the slings when the tubing head spool is deployed in water for all slings expect for sling 3. Form Figure 7.9, some snap forces in slings 1 and 4 are visualized. These extreme values may affect the statistics provided in Table 7.7, such as the mean tension in water and standard deviation.

Table 7.7: Statistics for tension in slings, 18m

	Max [N]	Min [N]	Mean [N] (total)	Standard deviation [N]	Mean [N] (water)
sling 1	157797	0	24814	27988	11116
sling 2	122040	0	25129	57162	40352
sling 3	81802	0	15074	40970	32716
sling 4	123702	0	31851	44100	19523

7.5.3. Alternative 3: Wellhead z position at 17m

The last alternative provided is positioning the tubing head spool at 17 meters above water level. The new coordinates are provided in Table 7.8.

sling 1	Body point coordinates relative to body coordinates			Body coordinates relative to centre coordinates			Body point coordinates relative to centre coordinates		
	x	y	z	x1	y1	z1	x0	y0	z0
Hook point 1	0.00	-0.20	-1.80	-24.50	27.50	25	-24.50	27.30	23.20
Wellhead point 1	-0.95	-0.64	1.25	-23.46	27.14	1	-24.41	26.50	18.25

Table 7.9: Data results for 17m

length in y-direction	0.80
length in x-direction	-0.09
hypotenuse1	0.81
length in z-direction, L	4.95
hypotenuse2, H	5.02
L/H	1.01
angle1	80.76
angle2	9.24

For this case the load angle factor only decreases by 0.01 from alternative 2. The small decrease in load angle factor will have very little to say on the added load for the slings.
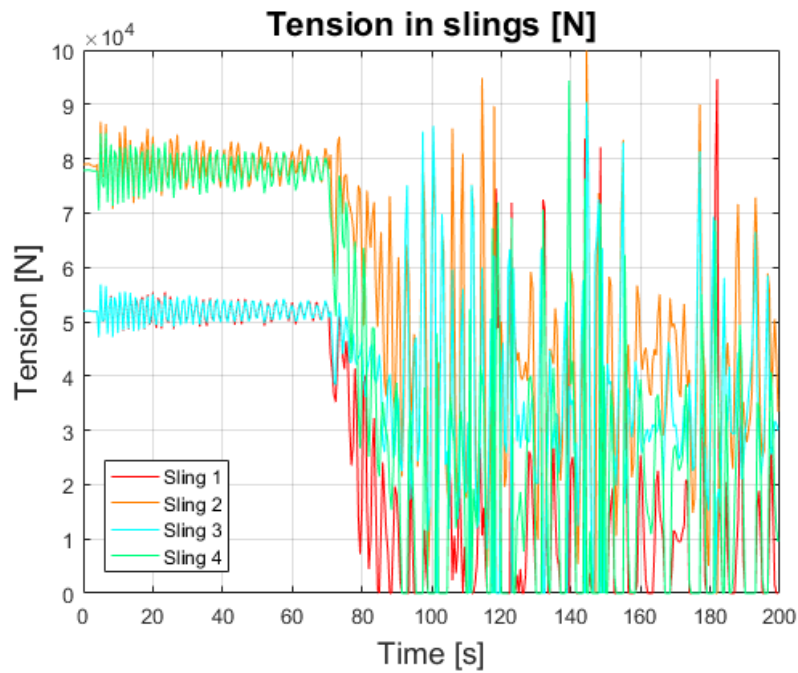
Figure 7.10: Tension in slings, 17m

Compared to alternative 2, the maximum tension when the tubing head spool is lifted above water level is slightly reduced. The standard deviation of the tension reduced as well for all slings.

Table 7.10: Statistics for tension in slings, 17m

	Max [N]	Min [N]	Mean [N] (total)	Standard deviation [N]	Mean [N] (water)
sling 1	94635	0	26413	24018	10215
sling 2	99879	0	55754	24666	39321
sling 3	90408	0	41092	16256	34016
sling 4	589183	0	42794	42324	19774

The large maximum displacement in sling 4 is due to a snap force. The value of the snap force was removed from Figure 7.10 due to visual effects.

7.5.4. Comparison
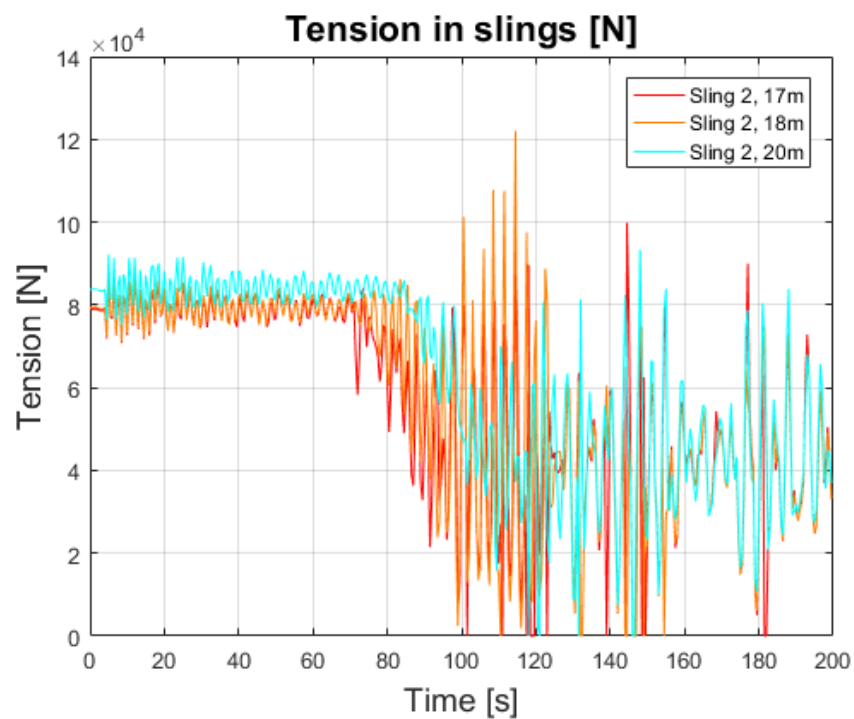
Figure 7.11: comparison of tension in sling 2

Figure 7.11 show a comparison of the tension in sling 2 for the three alternatives. The tension for alternative 1, shown in turquoise, have a larger tension in the sling when lifted above the water level than for the two other cases. However, the though the splash zone, the tension is higher for alternatives 2 and 3, shown in orange and red. This might be due to largest snap forced due to the increased sling length.

After the splash zone, the tension for the three alternatives remain close in values and variance to each other. This might be due to the decreased weight of the tubing head spool in water. Looking at the load angle factor, the difference between alternative 2 and 3 is small. Although the load angle factor is smaller for alternative 3, the increase of cost due to the increase in sling length must be considered. Based on the above results, alternative 2 is used further in the analysis with the tubing head spool located at 18 meters above water level.

7.6. Sling positions

For the following section, the calculation of the load angle factor in the slings for the remaining equipment is provided.

7.6.1. Sling position of suction anchor

Table 7.11: Coordinates for data input, Suction anchor

Sling 1	Body point coordinates relative to body coordinates			Body coordinates relative to centre coordinates			Body point coordinates relative to centre coordinates		
	x	y	z	x1	y1	z1	x0	y0	z0
Hook point 1	0	-0.2	-1.8	-24.5	27.5	25	-24.5	27.3	23.2
Suction anchor point 1	0	-2.5	5	-24.5	27.5	10	-24.5	25	15

Table 7.12: Data results for suction anchor

	10m	7m	Difference between 7m and 10m
length in y-direction	2.3	2.30	0.00
length in z-direction, H	8.2	11.20	3.00
Hypotenuse, L	8.52	11.43	2.91
L/H (Load angle factor)	1.04	1.02	-0.02
angle1	74.33	78.40	4.07
angle2	15.67	11.60	-4.07

Figure 7.12: Suction anchor sling positions

In this case, the angle changes less for each added meter of added height. To increase the angle from 74 to an angle of 78 degrees, approximately 3 meters of rope must be added to each sling. Therefore, considering the cost of the extra sling, it has been decided to stick to an angle of 74m and a load angle factor of 1.04, by placing the suction anchor at 7 meters above the water level.

7.6.2. Sling position of valve tree

Table 7.13: Coordinates for data input, valve tree

sling 1	Body point coordinates relative to body coordinates			Body coordinates relative to centre coordinates			Body point coordinates relative to centre coordinates		
	x	y	z	x1	y1	z1	x0	y0	z0
Hook point 1	-0.14	-0.14	-1.8	-24.5	27.5	25	-24.64	27.36	23.2
Suction anchor point 1	-2.375	-2.5	1.5	-24.5	27.5	12	-26.88	25	13.5

Table 7.14: Data results for valve tree

	12m	10m	Difference between 10m and 12m
Length in y-direction	2.235	2.235	0.000
Length in x-direction	2.360	2.360	0.000
Hypotenuse1	3.250	3.250	0.000
Length in z-direction, L	11.700	9.700	2.000
Hypotenuse 2, H	12.143	10.230	1.913
L/H (Load angle factor)	1.038	1.055	-0.017
angle1	74.474	71.475	3.000
angle2	15.526	18.525	-3.000

Figure 7.13: valve tree sling positions

In this case the difference between 12m and 10m is small, with the difference of 0.017 in the load angle factor. Therefore, 12 m above main sea level is chosen for the position of the valve tree at 12m above mean sea level, to save approximately 2 meters of extra rope for each sling.

7.6.3. Sling position of well jumper

Due to the length and geometry of the well jumper, a spreader beam is needed. In this case the only angle that is needed to take account for is the sling angle between the hook and the spreader beam. The angle of the slings between the spreader beam and the well jumper will be 90 degrees in this case, and therefore a load angle factor of 1.

sling 1	Body point coordinates relative to body coordinates			Body coordinates relative to centre coordinates			Body point coordinates relative to centre coordinates		
	x	y	z	x1	y1	z1	x0	y0	z0
Hook point 1	-0.2	0	-1.8	-24.5	24.25	29	-24.7	24.25	27.2
spreader beam point 1	-11	0	0	-24.5	24.25	11	-35.5	24.25	11
spreader beam point 3	-13	0	0	-24.5	24.25	11	-37.5	24.25	11
well jumper point 1	-13	0	2.75	-24.5	24.25	4	-37.5	24.25	6.75

Table 7.16: Data results for suction anchor

	Spreader beam 11m	Well jumper 4m
length in x-direction	10.80	0
length in z-direction, H	16.20	4.25
Hypotenuse, L	19.47	4.25
L/H (Load angle factor)	1.20	1
angle1	56.31	90
angle2	33.69	90
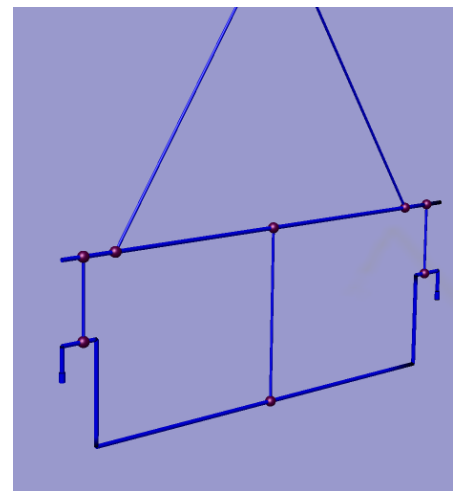
Figure 7.14: Well jumper sling positions

In this case it was necessary to take account for the extra height of the installed objects due to the spreader beam. The spreader beam could not be placed at a too small height above the mean water level. This is due to the height of the well jumper, which is 5.5m, or 2.75m above and below the well jumper coordinates. A way to solve this problem was to move the crane coordinates up and in the negative y direction so that the hook could be placed at 29m above the water level. With the provided calculated values provided in Table 7.16 and Table 7.17, the well jumper is placed 1.25 meters above the mean water level. The smallest possible load angle factor was 1.20, which means that each sling has an added factor of 0.20 to the tension. The angle calculated is within the limit provided in section 7.3. For further simulations in the report, the well head is placed 4 meters above the water level and the spreader beam is placed 11 meters above the water level.

7.6.4. Sling position of drill centre template

Table 7.17: Coordinates for data input, drill centre template

sling 1	Body point coordinates relative to body coordinates			Body coordinates relative to centre coordinates			Body point coordinates relative to centre coordinates		
	x	y	z	x1	y1	z1	x0	y0	z0
Hook point 1	-0.14	-0.14	-1.8	-24.5	24.25	29	-24.64	24.11	27.2
Template point 1	-6.5	-5.7	4.8	-24.5	24.25	7	-31	18.55	11.8

Table 7.18: Data results for drill centre template

	7m	10m	Difference between 10m and 7m
length in y-direction	5.56	5.56	0.00
length in x-direction	6.36	6.36	0.00
hypotenuse1	8.45	8.45	0.00
length in z-direction, L	15.40	12.40	-3.00
hypotenuse 2, H	17.56	15.00	-2.56
L/H (Load angle factor)	1.14	1.21	0.07
angle1	61.25	55.73	-5.52
angle2	28.75	34.27	5.52
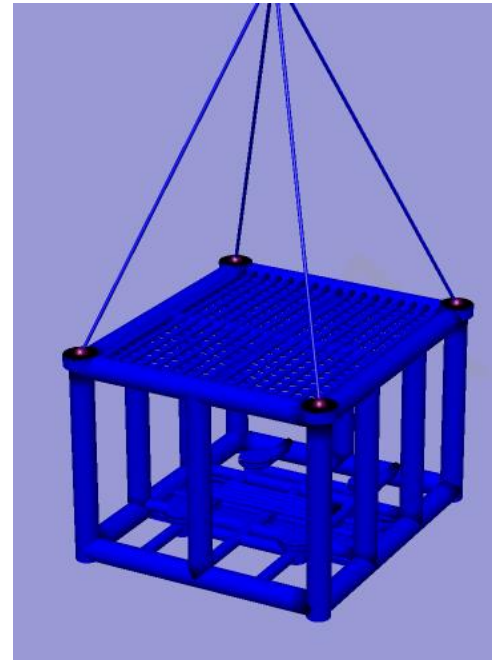
Figure 7.15: drill centre template sling positions

To increase the sling positions enough to get an angle above 60 degrees, the crane had to be moved up in the z and y direction, likewise the well jumper. Placing the drill centre template at 7 meters above the mean water level gives a load angle factor of 1.14 per sling and sling lengths of 17.56m. The template is positioned 7 meters above water level for the further simulations in the report.

8. Environment

In the following chapter, the effect of the environment during the installation and deployment process are discussed. The chapter takes account for the positioning of the vessel relative to the incoming weather direction, the wave and current data, the natural period and the installation time.

8.1. Current data

The current data is adapted from figure 6 in *Deepwater current profile data sources for riser engineering offshore Brazil.* (Harringston-Mission, et al., 2012)

The current data given in Table 8.1 are used for the main simulations. The current acts in the positive x direction of the simulation, see Figure 8.3. The current data starts of at 0.30 m/s at the mean water level, and reduced to 0.01 m/s at 4000 meters water depth. In between, the current reduces to 0.15 m/s at 350 meters water depth and increases to 0.25 m/s at 800 meters water depth.

Table 8.1: Current data

Depth [m]	Current [m/s]	Direction [degrees]
0	0.30	0
-350	0.15	0
-800	0.25	0
-1400	0.01	0
-4000	0.01	0
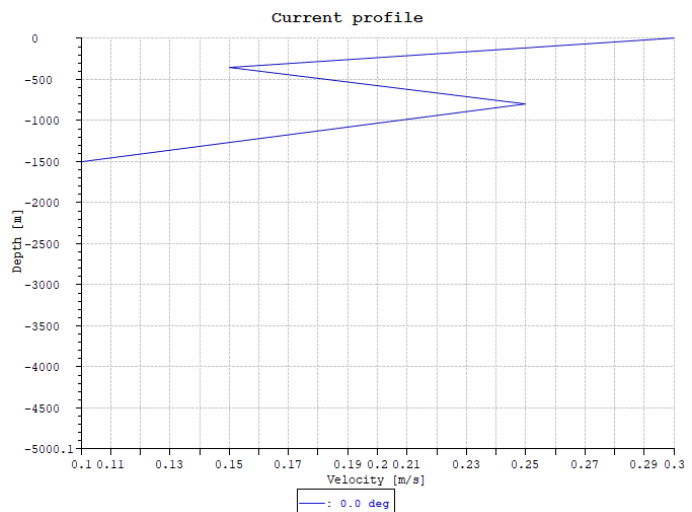
Figure 8.1: current profile from SIMO

To investigate the significance of the current, a reduced current data was made with half the velocity as the current data in Table 8.1. The reduced current data is shown in Table 8.2 below.

Table 8.2: Reduced current data

Depth [m]	Current [m/s]	Direction [degrees]
0	0.15	0
-350	0.075	0
-800	0.125	0
-1400	0.01	0
-4000	0.005	0
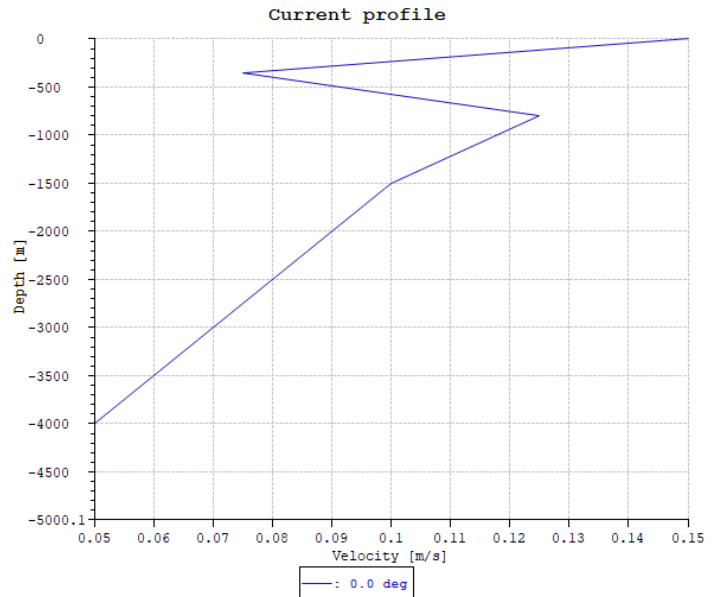
Figure 8.2: Reduced current profile from SIMO

The force on the equipment due to current is calculated by the formula given in section 5.3.3. Looking at the formula, one sees that the force is proportional to the exposed area of the equipment in the current direction, and the square of the current velocity.

To experience the maximum effect of the current, the current used in the simulation acts in the same direction at all water depths. For water depth of 4000 m the current may switch directions as the water depth increases. The change in directions of the current will reduce the effect of the equipment being displaced in one direction only.

8.2. Position

Most vessels today use dynamic positioning to position the vessel according to the incoming weather direction. To illustrate the effect of the positioning of the vessel, with respect to the incoming wave direction, a short simulation installing the suction anchor to approximately 200 m water depth was done. In the simulation, different condition sets were used with a constant Hs of 2 m and a Tp of 6m, and varying direction.

To investigate the effect of the direction of the incoming waves, eight different directions were chosen between 0 and 360, with intervals of 45 degrees. The data input and weather directions relative to the boat in SIMO is shown in Table 8.3 and Figure 8.3.

Table 8.3: Position input

Wave height, Hs	Wave period, Tp	position
2	6	0
2	6	45
2	6	90
2	6	135
2	6	180
2	6	225
2	6	270
2	6	315
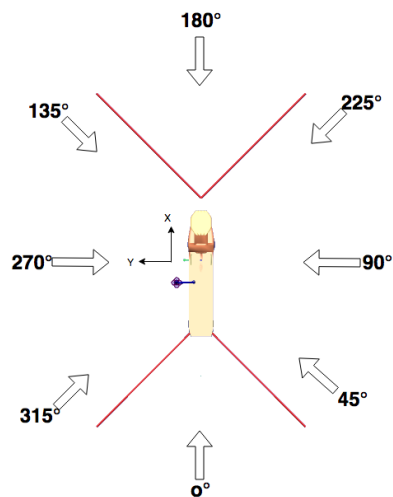
Figure 8.3: Positions relative to the vessel

8.2.1. Tension results

Figure 8.4 show a trend for the tension in the main liftwire. The tension in highest when the suction anchor is above water level, gradually decreases though the splash zone and has the largest variation in the upper water column. Throughout the deployment process, the tension in the main liftwire when the incoming weather comes in at 90 and 270 degrees stands out in Figure 8.4 and Figure 8.5. Figure 8.5 show a zoomed in section of the tension at the time interval of 220:300s. The figure illustrates the change in tension with respect to the incoming weather positions. The tension in the main liftwire for positions 90 and 270 varies more than that of the other directions. From Table 8.4, the highest maximum tension above water level occurs for positions 90 and 270 degrees, marked with red. This is in compliance with the high roll motions of the vessel due to the two weather directions.
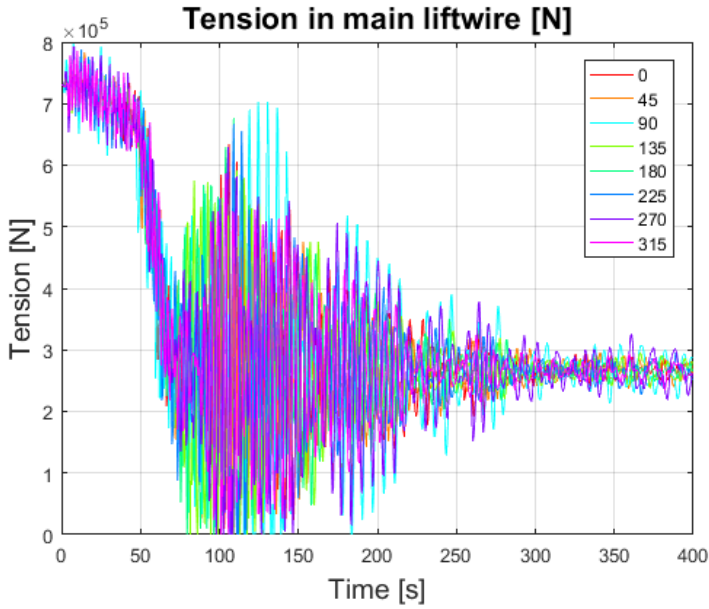
Figure 8.4: Tension in main liftwire
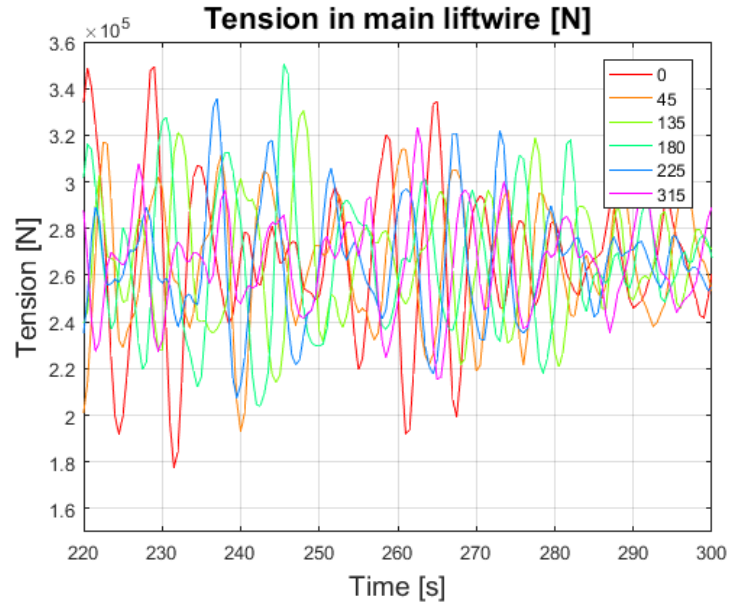
Figure 8.5: Tension in the main liftwire at a part of the simulation

The variation in the mean tension is small for the different incoming weather directions, a seen in Table 8.4. However, the standard deviation for the different directions are large. The smallest standard deviation of the tension occurs for the incoming wave direction of 45 degrees, and is largest for the incoming wave direction of 90 degrees.

Table 8.4:Tension statistics in main liftwire

	Max [N] (air)	Max [N] (water)	Min [N]	Mean [N]	Standard deviation [N] (upper water column)
0	777400	633940	602	331100	152260
45	782300	548290	4880	331000	141790
90	796800	702440	592	330300	211790
135	783900	591810	479	330600	168770
180	776300	675700	471	331200	166990
225	788000	666450	592	331400	147120
270	793400	628350	557	331200	157040
315	784400	587710	570	331300	147140

From the results above, the smallest maximum tension in air, is when the incoming waves are coming at 0 and 180 degrees to vessel. We now have two alternative wave directions. To find the better of the two, the x displacement of the suction anchor is investigated in the following section.

8.2.2. X displacement results

It is important to investigate the effect of the incoming wave direction with respect to the x displacement of the suction anchor. Figure 8.6 show a trend in the x displacement, where the weather incoming at 0, 45 and 315 degrees causes a slightly higher x displacement than of the other directions. The variation is slightly increasing as the suction anchor is installed though the water columns. As this is the results for an installation to only 200 m water depth, it is important to take account the effect for when the equipment is installed at further water depth. The most probable cause why the displacement is larger for 0, 45 and 315 degrees, are because these acts in the positive x direction of the vessel, as seen in Figure 8.3. This is the same direction as the current data used in the simulation, see section 8.1. The end position and the displacement of the three positions are marked in red in Table 8.5. The end position is the x position at 400s.
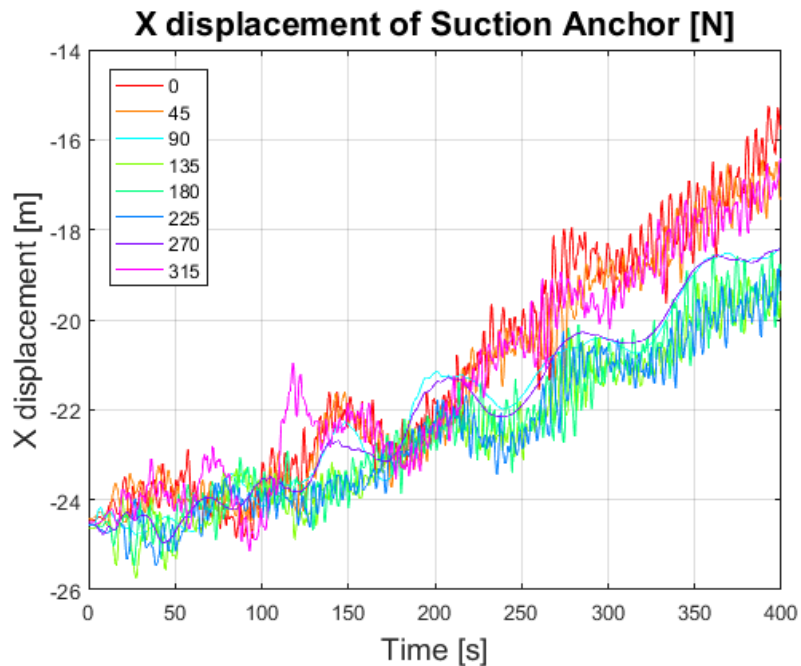
Figure 8.6:X displacement

From Figure 8.6 and Table 8.5, the smallest displacement is when the incoming wave direction is at 135, 180 and 225 degrees. These directions act in the negative x direction, which most likely is the cause of the smaller x displacement, which is the opposite direction of the current. Therefore, it is logical that the positions where the waves are acting in the positive x direction results in an additional displacement, and the positions acting in the negative x direction results in a reduced displacement. The two positions acting

on the ±y direction, 90 and 270 degrees, the x displacement lays at a median value with respect to the other values, which is most likely the displacement caused by the current alone.

Table 8.5: X displacement statistics

	Max [m]	Min [m]	Mean [m]	Start position [m]	End position [m]	Displacement [m]
0	-15.3	-24.9	-21.1	-24.5	-15.8	-8.7
45	-16.4	-24.6	-21.4	-24.5	-17.4	-7.1
90	-18.4	-24.8	-22.0	-24.5	-18.4	-6.1
135	-18.9	-25.8	-22.6	-24.5	-19.6	-4.9
180	-18.5	-25.5	-22.6	-24.5	-18.9	-5.6
225	-18.9	-25.5	-22.6	-24.5	-19.4	-5.1
270	-18.4	-25.0	-22.0	-24.5	-18.4	-6.1
315	-19.4	-25.2	-21.3	-24.5	-16.4	-8.1

When taking account both the effect of the tension in the main liftwire, and the x displacement of the suction anchor, positioning the vessel with the bow facing 180 degrees to the incoming waves is the safest and the most efficient position.

8.2.3. Shielding effect

When the waves come in at 180 degrees to the vessel, there is no shielding of the waves by the boat when the suction anchor is installed though the splash zone, and in the upper water column. To investigate this effect, simulations with a new condition set with five different direction from 150 to 210 at intervals of 15 degrees has been conducted, as shown in Table 8.6 and Figure 8.7.

Table 8.6: Data input

Wave height	wave period	position
2	6	150
2	6	165
2	6	180
2	6	195
2	6	210
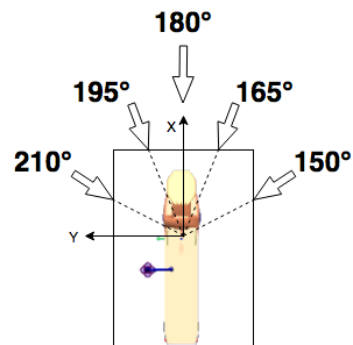
Figure 8.7: Positioning relative to vessel
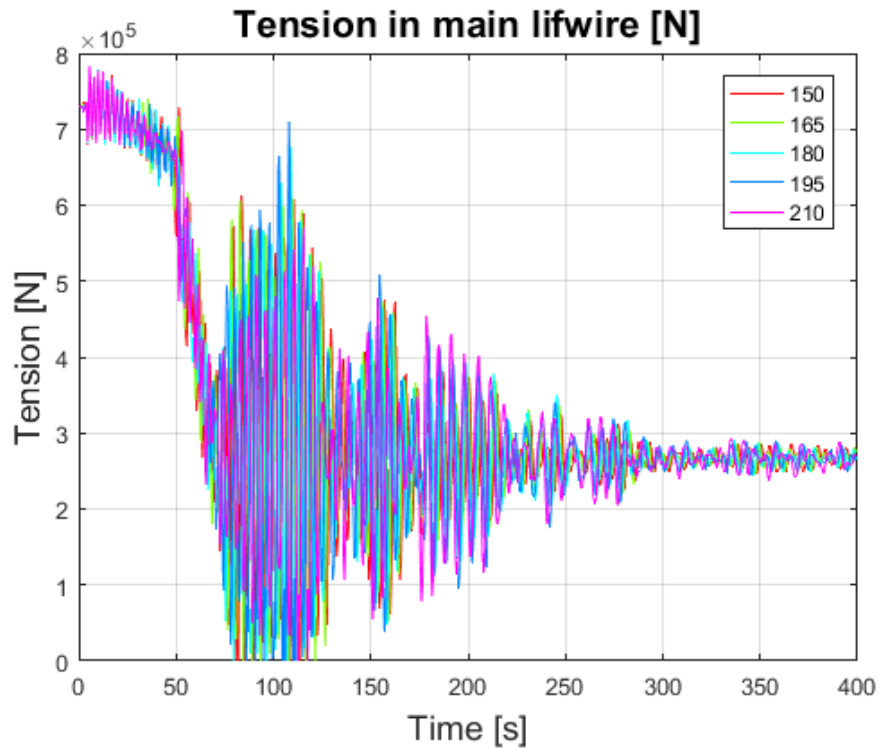
Figure 8.8: Tension in main liftwire

Table 8.7: Tension statistics

	Max [N] (air)	Max [N] (water)	Min [N]	Mean [N]	Standard Deviation [N] (water)
150	777600	612960	475	330900	173450
165	774700	606930	493	331200	174460
180	776300	675700	471	331200	166990
195	780900	710070	501	331100	174950
210	782200	571034	621	331300	131830

There is small difference in the maximum tension in air, and the mean tension throughout the deployment process for the different wave directions. These is a slight increase in maximum tension from 150 degrees to 210 degrees. The highest peak at the beginning of the water column is for 195 degrees at approximately 100s, marked in red in Table 8.7. The smallest standard deviation of the tension in the main liftwire occur when the incoming weather comes in at 210 degrees to the vessel. There are no clear results indicating the effect of the sheading from the boat.

8.2.3.2.   X displacement results
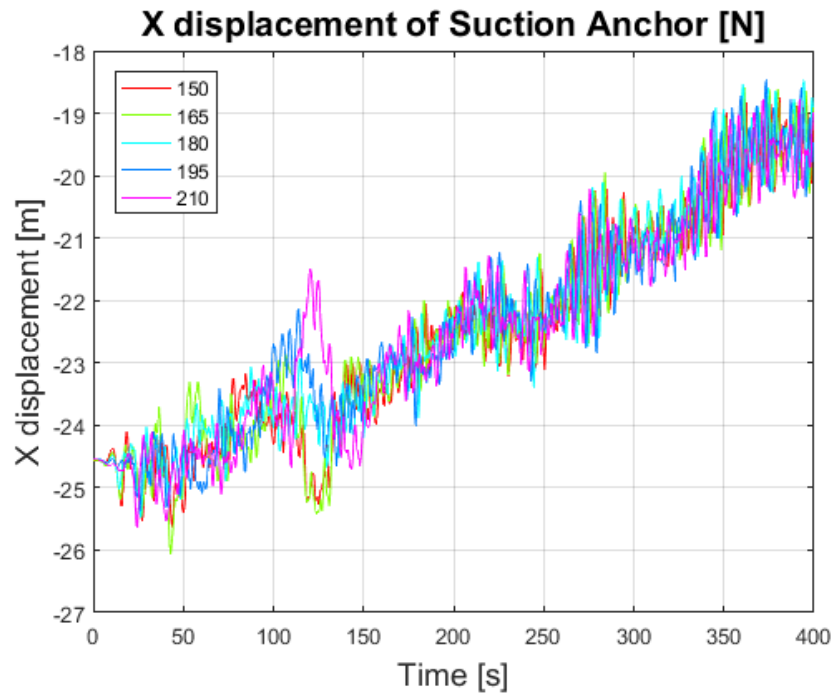
Figure 8.9: X displacement of suction anchor

Table 8.8: x displacement statistics

	Max [m]	Min [m]	Mean [m]	Start position [m]	End position [m]	Displacement [m]
150	-18.7	-25.6	-22.6	-24.5	-19.1	-5.4
165	-18.6	-26.1	-22.5	-24.5	-18.9	-5.6
180	-18.5	-25.5	-22.4	-24.5	-18.9	-5.6
195	-18.5	-25.4	-22.4	-24.5	-19.5	-5.0
210	-18.8	-25.6	-22.5	-24.5	-19.0	-5.5

As with the tension in the main sling, we see there is small difference in the displacement of the suction anchor. The differences in displacements are less than 1 m, and is therefore of little significance.

Further in the report, the incoming wave direction of 180 degrees will be used.

8.3. Wave data

As the installation is a weather restricted operation, looking at the effect of the Wave height and the wave period is important. For installation at 4000 m water depth, there are two offshore locations that are of interest. That is, the Gulf of Mexico and Offshore Brazil.

According to OTC 24304, the Brazilian Sea is classified as having an onerous environmental condition. Here, rapid load transfer is required, and an operational window of 24 hours may be appropriate. The Brazilian Sea is a harsh area due to the swell condition. South Gulf of Mexico is classified as having a mild environment condition, and an operational window of 72 hours is considered conservative. This does not take account for the hurricanes in the Gulf of Mexico. Both of the operational windows are within the operation time for the deployment in this report. (Zhang & Jeong, 2013)

To investigate the weather conditions in the South Gulf of Mexico and in Offshore Brazil, two different weather characteristics using distributions of 30-year wave height, Hs, and Peak period, Tp, is used from the OTC 24304. The Pelotas area has been chosen for Offshore Brazil, because it is the area of the Brazilian sea with the deepest water depth, 1007m. (Zhang & Jeong, 2013)

The weather conditions used are shown in Figure 8.10 and Figure 8.11 below. In the South Gulf of Mexico, the weather conditions shown in Figure 8.10 have a variation of Hs between 0.25 and 1.75, and a Tp between 2 and 8. For the Pelotas basin in Offshore Brazil, shown in Figure 8.11, are higher for both Hs and Tp. Hs varies between 1 and 4, and Tp between 5 and 13.

South Gulf of Mexico	Offshore Brazil, 1007m
Figure 8.10: Weather characteristics for Gulf of Mexico. (Zhang & Jeong, 2013)	*Figure 8.11: Weather characteristics for Offshore Brazil, Pelotas area. (Zhang & Jeong, 2013)*
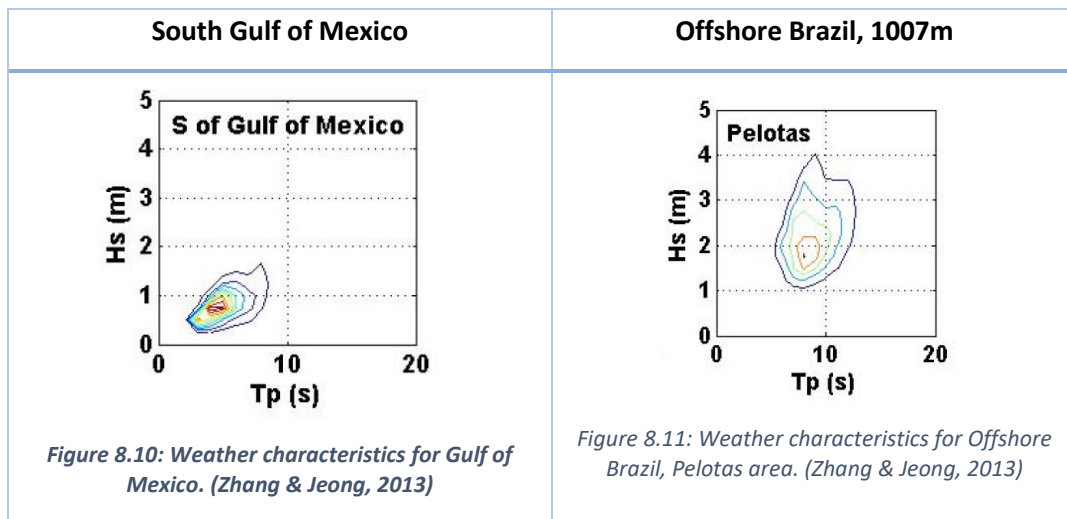
The weather characteristics data in Table 8.9 and Table 8.10 below are interpreted form Figure 8.10 and Figure 8.11 shown above.

Table 8.9: Weather characteristics in S Gulf of Mexico

Hs	Tp								
1			7	8					
1.5		6	7	8	9	10	11		
2	5	6	7	8	9	10	11	12	
2.5		6	7	8	9	10	11	12	13
3		6	7	8	9	10	11	12	13
3.5			7	8	9	10			
4				8	9	10			

Table 8.10: Weather characteristics in Offshore Brazil, Pelotas

Hs	Tp						
0.25		3	4				
0.5	2	3	4	5	6	7	
0.75		3	4	5	6	7	8
1		3	4	5	6	7	8
1.25			4	5	6	7	8
1.5				5	6	7	8
1.75							8

8.3.1. Condition sets

To investigate the effect of the Hs and Tp during the installation process, five different condition sets have been chosen. Three in which are taken from Offshore Brazil and Figure 8.11, and two in which are taken from the South Gulf of Mexico and Figure 8.10. From the weather characteristics from offshore Brazil, the data with Hs above 2.5 have been neglected as the maximum Hs for lifting operations are at 2.5 for light installations.

Wave height	wave period	position
1.5	6	180
1.5	7	180
1.5	8	180
1.5	9	180
1.5	10	180
1.5	11	180

Wave height	wave period	position
2	6	165
2	7	165
2	8	165
2	9	165
2	10	165
2	11	165
2	12	165

Wave height	wave period	position
2.5	6	165
2.5	7	165
2.5	8	165
2.5	9	165
2.5	10	165
2.5	11	165
2.5	12	165
2.5	13	165

8.3.1.2. Gulf of Mexico

Wave height	wave period	position
0.5	2	165
0.5	3	165
0.5	4	165
0.5	5	165
0.5	6	165
0.5	7	165

Wave height	wave period	position
1	3	165
1	4	165
1	5	165
1	6	165
1	7	165
1	8	165
1	9	165

8.3.2. Results

To investigate the effect of Hs and Tp we will look at the tension in the main liftwire, and the x displacement of the installed object. After the suction anchor reaches 3990 m water depth, the winch is stopped to let the suction anchor naturally fall into place. This is to investigate how far the suction anchor is able to correct its x position by itself.
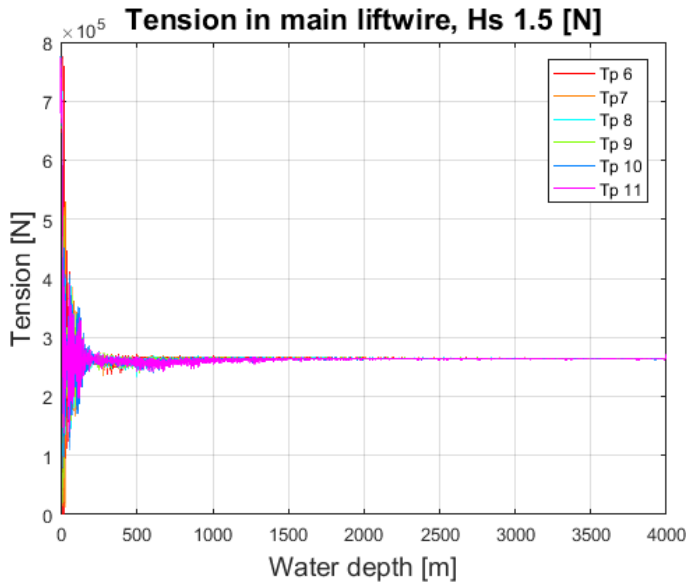
Figure 8.12: Tension in main liftwire, Hs 1.5
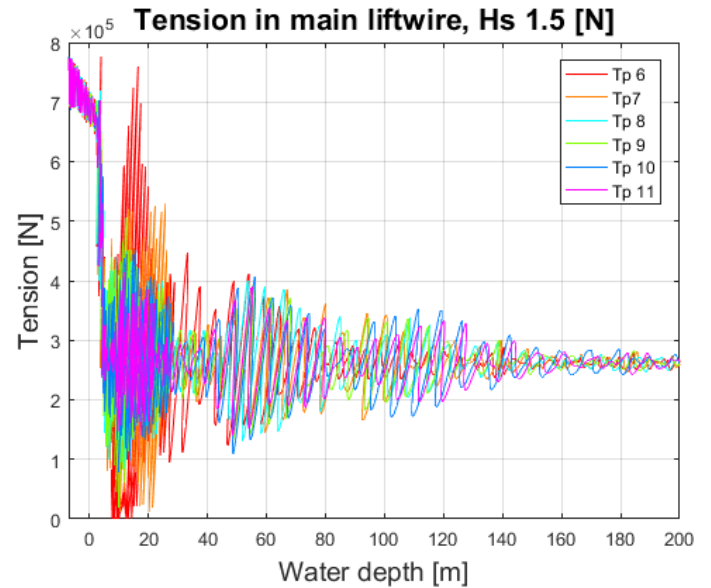
Figure 8.13: Tension in main liftwire (Hs 1.5), zoomed in

When investigating the effect of the wave period, Tp, there is a trend in the upper part of the water column. Figure 8.13 show the first part of the water column zoomed in to get a clearer view of the effect of the tension in the main liftwire. There is a pattern where the standard deviation and maximum tension decreases with increasing Tp, for the splash zone. The maximum tension shown in Table 8.11 is the maximum tension in the main liftwire when the suction anchor is lifted above water level. As for the mean tension, the effect is the same as in the upper part of the water column where the mean tension decreases with increasing Tp.

Table 8.11: Tension in main liftwire data, Hs 1.5

Tp	Max [N]	Min [N]	Mean [N]	Standard deviation [N]
6	775543	528	268974	50779
7	775663	11059	268803	48670
8	776265	84916	268580	46491
9	776344	19083	268317	46729
10	775596	78373	268002	46881
11	774535	139018	267697	45652

The effect of wave period is only significant for the upper part of the water column. However, the results are not of significance as the maximum tension in the liftwire is minimalistic affected by the wave data.

Since the effect of the Tp was small for the tension in the main liftwire, it is important to look at the effect with regards to the x displacement of the suction anchor.
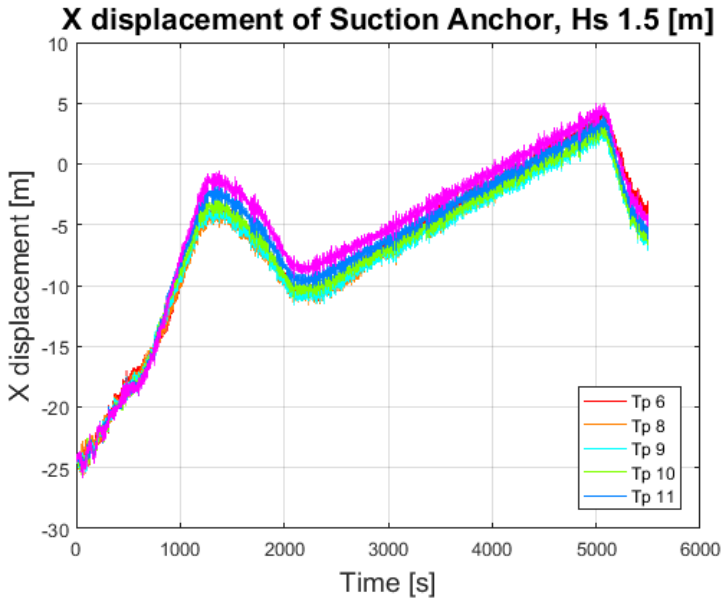
Figure 8.14: X displacement of suction anchor with respect to time. Hs 1.5
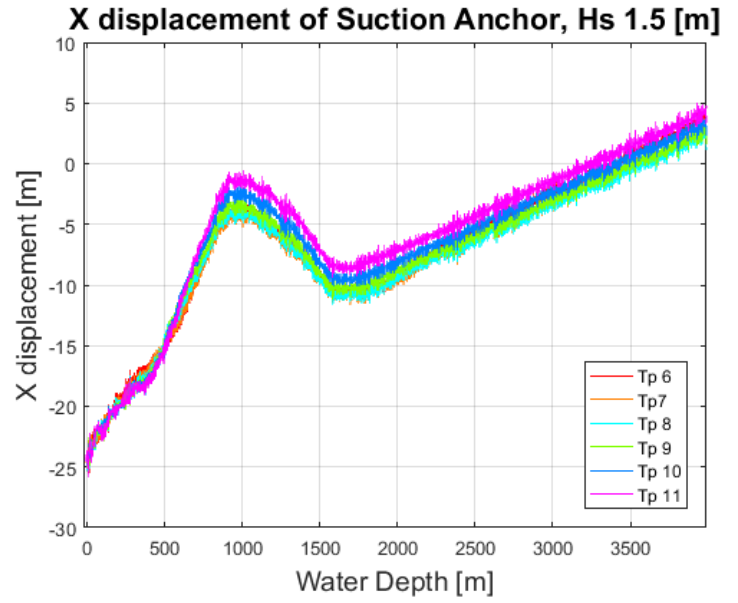
Figure 8.15: X displacement of suction anchor with respect to water depth. Hs 1.5

Figure 8.14 show the x displacment of the suction anchor with repect to time. This is to show the effect of the x displacment after the winch is stopped. Figure 8.15 show the x displacment of the suction anchor with respect to water depth. The effect shown in Figure 8.14 is neglected here because the fall back effect happens at approximately the same water depth of aournd 4000m., and is therefore not visualized in the graph.
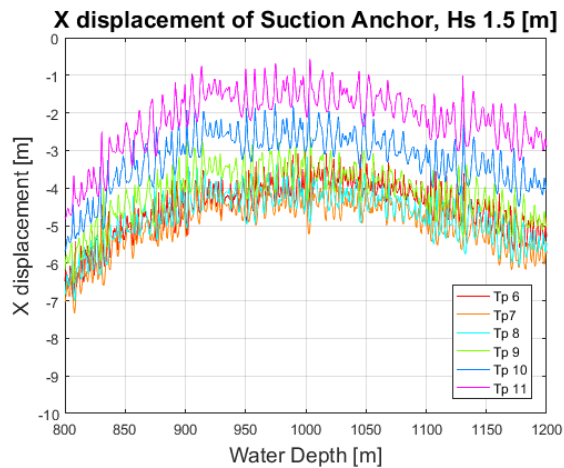
Figure 8.16: X displacement (Hs 1.5), zoomed in

121

From Figure 8.14 there is a trend with increasing x displacement with increasing Tp. Figure 8.16 is zoomed in on the first peak where the trend is clear from Tp 8 to Tp 11, but there is no trend for Tp 6 and Tp 7. Looking at the statistics in Table 8.12, the same trend is seen whereas the maximum and mean x position for Tp 8 to Tp 11 increases. For Tp 6 and Tp 7 the effect is opposite, where the displacement is increasing with decreasing Tp.

Table 8.12: x displacement statistics, Hs 1.5

Tp	Max [m]	Min [m]	Mean [m]	Standard derivation [m]
6	4.8	-25.4	-6.6	6.9
7	3.6	-25.6	-7.2	6.5
8	3.2	-25.4	-7.3	6.5
9	3.3	-25.6	-6.9	6.6
10	4.1	-25.5	-6.3	6.8
11	5.1	-25.8	-5.6	7.1

Table 8.13: x displacement data for Hs 1.5

Tp	Start position [m]	End position 1 [m]	Displacement 1 [m]	End position 2 [m]	Displacement 2 [m]
6	-24.5	4.8	29.3	-3.4	21.1
7	-24.5	3.6	28.1	-5.3	19.3
8	-24.5	3.2	27.7	-5.9	18.6
9	-24.5	3.3	27.8	-6.1	18.4
10	-24.5	4.1	28.6	-5.2	19.3
11	-24.5	5.1	29.6	-4.3	20.2

End position 1 in Table 8.12 is the maximum displacement, and end position 2 is the position at the end of the simulation. Displacement 1 is the displacement form the start position to the highest peak shown in Figure 8.14, the largest displacement is for Tp 11 and the second largest is for Tp 6. Displacement 2 is the x displacement from the start position to end position 2. Here the displacement has decreased for all the wave periods. Tp 6 has the largest displacement for displacement 2. The reduction in x position from end position 1 to end position 2 lays at approximately 9m for all wave periods.
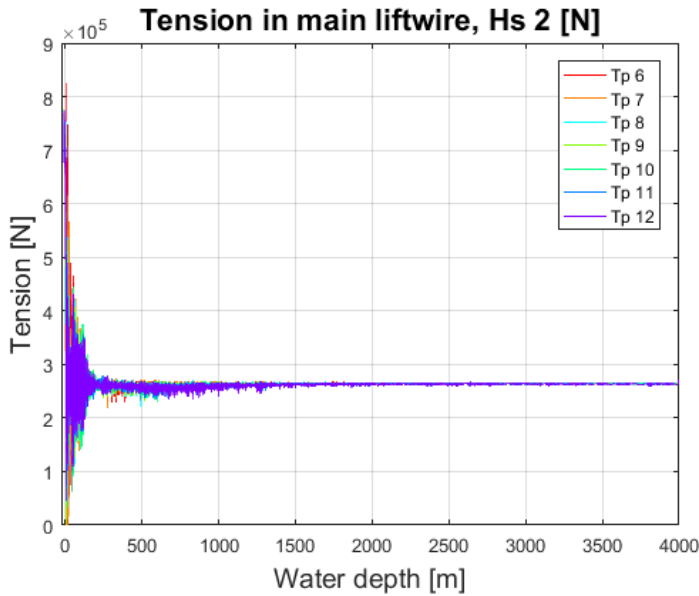
Figure 8.17: Tension in main liftwire, Hs 2
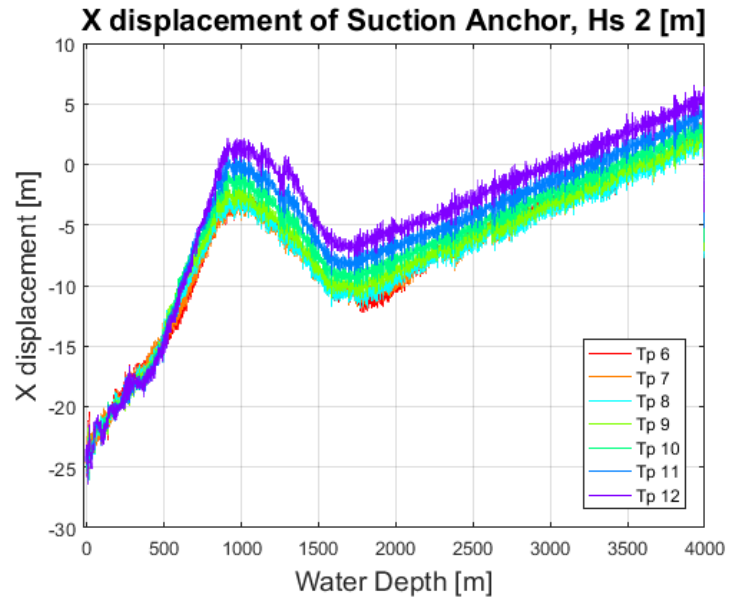
Figure 8.18: X displacement of suction anchor, Hs 2

The effect on the tension for condition set two, where the wave height is increased to 2 m, is similar to that of condition set two. The highest maximum tension is larger than for condition set 1, because the vessel will be more effected by the waves as the wave height increases. When the vessel is affected, the crane tip motion is also affected, thus the higher maximum tension in air.

Table 8.14: Tension in main liftwire data, Hs 2

Tp	Max [N]	Min [N]	Mean [N]	Standard deviation [N]
6	826361	489	268840	52637
7	775791	466	268635	50657
8	776619	30910	268419	48458
9	776751	1940	268149	47768
10	775765	58772	267826	47707
11	774352	94644	267513	46665
12	775149	44685	267148	47255

Shown in Table 8.14, the mean tension in the liftwire decreases with increasing wave period. For this case the maximum load of the liftwire is affected by the wave weather conditions, and therefore the weather is of more significance than that of the previous condition set.

Table 8.15: x displacement statistics, Hs 2

Tp	Max [m]	Min [m]	Mean [m]	Standard derivation [m]
6	4.0	-25.9	-7.0	6.5
7	3.4	-26.3	-7.2	6.3
8	2.8	-26.2	-7.3	6.3
9	3.1	-26.0	-6.8	6.4
10	4.0	-26.0	-6.1	6.7
11	5.2	-26.3	-5.3	7.1
12	6.5	-26.5	-4.2	7.5

Table 8.16: x displacement data for Hs 2

Tp	Start position [m]	End position 1 [m]	Displacement 1 [m]	End position 2 [m]	Displacement 2 [m]
6	-24.50	4.04	28.54	-4.55	19.95
7	-24.50	3.41	27.91	-5.39	19.11
8	-24.50	2.83	27.33	-6.13	18.37
9	-24.50	3.10	27.60	-6.30	18.20
10	-24.50	3.99	28.49	-5.18	19.32
11	-24.50	5.17	29.67	-4.07	20.43
12	-24.50	6.52	31.02	-3.54	20.96

The effect of the x displacement is also similar to that of condition set 1. However, in this case, the variation between each wave period is larger. For displacement 1, the largest displacement is for Tp 12. For displacement 2, the largest displacement is also Tp 12. In this case, Tp 6 has the third largest displacement for displacement 1 and 2.
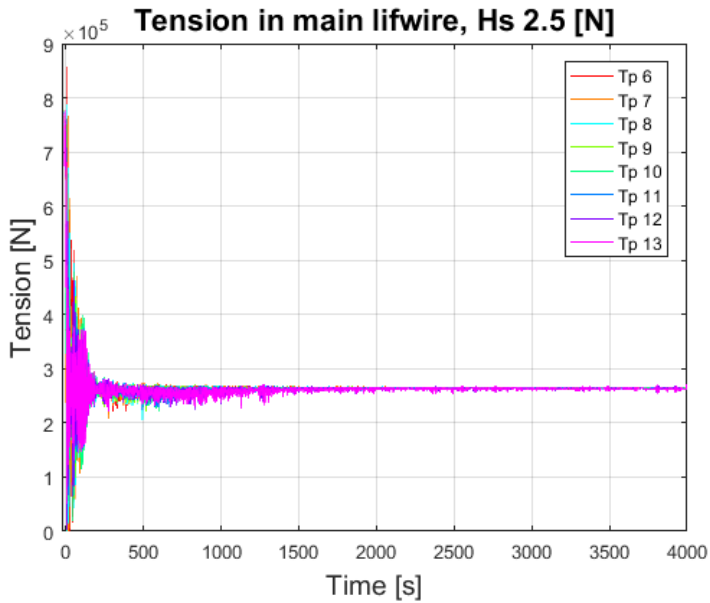
Figure 8.19: Tension in main liftwire, Hs 2.5
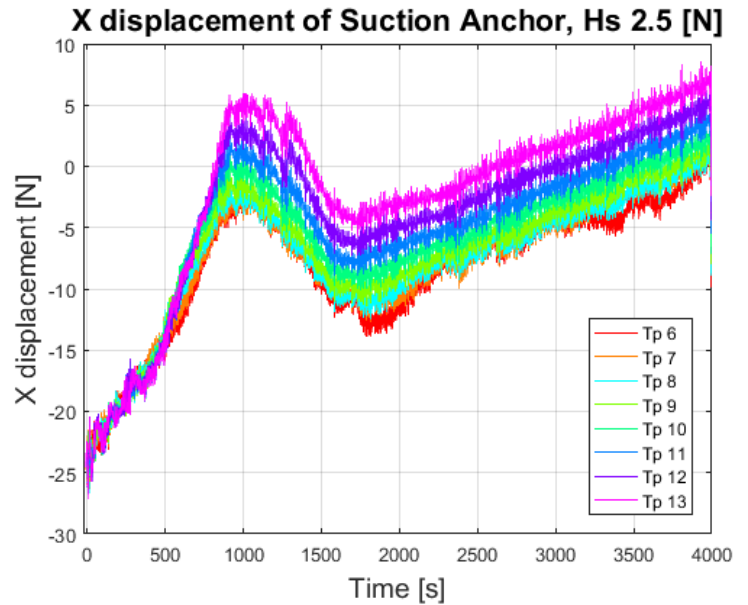
Figure 8.20: X displacement of suction anchor, Hs 2.5

In this case, the highest maximum tension is increased due to the effect of the higher Hs and its effect on the vessel and the crane tip. Therefore, the load on the liftwire is increased and is of more significance. In this case, the same trend is seen where the mean tension decreases with increasing Tp.

Table 8.17: Tension in main liftwire data, Hs 2.5

Tp	Max [N]	Min [N]	Mean [N]	Standard deviation [N]
6	857953	452	268739	54114
7	775841	484	268442	54777
8	788242	547	268211	50971
9	777177	6241	267952	48499
10	775957	12628	267630	49156
11	774616	38101	267297	47808
12	776745	4451	266926	48757
13	778580	51681	266531	47350

Looking at Figure 8.20 and Table 8.18, the variation of the displacements for the different wave periods are larger. The maximum x positions, and the displacements have increased when comparing to the cases with Hs 1.5 and Hs 2. For this case, Tp 6 has the second smallest displacement for both displacement 1 and displacement 2.

Table 8.18: x displacement statistics, Hs 2.5

Tp	Max [m]	Min [m]	Mean [m]	Standard derivation [m]
6	2.0	-25.9	-8.1	5.9
7	2.3	-26.5	-7.7	5.9
8	2.1	-26.7	-7.5	6.0
9	2.6	-26.5	-6.9	6.2
10	3.6	-26.5	-6.0	6.5
11	5.2	-26.8	-5.0	7.0
12	6.7	-27.0	-3.8	7.5
13	8.6	-27.1	-2.3	8.2

Table 8.19: x displacement data for Hs 2.5

Tp	Start position [m]	End position 1 [m]	Displacement 1 [m]	End position 2 [m]	Displacement 2 [m]
6	-24.50	2.00	26.50	-7.28	17.22
7	-24.50	2.33	26.83	-6.54	17.96
8	-24.50	2.10	26.60	-6.92	17.58
9	-24.50	2.58	27.08	-6.92	17.58
10	-24.50	3.56	28.06	-5.48	19.02
11	-24.50	5.17	29.67	-4.06	20.44
12	-24.50	6.72	31.22	-3.52	20.98
13	-24.50	8.56	33.06	-1.23	23.27

The trends in cases 1 through 3 have been similar. The only difference is the effect related to wave period for all cases. There seem to be a pattern switch around the wave period of 6 seconds.

For the two following condition sets, both the wave period and wave height is reduced. This is to simulate weather simulations similar to that of the South Gulf of Mexico as explained in section 0, and to investigate the effect of lower wave periods.
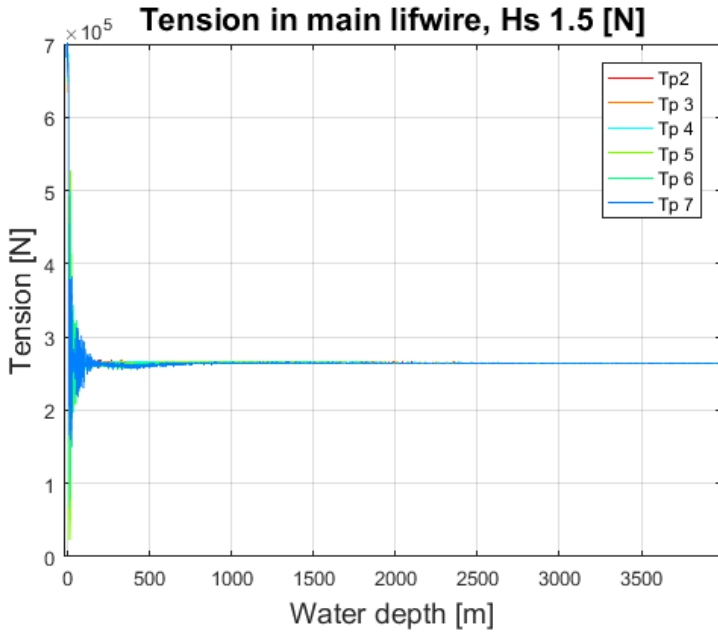
Figure 8.21: Tension in main liftwire, Hs 0.5   *Figure 8.22:X displacement of suction anchor, Hs 0.5*
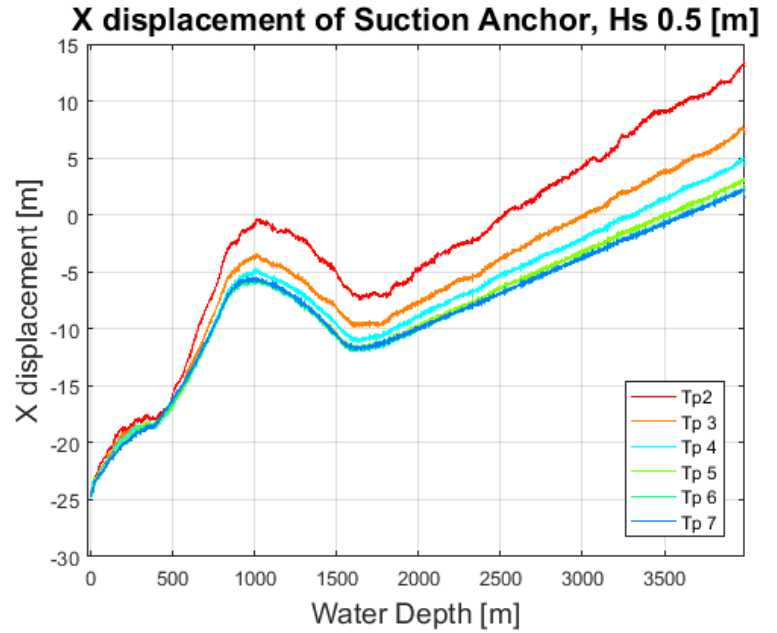
The tension shows the same trend as the for the previous condition sets. The maximum tension in the main liftwire increases with increasing wave period, and the mean tension decreases with increasing wave period. The standard deviation shown in Table 8.20 does not follow a specific pattern. The largest standard deviation of the tension is for wave period 5. The focus in this condition set will be on the x displacement.

Table 8.20: Tension in main liftwire data, Hs 0.5

Tp	Max [N]	Min [N]	Mean [N]	Standard derivation [N]
2	775240	194765	269617	44130
3	775278	209354	269625	44092
4	775257	98287	269548	44504
5	775088	23015	269402	47144
6	775115	66398	269225	45409
7	775382	149809	269020	44982

Observing Figure 8.22, the trend shown in the previous condition sets has clearly switched, as indicated in the previous cases. The displacement is now decreases with increasing wave period, see Table 8.21. The difference in displacement for each wave period has increased compared to the previous cases. The largest displacement is for Tp 2 for both displacement 1 and 2, shown in Table 8.22.

Table 8.21: x displacement statistics, Hs 0.5

Tp	Max [m]	Min [m]	Mean [m]	Standard derivation [m]
2	13.4	-24.7	-1.8	9.8
3	7.8	-24.6	-5.2	8.1
4	5.2	-24.8	-6.7	7.3
5	3.3	-24.6	-7.7	6.8
6	2.6	-24.7	-8.0	6.5
7	2.5	-24.8	-8.0	6.5

Table 8.22: x displacement data for Hs 0.5

Tp	Start position [m]	End position 1 [m]	Displacement 1 [m]	End position 2 [m]	Displacement 2 [m]
2	-24.5	13.4	37.9	8.6	33.1
3	-24.5	7.8	32.3	1.8	26.3
4	-24.5	5.2	29.7	-2.5	22.0
5	-24.5	3.3	27.8	-5.5	19.1
6	-24.5	2.6	27.1	-6.7	17.8
7	-24.5	2.5	27.0	-7.0	17.5

8.3.2.5. Condition set 5
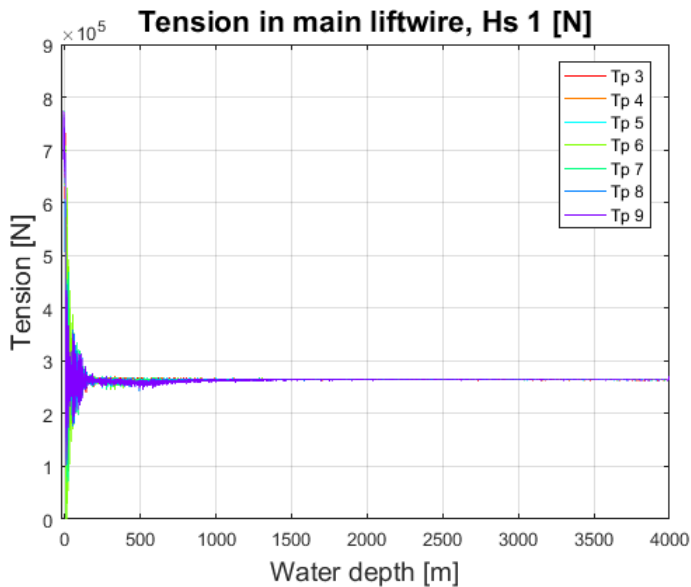
Figure 8.23: Tension in main liftwire, Hs 1
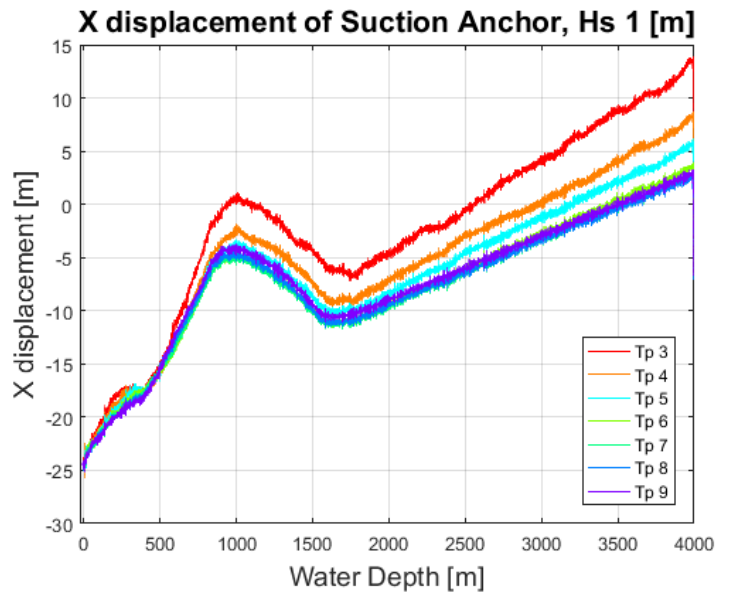
Figure 8.24: X displacement of suction anchor, Hs 1

128

The trend in the tension of the liftwire remains the same as the previous cases. For this condition set, the largest standard deviation for the tension in the main liftwire is for wave period 6.

Table 8.23: Tension in main liftwire data, Hs 1

Tp	Max [m]	Min [m]	Mean [m]	Standard derivation [m]
3	775353	134080	269400	44441
4	775281	18376	269407	45944
5	774940	522	269294	48356
6	774994	554	269110	49603
7	775524	68364	268933	46555
8	775917	102700	268706	45526
9	775956	100718	268443	45510

Looking at the x displacement in Figure 8.24, the trend is similar to that of the previous case. Due to the increase in the wave period, the displacement of the suction anchor increases. For condition set 4 and 5, the difference between displacement 1 and 2 increases with increasing Tp. This means that the suction anchor experiences more trouble with falling into place after the winch is stopped for the smaller wave periods.

Table 8.24: x displacement data, Hs 1

Tp	Max	Min	Mean	start position	End position 1	Displacement 1	End position 2	Displacement 2
2	13.97	-24.81	-1.49	-24.50	13.97	38.47	9.50	34.00
3	8.77	-25.71	-4.55	-24.50	8.77	33.27	2.21	26.71
4	6.15	-25.07	-5.95	-24.50	6.15	30.65	-1.33	23.17
5	3.96	-24.89	-7.18	-24.50	3.96	28.46	-4.58	19.92
6	3.23	-25.05	-7.55	-24.50	3.23	27.73	-5.89	18.61
7	3.06	-25.09	-7.48	-24.50	3.06	27.56	-6.24	18.26
8	3.26	-25.15	-7.12	-24.50	3.26	27.76	-6.27	18.23

8.3.3. Chosen wave data

The effect on the tension of the liftwire were similar for all cases, and was not affected significantly of the wave data. Therefore, the wave data used for further research will be based on the above results for the x displacement. It is important to investigate the worst weather condition the equipment may be installed during, therefore the condition set chosen are the worst cases for the wave displacements from each condition set. The chosen condition set is shown in Figure 8.21 below.

Table 8.25: Condition set for further research

	Hs	Tp
1	1.5	11
2	2	12
3	2.5	13
4	0.5	2
5	1	3

8.4. Horizontal water particle velocity for chosen condition set

To understand the effect of the wave height and the wave period during the installation process, it is important to investigate the horizontal water particle velocity for the chosen condition set shown in Table 8.25. The values in Table 8.28 are calculated with respect to the linear wave theory in section 5.2.

Table 8.26: Input data for horizontal velocity

	Wave conditions				
	1	**2**	**3**	**4**	**5**
Hs	1.5	2	2.5	0.5	1
Tp	11	12	13	2	3
g	9.81	9.81	9.81	9.81	9.81
L	1864.55	2218.97	2604.21	61.64	138.69
k	0.00	0.00	0.00	0.05	0.02
ω	0.57	0.52	0.48	3.14	2.09
ξ_0	0.75	1.00	1.25	0.25	0.50

Using the values in Table 8.26 the horizontal water particle velocity is calculated with respect to the water depth. ξ_0 is half the wave height for each wave condition.

Table 8.27: Horizontal water particle velocity for wave conditions

water depth	Wave conditions				
	1	2	3	4	5
ξ_0	0.00395	0.00442	0.00471	0.04030	0.03564
0	0.00395	0.00442	0.00471	0.03979	0.03537
-500	0.00339	0.00393	0.00429	3.40E-13	1.86E-05
-1000	0.00290	0.00349	0.00391	2.91E-24	9.77E-09
-1500	0.00249	0.00310	0.00356	2.49E-35	5.14E-12
-2000	0.00214	0.00276	0.00325	2.13E-46	2.7E-15
-2500	0.00183	0.00245	0.00296	1.83E-57	1.42E-18
-3000	0.00157	0.00218	0.00270	1.56E-68	7.46E-22
-3500	0.00135	0.00194	0.00246	1.34E-79	3.92E-25
-4000	0.00116	0.00172	0.00224	1.14E-90	2.06E-28

For wave conditions 1, 2 and 3 Table 8.27 show that the wave velocity at the mean water level is about 100 times smaller than the current velocity at the same water depth. As for wave conditions 4 and 5, the wave velocities are only 10 times smaller than the current velocity. Looking at Figure 8.25, below, the wave velocity starts at a higher value for wave conditions 4 and 5, where both wave height and wave period are low, than for wave conditions 1 through 3, where both wave height and wave period are high.
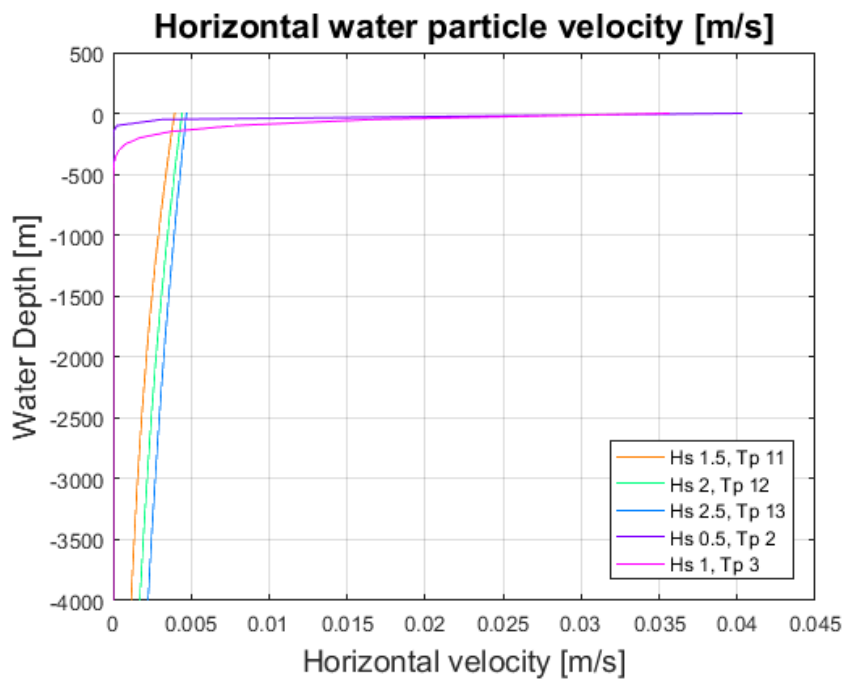
Figure 8.25: Horizontal water particle velocity for all wave conditions to 4000 m water depth

Figure 8.26 show that the horizontal velocity for wave conditions 1 through 3 decreases at a steady state to values of 0.00116, 0.00172 and 0.00244 m/s respectively at 4000 m water depth. On the other hand, for condition sets 4 and 5, shown in Figure 8.27, the horizontal decreases rapidly and reaches zero at water depth of 100 m and 400 m respectively.
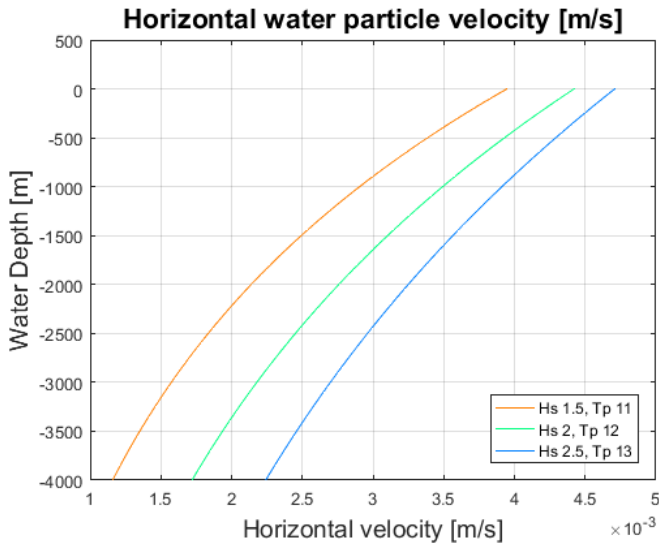
Figure 8.26: Horizontal water particle velocity for all wave conditions 1 through 3 to 4000 m water depth
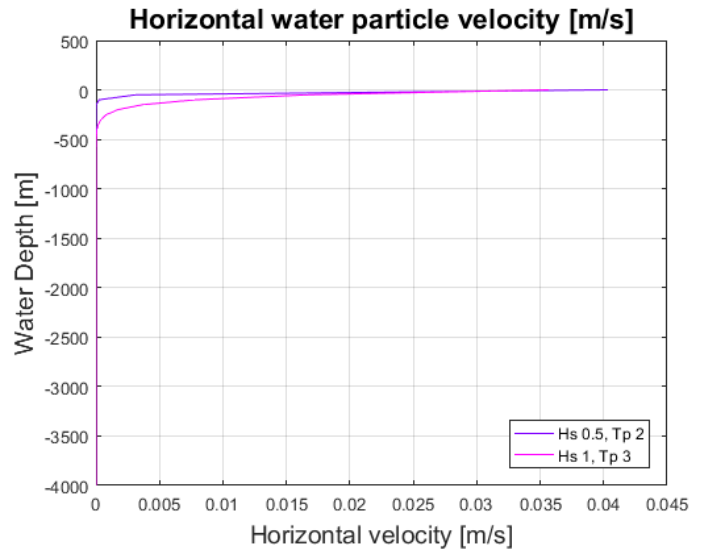
Figure 8.27: Horizontal water particle velocity for wave conditions 4 and 5 to 4000 m water depth

To get a clearer view of the horizontal velocity for wave conditions 4 and 5, a graph of the velocity to the water depth of 100 m were made, shown in Figure 8.28.
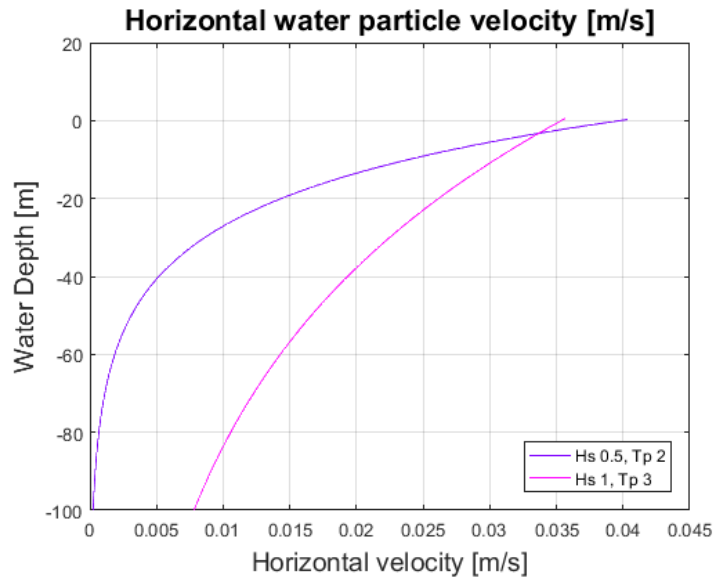
Figure 8.28: Horizontal water particle velocity for wave conditions 4 and 5 to 100 m water depth

Looking at Figure 8.28, condition set 5 which has a higher wave period and wave height, start at a slightly lower velocity than condition set 4. However, the velocity of the water particles decreases more rapidly for wave condition 4 than for 5.

Learning from this, wave conditions with low wave periods will affect the motion of the deployed equipment more in the upper water column than wave conditions with higher wave periods. Wave conditions with high wave periods will affect the motion of the equipment for a much longer period of time, as the horizontal velocity of the water particles decreases less rapidly than for wave conditions with low wave period.

8.5. Natural period

Due to the depth of the installation, it is important to consider the resonance oscillations in then rope. This is important when deciding what weather windows and wave periods are acceptable. Formula of Natural Period:

$$To = 2\pi \sqrt{\frac{(m + m_a)}{EA/L}}$$

Table 8.28: Natural Period data for Equipment

Water depth	Natural Period				
	Suction Anchor 112582 Kg	Well Jumper 13323 Kg	Tubing Head Spool 46145 kg	Valve tree 92347kg	Template 292595 kg
1	0.13	0.05	0.09	0.12	0.21
-1000	4.22	1.45	2.70	3.82	6.80
-2000	5.96	2.05	3.82	5.40	9.61
-3000	7.30	2.51	4.68	6.61	11.77
-4000	8.43	2.90	5.40	7.64	13.59

The masses of the equipment provided in Table 8.28 are the total mass including the mass of the hook and the added mass.

The results for the natural periods of the main liftwire varies according to the total weight of the equipment. Table 8.28 and Figure 8.30 show that the natural period has the widest range for the template, where it varies from 0 and all the way to 13.6s. This means that resonance in the main liftwire may occur

during the installation process in weather conditions with Peak periods between 0s and 13.6. As the equipment is continuously deployed in the water column, the eigen period will vary accordingly. This means that the chance of the main liftwire reaching resonance and lock-in only occurs for short periods, before the treat is over. The problem with resonance in the liftwire may be easily fixed by adding active heave compensation on the system.

The chance of the peak period of the waves being less than 5s is small, especially in offshore Brazil. Therefore, the problem of resonance in the main liftwire when installing the Well jumper and the tubing head spool will be neglected.
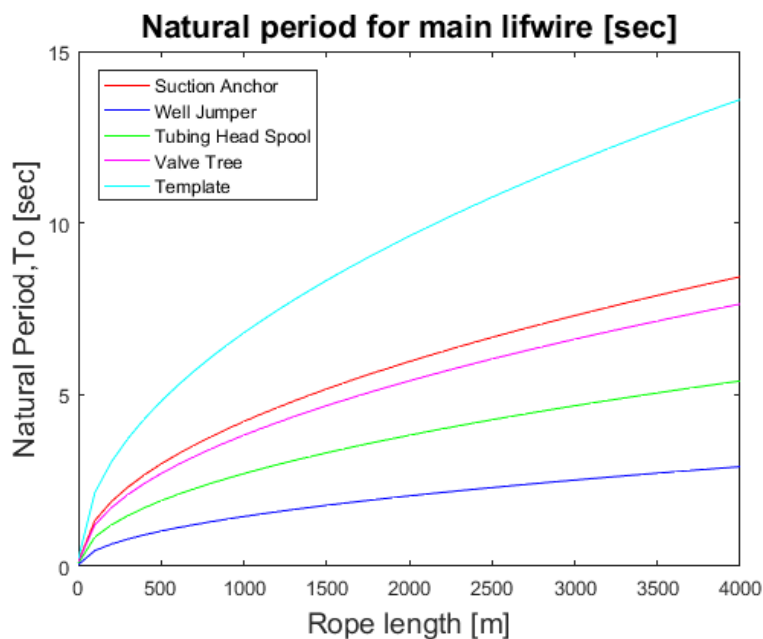
Figure 8.29: Natural period for equipment

8.6. Marine operations

According to DNV-OS-H101, marine operations shall be executed ensuring that the assumptions made in the planning and design process are fulfilled. This section is written with accordance to DNV-OS-H101. (Det Norske Veritas AS, 2011)

The purpose of the operational requirements is to ensure that:

- The (environmental) design criteria are not exceeded during the operation
- The operation is properly manned and organized
- Adequate surveys are performed before- and during the operation

134

- The operation is properly documented

8.6.1. Operation and design criteria

Marine operations may either be classified as weather restricted or as unrestricted. A weather restricted operation shall be of limited duration. In this thesis we will focus on weather restricted operations.

Following are some important definitions for marine operations

8.6.1.1.   Operation reference period - T_R

The operation reference period defines the duration of marine operations.

$$T_R = T_{POP} + T_C$$

T_R = Operation reference period

T_{POP} = planned operation period

T_C = estimated maximum contingency time

The start- and completion points for the intended operation or parts of the operation shall be clearly defined.

8.6.1.2.   Planned operation period - T_{POP}

The planned operation period should normally be based on a detailed schedule for the operation. Estimated time for each task in the schedule should be based on reasonable conservative assessment of experience with same or similar tasks. Frequently experienced time delaying incidents should be included in T_{POP}.

8.6.1.3.   Estimated contingency time - T_C

Contingency time shall be added to cover:

- General uncertainty in he planned operation time
- Possible contingency situations that will require additional time to complete the operation

If T_{POP} uncertainties and required time for contingency situations is not assessed in detail, the reference period should normally at least be taken as twice the planned operation period, i.e. $T_R \geq 2 \times T_{POP}$. An applied contingency time less than 6 hours is normally not accepted.

8.6.2. Weather restricted operations

Weather restricted operations are normally considered marine operations with a T_R less than 96 hours and a T_{POP} less than 72 hours. This is true for the installation time in this report. The planned operation period start point for a weather restricted operation shall normally be defined at the issuance of the last weather forecast.
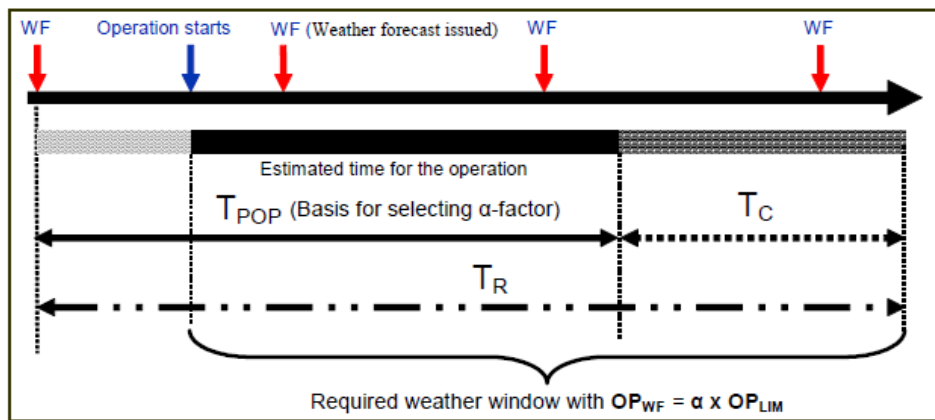
Figure 8.30: Operation periods. (Det Norske Veritas AS, 2011)

The operation shall only be considered completed when the object is in a safe condition. Restricted operations may be planned with environmental design conditions selected independent of statistical data, i.e. set by owner, operator or contractor. The start of weather restricted operations is conditional to acceptable weather forecast.

8.6.2.1. Operational limiting criteria

Limiting operational environmental criteria, OP_{LIM}, shall be established and cearly described in the marine operation manual. The OP_{LIM} shall not be taken greater than the minimum of:

- The environmental design criteria
- Maximum wind and waves for safe working – or transfer conditions for personnel
- Equipment specified weather restrictions
- Limiting weather conditions of diving system (if any)
- Limiting conditions for position keeping systems
- Any limitations identified, e.g. in HAZID/HAZO, based on operational experience with involved vessel(s), equipment, etc.
- Limiting weather conditions for carrying out identified contingency plans

8.6.2.2. *Forecasted- and monitored operational limits, Alpha factor*

Uncertainty in both monitoring and forecasting of the environmental conditions shall be considered. It is recommended that this is done by defining a forecasted operational criterion, OP_{WF}, defined as;

$$OP_{WF} = \alpha \times OP_{LIM}$$

The planned operation time from issuance of the weather forecast to the operation is completed shall be used as the minimum time for selection of the α-factor, shown in Figure 8.30 above.

The following should be used as guidelines for selecting the appropriate α-factor for waves:

- The expected uncertainty in the weather forecast should be calculated based on statistical data for the actual site and the operation schedule, i.e. T_{POP}.
- Reliable wave- and/or vessel response monitoring systems(s) and applied weather forecast level could be considered.

The tables for estimating the alfa factor is given in Appendix I: Alfa factor, DNV-OS-H101.

8.6.3. Weather forecast levels

Based on evaluations of the operational sensitivity to weather conditions and the operational reference period (T_R), a categorization of the operation into weather forecast levels A, B or C shall be made.

- Level A – applies to major marine operations sensitive to environmental conditions.
- Level B – applies to environmental sensitive operations of significant importance with regard to value and consequences.
- Level C – applies to conventional marine operations less sensitive to weather conditions, and carried out on a regular basis.

The list of typical level A, B and C operations are given in DNV-OS-H101 Section 4, page 34. Offshore lifting and subsea installations are typical Level B operations.

For level B operations:

- No meteorologist required on site
- 2 Independent WF sources required, where the most severe weather forecast is to be used
- The maximum WF interval is 12 hours

8.6.4. Calculation example
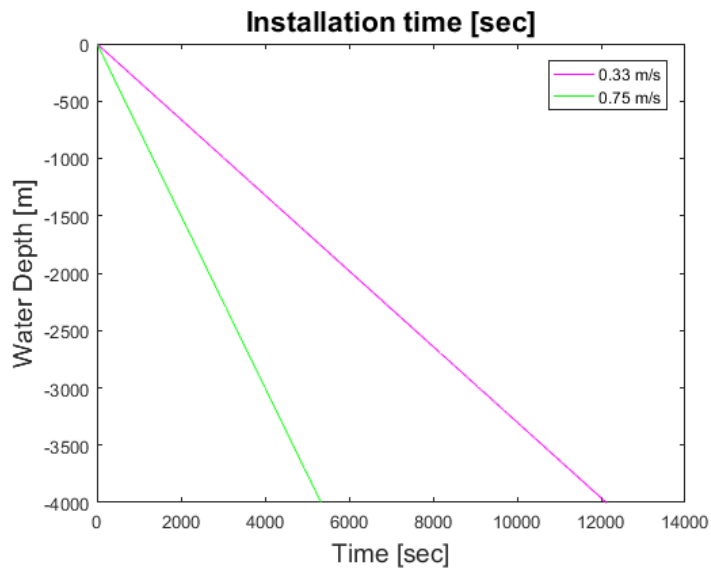
Figure 8.31: Deployment time of equipment to 4000 m

Table 8.29: Deployment time data to 4000 m

Deployment time	0.33 m/s	0.75 m/s
Seconds	12121.21	5333.33
Minutes	202.02	88.89
Hours	3.37 (3 h 22 min	1.48 (1 h 29 min)

Figure 8.31 and Table 8.29 show the installation time for equipment deployed with a winch speed of 0.33 m/s and 0.75 m/s. When considering the full operation time, the time of retrieval of the hook, as well as positioning of the subsea equipment must be taken into account.

Table 8.30: Planned operation time estimate

Planned operational time (hours)	0.33 m/s	0.75 m/s
Lift-off and over boarding	0.5	0.5
Deployment	3.37	1.48
Installation	4	4
Retrieval*	3.37	1.48
Total Planned Operational time, T_{POP}	11.24 hours	7.46 hours

*Assumed to be the same as deployment time.

To find the operational reference period, T_R, we need to calculate the contingency time, T_C. Using the minimum requirement that T_R must be minimum two times the planned operation time, we get an operational reference period of 22.48 and 14.92 hours respectively.

When estimating the alfa factor for the two different cases we use table 4-2 in Appendix I: Alfa factor, DNV-OS-H101. Assuming the design wave height is 2m for Offshore Brazil and 1m for South Gulf of Mexico, we get the following results:

	Alfa Factor
South Gulf of Mexico	0.68
Offshore Brazil	0.80

The alfa factor will be the same for both deployment times as the operational period for both deployment times are less than 12 hours.

Due to the short planned operation times of the installation, the weather will not be an issue if the weather is within the restrictions given for the installation.

9. Results and discussion

9.1. Steel versus fibre rope

Simulations deploying the suction anchor to 4000 m water depth using two different main liftwires were conducted. One simulation using fibre rope as main liftwire and one using steel wire as main liftwire. Both installations are installing a suction anchor with an accumulated mass of 70 tonnes, se section XX, in an environment with a wave height of 2 m and a wave period of 6 s. All values of tension in the results chapter are refers to the tension in the main liftwire at the cranetip. In this section the results from thee two simulations are provided and discussed to find the most optimal method.

9.1.1. Tension in the main liftwire
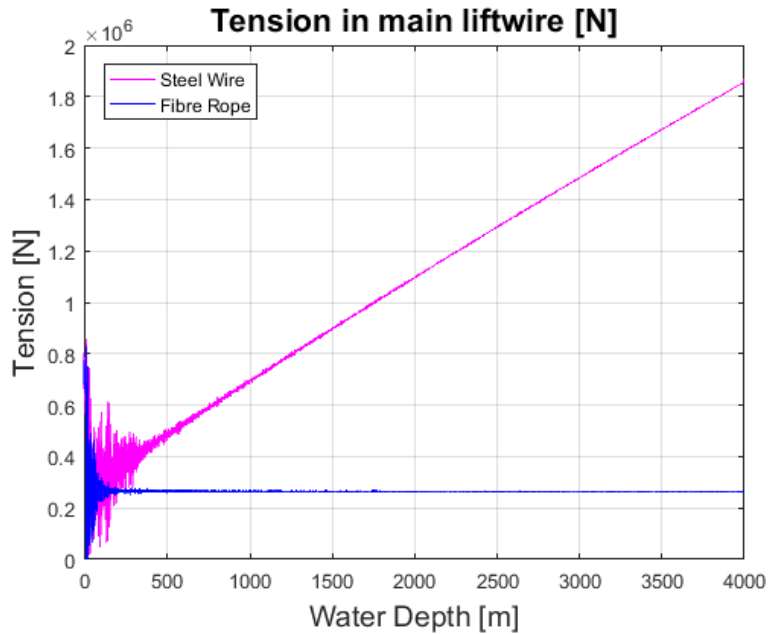
Figure 9.1: Tension in main liftwire, fibre rope vs steel wire

Table 9.1: Statistics of tension in main liftwire, fibre rope vs steel wire

	Max [N]	Min [N]	Mean [N]	Standard deviation [N]
Steel wire	1866991	12458	1131036	502161
Fibre rope	826361	489	269744	52503
Difference	1040630	11969	861292	449657

Figure 9.1 shows the difference in the tension in the main liftwire when using fibre rope or steel wire. As expected, the tension in main liftwire when using steel wire increases with increasing water depth. The

tension in the rope is proportional to the weight of the main liftwire. As the weight of the steel wire increases with increasing water depth, the tension in the main liftwire will also increase accordingly. The results simulated by SIMO fits the theory in section 3.1.1, and Figure 9.1 correlates to Figure 6.12 in section 6.4.2. The maximum tension in the main liftwire using steel wire is more than 1 million N higher than when using fibre rope. The maximum tension in the main liftwire when using fibre rope, see Table 9.1, refers to the tension before deployment, when the suction anchor is above sea level. The maximum tension in the main liftwire using fibre rope in the time interval of 75 to 490s (5m to 37m water depth) is calculated to find the maximum tension when the suction anchor is completely deployed in water. The results for both steel and fibre rope are given in Table 9.2. Considering the maximum tension for steel wire, Table 9.1, and the new maximum tension for fibre rope, Table 9.2, the difference in maximum tension is now 1.1 million N.

Table 9.2: Statistics for upper water column, time interval 75:190s (5 to 37 m depth)

	Max [N]	Min [N]	standard deviation [N]
steel wire	854600	12458	191800
Fibre rope	747380	489	183150
difference	107220	11969	8650

Table 9.3 show the difference in tension at water depth of 2000 m compared to the water depth of 4000 m. The difference in tension is small for deployment using fibre rope, due to the natural buoyancy of the fibre rope in water, the difference in tension between 2000 m and 4000 m is -772 N. However, for steel wire, the difference between 2000 m and 4000 m is approximately 750 thousand N.

Table 9.3: Tension in main liftwire, 2000 m and 4000 m water depth

	Tension at 2000 m [N]	Tension at 4000 m [N]	Difference [N]
Steel wire	1100077	1852228	752151
Fibre rope	265168.5	264396.6	-771.9
Difference	834908.5	1587831	752922.9

When installing equipment to 4000 m using fibre rope, the SWL of the crane must be a minimum of 84 tonnes when installing a suction anchor with a mass of 70tonnes. The restriction of the crane is due to the tension of the main liftwire when the installed equipment is above sea level, therefore the restriction of installation depth is not due to the tension in the main liftwire caused by the water depth of the

installation. The fibre rope crane used in these simulations has a 125 tonnes SWL or 250 tonnes SWL when used in two fall configuration.

The SWL of the crane must be at least 112 tonnes when installing to a water depth of 2000 m using steel wire, and 190 tonnes when installing to a water depth of 4000 m. When removing the weight of the suction anchor, the SWL of the crane must be at least 42 tonnes at 2000 m and 120 tonnes at 4000 m due to the weight of the steel wire alone.

9.1.2. X displacement

Shown in section 9.1.1, the differences in tension using steel wire and fibre rope are significant. This section explores the effect of the x displacement for the two different types of main liftwires.
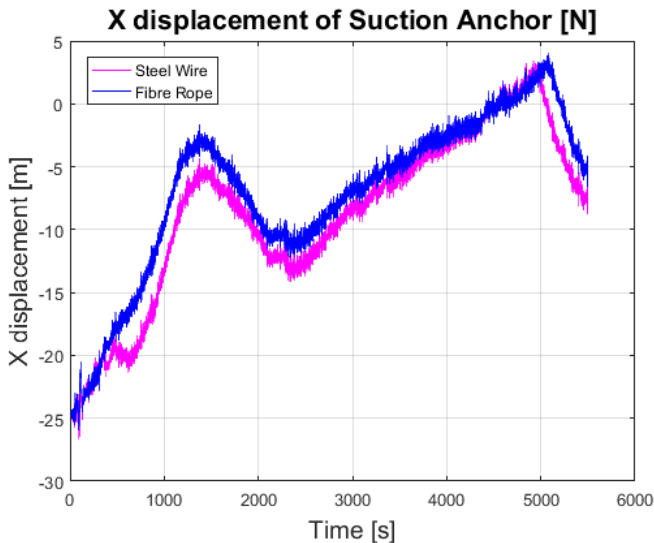
Figure 9.2: x displacement of suction anchor with respect to time
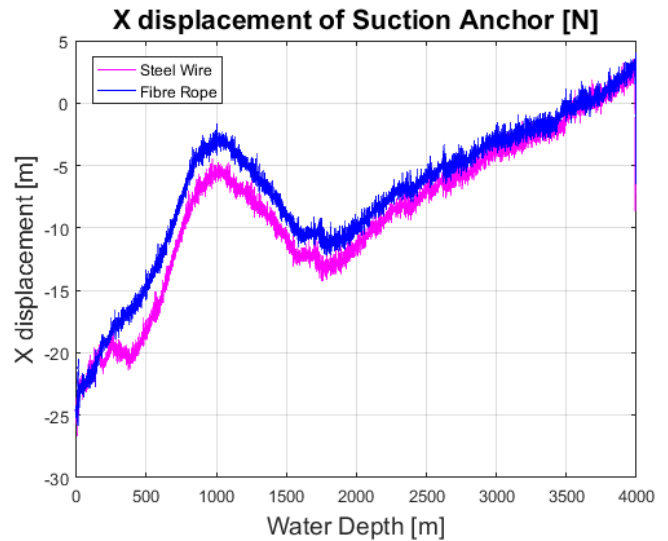
Figure 9.3: x displacement of suction anchor with respect to water depth

Figure 9.2 shows the x displacement of the suction anchor with respect to simulation time. Once the suction anchor reached a water depth of 3990 m, the winch was stopped. This happened at 4938s when using steel wire and 5065.5 s when using fibre rope, see Table 9.8. Looking at Figure 9.2 one sees that the suction anchor slowly starts falling back to its original x position once the winch is stopped, for both cases.

Table 9.4: data of x positions for suction anchor

	Start position	Max	End position
Fibre rope	-24.50	4.04	-4.55
steel wire	-24.50	3.47	-6.74

Table 9.4 shows the different x positions of the suction anchor at the different stages of the deployment. The start position is the position the suction anchor is modelled to start from. The maximum x position is the position in which the x displacement is at its maximum. In this simulation case, the maximum x position of the suction anchor is reached just before the winch is stopped. The end position is the x position the suction anchor ends up at after it has been allowed to fall closer to its original start position. The data for the end position is taken from the very end of the simulation at the time step of 5500 seconds. From this, it is shown that the effect of the weight of the two different main wirelines is minimal. Due to the added weight of the steel wire, the suction anchor reaches 3990 m a couple minutes faster, which then allows it to fall earlier back to its x position. Hence, the smaller x displacement.

Figure 9.3 shows the x displacement of the suction anchor with respect to water depth. The graph stopped at 4000 m water depth, and the effect of the fall back is not included. Looking at Table 9.5, the difference in maximum x displacement is just 0.5 meters for the two different cases. There is minimal effect of the x displacement with respect to main liftwire properties and weight in water.

Table 9.5: statistics for x displacement of the suction anchor

	Max [m]	Min [m]	Mean [m]	Standard deviation [m]	Start position [m]	Displacement [m]
Fibre rope	4.04	-25.90	-7.01	6.46	-24.50	28.54
steel wire	3.47	-26.66	-8.62	6.73	-24.50	27.97

Looking at the x displacement at 2000 m water depth and at 4000 m water depth, Table 9.6 shows that the difference between the two main liftwires are minimal for both 2000 m and 4000 m. The difference is less than 1 m for both water depths. However, the difference in x displacement between 2000 m and 4000 m are 13.58m and 12.97 for steel wire and fibre rope respectively. It would therefore be easier to position the equipment at the correct x position when installing at 2000 m than for 4000 m water depth.

Table 9.6: X displacement of suction anchor, 2000 m and 4000 m

	X displacement at 2000 m [m]	X displacement at 4000 m (3990 m) [m]	Difference [m]
Steel wire	-11.22	2.36	13.58
Fibre rope	-10.41	2.55	12.97
Difference	-0.81	-0.19	0.61

9.1.3. Z displacement

Looking at the z displacement, the time takes for the suction anchor to reach the desired water depth is investigated.
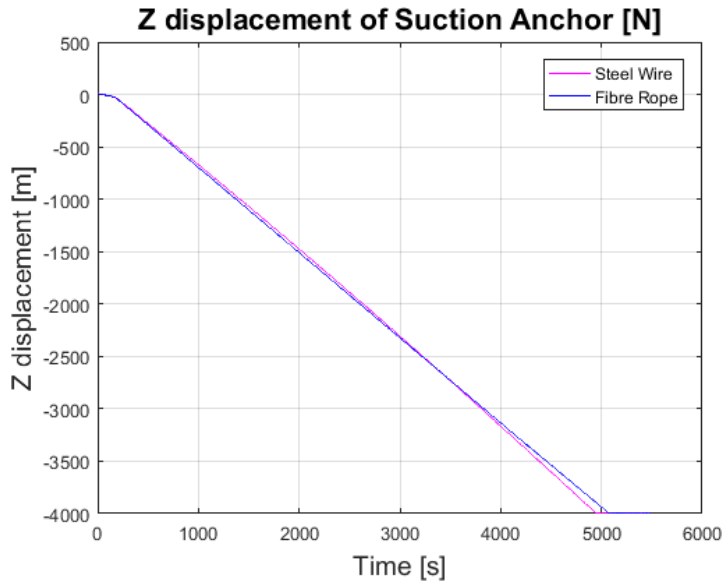
Figure 9.4: z displacement of suction anchor

When installing to a water depth of 2000 m, the deployment takes 44 minutes when using steel wire as the main liftwire, and 43 minutes when using fibre rope, see Table 9.7. There is only one minute separating the two cases, hence the effect of the liftwire properties is not significant for the selection of the main liftwire.

Table 9.7: Deployment time to 2000 m water depth

material	Deployment time [s] (2000 m)	Deployment time [h] (2000 m)
Steel Wire	2634.5	0.73 (44 min)
Fibre rope	2604	0.72 (43 min)

The time it takes for the suction anchor to reach 4000 m approximately doubles for both cases, compared to the time to reach 2000 m. The fibre rope case used 1 hour and 25 minutes, whereas the steel wire cases used 3 minutes less.

Table 9.8: Deployment time to 3990 m water depth

material	Deployment time [s] (4000 m)*	Deployment time [h] (4000 m)
Steel Wire	4938	1.37 (1 h 22 min)
Fibre rope	5065.5	1.41 (1h 25 min)

*Time it reaches 3990 m

When deciding between using fibre rope or steel wire as the main liftwire at an installation depth of 4000 m, the tension in the main liftwire during the deployment is of the biggest concern. The added weight in water of the steel wire causes an addition of 120 tonnes to the SWL of the deployment system. On the other hand, the weight of the fibre rope stays the same throughout the deployment of the equipment and no extra mass is added to the SWL of the deployment system.

9.2. Deployment of tubing head spool using fibre rope
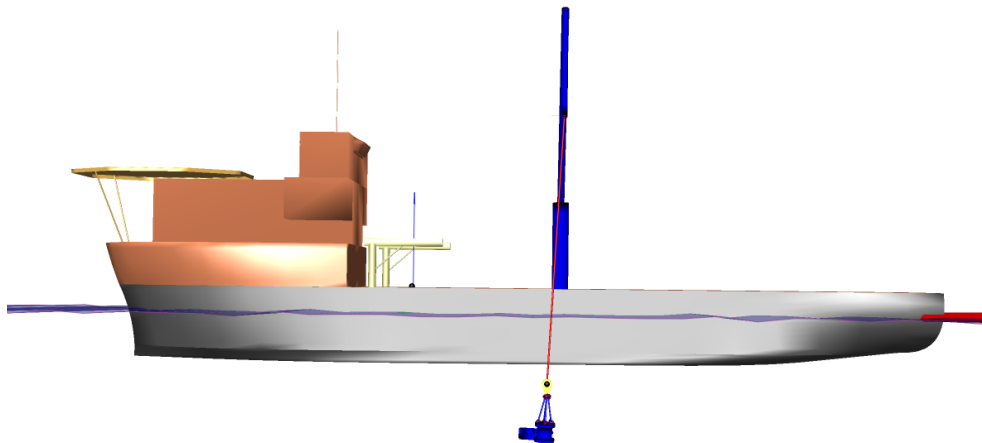
Figure 9.5: deployment of Tubing Head Spool using crane

The investigate the reliability of the SIMO model and simulation, the calculation of the weight of the object, the buoyancy force and the static weight of submerged object have been calculated and shown in Table 9.9 below. The calculations are conducted with respect to the theory in sections 5.3.1 and 5.3.2. The accumulated mass and volume of the model is retrieved from the SIMO model. The tension in the liftwire in air should be approximately the same as the weight of the object, and the tension in the liftwire in water should be approximately the same as the static weight of the submerged object.

146

Accumulated mass [kg]	26238
Accumulated volume [m³]	15.52
Weight of tubing head spool [N]	257395
Weight of hook [N]	39240
Total weight in air [N]	296635
Buoyancy force [N]	156047
Static weight of submerged object [N]	140587

9.2.1. Tension
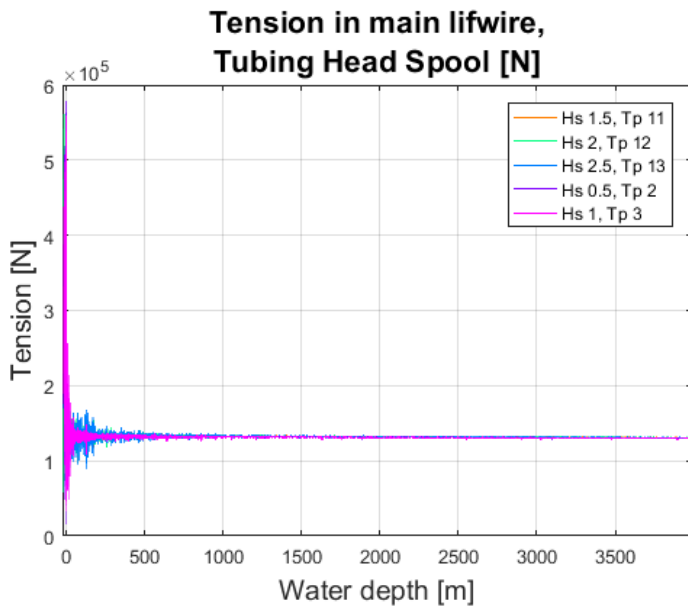
Figure 9.6: Tension in main liftwire, tubing head spool
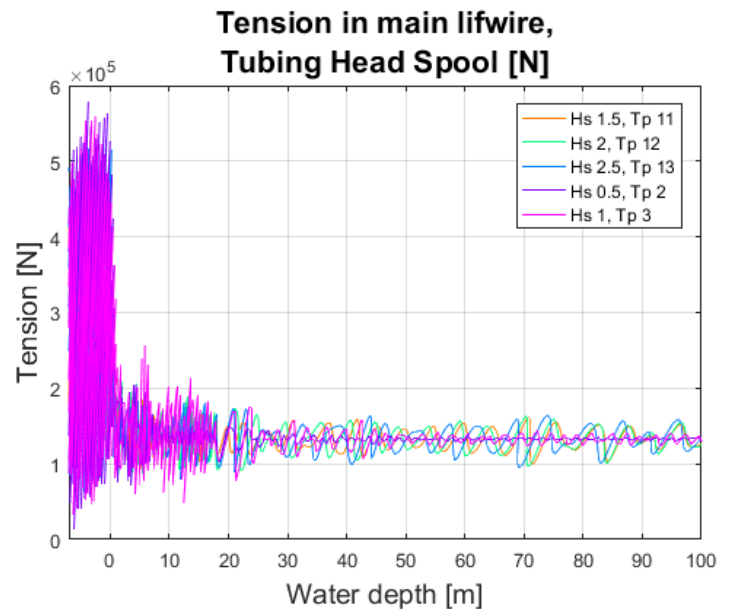
Figure 9.7: Tension in main liftwire, tubing head spool, to 100 m water depth

The tension of the main liftwire when installing the tubing head spool is shown in Figure 9.6 and Figure 9.7 with respect to the deployed water depth. Table 9.10, below, shows the statistics for the tension in the main liftwire as the tubing head spool is deployed to a water depth of 4000 m. The mean values are close for all five wave conditions. The mean value is close to that of the static weight of the submerged object, 140587 N. The reason why the mean value is slightly lower might be because SIMO takes account for the added mass and drag forces as the equipment is deployed though the water column. The results from the SIMO model is therefore in compliance with the theory.

Table 9.10: statistics of tension in main liftwire, tubing head spool

	Max [N]	Min [N]	Mean [N]	Standard deviation [N]
1	455796	88941	134562	22964
2	562064	58232	134536	24477
3	532345	62116	134513	26618
4	578328	14632	133893	26819
5	559194	33211	133529	26113

As the tension is somewhat constant after the splash zone and the upper column, the focus has been on the first 100 meters deployed, see Figure 9.7. Looking at Figure 9.7 one may notice that the highest variation, as well as the maximum and minimum value of the tension, shown in Table 9.10, are all from when the tubing head spool is lifted in air. To check if the values in the air matches the calculated value for the weight of the tubing head spool in air, see Table 9.9, one must look at the start value for the tension provided in Table 9.10. The start value is the tension of the main liftwire at 0 seconds. The tension value at the start position correlates with the calculated total weight of the hook and the tubing head spool. The calculated total weight of the system does not take into account the weight of the fibre rope, which is 120N/m.

To investigate the tension during the deployment in air, the mean and standard deviation was found for the time interval from 1:90s (16.98m to 0.2416m). The new statistics data are shown in Table 9.11 below. The standard deviation of the five wave conditions vary between 88 to 135 thousand N. The large differences in tension during the lifting in air, compared to the deployment though the water column, might be a result of the higher weight of the system in air and the motions experienced by the crane tip.

Table 9.11: statistics for TIME INTERVAL 1:90s

	Mean [N]	Standard deviation [N]
1	286700	87980
2	287100	107800
3	287300	135500
4	287500	139700
5	286700	127000

To investigate the difference between deploying to 2000 m and 4000 m, Figure 9.8 and Figure 9.9 shows the tension at the two water depths. The differences in the tension is minimal, but one can see that the variation in tension is less at 4000 m than at 2000 m. This might be caused by the effect of the wave conditions, explained in section 8.4. We also see that the tension is slightly smaller at 4000 m than at 2000 m. This is due to the fact that the weight of the fibre rope is set to -3N/m as it is deployed in the water column, meaning the buoyancy of the rope reduced the total weight and therefore the total tension of the system.
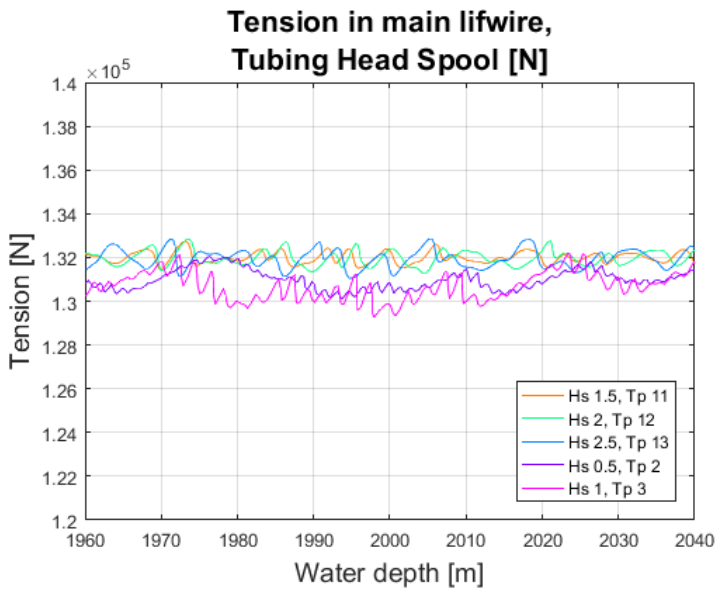
Figure 9.8: Tension in main liftwire at 2000 m, Tubing head spool
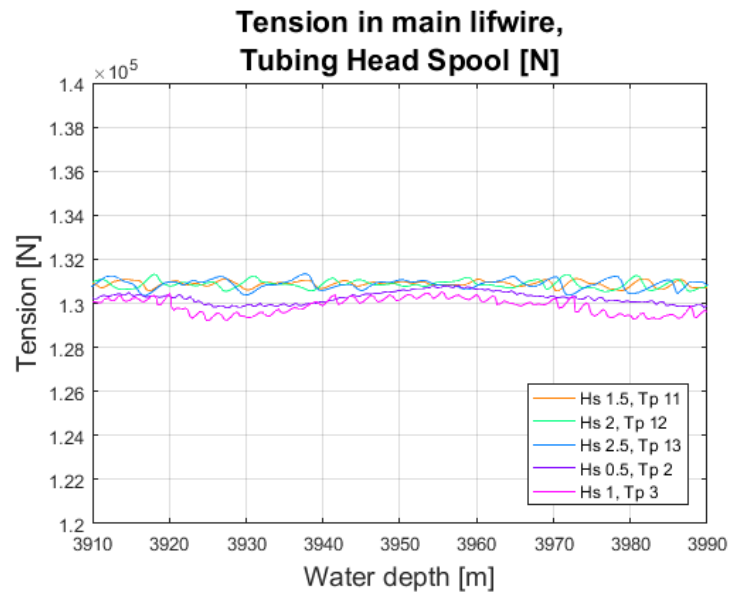
Figure 9.9: Tension in main liftwire at 4000 m, Tubing head spool

The values in Table 9.12 shows that the differences in tension varies with the different wave conditions. The largest difference between the tension at 4000 m and 2000 m is about -1500 N for wave conditions 1. The smallest difference is for wave condition 5. This correlates with the horizontal water particle velocity for the different wave conditions. For wave condition 5, the effect of the waves is neglected form when the installed equipment reaches about 100 m water depth.

Table 9.12: tension in main liftwire, 2000 m and 4000 m water depth, tubing head spool

	Tension at 2000 m [N]	Tension at 4000 m (3990 m) [N]	Difference [N]
1	132225	130759	-1466
2	132409	130899	-1510
3	131212	130726	-486
4	130633	130005	-628
5	129760	129622	-138

149

There is minimal effect of the tension in the main liftwire when using fibre rope as the main liftwire and deploying at five different wave conditions.

9.2.2. X displacement

The previous section demonstrated that the tension remained constant thought out the deployment process. In this section we are investigation the results for the x displacement of the tubing head spool.
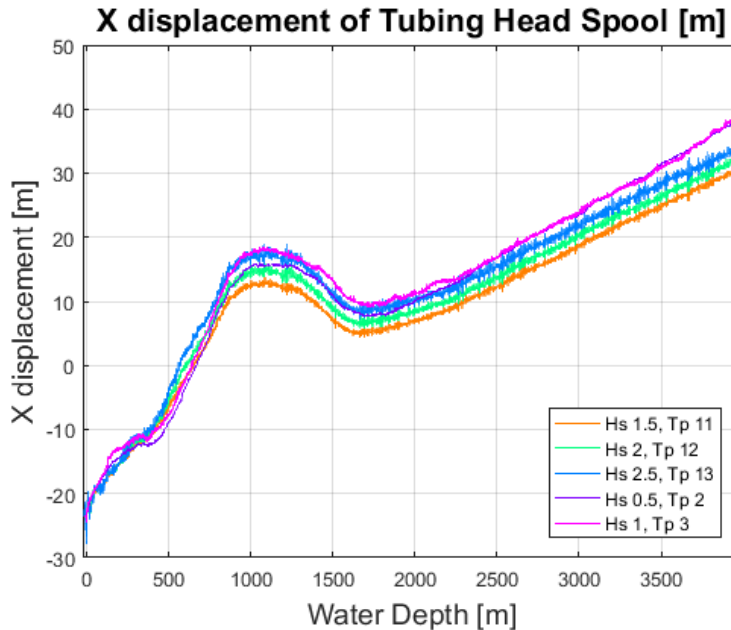
Figure 9.10: X displacement of Tubing head spool

The x displacement of the tubing head spool is shown in Figure 9.10 for all five wave conditions. The tubing head spool start at a x position of -24.5m. As the current is acting in the positive x direction, one sees that the x displacement of tubing head spool acts in the positive x direction as well. The horizontal water particle velocity due to the waves acts in the negative x direction, see section 8.4. From the mean water level to the water depth of 1400 m the current varies up in down in velocity, after 1400 m the current continues at a constant, low velocity. The effect of the current variation of velocities are seen in Figure 9.10.

Table 9.13 shows that the displacement in the positive x direction largest for wave condition 1 and smallest for wave condition 2. The differences might be a result of the horizontal water particle motions for wave conditions 1 through 3 acts in the negative x direction for a longer period of time that for wave conditions 4 and 5.

Table 9.13: Statistics of x displacement of tubing head spool

	Max [m]	Min [m]	Mean [m]	Standard deviation [m]	Start position [m]	Displacement [m]
1	33.34	-25.40	10.24	13.81	-24.50	57.84
2	35.24	-26.52	11.70	14.20	-24.50	59.74
3	36.93	-27.65	13.40	14.64	-24.50	61.43
4	41.35	-24.42	13.80	16.17	-24.50	65.85
5	42.51	-24.42	14.70	15.90	-24.50	67.01

As a contrast to the small differences in tension at 2000 and 4000 meters water depth, there is a clear difference in the x displacement at the two water depths in Figure 9.10. Figure 9.11 and Figure 9.12 show the displacement of the tubing head spool at 2000 m and 4000 m respectively. The variance of the x displacement is similar for both water depths. The difference between wave conditions 1 thought 3 is also similar for both cases. What is noticeable Figure 9.11 and Figure 9.12 are the x displacements for wave condition 4 and 5. At 2000 m the displacement in wave conditions 4 and 5 are similar to the three other conditions and increase at the same phase. However, closer to 4000 meters water depth they are farther apart from the other conditions and are increasing at a higher phase. This correlates to the water depth were the tubing head spool is no longer affected by the horizontal water particle velocity in the negative x direction for the different wave conditions.
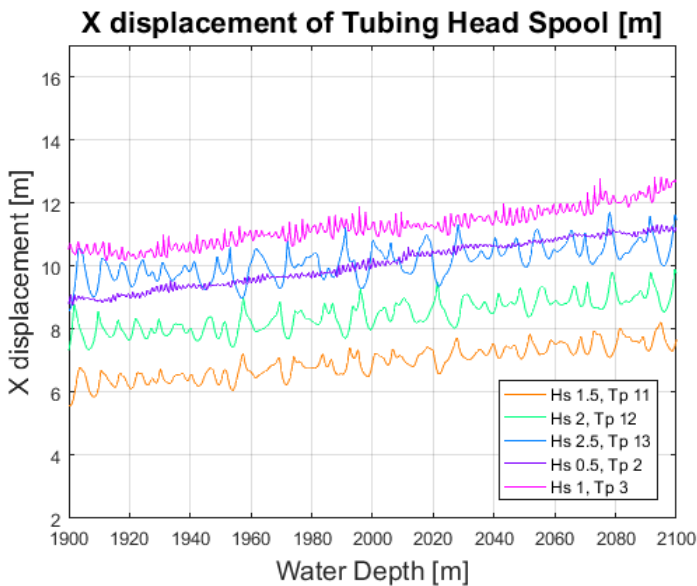
Figure 9.11: X displacement of tubing head spool at 2000 m
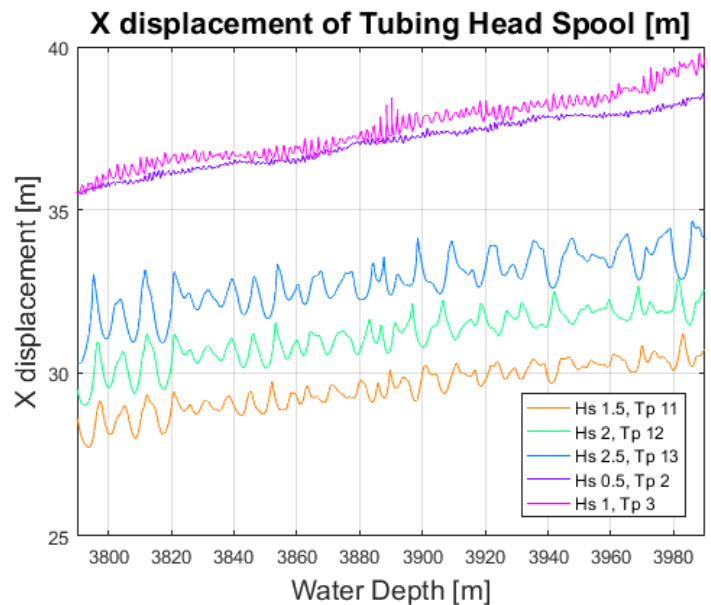
Figure 9.12: displacement of tubing head spool at 4000 m

Looking at the difference in x displacement from 2000 m to 4000 m, the difference is at about 24 meters for wave conditions 1 through 3 and at about 28 meters for wave condition 4 and 5. The additional x displacement at 4000 m makes it more challenging to position the tubing head spool after it has been deployed. At 2000 m the total x displacement of the tubing head spool for the different wave conditions lay between about 31m and 36m, whereas the displacement at 4000 m lies between about 55m and 64m.

Table 9.14: x displacement of tubing head spool, 2000 and 4000 m water depth

	X displacement at 2000 m [m]	X displacement at 4000 m (3990 m) [m]	Difference [m]
1	7.03	30.71	23.68
2	8.15	32.52	24.37
3	10.79	34.07	23.28
4	10.24	38.39	28.15
5	11.40	39.68	28.27

9.2.3. Y displacement
There are no current or waves acting in the y direction. However, other factors may come into play.
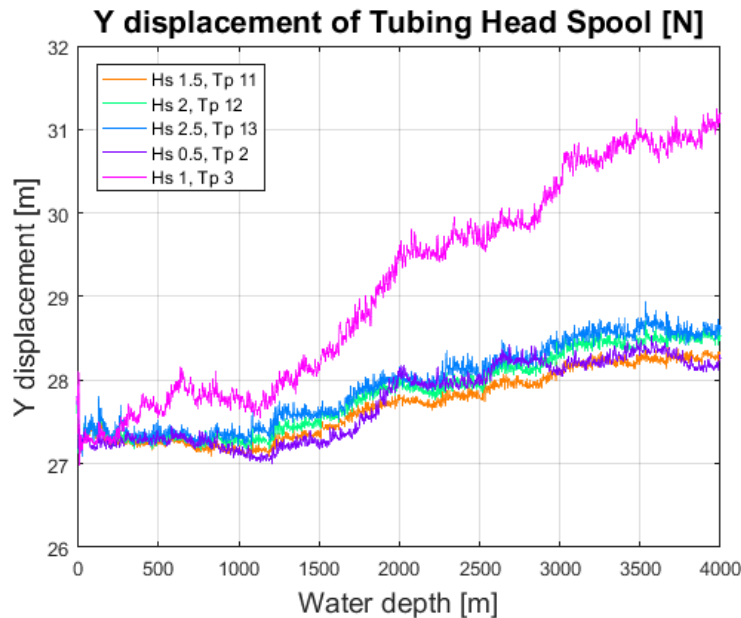
Figure 9.13: Y displacement of suction anchor

Unlike the x displacement where the displacement is large, the y displacement for the different wave conditions lies between 1 and 4 meters. We see from Figure 9.13 the there is a slight displacement in the positive y direction. This might be because the tubing head spool is not symmetric across the y axis.

	Max [m]	Min [m]	Mean [m]	Standard deviation [m]	Start position [m]	Displacement [m]
1	28.44	27.08	27.72	0.41	27.50	0.94
2	28.84	27.01	27.87	0.48	27.50	1.34
3	29.01	27.07	27.97	0.50	27.50	1.51
4	28.53	27.00	27.76	0.47	27.50	1.03
5	31.50	26.99	29.20	1.33	27.50	4.00

9.2.4. Z displacement

The z displacement shows the time it takes for the tubing head spool to reach the desired water depth of 4000 m. For this case the winch was not stopped before the tubing head spool reached 4000 m, and there is small variance in the z displacement caused by the heave period of the vessel. The heave motion of the tubing head spool is negligible as it is deployed though the water column, but will be present once the deployment is stopped.
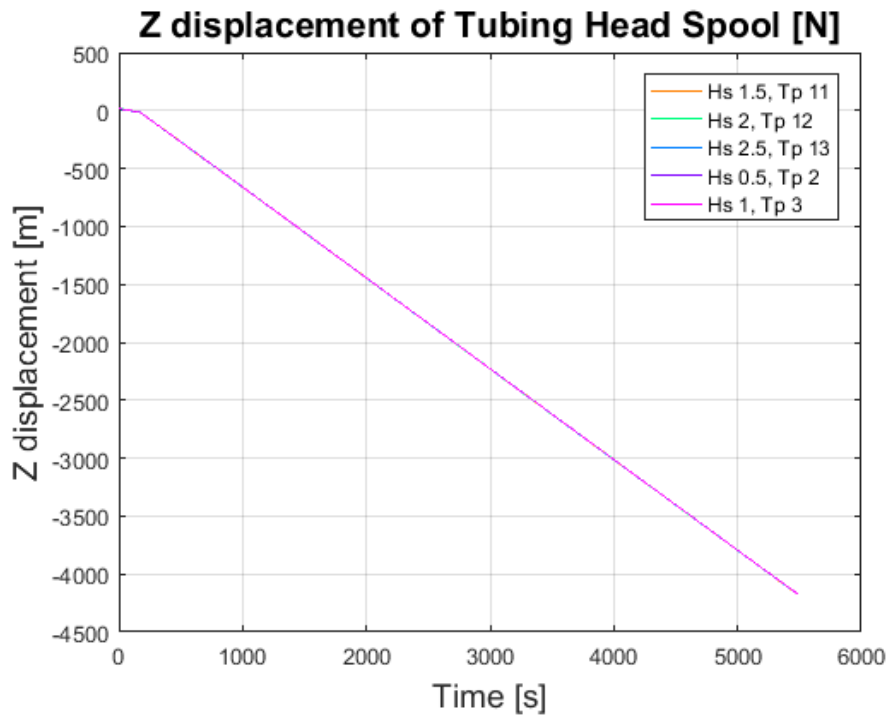
For all the five wave conditions the deployment takes 1 hour and 28 minutes for the tubing head spool to reach the water depth of 4000 m. The time it takes to 2000 m is about half the time.

	Z displacement time to 4000 m [s]	Z displacement time to 4000 m [hours]
1	5264	1.46 (1 hour 28 minutes)
2	5264	1.46 (1 hour 28 minutes)
3	5264	1.46 (1 hour 28 minutes)
4	5265.5	1.46 (1 hour 28 minutes)
5	5265	1.46 (1 hour 28 minutes)

9.2.5. Rotation

The last factors investigated for the tubing head spool is the rotation of the x-, y- and z-axis. The rotation about the x-axis is the roll motion, the rotation about the y axis is the pitch motion and the rotation about the z axis is the yaw motion. See Figure 5.1in section 5.1.

9.2.5.1. X rotation

The x rotation of the tubing head spool is roll motion of the tubing head spool as it is deployed.

Figure 9.14: x rotation of the tubing head spool with respect to time

Figure 9.15: x rotation of the tubing head spool with respect to time, for time interval 0:400s

Looking at Figure 9.14, one can see that the roll motion is larger when the tubing head spool is lifted in air, and in the upper water column. The area where the roll motion is largest is when it is deployed though the splash zone and in the upper water column. This is the area where the tubing head spool is most affected

154

by the different wave conditions. Figure 9.15 shows the first 400 seconds of the simulation where the tubing head spool is deployed from about 17 meters above the mean water level to a water depth of about 190 meters. At about 80 seconds, the tubing head spool starts to deploy though the splash zone, where the variance, maximum and minimum values of the x rotation are at its largest.

From Table 9.16 we see that wave condition 5 has the largest maximum, minimum and standard deviation, as seen in orange in Figure 9.15. The worst rotation is between -20.6 degrees and 9.6 degrees. The reason why the rotation is larger in the negative direction is due to the non-symmetric geometry of the tubing head spool.

Table 9.16: Statistics for x rotation of tubing head spool

	Max [deg.]	Min [deg.]	Mean [deg.]	Standard deviation [deg.]
1	3.60	-7.41	-2.12	0.47
2	5.74	-9.15	-2.12	0.63
3	5.14	-11.31	-2.12	0.59
4	6.75	-11.16	-2.31	0.64
5	9.62	-20.57	-2.46	1.08

9.2.5.2.   Y rotation

The y rotation is the pitch motion of the tubing head spool as it is deployed trough the water column.
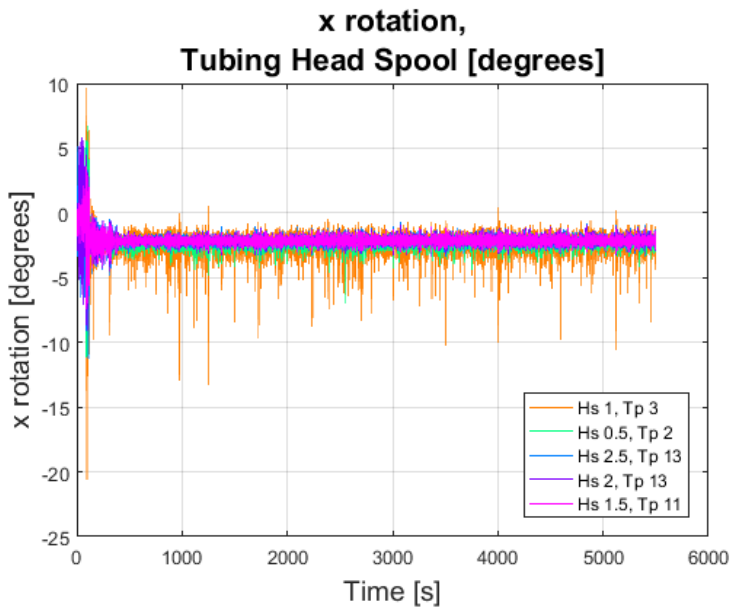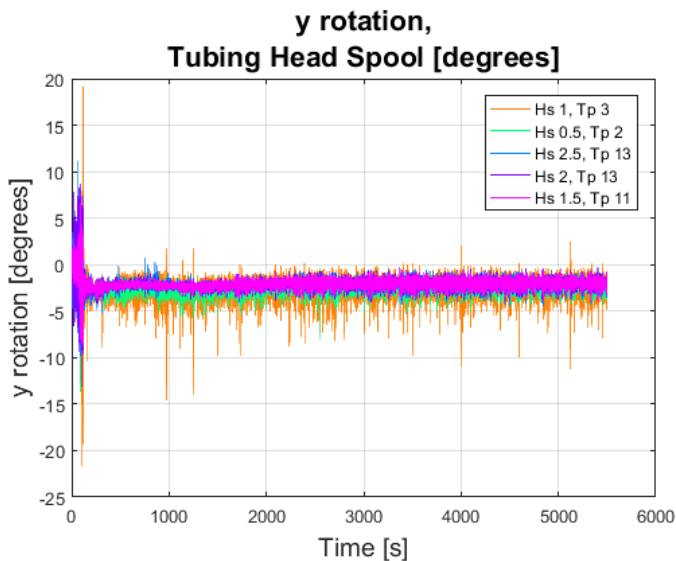

Figure 9.16: y rotation of the tubing head spool with respect to time
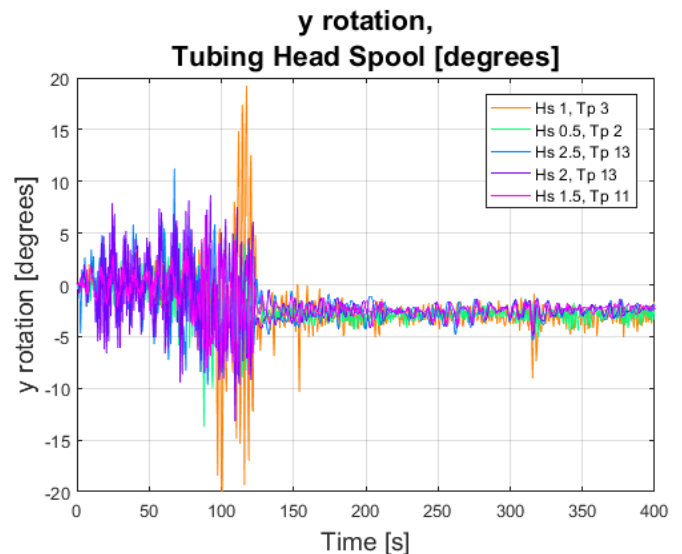
Figure 9.17: y rotation of the tubing head spool with respect to time, for time interval 0:400s

155

The trends are somewhat the same as for the x rotation, where the rotation is largest in the splash zone and the upper water column, and is highest for wave condition 5. However, for wave condition 5, the minimum and maximum rotation is almost the same values, which might indicate that the tubing head spool is more symmetric about the y-axis than the x-axis. Figure 9.17 shows that the average rotation about the y-axis lay between 0 and -5 degrees, therefore the tubing head spool is not quite symmetric about the y-axis. The shift in rotation from +/- 0 degrees to 0/-5 degrees might be caused by a shift in the centre of force in the system caused by the buoyancy force. As explained in section 7.5, the slings between the hook and the tubing head spool is located about the centre of gravity of the tubing head spool in air.

Table 9.17: statistics for y rotation of tubing head spool

	Max [deg.]	Min [deg.]	Mean [deg.]	Standard deviation [deg.]
1	6.64	-8.70	-2.10	0.64
2	8.61	-13.11	-2.12	0.84
3	11.18	-9.67	-2.14	0.81
4	5.45	-13.61	-2.47	0.81
5	19.13	-21.64	-2.66	1.45

9.2.5.3.   Z rotation

The z rotation of the tubing head spool is the yaw motion of the tubing head spool.

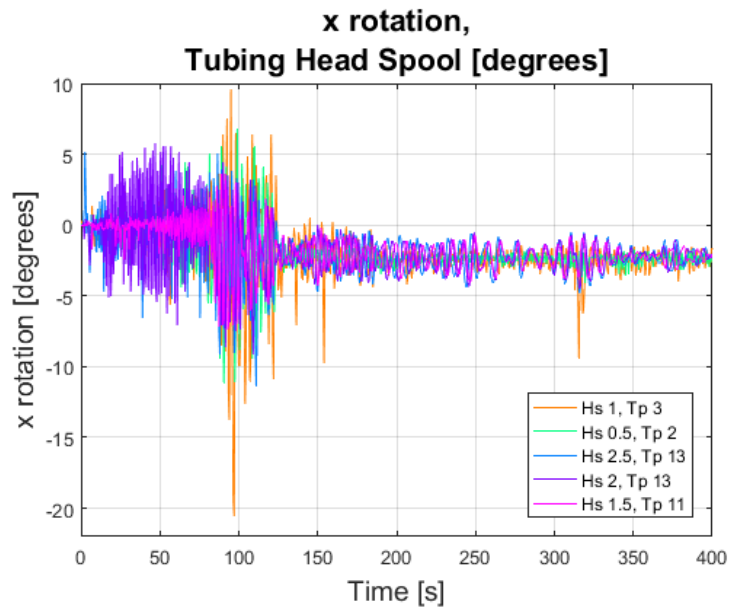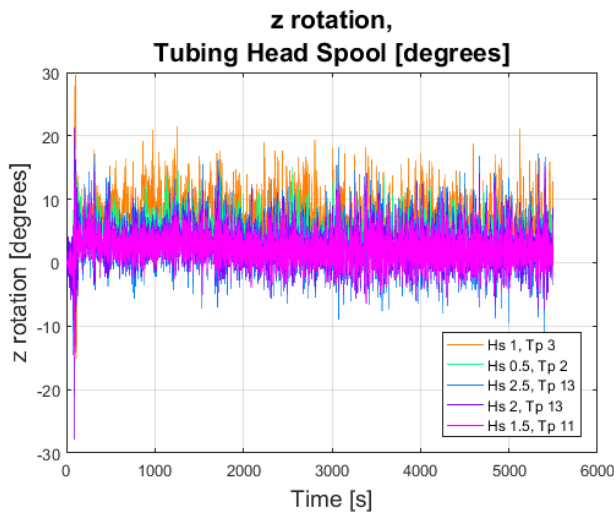*Figure 9.18: z rotation of the tubing head spool with respect to time, for time interval 0:400s*
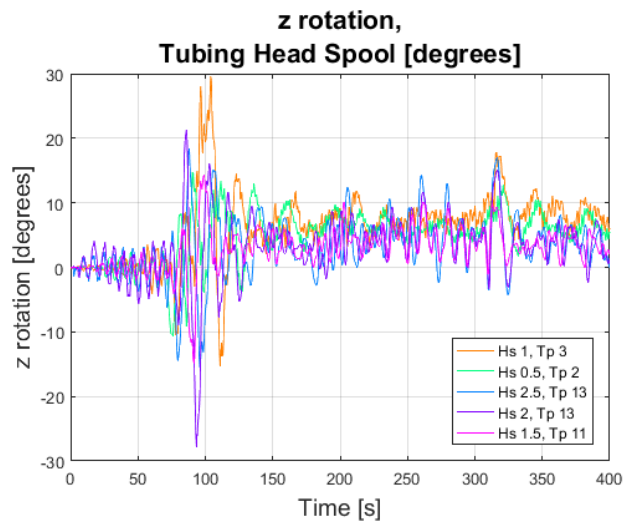
Figure 9.19: z rotation of the tubing head spool with respect to time, for time interval 0:400s

Different from the x and y rotation, the z rotation the standard deviation is larger throughout the whole deployment process. For the z rotation, the maximum rotation is found for wave condition 5, and the minimum rotation is found for wave condition 2, shown in Table 9.18. The mean rotation degree is smallest for condition set 1 and increases in degrees until condition set 5. The rotation values for the main deployment phase lay between -5 and +15 degrees, which means the rotation has shifted towards the positive degrees. This is opposite than for the x and y rotation.

Table 9.18: Statistics for y rotation of tubing head spool

	Max [deg.]	Min [deg.]	Mean [deg.]	Standard deviation [deg.]
1	14.21	-14.83	2.39	2.41
2	21.28	-27.86	2.73	3.19
3	18.35	-15.50	3.03	3.72
4	15.07	-10.54	4.85	2.41
5	29.51	-15.17	7.74	3.66

There is little effect of the rotation of the installed equipment as it is deployed though the water column. The rotations of the equipment will therefore not be focused on for the following sections.

9.3. Deployment of suction anchor using fibre rope
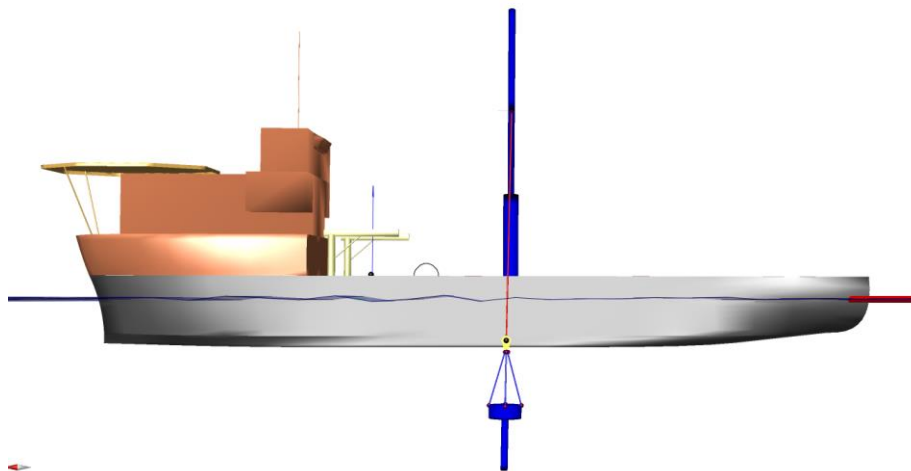
Figure 9.20: Deployment of suction anchor

The calculations in Table 9.19 is calculated the same way as for the Tubing head spool explained in section 9.2. The suction anchor has a larger accumulated mass and weight than the tubing head spool, and the geometry is symmetric across the z-axis.

Table 9.19: Calculated data for suction anchor

Accumulated mass [kg]	70456
Accumulated volume [m³]	45.55
Weight of suction anchor [N]	691173
Weight of hook [N]	39240
Total weight in air [N]	730414
Buoyancy force [N]	458017
Static weight of submerged object [N]	233157

For the suction anchor the focus will be on the tension in the main liftwire, and the x and y displacement of the suction anchor. Data for the x, y and z rotations of the suction anchor can be found in Appendix A: Results.

9.3.1. Tension

For the suction anchor, the difference in the weight in air is about 6 times the weight of the submerged weight. This affects the tension in the main liftwire.
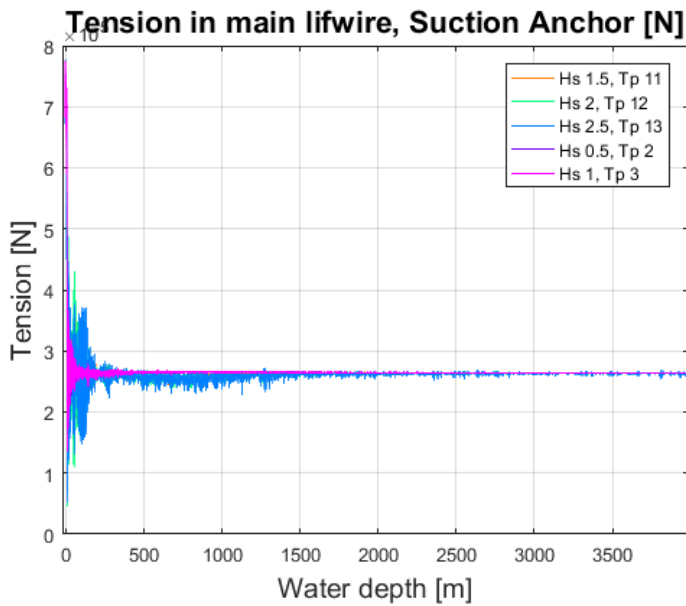
Figure 9.21: Tension in main liftwire, suction anchor
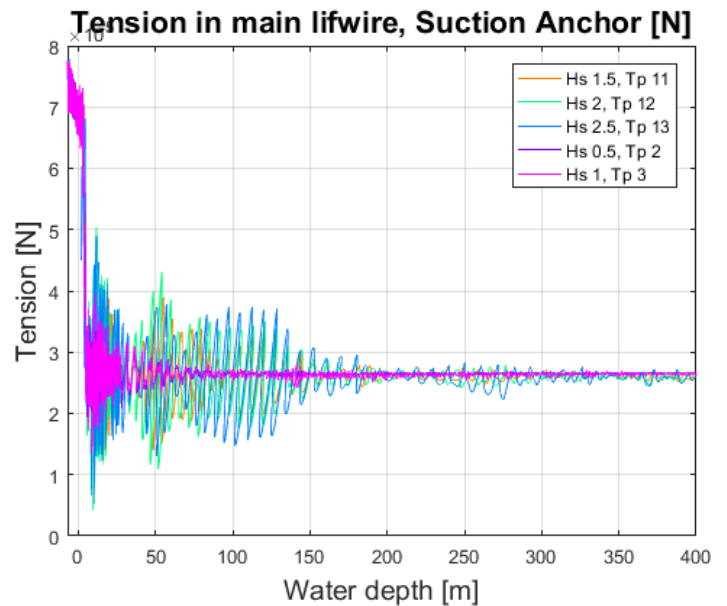
Figure 9.22: Tension in main liftwire, suction anchor, to 400 m water depth

The trend for the tension in the main liftwire is similar to that of the deployment of the tubing head spool. However, for the suction anchor, the tension is highest in air, varies in the upper water column, and remains somewhat constant throughout the deployment. The maximum tension for all wave conditions

lay at about 775 thousand N, which is the largest tension when the suction anchor is deployed in air. The start value shown in Table 9.20 is the tension at the very beginning of the simulation. The value fits with the value for the total weight of the system in air. The results are therefore true to the theory.

Table 9.20: statistics of tension in main liftwire, Suction anchor

	Max [N]	Min [N]	Mean [N]	Standard deviation [N]	Start value [N]
1	774651	139261	267698	45644	730464
2	774992	44806	267148	47246	730465
3	778418	51492	266531	47349	730464
4	775371	194891	269616	44127	730465
5	775482	135311	269399	44432	730465

The statistics for the time interval of 75 to 150s, water depth of 5.9 to 22.3m, is shown in Table 9.21. the maximum values for tension have now decreased and the values are different for each condition set. The maximum tension and standard deviation is largest for wave conditions 2 and 3. Snap forces in the main liftwire caused by the wave conditions might cause the high values.

Table 9.21: statistics of tension in main liftwire, for time interval 75:150s, Suction anchor

	Max [N]	Min [N]	Standard deviation [N]
1	413900	139300	66320
2	505600	45810	101100
3	489600	51490	90960
4	346200	194900	30590
5	394300	135300	48660

As for the tubing head spool, we will also look at the effect of the tension in the main liftwire the water depths of 2000 and 4000 m. The results are shown in in Figure 9.23 and Figure 9.24 below.
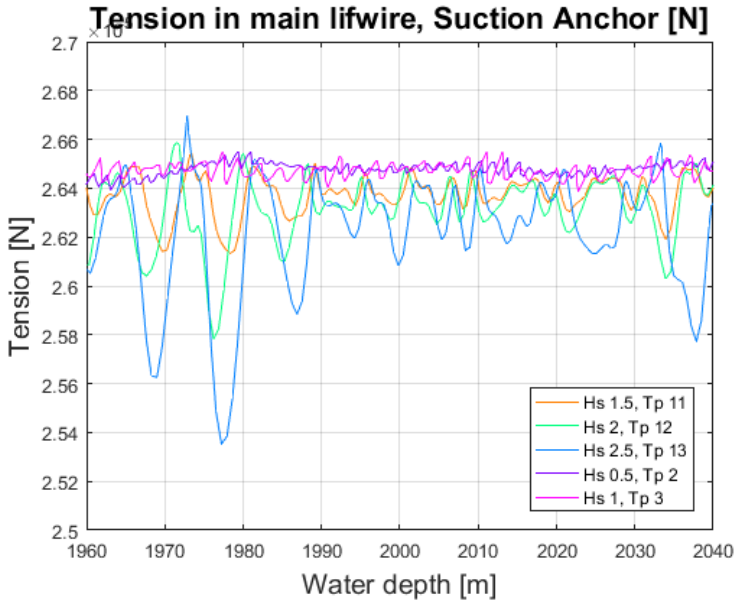
Figure 9.23: Tension in main liftwire at 2000 m, Tubing head spool
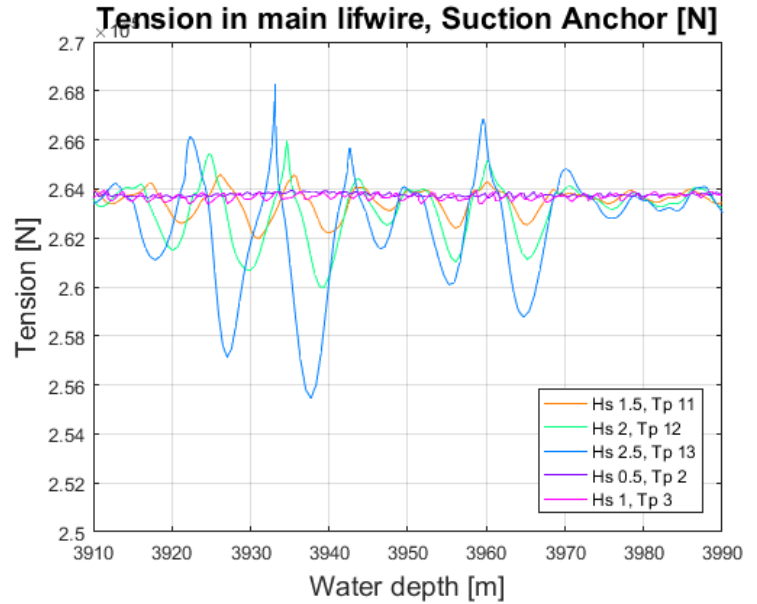
Figure 9.24: Tension in main liftwire at 4000 m, Tubing head spool

The tension in the main liftwire for wave conditions 4 and 5 remain constant for both water depths, with a slight decrease in tension at 4000 m, as seen for the tubing head spool. The variation in tension has settled at 4000 m compared to 2000 m. For condition sets 1 through 3, the tension varies more and lay at values slightly lower than for that of wave conditions 4 and 5, at 2000 m. At 4000 m the variation in the tension is smoother and the mean values are closer to the values of condition sets 4 and 5.

Table 9.22: tension in main liftwire, 2000 m and 4000 m water depth, Suction anchor

	Tension at 2000 m [N]	Tension at 4000 m (3990 m) [N]	Difference [N]
1	263511	263490	-21
2	264269	263182	-1088
3	261260	263024	1764
4	264992	263783	-1209
5	264734	263783	-951

The water depth of the installation does not affect the tension in the main liftwire. There is rather a slight decrease in tension from 2000 m to 4000 m due to the slightly negative buoyancy of the fibre rope.

9.3.2. X displacement

In this section, the x displacement of the suction anchor is investigated for deployment to 4000 m water depth. The suction has a round geometry, and a small cross-sectional area in the direction of the current.

160
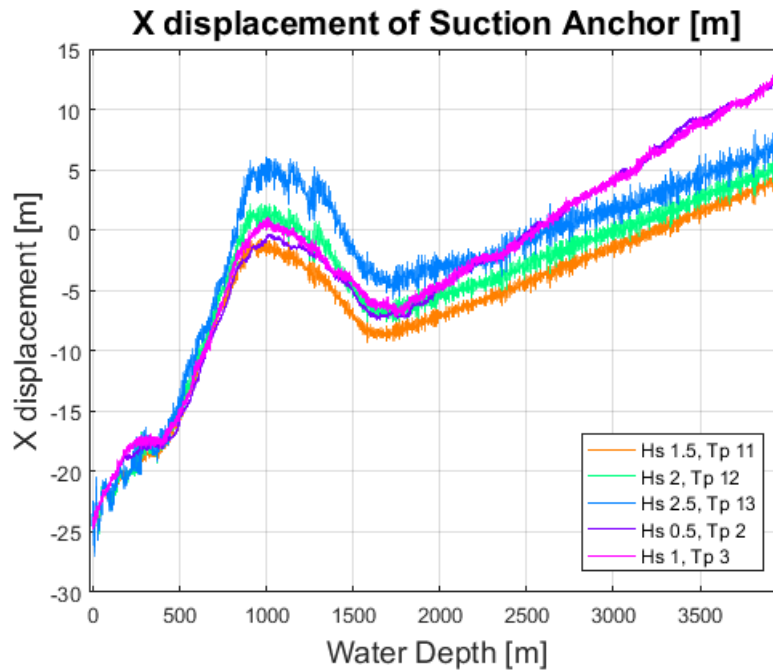
Figure 9.25: x displacement of suction anchor

The x displacement of the suction anchor is smaller than that for the tubing head spool, see section 9.2.2. This is the result of the higher weight and the smaller cross-sectional area in the current direction of the suction anchor. Both components of the suction anchor are round and smooth, therefore the force from the current will flow around the suction anchor. The largest displacement happens in wave conditions 4 and 5, with displacements of 38.1 and 38.6 m respectively.

Table 9.23: Statistics of x displacement of Suction anchor

	Max [m]	Min [m]	Mean [m]	Standard deviation [m]	Start position [m]	Displacement [m]
1	5.21	-25.79	-5.56	7.15	-24.50	29.71
2	6.66	-26.47	-4.19	7.54	-24.50	31.16
3	8.70	-27.09	-2.25	8.20	-24.50	33.20
4	13.56	-24.68	-1.77	9.83	-24.50	38.06
5	14.10	-24.81	-1.49	9.66	-24.50	38.60

The x displacements at 2000 m and 4000 m water depths are shown in Figure 9.26 and Figure 9.27. The same trend as for the tubing head spool is present here, where the displacement for wave condition s1 through 3 remains at the same phase and with approximately the same variation in x displacement

between the tree wave conditions. The x displacement for wave conditions 4 and 5 increase at a slightly higher pace at both 2000 m and 4000 m. The difference between the two water depths is that at 2000 m the x displacement for condition 4 and 5 lay at a median value of conditions 1 through 3, but at 4000 m they lie approximately 5 meters above.
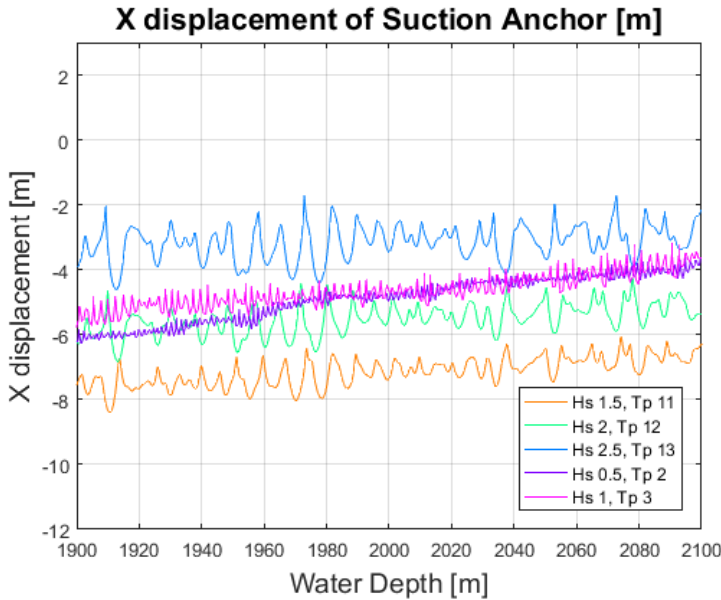
Figure 9.26: X displacement of suction anchor at 2000 m
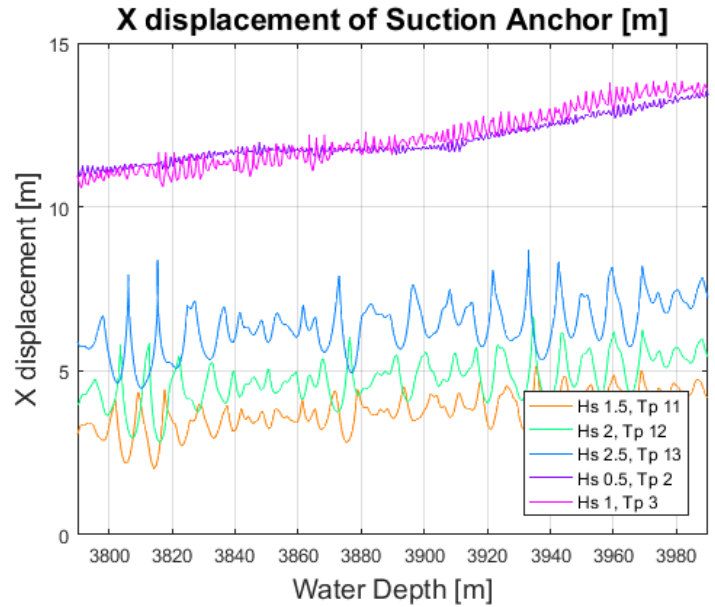
Figure 9.27: X displacement of suction anchor at 4000 m

From the water depth of 2000 m to 4000 m the difference in displacement lies at approximately 23.5m for wave conditions 1though 3 and at 28m for wave conditions 4 and 5.

Table 9.24: x displacement of suction anchor, 2000 m and 4000 m water depth

	X displacement at 2000 m [m]	X displacement at 4000 m [m]	Difference [m]
1	7.03	30.71	23.68
2	8.15	32.52	24.37
3	10.79	34.07	23.28
4	10.24	38.39	28.15
5	11.40	39.68	28.27

The x displacement of the suction anchor is not as significant as for the tubing head spool. A displacement of 35.9m at 2000 m and 64.2 at 4000 m is not impossible to fix with some simple installation support.

9.3.3. Y displacement
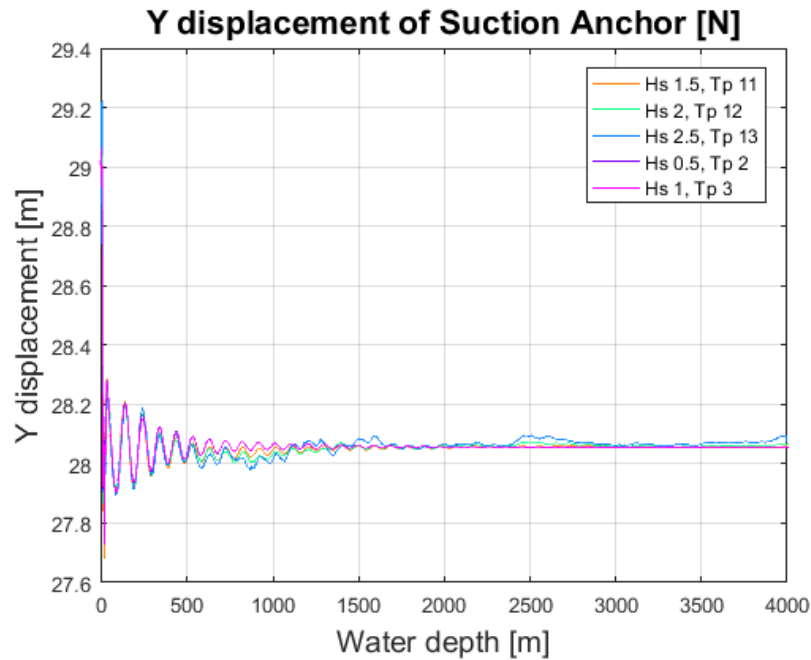
Figure 9.28: y displacement of suction anchor

As seen in Figure 9.13 and Table 9.25 the y displacement of the suction anchor is minimal. The largest y displacement is for wave condition 3, where the displacement is 1.72m. There are no significant differences in displacement between the different wave conditions. The reason for the small y displacement of the suction anchor may be due to the symmetry of the suction anchor.

Table 9.25: Statistics of y displacement of suction anchor

	Max [m]	Min [m]	Mean [m]	Standard deviation [m]	Start position [m]	Displacement [m]
1	29.08	27.68	28.06	0.10	27.50	1.58
2	29.14	27.74	28.06	0.10	27.50	1.64
3	29.23	27.82	28.07	0.10	27.50	1.73
4	29.06	27.75	28.07	0.10	27.50	1.56
5	29.06	27.73	28.07	0.10	27.50	1.56

9.3.4. Z displacement
The z displacement of the suction anchor is shown in Table 9.25 below.
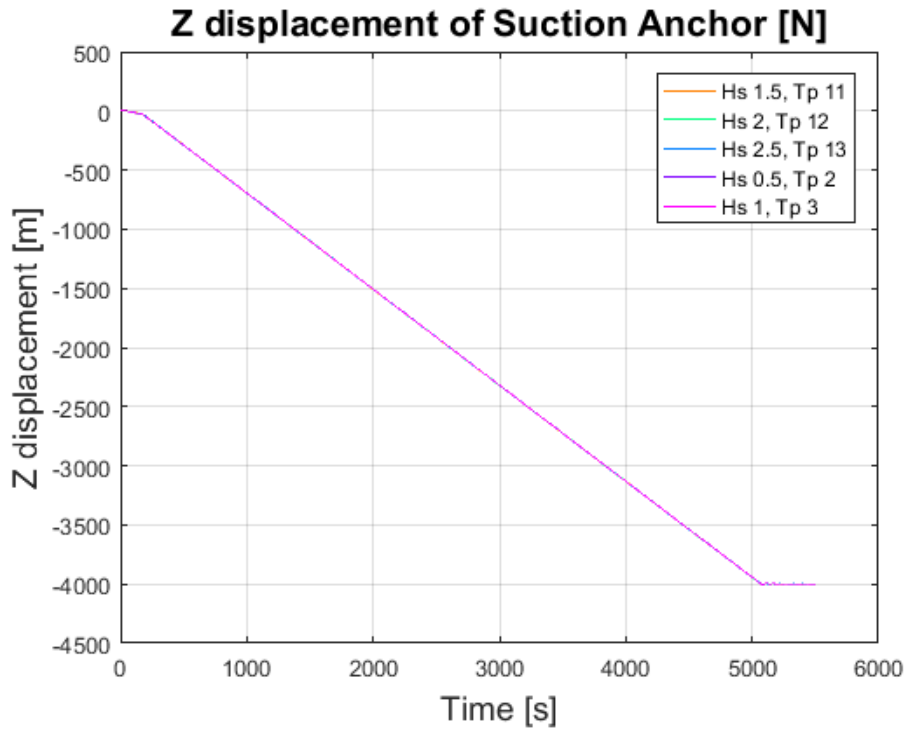
The suction anchor reached the desired water depth of 4000 m with a difference of 1 second for the five different wave conditions. The displacement time is 1 hour and 25 minutes for all five conditions, which is 3 minutes less than that of the tubing head spool.

Figure 9.29: z displacement of suction anchor

	Z displacement time to 4000 m [s]	Z displacement time to 4000 m [hours]
1	5072	1.41 (1 hour 25 minutes)
2	5072.5	1.41 (1 hour 25 minutes)
3	5072.5	1.41 (1 hour 25 minutes)
4	5073	1.41 (1 hour 25 minutes)
5	5073	1.41 (1 hour 25 minutes)

The winch was stopped after 5067 seconds when the suction anchor reached a water depth of 3995m. the simulation was continued to 5500 seconds. Figure 9.30 shows the heave motion of the after the winch has

been stopped. The heave motion is only present once the winch is stopped and is largest at the time the winch is stopped. The heave motion then decreases rapidly until it ends up at +/- 0.5m.
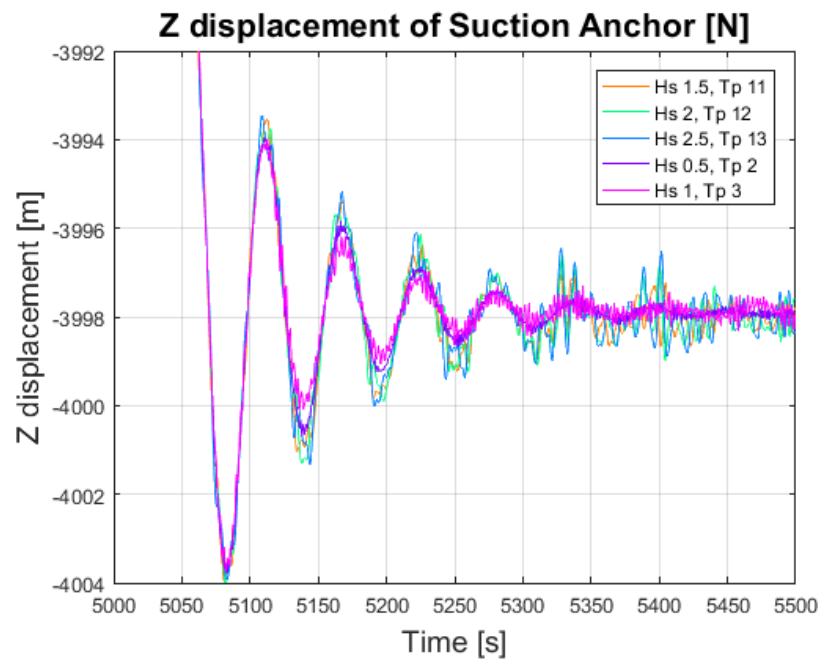
Figure 9.30: Heave motion of suction anchor

9.4. Deployment of valve tree using fibre rope
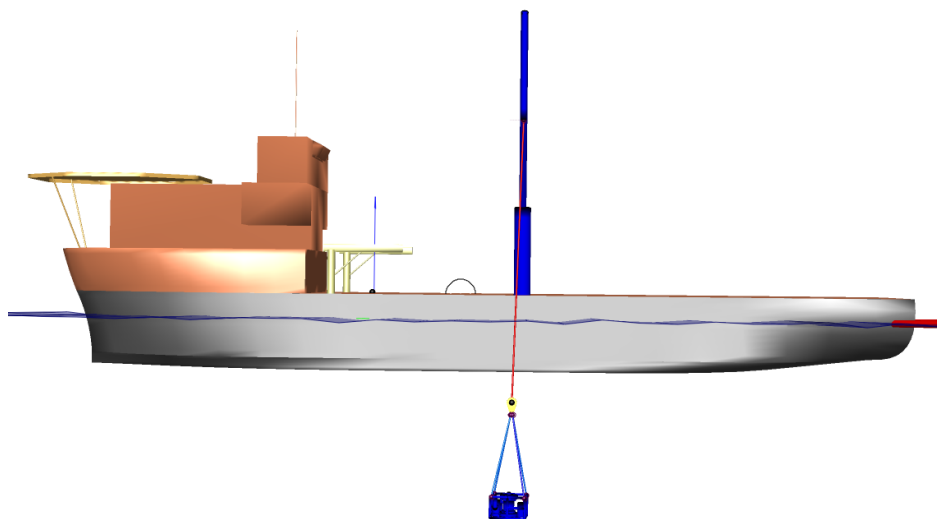
Figure 9.31: Deployment of valve tree

The values calculated in Table 9.26 are calculated with the same method as for the previous equipment, explained in section 9.1. Due to simulation time limitations, a simplified model of the valve tree was made. The simplified model has a weight that is approximately 70 thousand N lighter. The buoyancy force of the simplified model is also smaller due to the smaller volume of the valve tree. However, the static weight of the submerged valve tree is larger due to the smaller buoyancy force for the simplified model.

Table 9.26: Calculated data for valve tree

	Full	Simplified	Difference
Accumulated mass [kg]	57092	50000	-7092
Accumulated volume [m³]	47.17	23.55	-23.62
Weight of valve tree [N]	560073	490500	-69573
Weight of hook [N]	39240	39240	-
Total weight in air [N]	599313	529740	-69573
Buoyancy force [N]	474286	236751	-237535
Static weight of submerged object [N]	125027	292989	167963

9.4.1. Tension
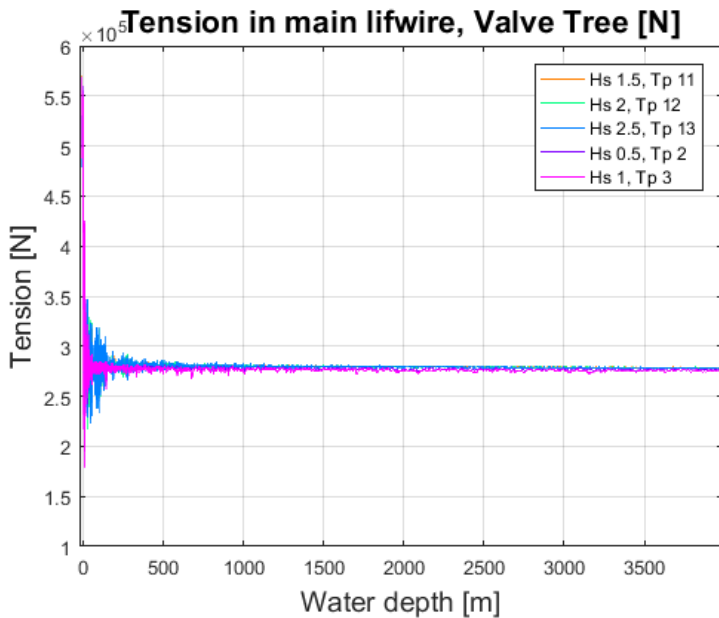
Figure 9.32: Tension in main liftwire, valve tree
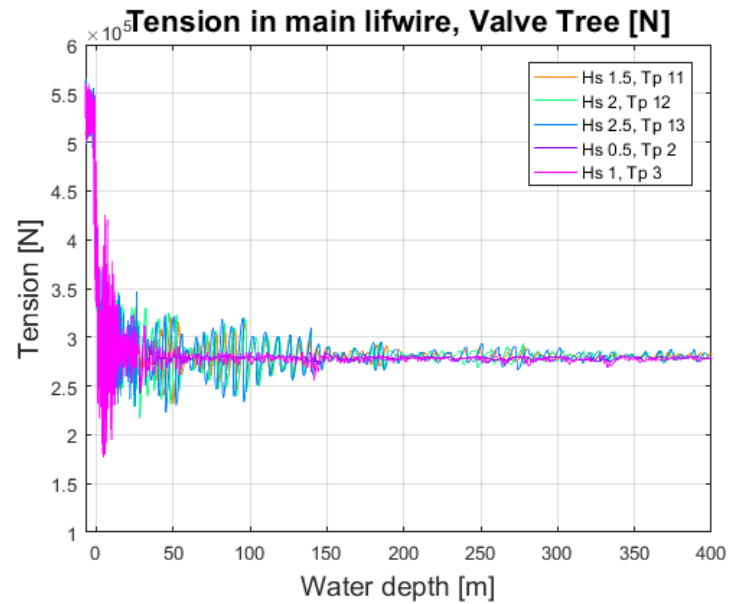
Figure 9.33: Tension in main liftwire, valve tree, to 400 m water depth

The tension in the main liftwire when installing the valve tree follow the same trend as the previous equipment. The tension is highest when the valve tree is lifted in air, and remains constant after the upper water column.

Table 9.27: statistics of tension in main liftwire, valve tree

	Max [N]	Min [N]	Mean [N]	Standard deviation [N]	Start value [N]
1	569845	231817	281938	21346	529379
2	569435	217437	281837	21600	529378
3	568663	222719	281749	21720	529378
4	568866	242720	279964	21112	529378
5	568841	178169	278809	22190	529379

The start value in Table 9.27 is the tension in the main liftwire at 0 seconds, the beginning of the simulation. The start value correlates to the calculated total weight in air for the system. Checking the value for the static weight of the submerged object to the mean tension for the deployment process, these values also correlate with each other, meaning the simulation fit the theory. The maximum value in Table 9.27 is the maximum tension in the main liftwire when the valve tree is lifted in air. New data for the time interval of 60:130s, water depth of 3.12 to 18.22m, was made to see the investigate the tension in the splash zone and the upper water column.

Table 9.28: statistics of tension in main liftwire, for time interval 60:130s, Valve tree

	Max [N]	Min [N]	Standard deviation [N]
1	340970	237000	26530
2	352910	238000	28450
3	357320	226100	3026
4	310050	270300	7445
5	424360	178200	47590

The max displacement, shown in Table 9.28, is highest for wave condition 5. Wave conditions 4 and 5 have the largest standard deviation in the splash zone and the upper water column. This correlates to the horizontal water particle motion of the two wave conditions in the upper water column. The peaks in tension in the splash zone could indicate snap forces.

Investigating the differences in the tension in the main liftwire at 2000 m and 4000 m, Figure 9.34 and Figure 9.35 show similar trends to the previous cases. The variation in tension for wave conditions 4 and 5 are larger at 2000 m that for 4000 m water depth. Tension in all five wave conditions are slightly reduced at the water depth of 4000 m.
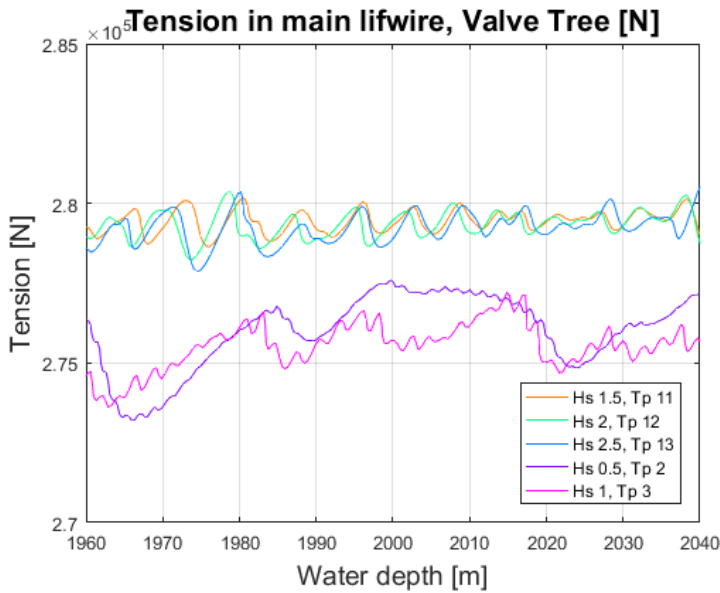
Figure 9.34: Tension in main liftwire at 2000 m, valve tree
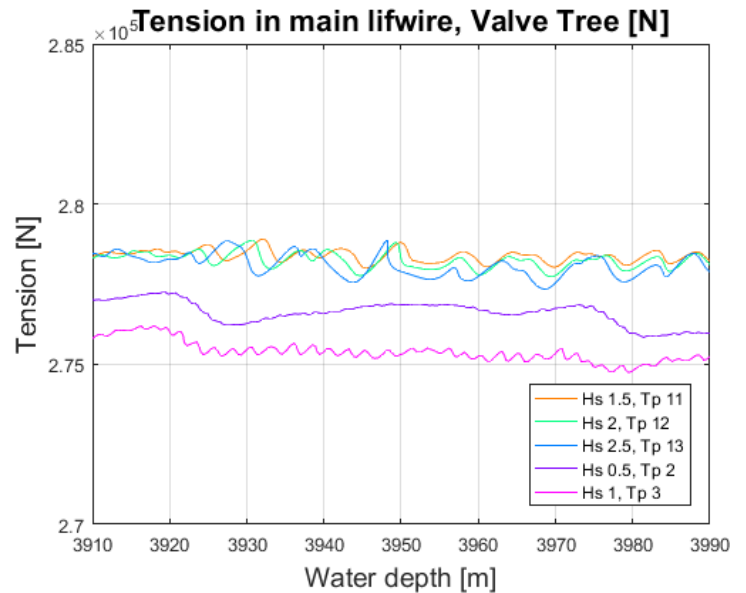
Figure 9.35: Tension in main liftwire at 2000 m, valve tree

The tension at both water depths are slightly lower for wave conditions 4 and 5. This might be due to the lower horizontal water particle motions caused by the wave conditions at the deep-water depths.

Table 9.29: tension in main liftwire, 2000 m and 4000 m water depth, valve tree

	Tension at 2000 m [N]	Tension at 4000 m (3990 m) [N]	Difference [N]
1	279316	278212	-1105
2	279483	278073	-1410
3	278940	277857	-1083
4	277562	275986	-1577
5	275699	275288	-411

For the valve tree the tension in the main liftwire it not affected significantly by the increasing water depth. There are no main issues with tension when installing the valve tree to 4000 m.

9.4.2. X displacement

When simplifying the valve tree for the SIMO simulation, slender elements were removed, reducing the affected cross-sectional area in the direction of the current. This might cause a smaller x displacement than for the actual modelled valve tree.
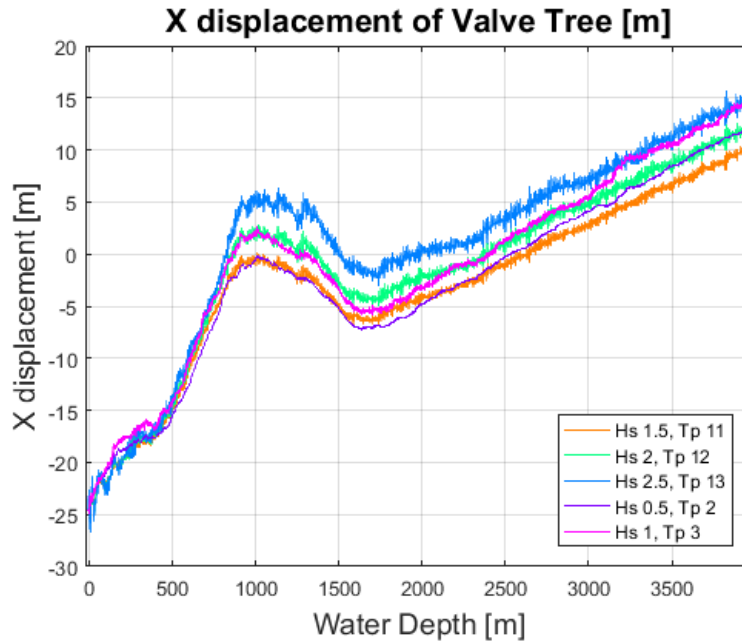
Figure 9.36: x displacement of suction anchor

The largest displacement of the suction anchor happens in wave conditions 3 and 5, where the largest displacement is at 43m for wave condition 5. The x displacement is larger than that of the suction anchor due to the larger cross-sectional area in the current direction, and smaller than that of the tubing head spool because of the larger weight.

Table 9.30: Statistics of x displacement of Suction anchor

	Max [m]	Min [m]	Mean [m]	Standard deviation [m]	Start position [m]	Displacement [m]
1	11.38	-25.36	-2.42	8.92	-24.50	35.88
2	13.79	-25.98	-0.65	9.56	-24.50	38.29
3	16.58	-26.63	1.51	10.38	-24.50	41.08
4	13.77	-24.59	-1.66	9.89	-24.50	38.27
5	18.60	-24.89	0.35	10.59	-24.50	43.10

Figure 9.37 and Figure 9.38 show the x displacement at the water depth of 2000 m and 4000 m respectively. The trend for the x displacement in wave condition 1 through 3 are similar to the previous

cases. However, a new trend is seen for the x displacement in wave condition 4 and 5. The gap between the x displacement for the two cases increase from 2000 m to 4000 m. The x displacement for wave conditions 4 and 5 increases at a higher rate than that of the other wave conditions. As a result, the x displacement in wave condition 4 and 5 start in the lower displacement range of the three other conditions at 2000 m, and shifts to the higher displacement range at 4000 m.
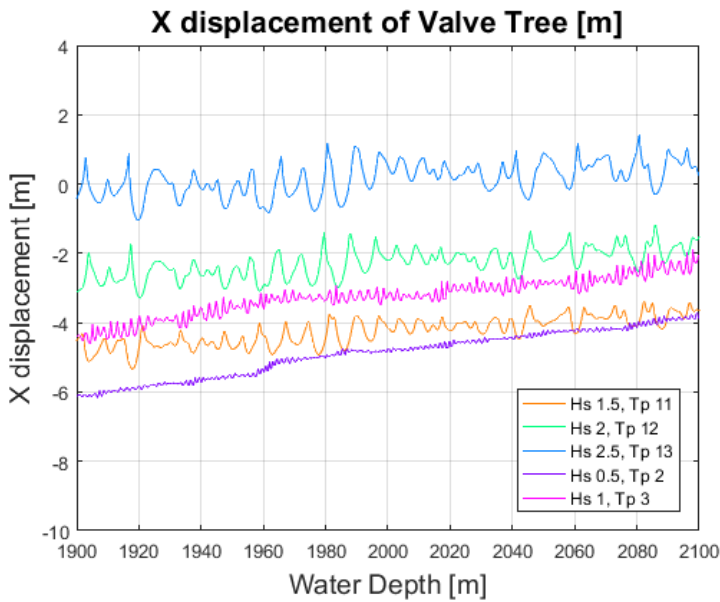
Figure 9.37: X displacement of valve tree at 2000 m
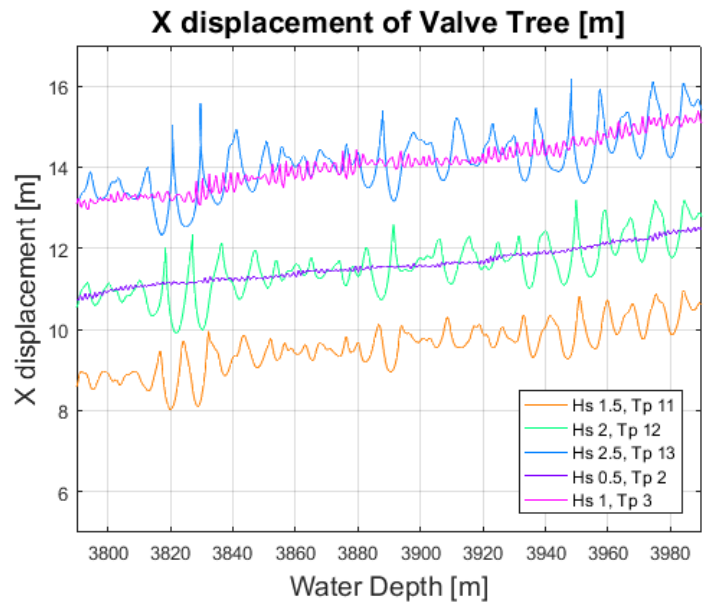
Figure 9.38: X displacement of valve tree at 4000 m

At 2000 m the largest x displacement is in wave condition 3 and the smallest in wave condition 4. On the other hand, the at 4000 m water depth the x displacement is largest for wave condition 3 and smallest for wave condition 1.

Table 9.31: x displacement of suction anchor, 2000 m and 4000 m water depth

	X displacement at 2000 m [m]	X displacement at 4000 m (3990 m) [m]	Difference [m]
1	-4.15	10.59	14.74
2	-2.20	12.74	14.94
3	0.48	15.32	14.83
4	-4.75	12.50	17.25
5	-3.18	15.07	18.25

The largest displacement at 2000 m is about 25m and the largest displacement at 4000 m is about 40 m. there is only 15 meters difference in the worst x displacement for the two water depths. Therefore, the x

displacement of the valve tree is not seen as a significant problem when installing a valve tree to a water depth of 4000 m.

9.4.3. Y displacement

Y displacement of Valve Tree [N]
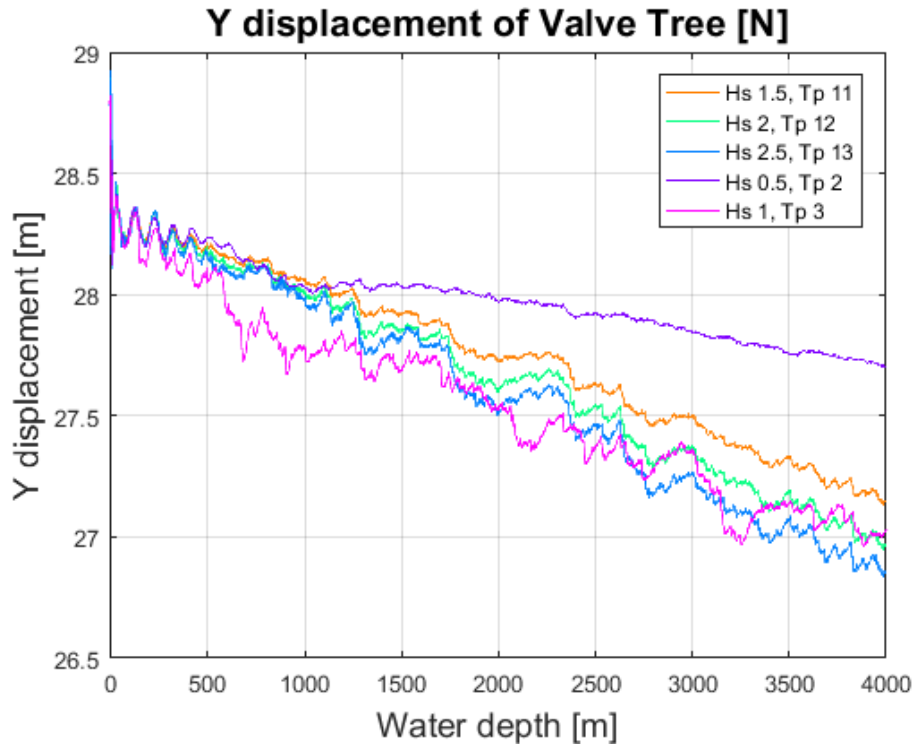
Figure 9.39: y displacement of valve tree

The modelled Y position of the valve tree is 27.5. looking at the Figure 9.39 and Table 9.32 the maximum y position start is 28.9. This could be caused by the centre of gravity of the valve tree in air, due to the un-symmetric body. Once the valve tree I deployed the y displacement shifts in the negative y direction. This is most likely caused by the centre of force of the valve tree in water, where the valve tree leans slightly towards the negative y direction during deployment.

Table 9.32: statistics of y displacement of valve tree

	Max [m]	Min [m]	Mean [m]	Standard deviation [m]	Start position [m]	Displacement [m]
1	28.87	27.13	27.74	0.37	27.50	1.74
2	28.89	26.95	27.65	0.42	27.50	1.95
3	28.92	26.83	27.58	0.46	27.50	2.09
4	28.82	27.64	27.97	0.19	27.50	1.18
5	28.82	26.57	27.51	0.44	27.50	2.25

Although there is a y displacement present, the displacement is at 2.25m at its largest, in wave condition 5. The y displacement is smallest for wave condition 4. The y displacement is not significant for the deployment of the valve tree to 4000 m.

9.4.4. Z displacement

Z displacement of Valve Tree [N]
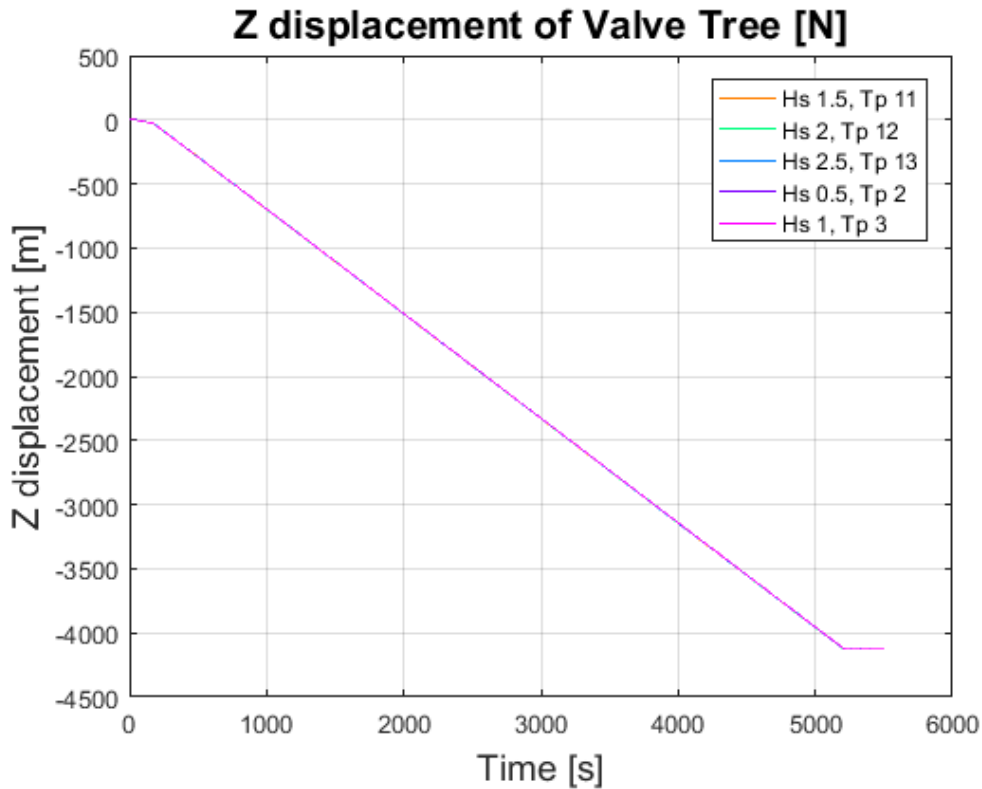
Figure 9.40: Z displacement of the valve tree

The valve tree reaches the water depth of 4000 m at the time between 5053.5s and 5057s for the different wave conditions. This correlates to a deployment time of 1 hours and 24 minutes, which is one minute faster than for the suction anchor and 4 minutes faster than for the tubing head spool.

Table 9.33: Deployment time of valve tree

	Z displacement time to 4000 m [s]	Z displacement time to 4000 m [hours]
1	5053.5	1.40 (1 hour 24 minutes)
2	5053.5	1.40 (1 hour 24 minutes)
3	5054	1.40 (1 hour 24 minutes)
4	5056	1.40 (1 hour 24 minutes)
5	5057	1.40 (1 hour 24 minutes)

Looking at Figure 9.41 there is a small presence of heave motion of the valve tree during the z displacement. Figure 9.41 show the z displacement from the water depth of 3970 m to 4000 m.
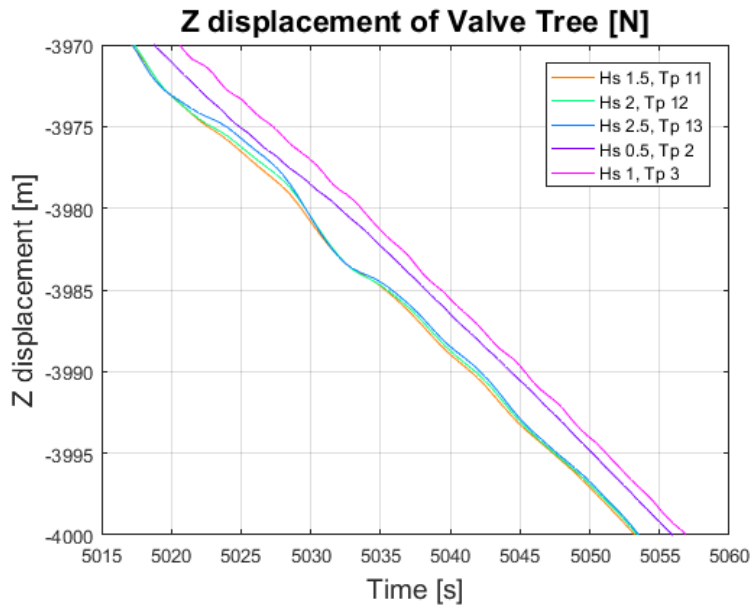
Figure 9.41: Heave motion during z displacement of valve tree

9.5. Deployment of well jumper using fibre rope

The well jumper is the smallest of the five equipment. The slings of the well jumper are supported by a spreader beam to reduce the tension in the slings.
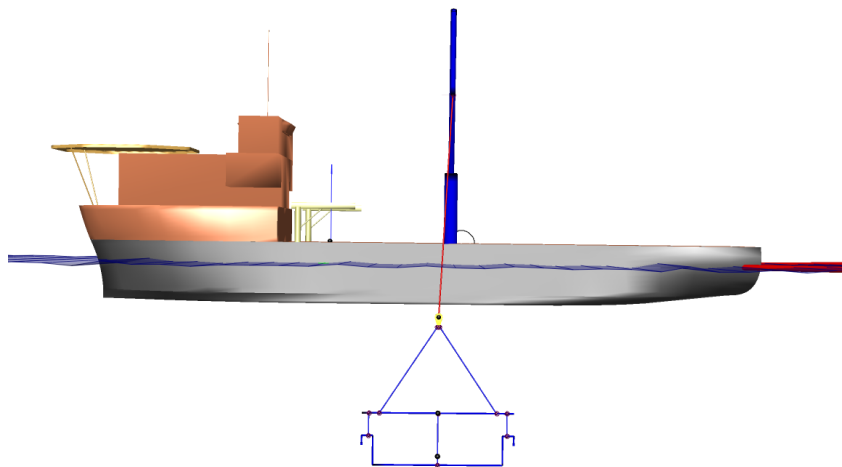
Figure 9.42: Deployment of well jumper

For the weight and buoyancy calculation, the spreader beam and the hook are included. The Total weight in air and static weight of submerged object is the sum of the tree bodies. The calculations are done with correlation to section 5.3.1 and 5.3.2.

Table 9.34: Calculations for spreader beam

	Well jumper	Spreader beam	Total
Accumulated mass [kg]	4498	2946	7443
Accumulated volume [m³]	1.10	0.71	1.81
Weight of slender elements [N]	44121	28898	73020
Weight of hook [N]	-	39240	39240
Total weight in air [N]	44121	68138	112260
Buoyancy force [N]	11034	7132	18166
Static weight of submerged object [N]	33088	61006	94094

9.5.1. Tension
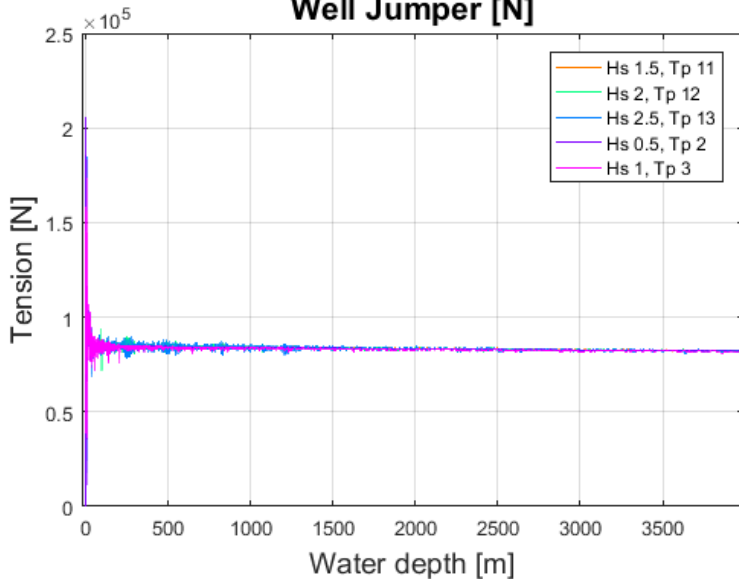
Figure 9.43: Tension in main liftwire for well jumper
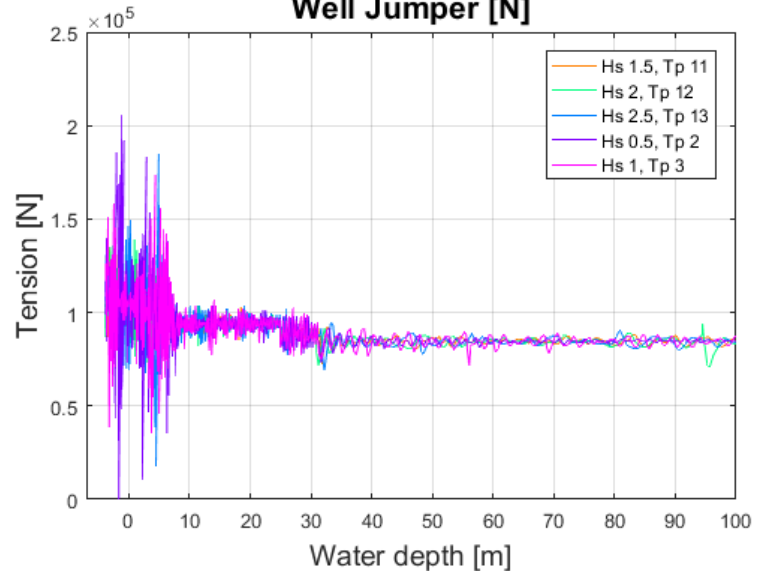
Figure 9.44: Tension in main liftwire, well jumper, to 100 m water depth

The tension in the main liftwire for the deployment of the well jumper show the follow the same trend as the previous cases. However, for this case, the maximum displacement shown in Figure 9.44 and Table 9.35 is experience by the rope during the deployment though the splash zone, and in the upper water column. The start value in Table 9.35 is the initial tension of the main liftwire at 0 second, where the well

174

jumper is lifted in air. The start value correlates to the calculated total weight in air shown in Table 9.34 above.

Table 9.35: statistics of tension in main liftwire, well jumper

	Max [N]	Min [N]	Mean [N]	Standard deviation [N]	Start value [N]
1	134988	68164	83988	3104	112172
2	138982	71364	83892	3206	112170
3	184549	17817	83809	3768	112171
4	205647	125	83809	4410	112172
5	173797	36029	83437	3816	112171

The mean value of the tension in the main liftwire during deployment is about 10k N lower than the calculated value of the static weight of the submerged equipment, see Table 9.34. The reason for the difference might be due to the negative weight in water of the fibre rope, which is -3.1 N/m. Also, the lift forces acting on the main liftwire when the well jumper is deployed with a skewness in the x direction. Taking a closer look at the tension in the main liftwire, one may notice that the tension is higher in the upper water column from 10 m to 30 m water depth. The mean tension for the time interval of 60-140 seconds, water depth of 7.5 to 24, is measured and shown in Table 9.36.

Table 9.36: Mean tension t time interval of 60:140s

	Mean [N]
1	94190
2	94200
3	94180
4	93940
5	93610

The mean tension in the main liftwire for the new time interval correlates to the static weight of the submerged equipment calculated in Table 9.34.

Figure 9.45 and Figure 9.46 show the tension in the main liftwire for the different wave conditions at the water depth of 2000 m and 4000 m. As the tension in the main liftwire is smaller due to the small weight of the well jumper and the components, the variation of the tension for each condition set is shown more clearly in Figure 9.45 and Figure 9.46, than in the previous cases.
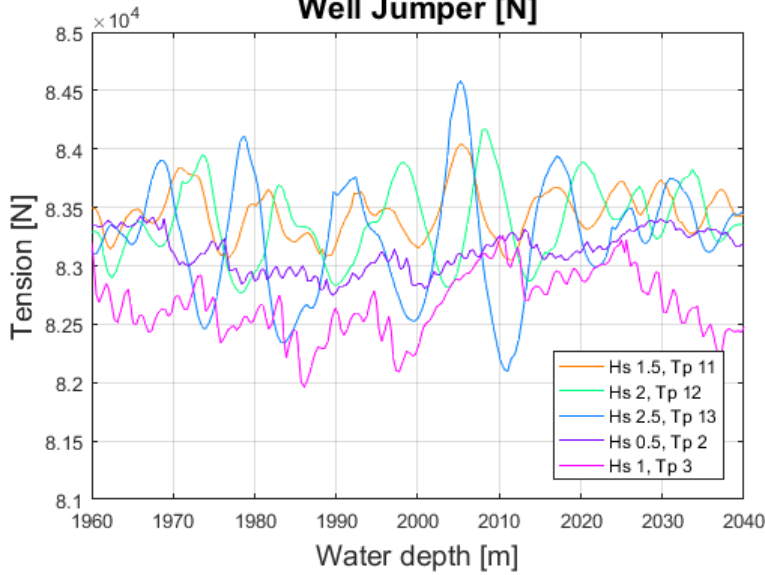
Figure 9.45: Tension in main liftwire at 2000 m, well jumper
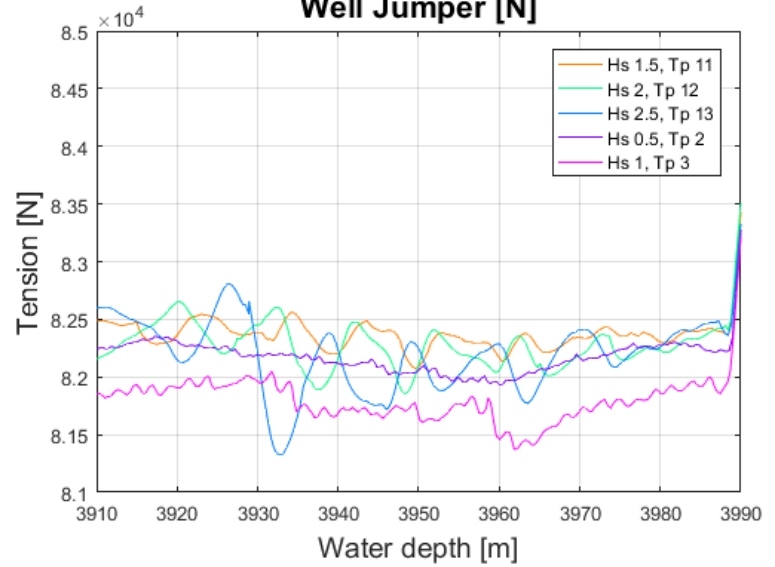
Figure 9.46: Tension in main liftwire at 4000 m, well jumper

The variation between the tensions are smaller than for the other cases. There is no clear gap between the tension in wave conditions 1 through 3, as seen in the previous cases, and the tension in wave conditions 4 and 5 is closer to the other values. The tension in the main liftwire decreases for all wave conditions from 2000 m to 4000 m. The values shown in Table 9.37 at the water depth of 3990 m does not give a good indication for the tension at 4000 m. This is due to the simulation duration, and looking at Figure 9.46, there is a sudden increase in the tension just before 3990 m. Values of tension at the water depth of 3980 m would give a better indication of the actual tension at 4000 m.

Table 9.37: tension in main liftwire, 2000 m and 4000 m water depth, well jumper

	Tension at 2000 m [N]	Tension at 4000 m (3990 m) [N]	Difference [N]
1	83151	83520	369
2	83570	83794	224
3	82552	83356	803
4	82845	83336	491
5	82344	83243	900

As for the previous cases, the tension is not affected significantly by the water depth of the installation.

9.5.2. X displacement

The suction anchor has a light weight, but the cross-sectional area is very small.
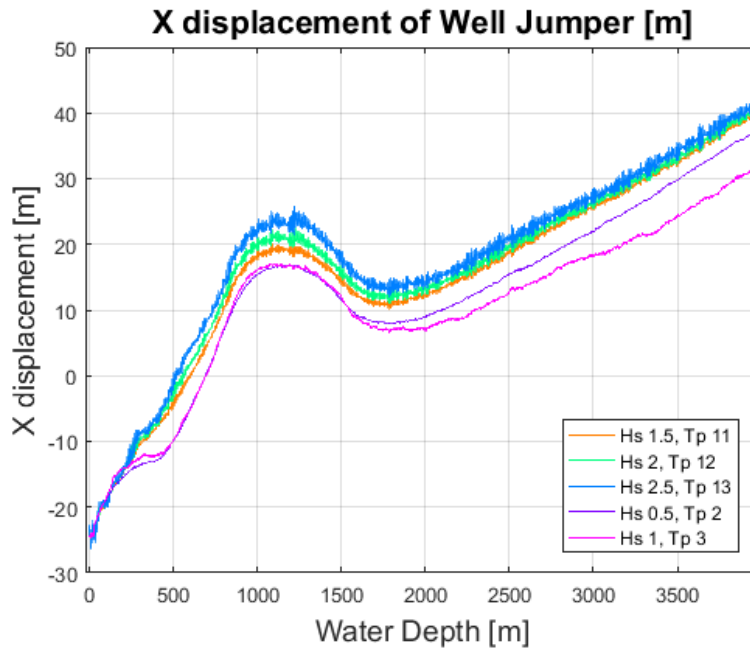
Figure 9.47: X displacement of suction anchor

The x displacement is similar to the x-displacement of the tubing head spool, see section 9.2.2. However, the in this case, the x displacement for wave conditions 4 and 5 are the smallest. This variance from the other cases could be related to the tiny cross-sectional area of the well jumper in the current direction. The main cause of the x displacement in this case might be due to the light weight of the well jumper and the spreader beam. The largest x displacement is for wave condition 3, with a x displacement of 67.5m.

	Max [m]	Min [m]	Mean [m]	Standard deviation [m]	Start position [m]	Displacement [m]
1	40.54	-25.25	15.71	16.00	-24.50	65.04
2	41.55	-25.85	16.64	16.04	-24.50	66.05
3	42.99	-26.50	17.94	16.20	-24.50	67.49
4	37.64	-24.53	12.72	15.79	-24.50	62.14
5	35.32	-24.62	10.78	14.08	-24.50	59.82

Figure 9.48 and Figure 9.49 show the x displacement at the water depths of 2000 m and 4000 m. Different from the other cases, is that the x displacement in wave conditions 4 and 5 are smaller at both 2000 m and 4000 m.
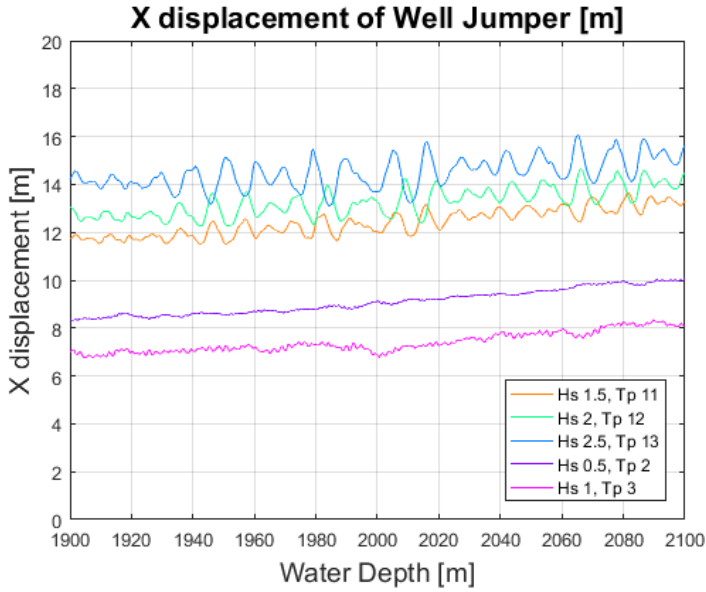
Figure 9.48: X displacement of well jumper at 2000 m
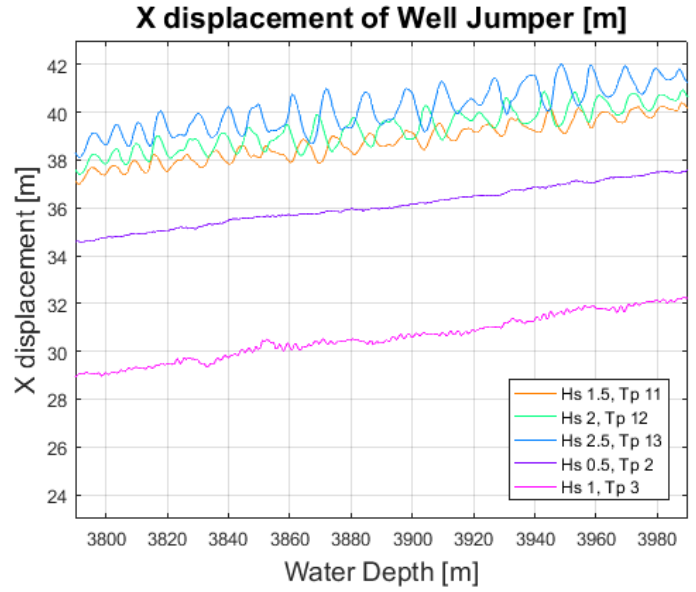
Figure 9.49: X displacement of well jumper at 4000 m

The x displacement between wave 4000 m and 2000 m is for wave condition 4, with a displacement of 28.5m. The largest x displacement is at 37.8m at 2000 m and 65.8m at 400 m, both in wave condition 3.

Table 9.38: x displacement of suction anchor, 2000 m and 4000 m water depth

	X displacement at 2000 m [m]	X displacement at 4000 m (3990 m) [m]	Difference [m]
1	12.02	40.15	28.13
2	13.27	40.59	27.31
3	13.70	41.25	27.55
4	9.13	37.59	28.47
5	6.81	32.25	25.44

The x displacement of the well jumper is a bigger issue for the well jumper due to the light weight. The largest x displacement at 4000 m, with a displacement of 67.5 meters, might be an issue when it comes to the positioning of the well jumper.

9.5.3. Y displacement
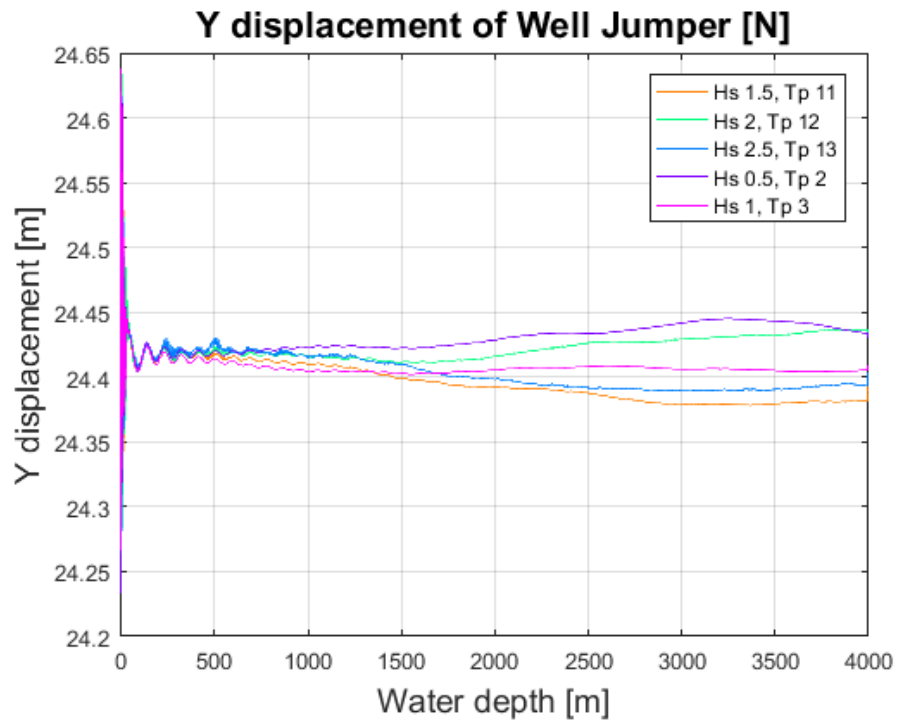
Figure 9.50: Y displacement of well jumper

	Max [m]	Min [m]	Mean [m]	Standard deviation [m]	Start position [m]	Displacement [m]
1	24.64	24.26	24.40	0.02	24.25	-0.39
2	24.64	24.26	24.42	0.02	24.25	-0.39
3	24.62	24.25	24.40	0.02	24.25	-0.37
4	24.62	24.23	24.43	0.01	24.25	-0.37
5	24.64	24.27	24.41	0.01	24.25	-0.39

9.5.4. Z displacement
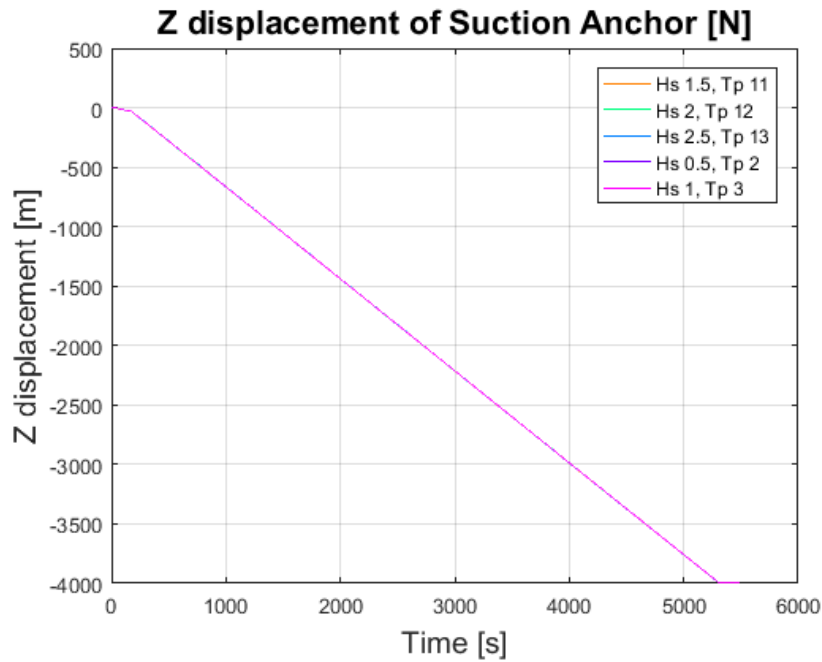
Figure 9.51: z displacement of well jumper

The simulation was stopped when the well jumper reached a water depth of 3994m, therefore the deployment time shown below is the time for the well jumper to deploy to a water depth of 3990 m. the deployment time of the well jumper to the water depth of 3990 m takes 1 hours and 28 minutes, which is the same time as the tubing head spool takes to deploy all the way to 4000 m. The most probable cause to the longer deployment time of the well jumper is due to the light weight, and the larger x displacement.

	Z displacement time to 3990 m [s]	Z displacement time to 4000 m [hours]
1	5302	1.47 (1 hour 28 minutes)
2	5302.5	1.47 (1 hour 28 minutes)
3	5302	1.47 (1 hour 28 minutes)
4	5302	1.47 (1 hour 28 minutes)
5	5302.5	1.47 (1 hour 28 minutes)

The winch is stopped as the well jumper reaches 1994m. Figure 9.52 show the heave motion of the well jumper after the winch is stopped. The heave motion is larger for wave conditions 1 through 3 than for wave conditions 4 and 5.
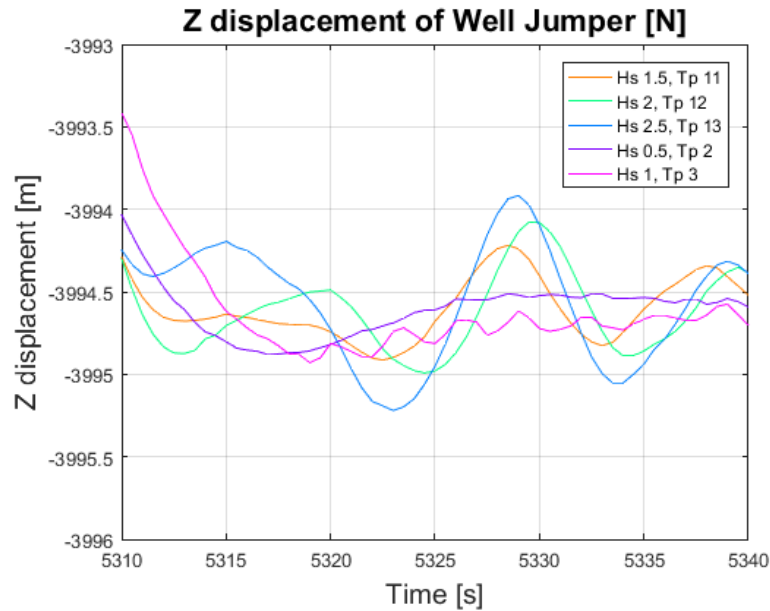
Figure 9.52: Heave motion of well jumper during z displacement

9.6. Deployment of drill centre template using fibre rope

The drill centre template is the largest and heaviest equipment installed. The simulation using the template was made to check for a limit using the fibre rope deployment method.
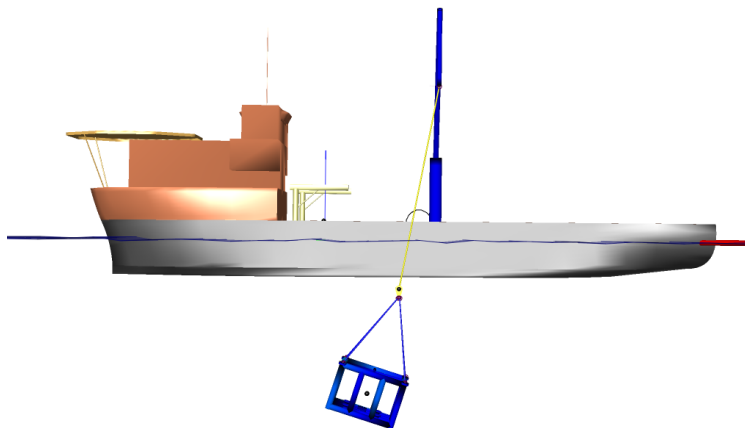
Figure 9.53: Deployment of Drill centre template

As with the valve tree, the modelled drill centre template was too complex for the simulation. Therefore, a simplified model was made for the drill centre template.

	Full	Simplified	Difference
Accumulated mass [kg]	189100	190030	930
Accumulated volume [m³]	206.59	176.95	-29.64
Weight of object [N]	1855071	1864194	9123
Weight of hook [N]	39240	39240	-
Total weight in air [N]	1894311	1903434	9123
Buoyancy force [N]	2077314	1779276	-298038
Static weight of submerged object [N]	-183003	124158	307161

When simplifying the model, slender elements were removed, reducing the volume of the body. Due to the reduction of the volume, the buoyancy force of the simplified model is reduced, hence the static weight of the submerged equipment in water is decreased.

9.6.1. Drill centre template discrepancy

1) Initial	2) Splash zone	3) Deployed
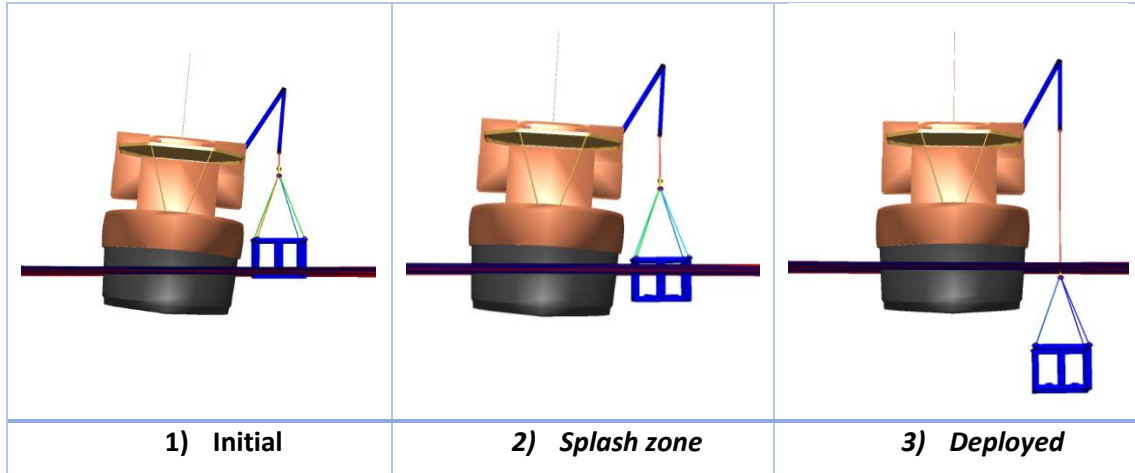
Figure 9.54: Roll of vessel due to weight of drill centre template

A discrepancy occurred when simulating the drill centre template. Due to the large weight of the drill centre template in air, roll motion in the negative x direction of the vessel occurred at the initial stages of the deployment, see Figure 9.55. The roll motion results in parts of the drill centre template being deployed in water at the start position of the deployment, rather than being above the sea level. In Figure 9.54 the position of the vessel and the drill centre template at the initial phase, during the splash zone and

the fully deployed stage. From Figure 9.54 we see that once the template is fully deployed, the roll of the vessel stabilized to around 0 degrees. The phenomena is seen in Figure 9.55 below.
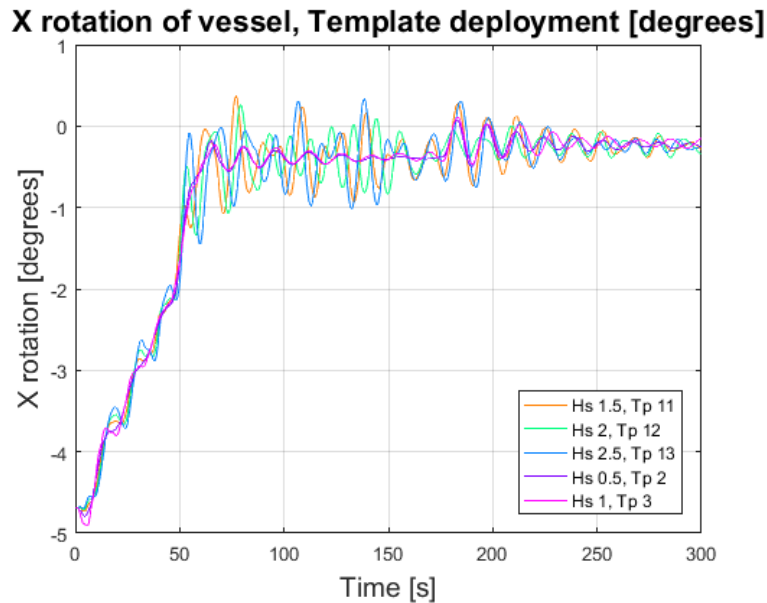
Figure 9.55:X rotation of vessel, template deployment

For the calculated values of weight and buoyancy to fit the model, an additional static weight was calculated. To find the appropriate percentage of deployed volume at the initial position, the calculations were made such that the static weight of the partially submerged drill centre template correlated to the start value found in the simulation results, see Table 9.40 in section 9.6.2 below. For the initial tension to correlate to the static weight of the object when 36.8% of the volume of the drill centre template was deployed.

Table 9.39: New calculations for drill centre template

Accumulated mass [kg]	190030
Accumulated volume [m³]	176.95
36.8 % of accumulated volume [m³]	65.1176
Weight of object [N]	1864194.3
Weight of hook [N]	39240
Total weight in air [N]	1903434.3
Buoyancy force [N]	1779276.488
Buoyancy force of 36.8% of volume submerged [N]	654773.7474
Static weight of submerged object [N]	124157.8125
Static weight of 36.8 % submerged object [N]	1248660.553

9.6.2. Tension
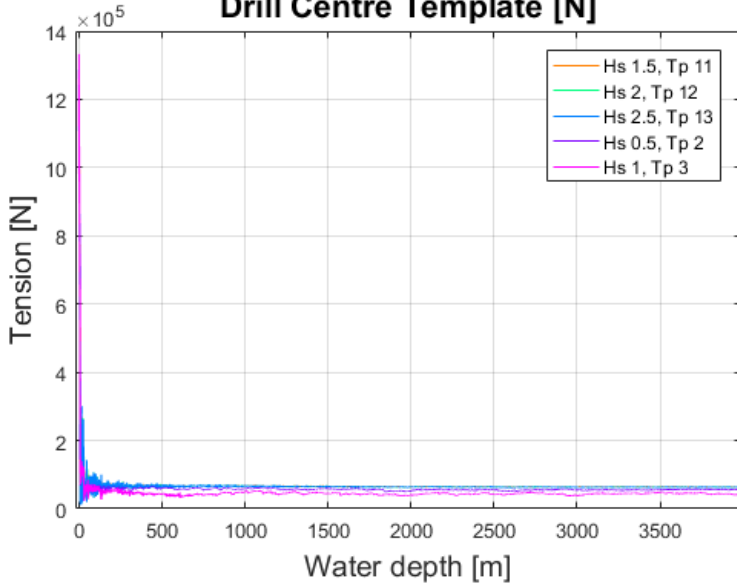
Figure 9.56: Tension in main liftwire for drill centre template
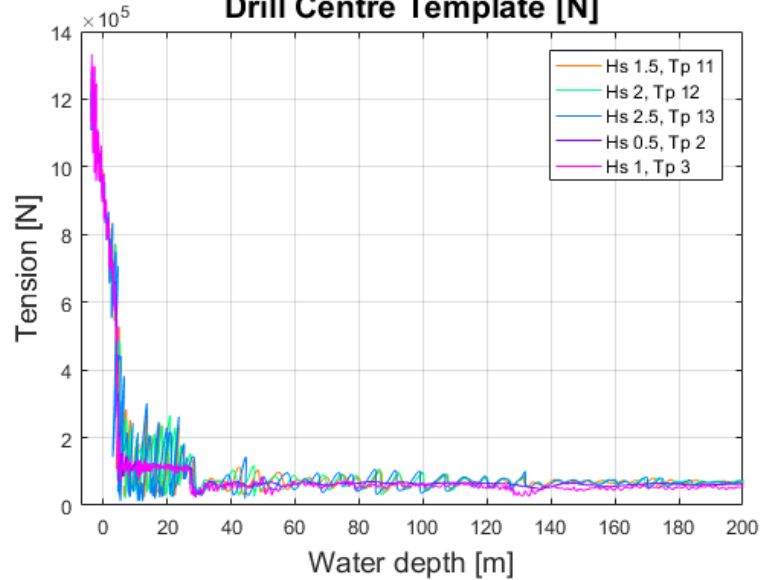
Figure 9.57: Tension in main liftwire, drill centre template, to 100 m water depth

The tension in the main liftwire when deploying the drill centre template show similar trends to that of the valve tree, where the tension is significantly higher in air, and that for the well jumper, where there is a sudden drop in tension at about 30 m water depth. As explained in section 9.6.1, the start value and maximum value correlated to the template being about 36.8% deployed in the initial stage of the simulation. The actual tension in air would be closer to 1.9 million N.

Table 9.40: statistics of tension in main liftwire, drill centre template

	Max [N]	Min [N]	Mean [N]	Standard deviation [N]	Start value [N]
1	1266063	24455	74440	82389	1248513
2	1274183	20169	74159	82559	1248515
3	1285072	11999	73975	82804	1248515
4	1281644	28519	66462	82739	1248513
5	1333107	22643	54623	84420	1248514

The mean values shown in Table 9.40 does not correlate with the static weight of the submerged object. As for the well jumper, this might be due to the sudden drop in tension at 30 m water depth. The drop might indicate a shift in x displacement, and therefore lift forces acting on the main liftwire could reduce the tension. A new mean value is found for the time interval of 70:160s, at a water depth from 7 to 25m,

184

is found. This is the time interval before the tension drop. The mean values of tension from the time interval correlates to the static weight of the submerged drill centre template shown in Table 9.39.

	Mean tension [N]
1	116000
2	114400
3	116000
4	115300
5	111800

Figure 9.58 and Figure 9.59 show the tension in the main liftwire for the five wave conditions for when the drill centre template is deployed to the water depths of 2000 m and 4000 m. The trends in the two figures are similar to the trends shown for the tension in the main liftwire for the deployment of the valve tree, see section 9.4.1.
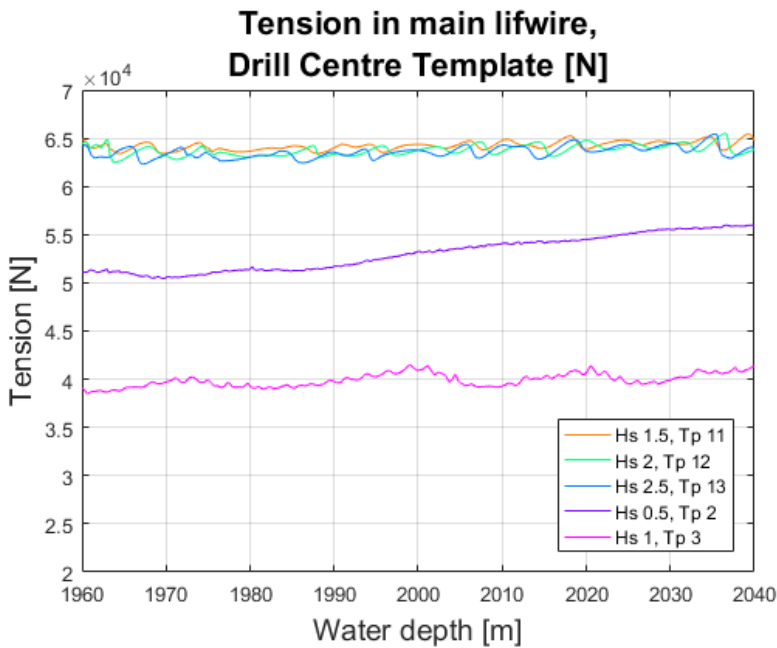
Figure 9.58: Tension in main liftwire at 2000 m, Drill centre template
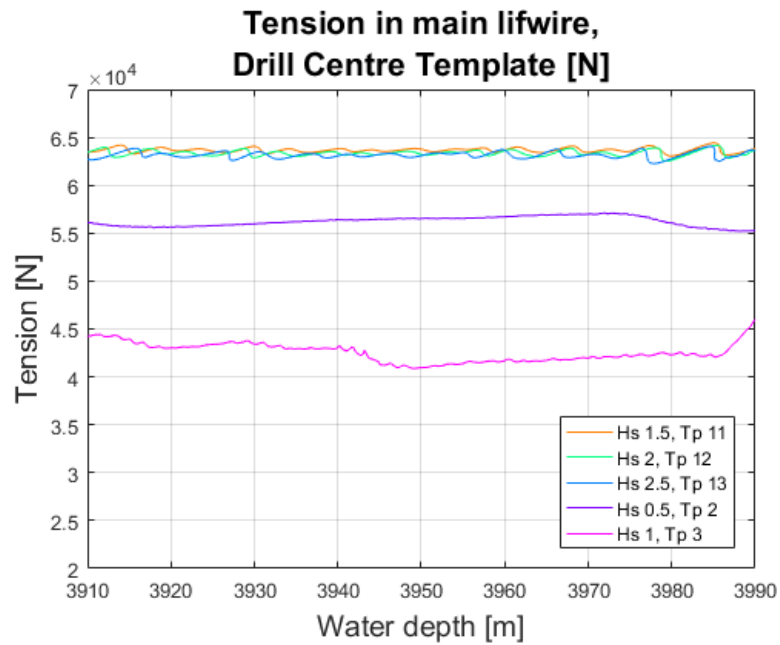
Figure 9.59: Tension in main liftwire at 4000 m, Drill centre template

The tension in condition sets 1 through 3 show little variance between each other, and decreases slightly from 2000 to 4000 m water depth. However, the tension in wave conditions 4 and 5 are about 10k N apart

at both 2000 m and 4000 m, and there is a slight increase in tension from 2000 m to 4000 m. The increase in tension in shown in Table 9.42 below.

Table 9.42: tension in main liftwire, 2000 m and 4000 m water depth, drill centre template

	Tension at 2000 m [N]	Tension at 4000 m (3990 m) [N]	Difference [N]
1	64347	63866	-481
2	63845	63694	-151
3	63735	63603	-132
4	53284	55236	1952
5	40961	46027	5066

As for the four other equipment, the tension is not significantly affected by the increase in water depth from 2000 m to 4000 m.

9.6.3. X displacement

The template has both the largest dimension and the largest weight. The dimensions of the template in the direction of the current is 11.4m by 9.1m.
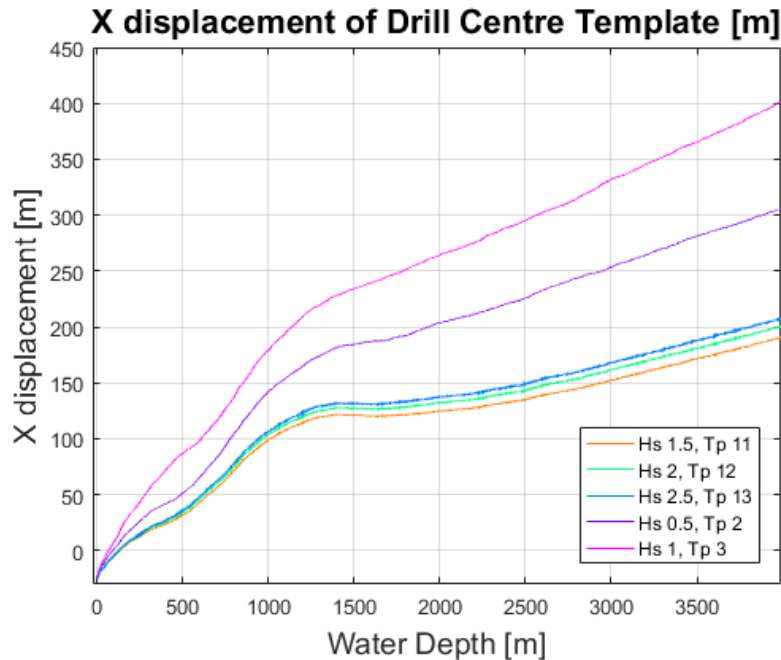
Figure 9.60: x displacement of drill Centre template

Different from the previous results, there is a clear and large difference in x displacement depending on the wave conditions, especially in wave conditions 4 and 5. The difference in the x displacement in wave

conditions 1 through 3 is minimal, where wave condition 1 is smallest wit 218m displacement, and wave condition 3 largest with 236m displacement. As stated above, the drill centre template has the largest cross-sectional area in the direction of the current. Because the x displacement due to current is calculated with respect to the cross-sectional area and the velocity of the current, it is understandable why the x displacement of the drill centre template is much larger than for the other equipment.

Table 9.43: Statistics of x displacement of drill centre template

	Max [m]	Min [m]	Mean [m]	Standard deviation [m]	Start position [m]	Displacement [m]
1	193.93	-24.62	114.36	57.02	-24.50	218.43
2	204.51	-24.98	120.89	59.94	-24.50	229.01
3	211.57	-25.17	125.38	62.01	-24.50	236.07
4	310.00	-24.46	183.70	92.08	-24.50	334.50
5	403.90	-24.57	238.65	116.70	-24.50	428.40

The x displacement is largest for wave condition 5, which has a x displacement of 428m. That is almost half a kilometer off its original x position. For wave condition 4, the x displacement is about 100 m less.

Figure 9.61 and Figure 9.62 show the x displacement of the drill centre template at the water depths of 2000 m and 4000 m. different from the previous cases, the x displacement for both water depths are large. The smallest x displacement at 2000 m is larger than the largest x displacement at 4000 m for the previous equipment. the increase in x displacement between 2000 m and 4000 m follow the approximately same phase for all wave conditions.
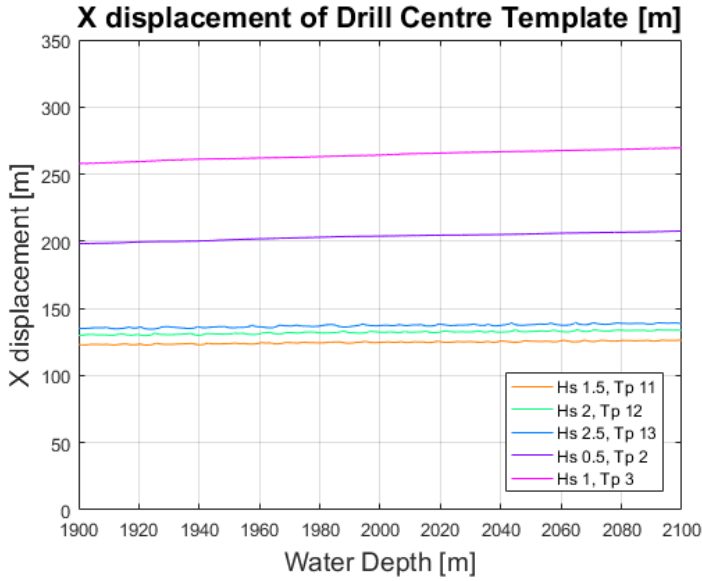
Figure 9.61: X displacement of drill centre template at 2000 m
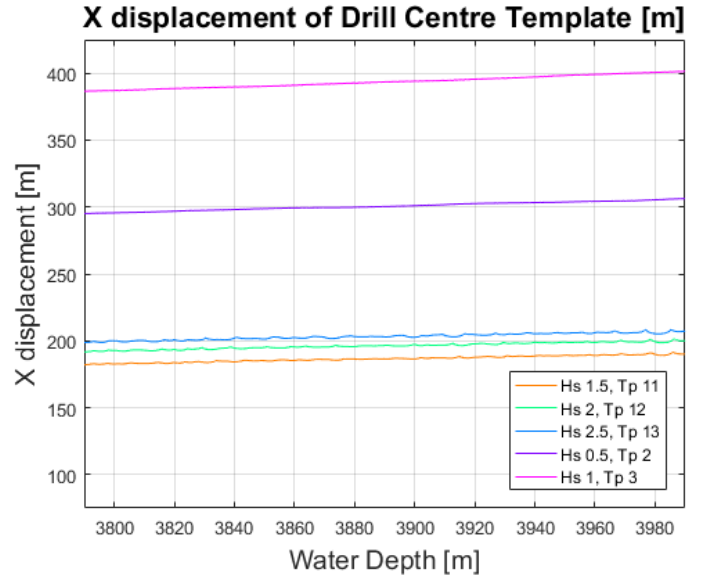
Figure 9.62: X displacement of drill centre template at 4000 m

Already at 2000 m, the drill centre template has shifted x positions to above 100 m. as stated above, this is more than for the largest shifts in x position for all four previous cases. The x displacements from 2000 m to 4000 m is 65.4m for wave condition 1 to 137.4m for wave condition 5.

	X displacement at 2000 m [m]	X displacement at 4000 m (3990 m) [m]	Difference [m]
1	124.76	190.13	65.37
2	132.30	200.11	67.81
3	137.27	207.41	70.14
4	203.92	306.21	102.29
5	264.20	401.56	137.36

The x displacement at both 2000 m and 4000 m is very large. Some type of positioning means should be used in order to reduce the large displacement in the x direction.

9.6.4. Y displacement
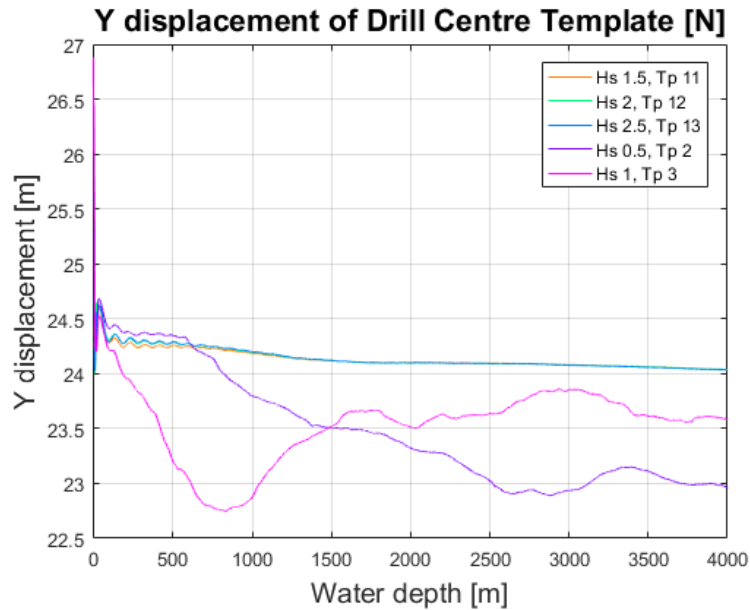
Figure 9.63: Y displacement of Drill centre template

As for the other equipment, the displacement in y direction for the drill centre template is minimalistic. The largest displacement is for in both positive and negative y direction is in wave condition 5. The y displacement in the positive y direction is similar for all wave conditions, but the difference in the negative y direction is neglectable for wave conditions 1 through 3 and about 1.5m for wave conditions 4 and 5.

Table 9.44: statistics for Y displacement of Drill centre template

	Max [m]	Min [m]	Mean [m]	Standard deviation [m]	Start position [m]	Displacement, +y [m]	displacement, -y [m]
1	26.78	24.03	24.15	0.22	24.25	2.53	0.22
2	26.77	24.00	24.16	0.22	24.25	2.52	0.25
3	26.75	24.02	24.16	0.22	24.25	2.50	0.23
4	26.81	22.89	23.51	0.58	24.25	2.56	1.36
5	26.88	22.75	23.59	0.43	24.25	2.63	1.50

Compared to the large displacement in the x direction, the y displacement is not significant.

9.6.5. Z displacement
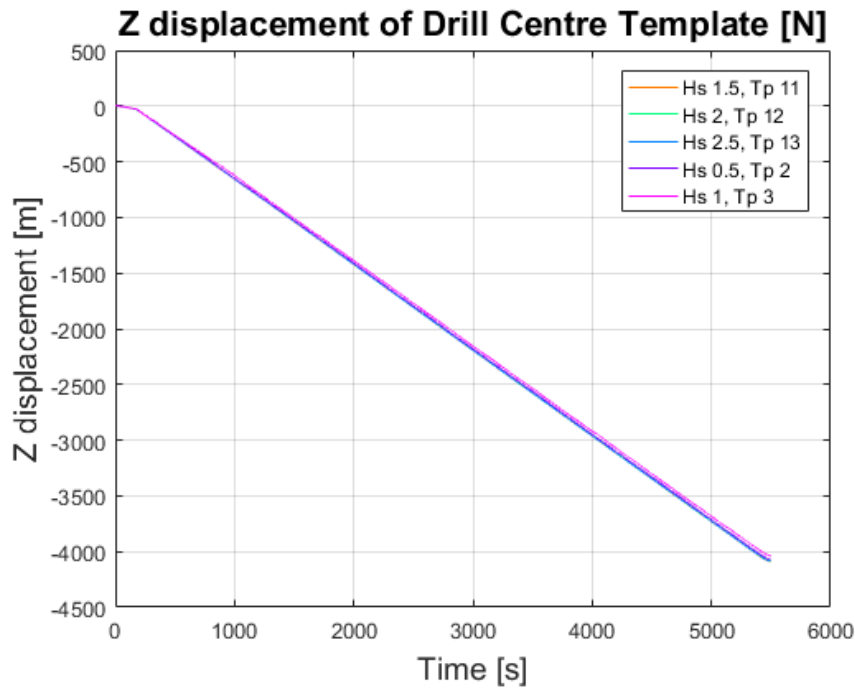
Figure 9.64: x displacement of the drill centre template

Figure 9.64 show the deployment time for the drill centre template to reach 4000 m water depth. Different from the previous cases, the displacement time varies more for each wave condition. There are 68 seconds separating the largest and smallest displacement time. For wave conditions 1 through 4, the displacement time is 1 hour and 29 minutes, and for wave condition 5 it takes one minute extra.

	Z displacement time to 3990 m [s]	Z displacement time to 4000 m [hours]
1	5352.5	1.49 (1 hour 29 minutes)
2	5354	1.49 (1 hour 29 minutes)
3	5354.5	1.49 (1 hour 29 minutes)
4	5375.5	1.49 (1 hour 29 minutes)
5	5420.5	1.51 (1 hour 30 minutes)

The difference in displacement times might be due to the differences in x displacement, where the wave condition with the largest x displacement is the slowest. The displacement times to 2000 minutes are approximately half the time.

190

9.6.6. Reduced current

To investigate the effect of the current, the drill centre template has been modelled in a new current which is half the previous current, see section 8.1. In this section we will investigate the effect of the reduced current, especially the effect on the x displacement.

9.6.6.1. Tension
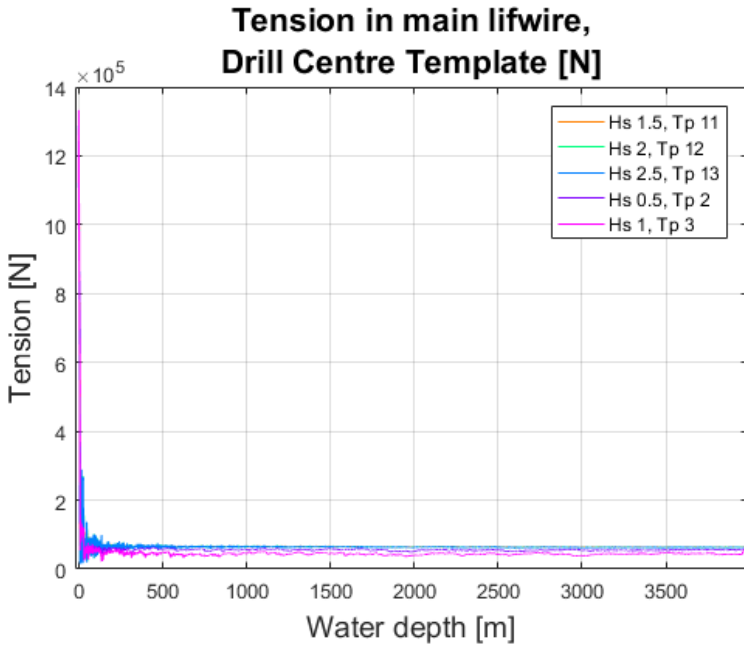
Figure 9.65: Tension in main liftwire, drill centre template, reduced current
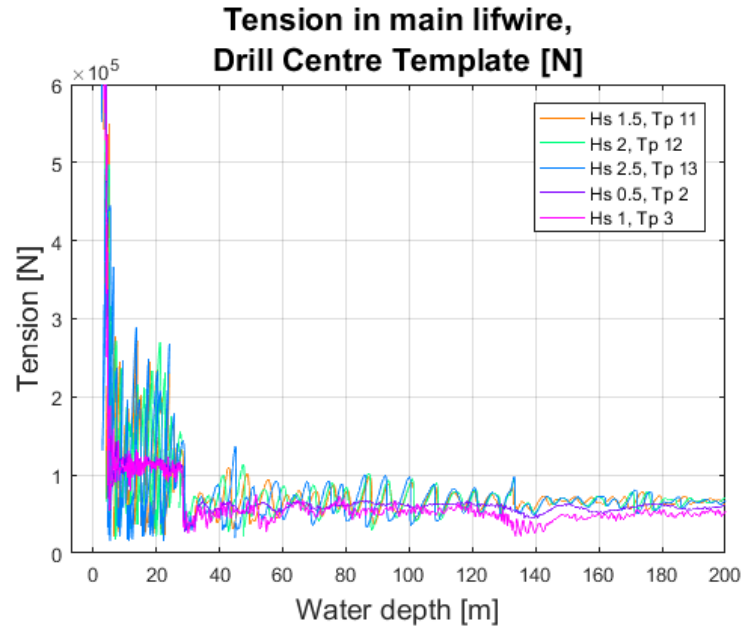
Figure 9.66: Tension in main liftwire, drill centre template, to 100 m water depth, reduced current

The tension in the main liftwire is approximately the same as for the larger current. There is e slight decrease in the mean tension throughout the deployment process. The smaller current will affect the motion of the drill centre template to a lesser extent than for the larger current. The small reduction tension may indicate less snap forces in the splash zone and upper water column due to current motion.

Table 9.45: statistics for tension in main liftwire, drill centre template, reduced tension

	Max [N]	Min [N]	Mean [N]	Standard deviation [N]
1	1266917	22696	74282	82588
2	1275157	19189	73963	82784
3	1286009	15062	73758	82995
4	1280635	27971	65922	82966
5	1332987	22112	54742	84543

Looking at the formula for horizontal water particle motion, see section 8.4, we see that the force I directly proportionate to the square of the current velocity. The force on the should therefore be 4 times as smaller for the reduced current.
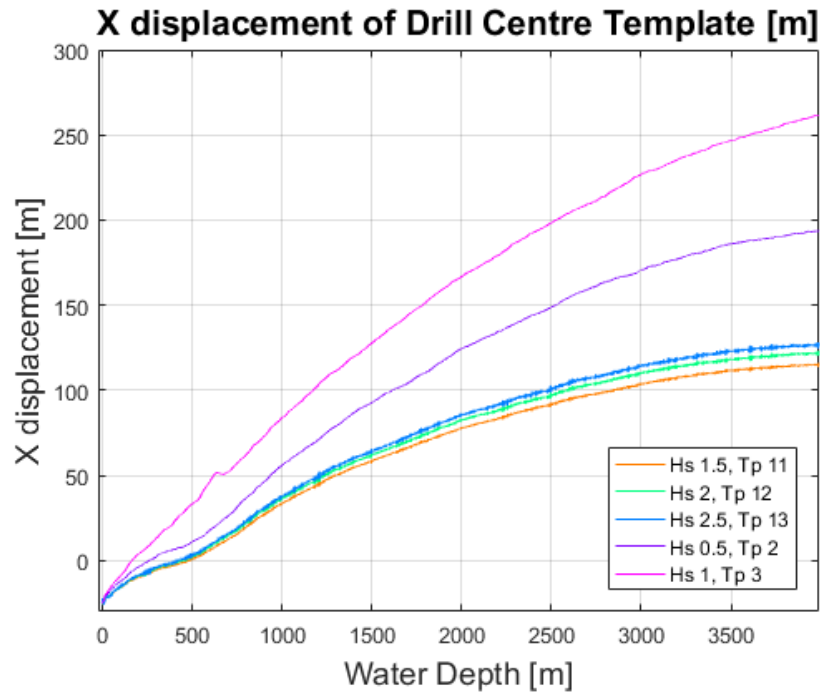
Figure 9.67: X displacement of drill centre template, reduced current

The x displacement of the for wave condition 5 is reduced by 142 meters, and the x displacement for wave condition 1 is reduced by 78m. We see from Figure 9.67 that the phase of the displacement to 500 m water depth has significantly reduced, but once the drill centre template reaches a certain water depth, the x displacement continues at a mostly constant phase. Even though the current is small after 1400 m, the x displacement will continue to grow.

Table 9.46: statistics of X displacement of drill centre template, reduced current

	Max [m]	Min [m]	Mean [m]	Standard deviation [m]	Start position [m]	Displacement [m]
1	116.07	-25.17	64.94	44.00	-24.50	140.57
2	122.98	-25.53	69.17	46.11	-24.50	147.48
3	128.32	-25.99	72.00	47.66	-24.50	152.82
4	194.09	-24.51	108.41	69.05	-24.50	218.59
5	262.17	-24.64	148.01	87.01	-24.50	286.67

The reduction of the current reduced the x displacement to some extent, but the need for positioning means is still present.

9.6.6.3. Y displacement
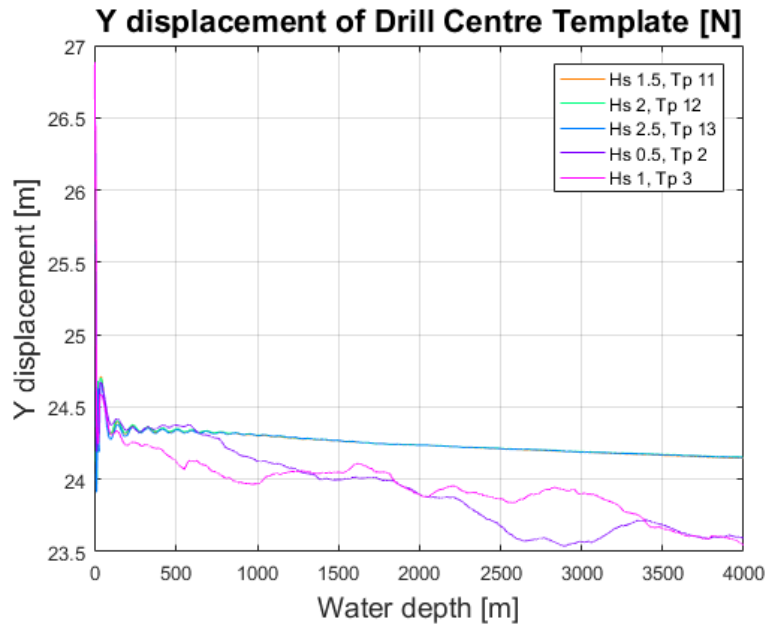
Figure 9.68: y displacement of drill centre template, reduced current

The difference in the y displacement is neglectable. The only difference is a visual difference of the negative y displacement for wave conditions 4 and 5, and a slight reduction in the negative y displacement for the two wave conditions.

Table 9.47: Statistics of y displacement of drill centre template, reduced current

	Max [m]	Min [m]	Mean [m]	Standard deviation [m]	Start position [m]	Displacement, +y [m]	displacement, -y [m]
1	26.78	23.93	24.26	0.20	24.25	2.53	0.32
2	26.77	23.94	24.27	0.21	24.25	2.52	0.31
3	26.75	23.91	24.26	0.20	24.25	2.50	0.34
4	26.81	23.54	23.94	0.37	24.25	2.56	0.71
5	26.88	23.54	23.97	0.30	24.25	2.63	0.71

9.6.7. No current

To investigate the effect of the wave conditions with no current present, the current was set to "no current" in the SIMO simulation, and was simulated for the drill centre template.

9.6.7.1. Tension
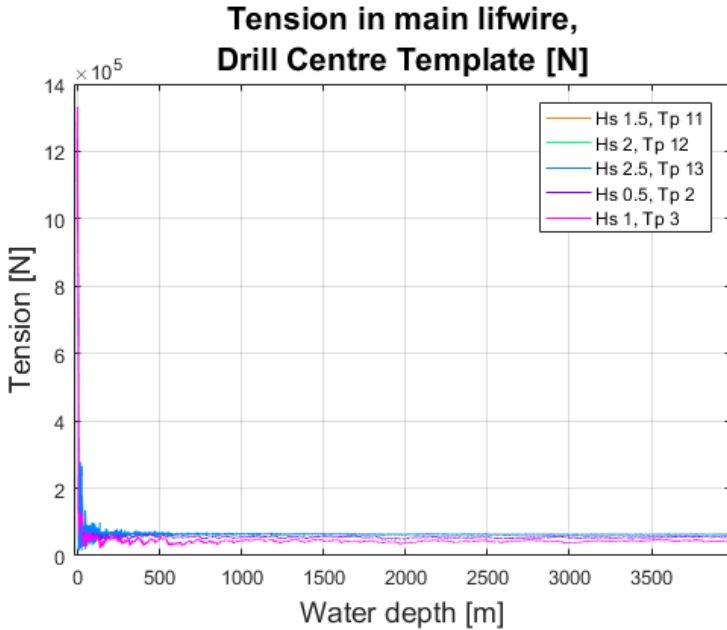
Figure 9.69: Tension in main liftwire, drill centre template, no current
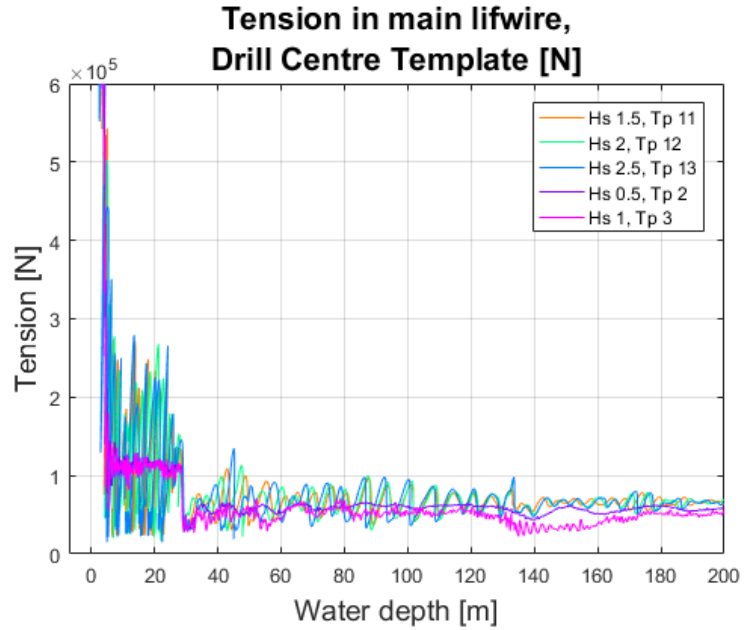
Figure 9.70: Tension in main liftwire, drill centre template, to 100 m water depth, no current

Compared to the two previous cases with there is a small decrease in mean tension in main liftwire when deploying the drill centre template though the water column with no current present. The drop in tension after 30 m is also present for this case. This might be due to the smaller effect of the waves after the position. This effect happens for the well jumper and drill centre template, where a different crane is used, which could have some effect on the tension due to crane tip motions. Another reason for the drop might be an error in the model setup.

Table 9.48: statistics for tension in main liftwire, drill centre template, no current

	Max [N]	Min [N]	Mean [N]	Standard deviation [N]
1	1267348	21144	73700	82618
2	1275531	16357	73358	82816
3	1286299	14912	73126	82998
4	1281421	27608	65000	83034
5	1332553	22285	53685	84625

9.6.7.2. X displacement

For this result, we see how much the current affects the displacement for the equipment in the current direction.
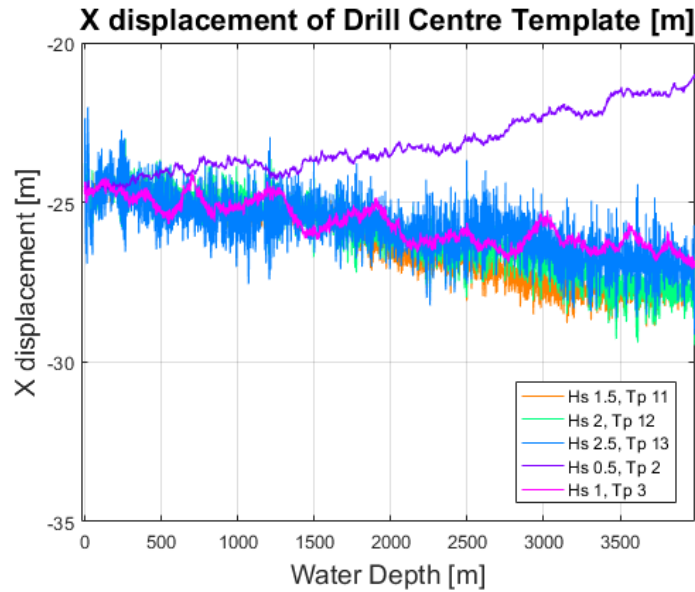
Figure 9.71: X displacement of drill centre template, no current

As expected, the x displacement is a lot less when there is no current present. The x displacement of the drill centre template is only affected by the horizontal wave particle motion due to the wave conditions. The largest x displacement wave conditions 1, 2, 3 and 5 are all in the negative x direction, whereas the largest x displacement for wave condition 4 is in the positive x direction. The reason for this might be due to the effect of the horizontal water particle velocity for wave condition 4 is only present until 100 m water depth.

Table 9.49: statistics of X displacement of drill centre template, no current

	Max [m]	Min [m]	Mean [m]	Standard deviation [m]	Start position [m]	Displacement, +x [m]	displacement, -x [m]
1	-23.21	-29.04	-26.30	1.25	-24.50	1.29	4.54
2	-22.84	-29.57	-26.02	1.18	-24.50	1.66	5.07
3	-22.02	-29.16	-25.78	0.99	-24.50	2.49	4.66
4	-20.94	-25.01	-23.15	1.00	-24.50	3.56	0.51
5	-24.06	-27.39	-25.68	0.71	-24.50	0.44	2.89

We see from this that the current data at the installation site is important when deciding what positioning measures are necessary.

9.6.7.3.   Y displacement
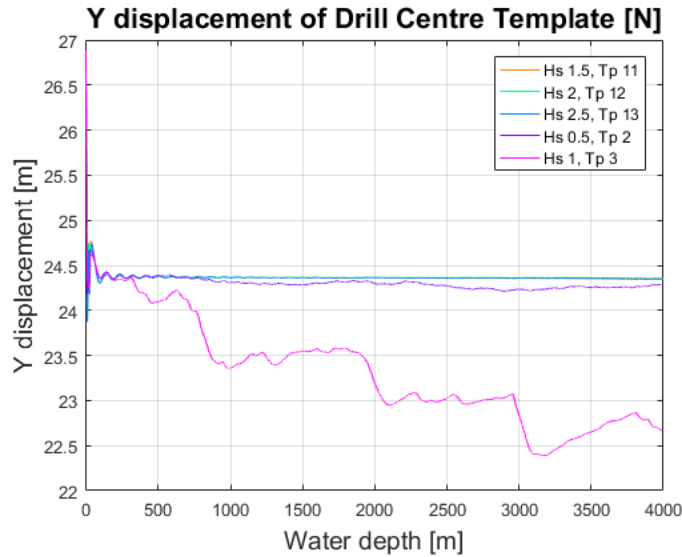
Figure 9.72: Y displacement of drill centre template, no current

The only difference from the current and reduced current case when it comes to y displacement of the drill centre template, is that there is less y displacement in the negative y direction for wave condition 4, and more for wave condition 5.

Table 9.50: statistics for Y displacement of drill centre template, no current

	Max [m]	Min [m]	Mean [m]	Standard deviation [m]	Start position [m]	Displacement, +y [m]	displacement, -y [m]
1	26.78	23.89	24.38	0.18	24.25	2.53	0.36
2	26.77	23.90	24.38	0.18	24.25	2.52	0.35
3	26.75	23.87	24.38	0.18	24.25	2.50	0.38
4	26.81	24.18	24.32	0.19	24.25	2.56	0.07
5	26.89	22.39	23.34	0.65	24.25	2.64	1.86

10. Conclusion and recommendation for further work

10.1. Conclusion

Using fibre rope as an alternative to conventional steel wire for the main liftwire is demonstrated to be fully possible. When installing subsea equipment in water depths down to 4000 m, the main factor when deciding between using fibre rope and steel wire is the tension in the main liftwire during the deployment. The added weight in water of the steel wire requires an additional 120 tonnes to the SWL of the deployment system. On the other hand, the weight of the fibre rope in water is negligible throughout the deployment of the equipment. Therefore, when choosing a deployment system using fibre rope, the SWL is only dependent on the mass of the installed equipment.

For the simulations using fibre rope, the maximum tension in the main liftwire occurs when the equipment is lifted above sea level. The tension in air is very close to the calculated total weight in air of the equipment. The mean tension in the main liftwire when lifted though the water column correlates to the calculated submerged weight in water of the equipment. There are no significant challenges with tension in the main liftwire when the equipment is deployed to 4000 m.

The main concern with deep-water deployment is the x displacement of the installed equipment. The challenge was found to be equally present for both fibre rope and steel wire. The x displacement was simulated relative to the weight and geometry of the several types of equipment. The largest x displacement occurred when deploying the drill centre template to 4000 m, with a maximum displacement value of 430 m. The smallest displacement occurred for the suction anchor, with a maximum displacement of approximately 40 m. The x displacement of the equipment was significantly larger at 4000 m water depth compared with the water depth of 2000 m.

The x displacement was found to be dependent on the current velocity and the wave conditions. As the current was acting in the positive x direction, the displacement occurred in the x direction. When reducing the current by halving the current velocity, there was a reduction in the x displacement. However, the reduction was not halved, but decreased by approximately 140m, or approximately 33% for the worst wave condition. Even though the current below 1400 m water depth had a velocity of just 0.01 m/s, the x displacement continued to increase as the equipment was continued to be deployed though the water column.

The waves were simulated to operate in the opposite direction of the current, and therefore helped with reducing the x displacement. Out of the five wave conditions simulated, the wave conditions with small wave period and small wave height affected the x displacement the most, since the counter effect to the current was only working in the shallower depths. With exception for the low weight well jumper, the smallest x displacement for all equipment occurred for wave condition 1, having a wave height of 1.5 m and a wave period of 11 s.

When installing subsea equipment in water depths of 4000 meters it is important to have a good model of the wave and current profile in the area. Depending on the current data, the installation will rely on proper positioning methods. For the equipment with the least displacement, a ROV could be used to position the equipment after it had been deployed to the desired water depth. However, for the equipment with the larger displacement, such as the drill centre template, other positioning measures must be applied.

10.2.   Recommendations for further work

The simulations in this thesis is modelled for one current dataset only. For further work it is recommended to look at a larger spectre of current data, as the current is varying for the different installation sites. The simulations are done without using heave compensation for the winch, which may be included in further simulations.

Investigating positioning measures designed to work at 4000 meters water depth is recommended.

11. References

Aquaterra Energy. (n.d.). *Susbea drill centre templates.* Retrieved April 2018, from Aquaterra Energy.

Aquaterra Energy. (n.d.). *Aquaterra energy helps support first oil for catcher*. Retrieved April 2018, from Aquaterra Energy: https://www.aquaterraenergy.com/aquaterra-energy-helps-support-first-oil-for-catcher/

Bai, Y., & Bai, Q. (2010). *Subsea Engineering Handbook.* Burlington, Kidlington: Gulf Professional Publishing.

Bull, S., Bunes, Ø., Davidson, D., Ingberg, P., Paterson, J., & Torben, S. R. (2007). Fiber Rope Deployment System For Ultra Deep water Installations. *Offshore Technology Conference. OTC18932.* Houston.

Bunes, Ø., Ingeberg, P., Torben, S., & Teigen, P. (2008). Fiber Rope Deployment System and Rope Management Process. *International Offshore and Polar Engineering Conference.* Vancouver.

Cheveron, Statoil. (2018, February). *Oilfield Wiki*. Retrieved from Jumpers: http://www.oilfieldwiki.com/wiki/Jumpers#Well_jumpers

Company, G. E. (2011). *Subsea Systems.* Retrieved 2018, from GE Oil & Gas: https://www.geoilandgas.com/sites/geog/files/345_GE_SS_Subsea_Trees_Pages_280113.pdf

Davies, S., & Ramberg, R. M. (2016, October 01). *Gullfaks, Asgard represent world-firsts in subsea compression.* Retrieved from Offshore Magazine: http://www.offshore-mag.com/articles/print/volume-76/issue-1/subsea/gullfaks-asgard-represent-world-firsts-in-subsea-compression.html

Det Norske Veritas AS. (2009). *DNV-OS-H103 Modelling and analysis of marine operation.* DNV.

Det Norske Veritas AS. (2011). *Marine Operations, General. DNV-OS_H101.* DNV.

DNV. (2009). *DNV-OS-H103 Modelling and analysis of marine operation.* Det Norks eVeritas.

EPG. (2018, February). Retrieved from epgsa: http://epgsa.com/epgen/index.php/portfolio/suction-anchors-for-aasta-hansteen/

FishSAFE. (n.d.). *Subsea Templates & Manifolds*. Retrieved February 2018, from fishsafe: http://www.fishsafe.eu/en/offshore-structures/subsea-structures/subsea-templates-manifolds.aspx

FMC Technologies. (2018, February). *Tubing Heads*. Retrieved from FMC TEchnologies: http://www.fmctechnologies.com/SurfaceWellhead/Technologies/ConventionalWellhead/TubingHeads.aspx#

GE Oil&Gas. (2018, February). *Subsea Production Systems*. Retrieved from GE oil and gas: https://www.geoilandgas.com/catalog/mobile/subseaproductionsys.html?stream=upstream

Gjerde, B. (2015). *Going deeper with fibre.* Retrieved from Rolls-Royce: https://www.rolls-royce.com/~/media/Files/R/Rolls-Royce/documents/customers/marine/id25-fibre-rope.pdf

Gudmestad, O. (2015). *Marine Technology and Operations.* WIT Press.

Harringston-Mission, L., Herry, C., Jeans, G., Lima, J. A., Maisondieu, C., & Prevosto, M. (2012). Deepwater durrent profile data sources for riser engineering offshore brazil. *ASME Conference on Ocean, Offshore and Artic Engineering.* Rio de Janeiro.

He, M., Li, H., Wang, A., Xu, J., Yang, Y., & Zhu, S. (2012). Latest Progress in Deepwater Installation Technologies. *International Offshore and Polar Engineering Conference.* Thodes: International Society of Offhore and Polar Engineers.

He, M., Wang, A. M., Xu, J., Zhang, C., & Zhu, S. (2013). Pendulous Installation Method and its Installation Analysis for a Deeowater Manifold in South China Sea. *International Offshore and Polar Engineering.* Anchorage: International Society of Offshore and Polar Engineers (ISOPE).

Ingberg, P., & Torben, S. (2006). Development of a Fiber Rope Based Development System for Deep Water Application. *International Offshore and Polar Engineering Conference.* San Fransisco: The International Society of Offshore and Polar Engineers.

Ingeberg, P., & Torben, S. (2011). Field Pilot of Subsea Equipment Installation in Deep Water unssing Fibre Rope in Two-fall Arrangement. *Offshore Technology conference. OTC 21204.* Houston.

InterMoor. (2018, February). *How do sucttion piles work?* Retrieved from Imtermoor: http://intermoorblog.com/how-suction-piles-work/

Lankhorst Ropes. (n.d.). *Deep water deployment ropes.* Nogueira - Maia: Lankhorst Ropes Offshore Devision.

Lu, Y., Chun, L., Manzano-Ruiz, J. J., Janardhanan, K., & Perng, Y.-Y. (n.d.). *Flo-Induced Vibration in Subsea Jumper Sunbject to Downstream Slug and Ocean Current.* Retrieved February 2018, from The American Society of Mechnica Engineers: http://offshoremechanics.asmedigitalcollection.asme.org/article.aspx?articleid=2499409

Manning, M. (2016, October 28). *Offshore oil prodution in deepwater and ultra-deepwater is increasing*. Retrieved from U.S Energy Information Administration: https://www.eia.gov/todayinenergy/detail.php?id=28552

Marintek. (2003). *Deep-Water Marine Operations.* Trondheim: SINTEF.

Mouhandiz, A.-A. e., & Troost, S. (2013). Subsea Templates Installation at North Sea using HLV THIALF. *International Offshore and Polar Engineering.* Anchorage: International Society of Offshore and Polar Engineers .

National Oilwell Varco, Rig systems. (2017, October). *Next Generation Subsea Knuckle Boom Crane.* Retrieved from NOV: http://nov.com/Segments/Rig_Systems/Offshore/Lifting_and_Handling/Product_Catalogue/Cranes/Next_Generation_Subsea_Knuckle_Boom_Cranes/Next_Generation_Subsea_Knuckle_Boom_Crane.aspx

Offshore Energy Today staff. (2011, November 18). *USA: Shell's Tobago Offshore Field Breaks Depth Record for Subsea Production*. Retrieved from Offshore Energy Today: http://www.offshoreenergytoday.com/usa-shells-tobago-offshore-field-breaks-depth-record-for-subsea-production/

Offshore Fleet Journal. (n.d.). *Deepwater construction vessel*. Retrieved May 2018, from Offshore fleet: http://offshore-fleet.com/data/deepwater-construction-vessel.htm

OrcaFlex. (n.d.). *Orcina.* Retrieved April 2018, from Rope/Wire: Axial and Bending Stiffness: https://www.orcina.com/SoftwareProducts/OrcaFlex/Documentation/Help/Content/html/RopeWire,AxialandBendingStiffness.htm

Rolls-Royce Marine AS. (2017). *Rolls-Royce subsea cranes. Fiber rope cranes (DDC50FR).* Hareid: Rolls-Royce Marine AS.

Rolls-Royce Marine AS. (2017). *Rolls-royce subsea cranes. Fiber rope cranes (FRC 150t).* Hareid: Rolls Royce.

Rolls-Royce Marine AS. (2017). *Rolls-royce subsea cranes. Fiber rope cranes (FRC 250t).* Hareid: Rolls-Royce Marine AS.

Rolls-Royse Marine AS. (2010). *CTCU fact sheet.* Rolls-Royse Marine.

Samson Rope Tenchnologies, inc. (2014). *Quantum-12.* Ferndale: Samson.

Schlumberger. (2018, February). *Oilfield Glossary*. Retrieved from Schlumberger: http://www.glossary.oilfield.slb.com/Terms/t/tubing_head.aspx

Technical standards committe. (2015). *Guidelines for marine lifting and lowering operations.* Gl Noble Denton.

TTS Group ASA. (2017, October). *A-frames.* Retrieved from TTS Group : http://www.ttsgroup.com/Products/A-frames/
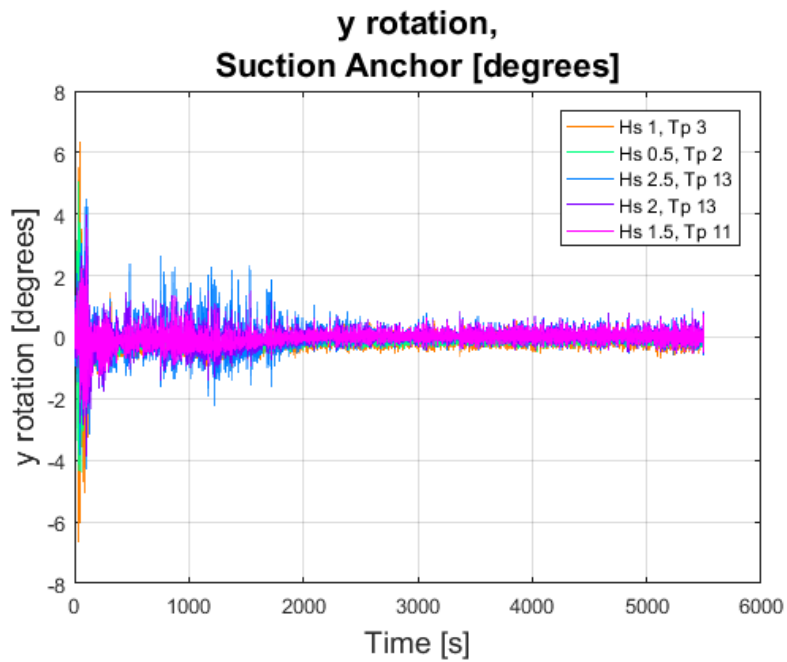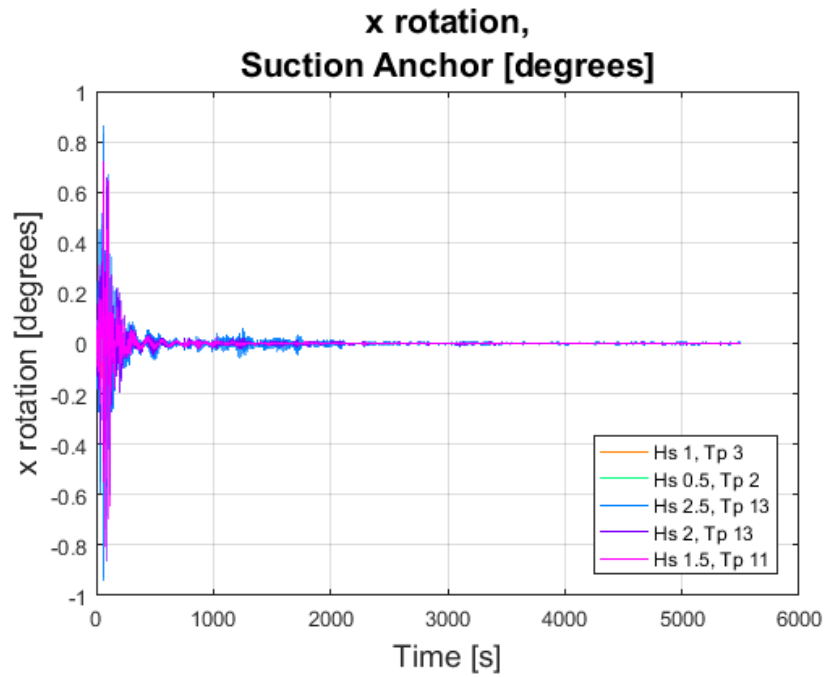
WSH Council. (2014). *Guidelines for Creating Lifting Plan for Lifting Operations in Workplaces.* WSH Council.
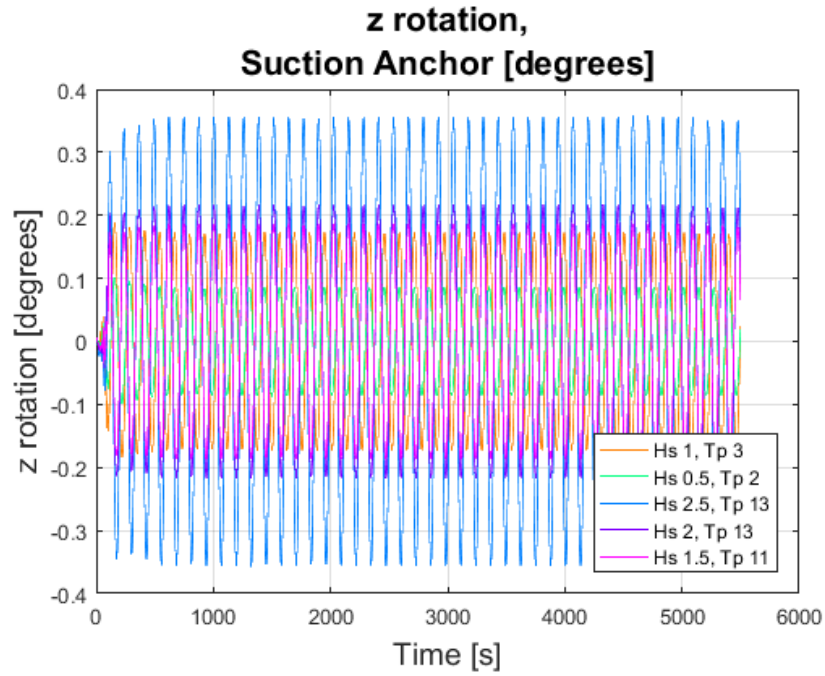
Zhang , W., & Jeong, C. (2013). *OTC 25304 Flat-over Feasibility in Brazilian Sea Water .* Rio de Janeiro : Offshore Technology Conferance .

Appendix

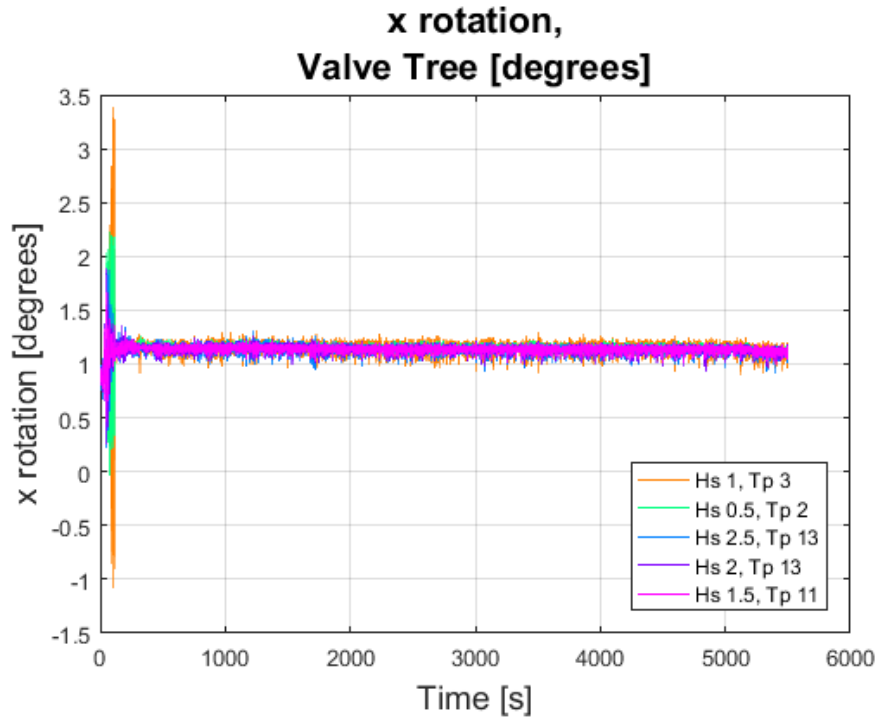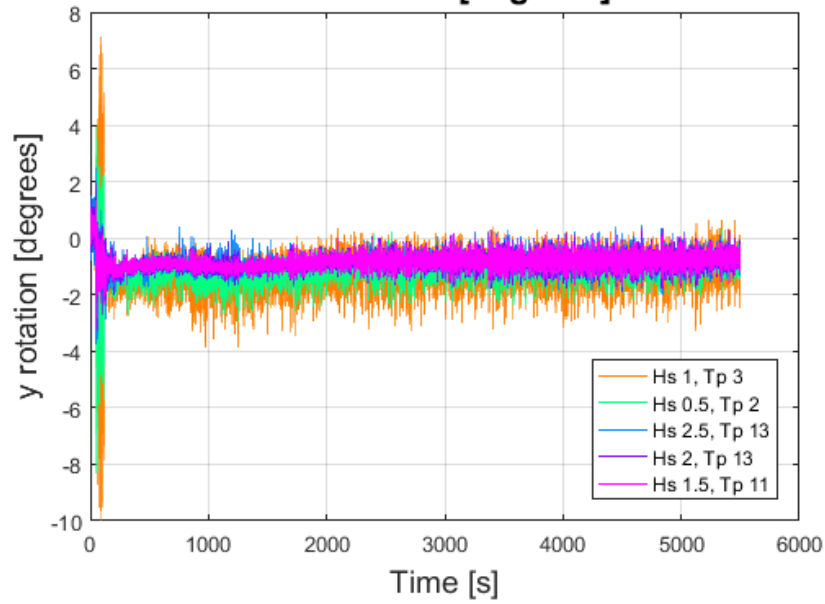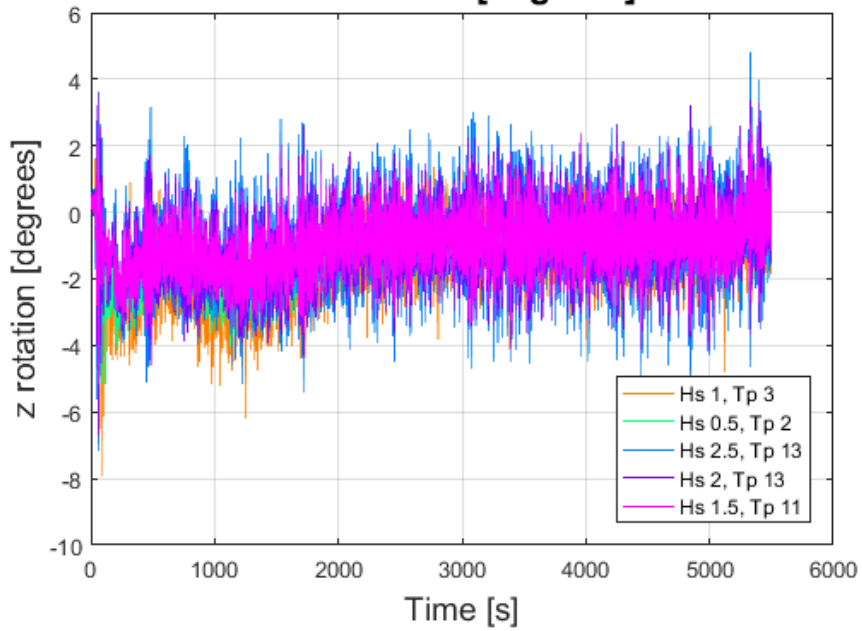## Appendix A: Results

Suction anchor rotation

Valve tree rotation

y rotation,
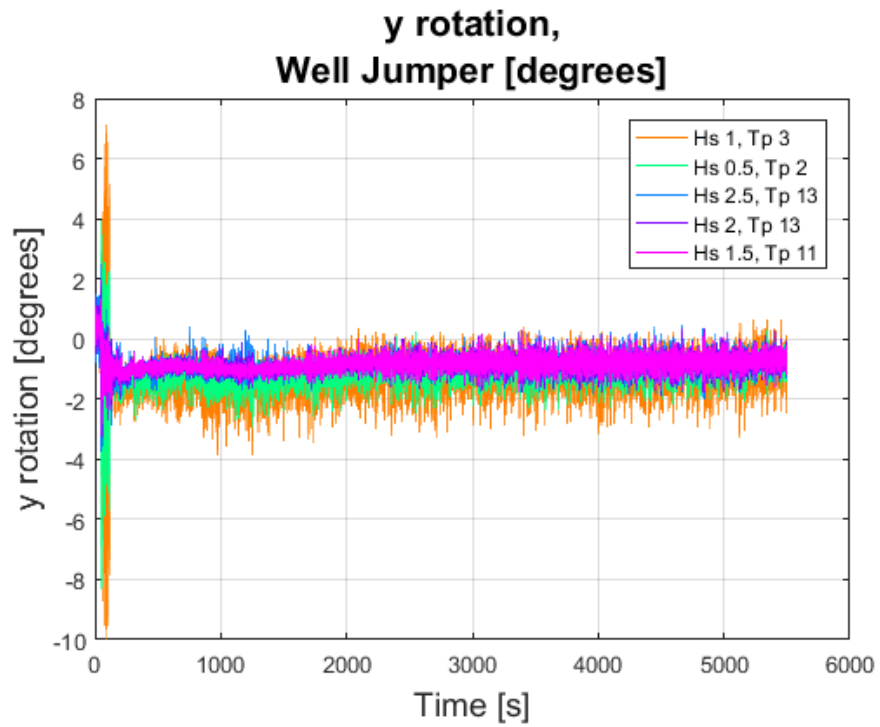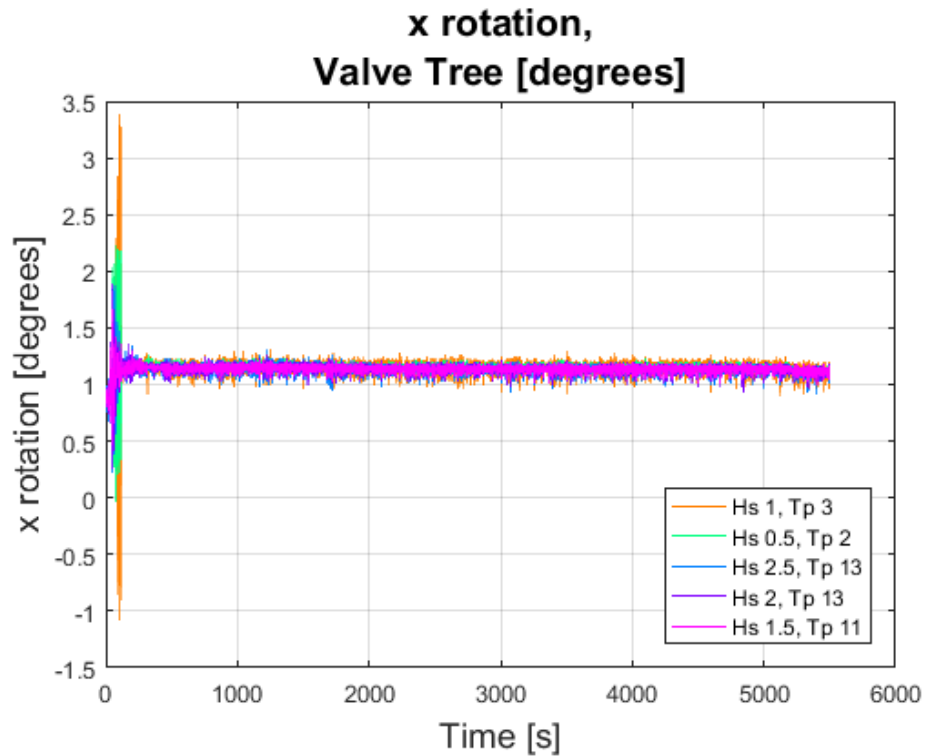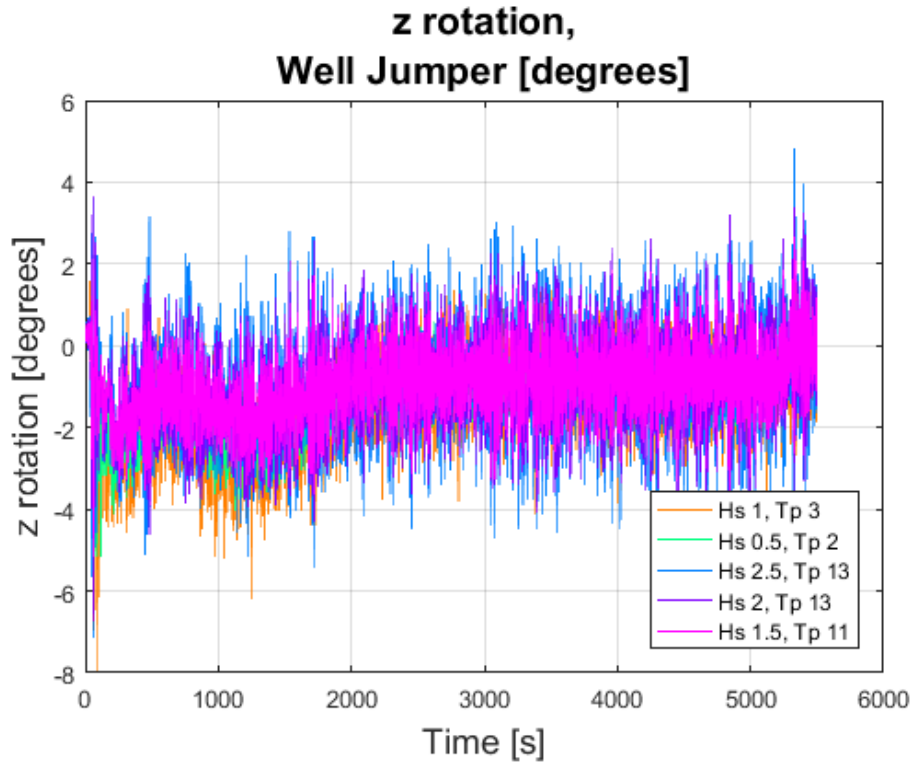Valve Tree [degrees]

z rotation,
Valve Tree [degrees]

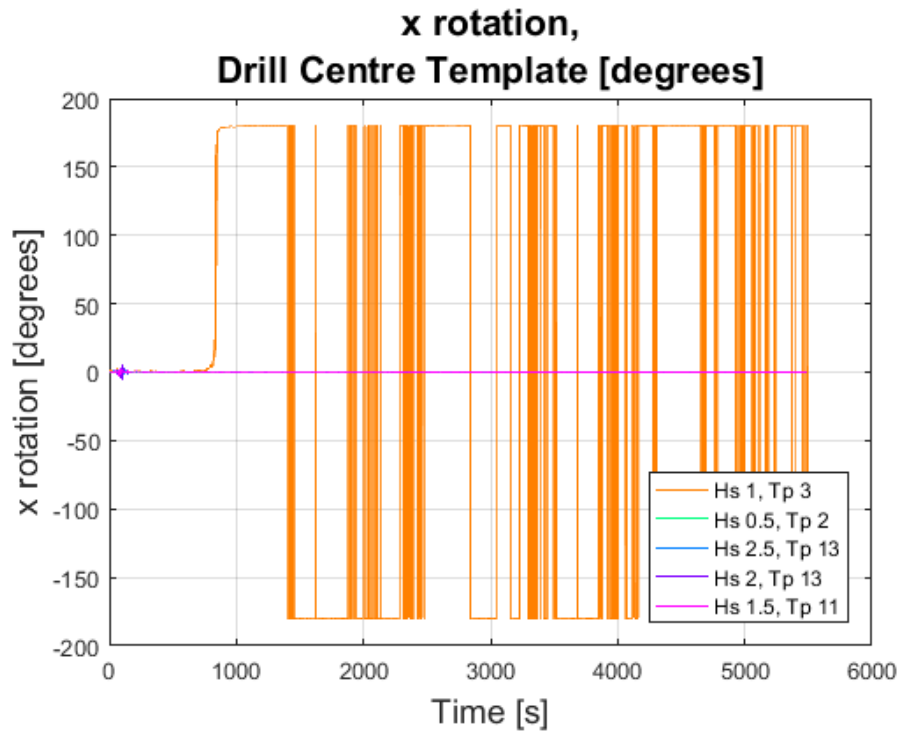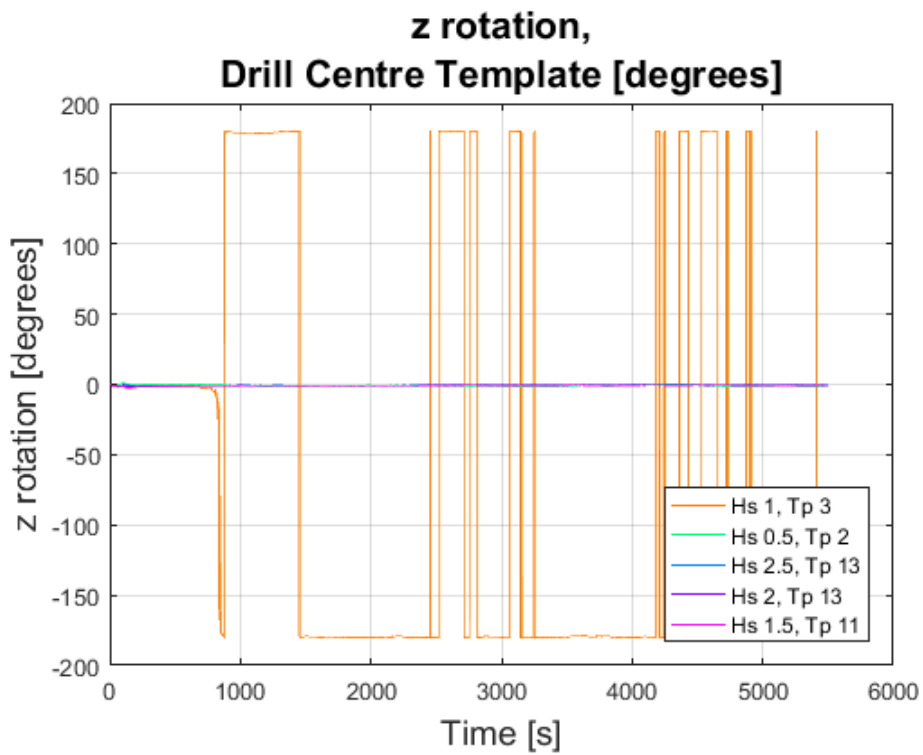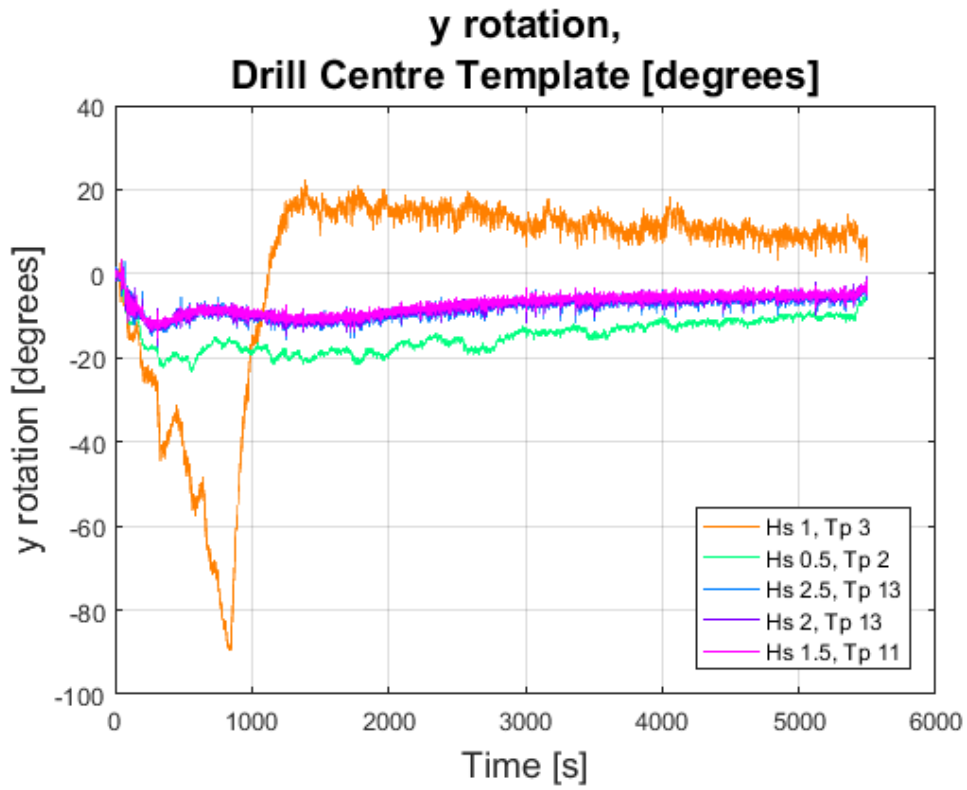Well jumper rotation

z rotation,
Well Jumper [degrees]

Drill centre template rotation

x rotation,
Drill Centre Template [degrees]

y rotation,
Drill Centre Template [degrees]

z rotation,
Drill Centre Template [degrees]

Quantum-12

PRODUCT CODE: 873

APPLICATIONS

> Winch Line / Offshore
> Lifting Sling / Offshore
> Working Line / Offshore

FEATURES AND BENEFITS

> Easy to handle
> Easy to splice
> Excellent grip
> Floats
> Lightweight
> Wire rope replacement
> Easy to inspect
> Excellent abrasion resistance
> Flexible
> High strength
> Samthane coated
> High coefficient of friction

SPECIFICATIONS

FIBER: Dyneema® - Polyester Blend

SPECIFIC GRAVITY: .99

SPLICE/CLASS: 12-Strand Class II

ELASTIC ELONGATION PERCENTAGE:
At % of break strength
10%..............0.65%
20%..............0.75%
30%..............0.90%

Quantum-12 is a lightweight, high-strength, floating rope that can grip on a capstan or H-bitt. The patented DPX™ fiber technology provides superior abrasion and cut resistance, but with a higher coefficient of friction than other high modulus polyethylene ropes. The 12-strand construction provides added flexibility, improved handling, and easy splicing. The vivid green Samthane coating provides excellent visibility and additional abrasion resistance.

COLOR: Vivid green, some sizes also available by special order in black, blue, green, orange, or yellow

DIAM. (inch)	CIRC. (inch)	WEIGHT PER 100 FT. (lbs)	AVG. STRENGTH (lbs)	MIN. STRENGTH (lbs)	DIAM. (mm)	CIRC. (mm)	WEIGHT PER 100 M (kg)	AVG. STRENGTH (kg)	MIN. STRENGTH (kg)	ISO 2307 STRENGTH (metric tons)
3/4"	2 1/4"	11.8	45,300	40,800	18	54	17.6	20,500	18,500	20.5
7/8"	2 3/4"	15.2	62,500	56,300	22	66	22.6	28,400	25,500	28.4
1"	3"	21.0	82,500	74,300	24	72	31.2	37,400	33,700	37.4
1 1/8"	3 1/2"	25.5	105,000	94,500	28	84	37.9	47,600	42,900	47.6
1 1/4"	3 3/4"	31.0	131,000	118,000	30	90	46.1	59,400	53,500	59.4
1 5/16"	4"	33.0	146,000	131,000	32	96	49.1	66,200	59,600	66.2
1 3/8"	4 1/8"	37.5	162,000	146,000	34	100	55.8	73,500	66,100	73.5
1 1/2"	4 1/2"	44.7	191,000	172,000	36	108	66.5	86,600	78,000	86.6
1 5/8"	5"	50.0	226,000	203,000	40	120	74.4	103,000	92,300	103
1 3/4"	5 1/2"	60.8	265,000	239,000	44	132	90.5	120,000	108,000	120
2"	6"	79.4	349,000	314,000	48	144	118	158,000	142,000	158
2 1/8"	6 1/2"	89.6	397,000	357,000	52	156	133	180,000	162,000	180

ISO strength specifications are for unspliced rope. All other strength specifications are for spliced rope.

SPECIFICATIONS CONTINUE ON NEXT PAGE...

samson
THE STRONGEST NAME IN ROPE

PRODUCT CODE: 873

CONTINUED...

DIAM. (inch)	CIRC. (inch)	WEIGHT PER 100 FT. (lbs)	AVG. STRENGTH (lbs)	MIN. STRENGTH (lbs)	DIAM. (mm)	CIRC. (mm)	WEIGHT PER 100 M (kg)	AVG. STRENGTH (kg)	MIN. STRENGTH (kg)	ISO 2307 STRENGTH (metric tons)
2 1/4"	7"	100	448,000	403,000	56	168	149	203,000	183,000	203
2 3/8"	7 1/8"	112	503,000	453,000	57	174	167	228,000	205,000	228
2 1/2"	7 1/2"	125	562,000	506,000	60	180	186	255,000	229,000	255
2 5/8"	8"	138	625,000	563,000	64	192	205	284,000	255,000	284
2 3/4"	8 1/2"	155	682,000	614,000	68	204	231	309,000	278,000	309
3"	9"	179	807,000	726,000	72	216	266	366,000	329,000	366
3 1/4"	10"	213	943,000	849,000	80	240	317	428,000	385,000	428
3 5/8"	11"	266	1,167,000	1,050,000	88	264	396	529,000	476,000	529
4"	12"	324	1,413,000	1,272,000	96	288	482	641,000	577,000	641
4 1/4"	13"	366	1,587,000	1,428,000	104	312	545	720,000	648,000	720
4 5/8"	14"	447	1,869,000	1,682,000	112	336	665	848,000	763,000	848
5"	15"	523	2,173,000	1,956,000	120	360	778	986,000	887,000	986
5 1/4"	16"	577	2,376,000	2,138,000	128	384	859	1,078,000	970,000	1078
5 1/2"	16 1/2"	634	2,573,000	2,316,000	134	400	943	1,167,000	1,050,000	1167
5 5/8"	17"	656	2,691,000	2,422,000	142	426	976	1,221,000	1,099,000	1221
6"	18"	755	3,003,000	2,703,000	152	456	1123	1,362,000	1,226,000	1362
6 1/4"	19"	820	3,204,000	2,884,000	158	474	1220	1,453,000	1,308,000	1453
6 5/8"	20"	922	3,579,000	3,221,000	168	504	1372	1,623,000	1,461,000	1623

ISO strength specifications are for unspliced rope. All other strength specifications are for spliced rope.

samson
THE STRONGEST NAME IN ROPE

Appendix C: Lankhorst rope

OFFSHORE

LankoDeep® AHC is a 12 strand braided rope where each strand is a 3 strand rope, resulting in a 12x3 patented construction, with dark grey color. Raw material is Dyneema® fully optimized for Cyclic Bending Over Sheave (CBOS) fatigue.

LankoDeep® AHC

| ø Rope [mm]	weight in air [kg/m]	weight in water [kg/m]	MBF (spliced) [Ton]
48	1,49	-0,039	148
52	1,76	-0,046	172
56	2,08	-0,054	199
60	2,39	-0,062	225
64	2,72	-0,071	256
68	3,07	-0,080	288
72	3,43	-0,089	320
76	3,82	-0,099	339
80	4,24	-0,110	360
88	5,09	-0,132	424
96	6,04	-0,157	497
104	7,10	-0,185	543
112	8,23	-0,214	623
120	9,45	-0,246	708
128	10,77	-0,280	796
136	12,19	-0,317	886
144	13,61	-0,354	989
152	15,18	-0,395	1.109
160	16,81	-0,437	1.238

SPECIFIC GRAVITY	• 0,98
UV-RESISTANCE	• excellent
ABRASION RESISTANCE	• excellent
CHEMICAL RESISTANCE	• good
MELTING POINT	• approx. 147°C
CONSTRUCTION	• 12-strand plaited
COLOUR	• dark grey
WATERABSORPTION	• 0%

Load / Extension curve
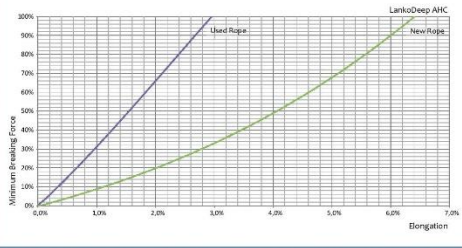
Cyclic Bending Over Sheaves (CBOS)

www.lankhorstropes.com

211

30.11.2017

Fact sheet

Rolls-Royce
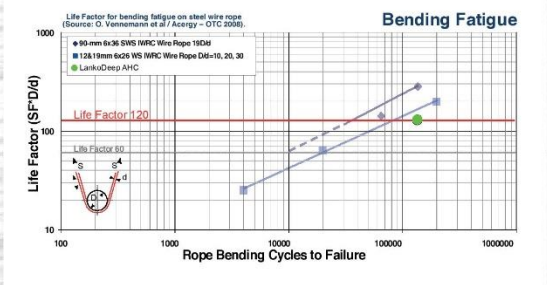
Cable traction control unit – CTCU

Fact sheet

The unique CTCU-technology has been developed through one of the most comprehensive processes ever by joint offshore industry efforts, and offers superior performance for our fibre rope deployment system.

The CTCU-technology has been designed to accommodate lifting capacities required to install subsea equipment safely and effectively to the seabed in shallow to ultra-deep waters. The CTCU is the main part of the complete fibre rope deployment system, and assures handling of fibre ropes and cables in the most careful manner.

High speed performance and the use of spliceable and repairable light-weight fibre ropes, instead of heavy steelwire, offers great benefits.

Field-proven units with a long track-record, now ranging from 20 – 125 Te capacities are operating in areas such as oceanography, seismic and subsea equipment installation.

A complete fibre rope deployment system includes high performance active heave compensation, proven to compensate for more than 95% of vessel motions. In addition to constant tension, pull limit and specially developed landing and lift-off functions, a rope management system is an integral part of the control system for monitoring rope bend fatigue.

30 Te CTCU

50 Te FRDS

125 Te FRDS

Technical specification

Calculation basis	DNV "Standard for certification No. 2.22 - Lifting appliances", 2008.				
Safe working load (SWL)	30 Te	50 Te	75 Te	125 Te	250 Te
Maximum dynamic load	48 Te	80 Te	97.5 Te	162.5 Te	325 Te
Launch/Recovery speed @ SWL *	1.0 m/s	1.0/0.5 m/s	0.75/0.4 m/s	0.5/0.3 m/s	0.5/0.3 m/s
Launch/Recovery speed @ 50% SWL	2.0 m/s	2.0/1.0 m/s	1.5/0.8 m/s	1.0/0.6 m/s	1.0/0.6 m/s
AHC speed	N/A	2.0 m/s	1.75 m/s	1.5 m/s	1.5 m/s
Constant tension range	N/A	5-45 Te	10-65 Te	15-110 Te	30-200 Te
Fibre rope diameter	30 mm	56 mm	68 mm	88 mm	136 mm
Storage winch capacity *	8000 m +	4500 m +	3500 m +	7000 m +	4000 m +
Peak power consumption *	450 kW	850 kW	850 kW	1000 kW	2000 kW

* Performance can be adapted to customer requirements.

Rolls-Royce

CTCU-2 of 2-160610

Fact Sheet

Rolls-Royce

Rolls-Royce subsea cranes

Fibre rope cranes (FRC 150t)
Working better deeper

The crane is designed for continuous operation in a tough and corrosive offshore environment with focus on efficient and safe load handling.

Fibre rope cranes

A range of offshore cranes up to 400 tonnes load using field proven Rolls-Royce fibre rope handling technology is now launched. The crane structure has an integrated operator cabin and the fibre rope runs over large diameter sheaves.

Below deck is a compact CTCU (cable traction control unit) which forms the crane winch, provides active heave compensation and stores the rope on a reel. This system has a proven track record of more than 10 years. Particular attention has been made to ease of access and maintenance of all main components.

Because the selected rope has neutral buoyancy, the crane can handle loads to its full rated capacity down to 4,500 metres water depth. Cranes using heavy steel wire must begin derating at depths more than about 700m, so by 2,500m a 400t wire crane can only handle the same load as a 250t FRC.

The Rolls-Royce rope management system monitors rope condition enabling abraded or damaged sections to be easily repaired by splicing onboard.

General design features

- Field proven CTCU technology for fibre rope handling
- Smart integration in vessel – below deck
- Innovative crane structure – reduced weight
- High-end control system
- Active heave compensation
- Constant tension, with auto landing and auto lift-off mode
- Pull limit and controlled emergency pay-out function
- State-of-the-art operator cabin
- High quality – low maintenance, robust and field proven technology
- Cost efficient logistics for rope replacement
- In-field splicing of rope
- Easy inspection of rope

- Rope management system – full wear traceability
- DNV GL certification

Options

- Auxiliary winch
- Personnel lifting
- Tugger winches
- Remote access
- Anti-collision system
- Pedestal
- Heavy lift double fall arrangement
- Health monitoring

Fact Sheet

Cabin

A sound insulated state-of-the-art cabin houses the operator's chair with redundant touch screens, camera monitors, a writing desk and a co-pilot chair. Heating and air conditioning allows the operator to work comfortably and efficiently in all climates.
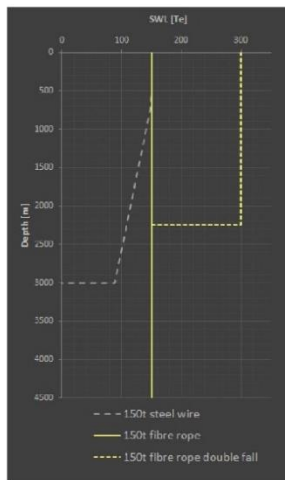
CTCU

Fibre rope handling is taken care of below deck, in a compact system using the field-proven Rolls-Royce cable traction control unit (CTCU), which assures reliable and predictable rope spooling and storage in all conditions.

| SWL	150t
Operating depth	4500 m
Min outreach	7 m
Max outreach	31 m
Winch speed	0 - 1.5 m/s (all layers)*
AHC capacity (Peak to peak)	4.8 m at 10 s period (150t, all layers)
Heavy lift capacity (double fall)	300t at 2250 m
Aux winch capacity	10t / 20t
Tugger winch capacity	5t
Slewing	+/-200 degrees rotation
Peak power consumption	1300 kW
Certification	DNVGL-ST-E407 "Rope based deployment and recovery systems for designed service"

Approximate values, provided for information only. Specifications may vary for given applications.
* Varies according to applied load.

The graphs to right compare the subsea lifting capacity of fibre rope vs. steel wire. Unlike steel wire, fibre rope suffers no depth derating as it has neutral buoyancy. In addition, the fibre rope's twist free construction enables deepwater operations in double fall which effectively doubles the crane's lifting capacity.

Use of steel wires practically stops at approx. 3000 m due to size of handling equipment and high water pressure causing wire core corrosion issues.

Fibre rope crane 150t vs. 150t steel wire
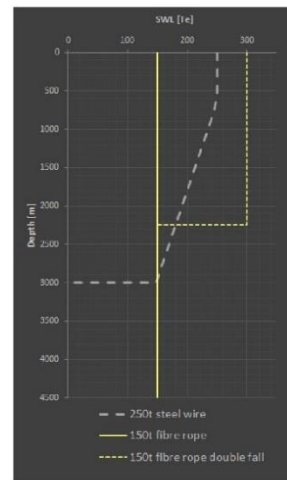
Fibre rope crane 150t vs. 250t steel wire

Fact Sheet

Rolls-Royce

Rolls-Royce subsea cranes

Fibre rope cranes (FRC 250t)
Working better deeper

The crane is designed for continuous operation in a tough and corrosive offshore environment with focus on efficient and safe load handling.

Fibre rope cranes

A range of offshore cranes up to 400 tonnes load using field proven Rolls-Royce fibre rope handling technology is now launched. The crane structure has an integrated operator cabin and the fibre rope runs over large diameter sheaves.

Below deck is a compact CTCU (cable traction control unit) which forms the crane winch, provides active heave compensation and stores the rope on a reel. This system has a proven track record of more than 10 years. Particular attention has been made to ease of access and maintenance of all main components.

Because the selected rope has neutral buoyancy, the crane can handle loads to its full rated capacity down to 4,500 metres water depth. Cranes using heavy steel wire must begin derating at depths more than about 700m, so by 2,500m a 400t wire crane can only handle the same load as a 250t FRC.

The Rolls-Royce rope management system monitors rope condition enabling abraded or damaged sections to be easily repaired by splicing onboard.

General design features

- Field proven CTCU technology for fibre rope handling
- Smart integration in vessel – below deck
- Innovative crane structure – reduced weight
- High-end control system
- Active heave compensation
- Constant tension, with auto landing and auto lift-off mode
- Pull limit and controlled emergency pay-out function
- State-of-the-art operator cabin
- High quality – low maintenance, robust and field proven technology
- Cost efficient logistics for rope replacement
- In-field splicing of rope
- Easy inspection of rope

- Rope management system – full wear traceability
- DNV GL certification

Options

- Auxiliary winch
- Personnel lifting
- Tugger winches
- Remote access
- Anti-collision system
- Pedestal
- Heavy lift double fall arrangement
- Health monitoring

Fact Sheet

Cabin

A sound insulated state-of-the-art cabin houses the operator's chair with redundant touch screens, camera monitors, a writing desk and a co-pilot chair. Heating and air conditioning allows the operator to work comfortably and efficiently in all climates.
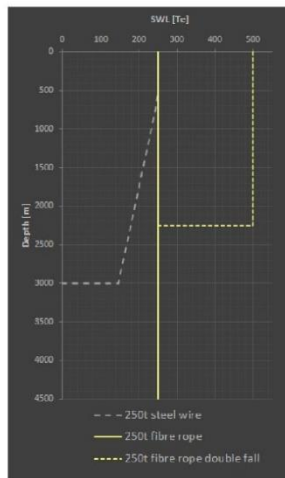
CTCU

Fibre rope handling is taken care of below deck, in a compact system using the field-proven Rolls-Royce cable traction control unit (CTCU), which assures reliable and predictable rope spooling and storage in all conditions.

| SWL	250t
Operating depth	4500 m
Min outreach	11 m
Max outreach	40 m
Winch speed	0 - 1.5 m/s (all layers)*
AHC capacity (Peak to peak)	4.8 m at 10 s period (150t, all layers) 3.2 m at 10 s period (250t, all layers)
Heavy lift capacity (double fall)	500T at 2250 m
Aux winch capacity	10 / 20t
Tugger winch capacity	5t
Slewing	+/-200 degrees rotation
Peak power consumption	2300 kW
Certification	DNVGL-ST-E407 "Rope based deployment and recovery systems for designed service"

Approximate values, provided for information only. Specifications may vary for given applications.
* Varies according to applied load.

The graphs to right compare the subsea lifting capacity of fibre rope vs. steel wire. Unlike steel wire, fibre rope suffers no depth derating as it has neutral buoyancy. In addition, the fibre rope's twist free construction enables deepwater operations in double fall which effectively doubles the crane's lifting capacity.

Use of steel wires practically stops at approx. 3000 m due to size of handling equipment and high water pressure causing wire core corrosion issues.

Fibre rope crane 250t vs. 250t steel wire
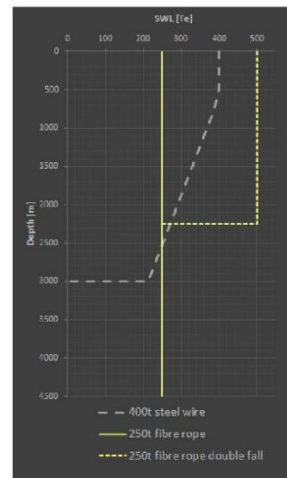
Fibre rope crane 250t vs. 400t steel wire

217

Fact Sheet

Rolls-Royce

Rolls-Royce subsea cranes

Fibre rope cranes (DDC50FR)
Working better deeper

The crane is designed for continuous operation in a tough and corrosive offshore environment with focus on efficient and safe load handling.

Fibre rope cranes

A range of offshore cranes up to 400 tonnes load using field proven Rolls-Royce fibre rope handling technology is now launched. The crane structure have been adapted to handle fibre rope, utilizing the field proven CTCU (cable traction control unit) which forms the crane winch, provides active heave compensation and stores the rope on a reel. This system has a proven track record of more than 10 years. Particular attention has been made to ease of access and maintenance of all main components.

Because the selected rope has neutral buoyancy, the crane can handle loads to its full rated capacity down to its maximum water depth. Cranes using heavy steel wire must begin derating at depths more than about 700m, so by 2,500m a 400t wire crane can only handle the same load as a 250t FRC.

The Rolls-Royce rope management system monitors rope condition enabling abraded or damaged sections to be easliy repaired by splicing onboard.
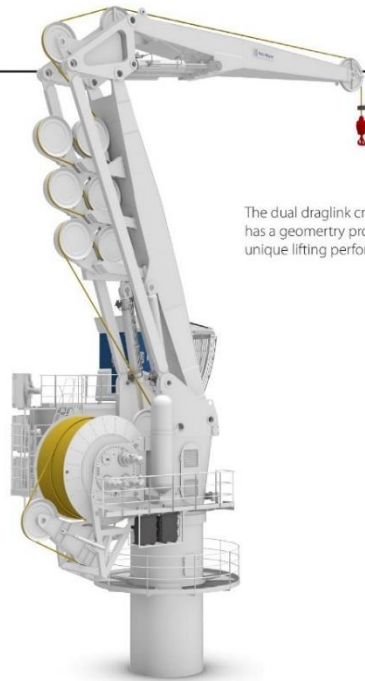
The dual draglink crane has a geomertry providing unique lifting performance.

General design features

- Field proven CTCU technology for fibre rope handling
- Innovative crane structure – increased lifting height
- High-end control system
- Active heave compensation
- Constant tension, with auto landing and auto lift-off mode
- Pull limit and controlled emergency pay-out function
- State-of-the-art operator cabin
- High quality – low maintenance, robust and field proven technology
- Cost efficient logistics for rope replacement
- In-field splicing of rope
- Easy inspection of rope

- Rope management system – full wear traceability
- DNV GL certification – others upon request

Options

- Auxiliary winch
- Personnel lifting
- Tugger winches
- Remote access
- Anti-collision system
- Pedestal
- Heavy lift double fall arrangement
- Health monitoring

Fact Sheet

Cabin

A sound insulated state-of-the-art cabin houses the operator's chair with redundant touch screens, camera monitors, a writing desk and a co-pilot chair. Heating and air conditioning allows the operator to work comfortably and efficiently in all climates.
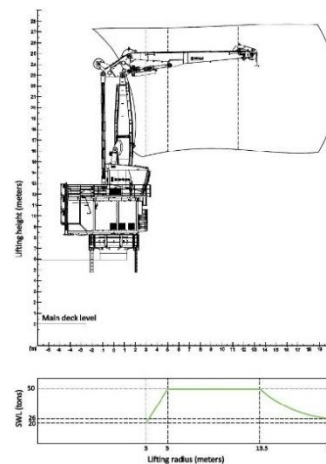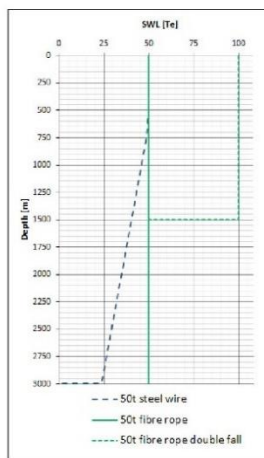
CTCU

Fibre rope handling is taken care of using the field-proven Rolls-Royce cable traction control unit (CTCU), which assures reliable and predictable rope spooling and storage in all conditions.

SWL	50t
Operating depth	3000 m
Min outreach	3 m
Max outreach	20 m
AHC capacity (Peak to peak)	6 m at 8 s (50t, all depths)
Heavy lift capacity (double fall)	100t at 1500 m
Tugger winch capacity	3t
Slewing	+/-360 degrees continuous
Peak power consumption	850 kW
Certification	DNVGL-ST-E407 "Rope based deployment and recovery systems for designed service"

Approximate values, provided for information only. Specifications may vary for given applications.

The graph to the right compares the subsea lifting capacity of fibre rope vs. steel wire. Unlike steel wire, fibre rope suffers no depth derating as it has neutral buoyancy. In addition, the fibre rope's twist free construction enables deepwater operations in double fall which effectivly doubles the crane's lifting capacity.

Use of steel wires practically stops at approx. 3000 m due to size of handling equipment and high water pressure causing wire core corrosion issues.

Your partner for a Lifetime of Lifting

NOV has developed a ground-breaking crane concept purpose-built for fiber rope that will revolutionize the subsea crane market. This sleek outward design provides a glimpse into what lies beneath the surface. This innovative lifting system allows the unit to maintain its full lifting capacity at any operational depth; for example, a 400 t capacity NOV Trident Crane allows the user to bring an actual 400 t load to whatever depth chosen.

Lifting Operation Station (LOS)

cranes@nov.com   nov.com

NOV Trident Crane

The innovative hoisting system includes the patent pending "winch on king" concept and a spooling system that is designed specifically for the use of fiber rope. It utilizes a unique rope protection system which ensures that the rope temperature is conditioned and protects the rope from environmental exposure. The versatile design allows the use of fiber rope, hybrid rope , or steel wire, depending on the needs of the customer.

We believe in purposeful innovation, as such this new design will not only increase safety and improve the ability of the vessel, it will also redefine how the crane is operated with the introduction of the new Lifting Operation Station (LOS). By integrating LOS into the superstructure of the vessel near the bridge, the Trident Crane enables close communication during lifting operations onboard.

	NOV Trident using Fiber Rope	Traditional crane using Steel Wire Rope
Same 400t load @ 3000m depth		=
Lighter		
Able to install on smaller ship	<	
Energy savings	<	
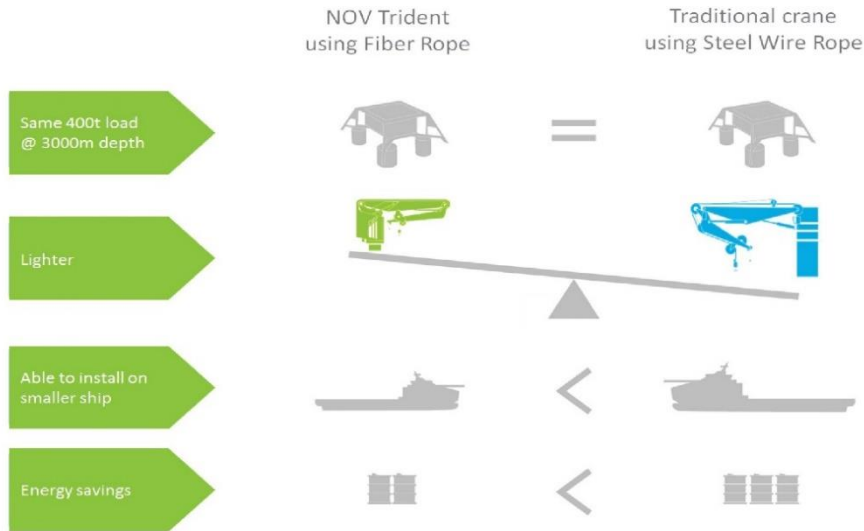
Key Features

Fiber Rope

- No loss of hook capacity in deepwater operations
- Purpose-built for fiber rope, but can also handle hybrid rope or steel wire
- No corrosion issues
- Fiber rope protection system

Lifting Operation Station (LOS)

- Safer, more efficient preparation, mobilization, and lifting operation
- Near vessel bridge location; crane operator no longer isolated in crane
- Extended operation possibilities, including possibilities for planning, simulation and training activities
- State-of-the-art dome offering benefit of impossible views, augmented reality, wave timing feature and timeline feature
- Improved human machine interface
- Increased safety for personnel on deck

Crane Features

- Lower weigth
- Reduced installation and commissioning – compared to below deck winch systems
- Lower CoG of crane system – compared to crane with winch above deck
- Electrically and/or hydraulically operated

NOV has a pending patent application directed to features and methods of the lifting crane design

cranes@nov.com

nov.com

Appendix I: Alfa factor, DNV-OS-H101

705 In the North Sea and the Norwegian Sea the α-factor should normally be selected according to the relevant Table 4-1 through Table 4-5. Table 4-1is applicable if one weather forecast (Level C) or the mean value of two or more forecasts is applied, while Table 4-2 through Table 4-5 cover special cases. The table(s) should also be used as a guideline for other offshore areas.

Guidance note:

The tabulated alpha factors are based on the work performed in a Joint Industry Project during the years 2005-2007 with the aim to establish a revised set of α-factors for European waters. For details of the JIP is referred to DNV Report 2006_1756 Rev. 03, "DNV Marine Operation Rules, Revised Alpha Factor JIP Project".

---e-n-d---of---G-u-i-d-a-n-c-e---n-o-t-e---

Table 4-1 α-factor for waves, base case

Operational Period [h]	Design Wave Height [m]						
	$H_s = 1$	$1 < H_s < 2$	$H_s = 2 = 2$	$2 < H_s < 4$	$H_s = 4$	$4 < H_s < 6$	$H_s \geq 6$
$T_{POP} \leq 12$	0.65	Linear Interpolation	0.76	Linear Interpolation	0.79	Linear Interpolation	0.80
$T_{POP} \leq 24$	0.63		0.73		0.76		0.78
$T_{POP} \leq 36$	0.62		0.71		0.73		0.76
$T_{POP} \leq 48$	0.60		0.68		0.71		0.74
$T_{POP} \leq 72$	0.55		0.63		0.68		0.72

Note 1: Note that the operational period used as basis for finding the α-factor may be defined by T_{POP}. However, required forecasted length of weather windows for the operations shall be defined by the operation reference period - TR. *See* Figure 1.

Note 2: The α-factor could be assumed to vary in time for one operation. E.g. for an operation with $T_{POP} = 36$ hours, $H_s = 4.0$ m, the α-factor is 0.79 for the first 12 hours, 0.76 for the next 12 hours and 0.73 for the last 12 hours of the operation.

Note 3: Design wave heights less than one (1) meter are normally not applicable for offshore operations. If a smaller design wave height nevertheless has been applied the alpha factor should be duly considered in each case.

706 Special considerations should be made regarding uncertainty in the wave periods. I.e. if the operation is particularly sensitive to some wave periods (e.g. swell), also uncertainty in the forecasted wave periods shall be considered.

707 If the available weather forecasting services could be regarded as level B, and the highest forecasted wave height(s) from at least two recognized and pre-defined sources is (are) considered, the α-factors could be taken according to Table 4-2. The notes to Table 4-1 apply.

Table 4-2 α-factor for waves, Level B highest forecast

Operational Period [h]	Design Wave Height [m]						
	$H_s = 1$	$1 < H_s < 2$	$H_s = 2$	$2 < H_s < 4$	$H_s = 4$	$4 < H_s < 6$	$H_s \geq 6$
$T_{POP} \leq 12$	0.68	Linear Interpolation	0.80	Linear Interpolation	0.83	Linear Interpolation	0.84
$T_{POP} \leq 24$	0.66		0.77		0.80		0.82
$T_{POP} \leq 36$	0.65		0.75		0.77		0.80
$T_{POP} \leq 48$	0.63		0.71		0.75		0.78
$T_{POP} \leq 72$	0.58		0.66		0.71		0.76

708 If the weather forecasting services are Level A including a meteorologist at site that issues/verifies the weather forecast, the α-factors could be taken according to Table 4-3. The notes to Table 4-1 apply.

Table 4-3 α-factor for waves, Level A with meteorologist at site

Operational Period [h]	Design Wave Height [m]						
	$H_s = 1$	$1 < H_s < 2$	$H_s = 2$	$2 < H_s < 4$	$H_s = 4$	$4 < H_s < 6$	$H_s \geq 6$
$T_{POP} \leq 12$	0.72	Linear Interpolation	0.84	Linear Interpolation	0.87	Linear Interpolation	0.88
$T_{POP} \leq 24$	0.69		0.80		0.84		0.86
$T_{POP} \leq 36$	0.68		0.78		0.80		0.84
$T_{POP} \leq 48$	0.66		0.75		0.78		0.81
$T_{POP} \leq 72$	0.61		0.69		0.75		0.79

709 If the weather forecast(s) are properly calibrated based on monitoring as described in D300, the α-factors could be taken according to Table 4-4. The notes to Table 4-1 apply.

Table 4-4 α-factor for waves, monitoring

Operational Period [h]	Design Wave Height [m]						
	$H_s = 1$	$1 < H_s < 2$	$H_s = 2$	$2 < H_s < 4$	$H_s = 4$	$4 < H_s < 6$	$H_s \geq 6$
$T_{POP} \leq 4$	0.9	Linear Inter-polation	0.95	Linear Inter-polation	1.0	Linear Inter-polation	1.0
$T_{POP} \leq 12$	0.72		0.84		0.87		0.88
$T_{POP} \leq 24$	0.66		0.77		0.80		0.82
$T_{POP} > 24$	According to Table 4-1 or Table 4-2 as applicable						

710 If the weather forecast(s) are properly calibrated based on monitoring as described in D300, and the weather forecast is issued/verified by a meteorologist at site the α-factors could be taken according to Table 4-5. The notes to Table 4-1 apply.

Table 4-5 α-factor for waves, monitoring & Level A with meteorologist

Operational Period [h]	Design Wave Height [m]						
	$H_s = 1$	$1 < H_s < 2$	$H_s = 2$	$2 < H_s < 4$	$H_s = 4$	$4 < H_s < 6$	$H_s \geq 6$
$T_{POP} \leq 4$	0.9	Linear Inter-polation	0.95	Linear Inter-polation	1.0	Linear Inter-polation	1.0
$T_{POP} \leq 12$	0.78		0.91		0.95		0.96
$T_{POP} \leq 24$	0.72		0.84		0.87		0.90
$T_{POP} > 24$	According to Table 4-3						

711 The appropriate α-factor for wind should be selected (estimated) considering the items listed below.

— Statistical data and local experience for the actual site.
— Planned operation period from issuance of weather forecast, T_{POP}.
— Applied wind speed compared with the maximum possible wind speed, i.e. 10 year return wind speed.
— Criticality of exceeding the design wind speed, e.g. by considering the contribution from wind on the total design load.